



## Identification and functional characterization of new regulators of sensory neurogenesis in *Xenopus laevis*

|                  |   |
|------------------|---|
| Title            | Identification and functional characterization of new regulators of sensory neurogenesis in <i>Xenopus laevis</i> |
| Author(s)        | Hutlet, Bertrand  |
| Publication Date | 2025-02-04  |
| Publisher        | University of Galway  |

**Identification and functional characterization  
of new regulators of sensory neurogenesis  
in *Xenopus laevis***

*A thesis submitted in partial fulfilment of the requirements of the University of Galway  
for the degree of Doctor of Philosophy*

Author: Bertrand Hutlet

Supervisor: Dr Gerhard Schlosser

School of Biological and Chemical Sciences

University of Galway

Thesis submission: October 2024

# Table of Contents

|  |            |
|--|------------|
| <b>Declaration .....</b>   | <b>v</b>   |
| <b>Acknowledgements .....</b>  | <b>vi</b>  |
| <b>Abstract.....</b>   | <b>vii</b> |
| <b>Chapter 1. Introduction .....</b>   | <b>1</b>   |
| 1.1. The vertebrate "New Head" .....   | 1          |
| 1.2. Cranial placodes and their derivatives.....                                       | 2          |
| 1.3. Induction of the ectodermal territories.....                                      | 5          |
| 1.4. Placode segregation.....  | 8          |
| 1.5. Six1 and Eya1 .....   | 10         |
| 1.5.1. Six1 .....  | 10         |
| 1.5.2. Eya1.....   | 11         |
| 1.5.3. Roles in placode development.....   | 12         |
| 1.6. Regulation of placodal neurogenesis.....  | 13         |
| 1.6.1. SoxB1 transcription factors.....  | 14         |
| 1.6.2. Proneural bHLH transcription factors .....                                      | 16         |
| 1.6.3. Roles of Six1 and Eya1 in cell proliferation and neuronal differentiation ..... | 17         |
| 1.7. <i>Xenopus laevis</i> as a model for the study of placodal biology .....          | 20         |
| 1.8. Aim of the project .....  | 20         |
| <b>Chapter 2. Materials and Methods .....</b>  | <b>22</b>  |
| 2.1. Animals.....  | 22         |
| 2.1.1. Induction of egg laying.....  | 22         |
| 2.1.2. In vitro fertilization .....  | 22         |
| 2.2. Molecular methods.....  | 23         |
| 2.2.1. RNA extraction .....  | 23         |
| 2.2.2. cDNA generation.....  | 23         |
| 2.2.3. Yeast two-hybrid screening.....   | 24         |
| 2.2.4. PCR primers design .....  | 26         |
| 2.2.5. PCR amplification .....   | 26         |
| 2.2.6. Agarose gel electrophoresis.....  | 26         |
| 2.2.7. Agarose gel DNA extraction .....  | 27         |
| 2.2.8. Subcloning.....   | 27         |
| 2.2.9. Bacterial transformation.....   | 27         |

|         |   |    |
|---------|---|----|
| 2.2.10. | Miniprep.....   | 28 |
| 2.2.11. | Restriction test digest .....   | 28 |
| 2.2.12. | Midiprep.....   | 29 |
| 2.2.13. | Plasmid linearization .....   | 29 |
| 2.2.14. | mRNA synthesis for microinjection.....                                | 29 |
| 2.2.15. | RNA probes synthesis for <i>in situ</i> hybridization .....           | 30 |
| 2.2.16. | Microinjection of mRNA or morpholino antisense oligonucleotides ..... | 31 |
| 2.2.17. | Embryo fixation and X-gal staining .....                              | 34 |
| 2.2.18. | Whole mount <i>in situ</i> hybridization .....                        | 34 |
| 2.2.19. | TnT <i>in vitro</i> transcription and translation .....               | 36 |
| 2.2.20. | Protein extraction .....  | 36 |
| 2.2.21. | Co-immunoprecipitation.....   | 37 |
| 2.2.22. | Polyacrylamide gel electrophoresis (PAGE) .....                       | 38 |
| 2.2.23. | Western blotting.....   | 38 |
| 2.3.    | Microscopy.....   | 39 |
| 2.4.    | Data analysis .....   | 40 |
| 2.4.1.  | DAVID .....   | 40 |
| 2.4.2.  | Panther.....  | 40 |

### **Chapter 3. Candidate Protein Interaction Partners of Eya1: Identification and Expression ..... 41**

|        |  |    |
|--------|--|----|
| 3.1.   | Yeast two-hybrid screening .....                         | 41 |
| 3.2.   | Candidate Eya1 interactants ontology and selection ..... | 42 |
| 3.3.   | Candidate Eya1 interactants expression patterns .....    | 46 |
| 3.3.1. | Stage 14-18 .....  | 47 |
| 3.3.2. | Stage 22.....  | 50 |
| 3.3.3. | Stage 27.....  | 53 |
| 3.3.4. | Stage 34.....  | 56 |
| 3.4.   | Candidate Eya1 interactants single cell atlas data.....  | 58 |
| 3.5.   | Conclusion.....  | 59 |

### **Chapter 4. Validation of Interaction between Eya1 and Candidate Cofactors ..... 61**

|        |  |    |
|--------|--|----|
| 4.1.   | Co-immunoprecipitation of Eya1 and candidate cofactors ..... | 61 |
| 4.1.1. | Flag-tagged candidates .....                                 | 61 |
| 4.1.2. | (Twin-)Strep-tagged Pias4.....                               | 62 |
| 4.1.3. | eGFP-tagged candidates .....                                 | 62 |

|  |  |            |
|--|--|------------|
| 4.1.4.   | Co-immunoprecipitation experiments.....  | 63         |
| 4.2.   | One-by-one validation by solid growth tests (by Hybrigenics).....                      | 71         |
| 4.3.   | Mass spectrometry .....  | 73         |
| 4.4.   | Conclusion.....  | 77         |
| <b>Chapter 5. Roles of Pias4 and Smarce1 in Sensory Neurogenesis .....</b> |  | <b>83</b>  |
| 5.1.   | Introduction .....   | 83         |
| 5.2.   | Morpholinos specificity and efficacy .....   | 84         |
| 5.2.1.   | <i>Pias4.L</i> morpholino .....  | 84         |
| 5.2.2.   | <i>Smarce1.LS</i> morpholinos.....   | 84         |
| 5.3.   | Effects of <i>pias4</i> gain- and loss-of-function in sensory neurogenesis.....        | 86         |
| 5.3.1.   | <i>Pias4</i> loss of function .....  | 87         |
| 5.3.2.   | <i>Pias4</i> gain of function.....   | 91         |
| 5.3.3.   | <i>Pias4</i> gain- and loss-of-function: summary.....                                  | 95         |
| 5.4.   | Effects of <i>smarce1</i> gain- and loss-of-function in sensory neurogenesis.....      | 95         |
| 5.4.1.   | <i>Smarce1</i> loss of function.....   | 97         |
| 5.4.2.   | <i>Smarce1</i> gain of function .....  | 101        |
| 5.4.3.   | <i>Smarce1</i> gain- and loss-of-function: summary .....                               | 104        |
| 5.5.   | Conclusion.....  | 104        |
| <b>Chapter 6. Discussion.....</b>  |  | <b>106</b> |
| 6.1.   | Introduction .....   | 106        |
| 6.2.   | Confirming Eya1 interaction partners.....  | 106        |
| 6.2.1.   | Solid growth tests .....   | 107        |
| 6.2.2.   | Co-IP followed by western blotting .....   | 107        |
| 6.2.3.   | Co-IP followed by mass spectrometry .....  | 108        |
| 6.2.4.   | Y2H-based vs co-IP-based results .....   | 110        |
| 6.3.   | Developmental expression of selected candidate Eya1 interactants.....                  | 111        |
| 6.3.1.   | Expression patterns: previous data and updates.....                                    | 111        |
| 6.3.2.   | Expression in the PPE and its derivatives.....   | 113        |
| 6.3.3.   | Expression in other areas of <i>eya1</i> expression.....                               | 114        |
| 6.3.4.   | Expression in areas with no <i>eya1</i> expression .....                               | 114        |
| 6.4.   | The known functions of candidate Eya1 interactants are interconnected.....             | 115        |
| 6.4.1.   | Pias E3 ligases and SUMOylation: general functions.....                                | 115        |
| 6.4.2.   | Pias, SUMOylation of transcription factors and regulation of signaling pathways<br>116 |            |
| 6.4.3.   | Pias, SUMOylation, Sox and neuronal differentiation .....                              | 117        |
| 6.4.4.   | Pias, SUMOylation, Msh6, Zmym3 and DNA repair .....                                    | 118        |

|  |  |            |
|--|--|------------|
| 6.4.5.   | Smarce1, Zmym, SUMOylation and chromatin modification .....        | 119        |
| 6.5.   | Garre1 and the CCR4-NOT deadenylase complex .....                  | 120        |
| 6.6.   | Roles of Pias4 and Smarce1 in sensory neurogenesis .....           | 121        |
| 6.7.   | Summary and Conclusion .....                                       | 123        |
| <b>Bibliography .....</b>                                  |  | <b>125</b> |
| <b>Appendix A. Solutions.....</b>                          |  | <b>163</b> |
| A.1.   | General solutions .....  | 163        |
| A.2.   | Solutions for X-gal staining and <i>in situ</i> hybridization..... | 164        |
| A.3.   | Solutions for co-immunoprecipitation.....                          | 170        |
| A.4.   | Solutions for PAGE and western blotting.....                       | 171        |
| <b>Appendix B. Primers list and PCR protocol .....</b>     |  | <b>173</b> |
| <b>Appendix C. Sense <i>in situ</i> hybridization.....</b> |  | <b>175</b> |
| <b>Appendix D. MS/MS probable contaminants .....</b>       |  | <b>176</b> |

## Declaration

This thesis has not been submitted in whole, or in part, to this or any other university for any other degree and is solely that of the author.

This study was funded by a College of Science scholarship, a Beckman Fund Award and a Thomas Crawford Hayes Research Award from the University of Galway.

Bertrand Hutlet

A handwritten signature in blue ink, appearing to read 'Hutlet', is positioned to the right of the author's name.

# Acknowledgements

Firstly, I would like to thank my supervisor, Dr. Gerhard Schlosser, for giving me the opportunity to carry out this project in his team, and for his availability, guidance and unwavering support throughout this long journey.

I am grateful to have worked with my fellow team members Suad Almasoudi, Mohamed El Amri, Haris Bin Fida, Merin Lawrence and Bahareh Estiri, and with the members of Prof. Uri Frank's team I have known over the years, who all contributed to make the day-to-day laboratory work a pleasant and enriching experience.

I would also like to thank Yolanda, Natasha, Silke, Svitlana, Cecilia and the other BRU members, who looked or are still looking after our frogs with great care and professionalism.

Finally, I want to thank my parents, who have supported me unconditionally during my studies.

## Abstract

Whether to keep dividing or to differentiate is one of the key decisions cells have to make during animal development and adult life. However, very little is currently known about how this important balancing act is regulated. This study addresses this question focusing on cranial sensory cells and the sensory neurons that innervate them.

In previous studies, a protein complex of the transcription factor Six1 and its cofactor Eya1 has been identified as a key regulator of these sensory cells and neurons and several studies suggested that this protein complex is required for both maintenance of neuronal/sensory progenitors and neuronal or sensory differentiation. This suggests that this protein complex plays an important role in regulating the balance between proliferating progenitors and differentiating cells. While the precise mechanism is obscure, interactions with different cofactors in a context-dependent manner probably play a decisive role.

Based on a yeast two-hybrid protein interaction screen, the present study identified multiple putative protein interaction partners of Eya1. The developmental expression profiles of genes coding for five candidate Eya1 interactants (Garre1, Msh6, Pias4, Smarce1 and Zmym3) in *Xenopus laevis* are consistent with roles in the development of cranial sensory neurons, possibly in cooperation and/or interaction with Eya1. Even though no direct interaction between Eya1 and these candidates could be confirmed, gain and loss of function experiments performed in this study show that Pias4 and Smarce1 have important functions in sensory neurogenesis, with both proteins being required for the differentiation of sensory neurons and Pias4 potentially playing an additional role in neuronal progenitor formation.

# Chapter 1. Introduction

## 1.1. The vertebrate "New Head"

In 1983 Carl Gans and Glen Northcutt formulated the idea that the main innovation of vertebrates was their "New Head" (Gans and Northcutt, 1983; Northcutt and Gans, 1983): the concentration of sophisticated, paired sensory organs on the anterior part of the head constitutes a novelty that distinguishes the vertebrates from other chordates, and is related to the emergence of an active predatory lifestyle. These novel structures include paired eyes, ears, olfactory and gustatory systems, the lateral line system in fishes and amphibians, and a series of cranial nerves and ganglia (Gans and Northcutt, 1983; Northcutt and Gans, 1983). The craniofacial skeleton, encapsulating the brain and supporting the cranial sensory structures, is also a novel feature of the vertebrate head. At the embryological level, it has been shown that these sensory structures arise mainly from two ectodermal cell populations, that are also specific to vertebrates: the neural crest and cranial placodes (Gans and Northcutt, 1983; Glenn Northcutt, 2005; Northcutt and Gans, 1983) (reviewed in Koontz et al., 2023).

The neural crest is a population of embryonic stem cells that delaminate from the roof plate of the neural tube during neurulation and migrate throughout the body, differentiating into multiple cell types and contributing to a wide array of structures, such as most neurons and glia of the peripheral nervous system, craniofacial skeleton and connective tissues, endothelial cells in blood vessels, cardiac tissues, endocrine glands (e.g. chromaffin cells of the adrenal medulla) and pigment cells (melanocytes) (reviewed in Baker and Bronner-Fraser, 2001; Dupin et al., 2018; Le Douarin and Kalcheim, 1999; Park and Saint-Jeannet, 2010; Rothstein et al., 2018; Schlosser, 2006, 2010; Simoes-Costa and Bronner, 2015).

Cranial placodes are discrete, transient thickenings emerging from the coalescence and apicobasal elongation of ectodermal cells within a common horseshoe-shaped precursor domain, the pre-placodal ectoderm (PPE), surrounding the anterior neural plate and neural crest domain after gastrulation. These placodes undergo

morphogenetic processes like invagination or sprouting, and like neural crest cells, placodal cells are able to delaminate from their epithelium, to migrate and to differentiate into a variety of cell types, mainly contributing to the formation of the cranial sensory organs and ganglia (reviewed in Baker and Bronner-Fraser, 2001; Park and Saint-Jeannet, 2010; Schlosser, 2006, 2010). An overview of cranial placodes and a brief description of their derivatives is provided in the next section. For an extensive work on sensory/neuronal differentiation and cranial placodes development and evolution, see (Schlosser, 2021a; Schlosser, 2021b).

## 1.2. Cranial placodes and their derivatives

Cranial placodes include in most vertebrates the adenohipophyseal, olfactory, lens, profundal and trigeminal placodes, a series of epibranchial placodes, the otic placode, and a series of lateral line placodes (Fig. 1.1).

The unpaired adenohipophyseal placode is, together with the lens placode, the only non-neurogenic cranial placode. It is located in the most anterior part of the ectoderm, rostral to the mouth, and gives rise to the rostral lobe of the pituitary gland, or adenohipophysis (reviewed in Davis et al., 2013; Rizzoti and Lovell-Badge, 2005; Zhu et al., 2007). This gland regulates many physiological processes, like stress, lactation, growth and reproduction, through the release of different classes of hormones (Norris and Carr, 2021).

The olfactory placode produces the primary chemosensory neurons, supporting cells and mucus-producing cells of the olfactory and vomeronasal epithelia, that are specialized in the detection of odors and pheromones, respectively (Buck, 2004; Couly and Le Douarin, 1985; Hansen and Zeiske, 1993; Klein and Graziadei, 1983; Touhara and Vosshall, 2009). Some cells delaminate from the olfactory epithelium to colonize regions of the forebrain, where they control the gonadotropin release from the pituitary gland through the production of Gonadotropin Releasing Hormone (GnRH) (elAmraoui and Dubois, 1993; Northcutt and Muske, 1994; Yamamoto et al., 1996) (reviewed in Schwarting et al., 2007; Wray, 2010).

The lens of the eye arises from the lens placode. Following its invagination into a lens vesicle, its outer cells will form the lens epithelium, while the inner lens fiber cells will accumulate crystalline and fill the lens vesicle (reviewed in Chow and Lang, 2001; Cvekl and Duncan, 2007; Cvekl and Zhang, 2017; Kondoh, 2008; Lovicu and McAvoy, 2005; Medina-Martinez and Jamrich, 2007).

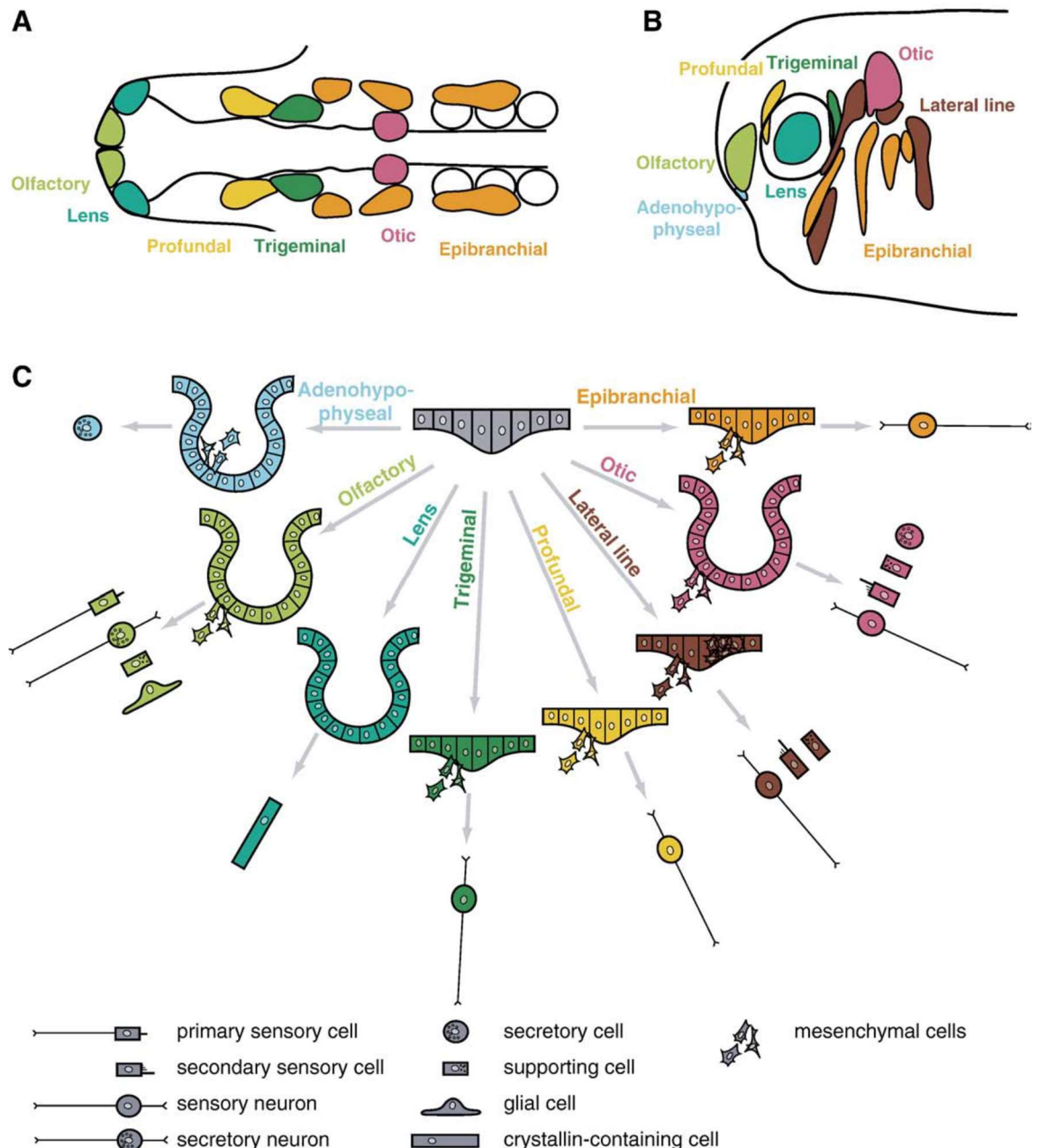
The somatosensory neurons of the profundal and trigeminal ganglia, that receive sensory inputs relating to temperature, touch and pain in the head, are formed in part by neural crest cells, and in part by migratory cells that delaminate from the profundal and trigeminal placodes (Ayer-Le Lievre and Le Douarin, 1982; Begbie et al., 2002; D'Amico-Martel and Noden, 1983; Hamburger, 1961; Noden, 1980a, b; Schlosser and Northcutt, 2000).

In fishes and amphibians, the lateral line system is composed of a series of small mechanosensory organs running along each side of the body, that allow the animal to detect weak water movements via hair cells. In some species, the lateral line also bears modified hair cells that act as electroreceptors, enabling the detection of electric fields. These hair cells, along with the somatosensory neurons innervating them and supporting cells, arise from the lateral line placodes (reviewed in Ghysen and Dambly-Chaudiere, 2004; Gibbs, 2004; Ma and Raible, 2009; Piotrowski and Baker, 2014; Schlosser, 2002).

The otic placode forms both the auditory and vestibular parts of the inner ear. These include specialized hair cells, supporting cells, and endolymph-producing cells. The somatosensory neurons of the vestibulocochlear ganglia, which innervate the hair cells, are also derived from the otic placode (reviewed in Alsina et al., 2009; Bok et al., 2007; Fekete and Wu, 2002; Magarinos et al., 2012; Maier et al., 2014; Whitfield, 2015; Wu and Kelley, 2012).

The epibranchial placodes produce viscerosensory neurons that contribute to the ganglia of the facial, glossopharyngeal and vagal nerves, and that receive input from the visceral organs and gustatory information from the taste buds in the mouth cavity (reviewed in Harlow and Barlow, 2007; Krimm, 2007; Ladher et al., 2010; Northcutt, 2004).

Other types of placodes are specific to some taxa: hypobranchial placodes can be found in some amphibians and generate sensory neurons whose function is unknown (Schlosser, 2003; Schlosser and Northcutt, 2000). The paratympanic placode gives rise to the paratympanic organ and its afferent neurons. This mechanosensory organ can be found in the middle ear of birds, and may provide barometric perception (O'Neill et al., 2012).



**Fig. 1.1.** Cranial placodes in and their cellular derivatives in vertebrates. (A) Dorsal view of 10-13 somite chick embryo (modified from Streit, 2004). (B) Lateral view of tailbud stage *Xenopus* embryo (modified from Schlosser and Northcutt, 2000). (C) Cranial placodes morphogenesis and cellular derivatives (modified from Schlosser, 2005). Adenohypophyseal, olfactory, lens and otic placodes undergo invagination. Epithelial-mesenchymal transition (EMT) occurs in all placodes, except the lens placode.

### 1.3. Induction of the ectodermal territories

In the early neurula, the neural plate that will fold and become the neural tube during neurulation is the most dorsal/medial ectodermal territory. It is flanked laterally along its anterior-posterior axis by the neural crest domains, and the pre-placodal ectoderm (PPE) surrounds both the neural plate and the neural crest domains anteriorly. The rest of the ectoderm (the most ventral/lateral part) constitutes the epidermis.

These ectodermal territories are established during gastrulation. The first step in the determination of ectodermal cell fates is a process called neural induction: dorsally, signals coming from the organizer (a signaling center in the prospective dorsal mesoderm) commit the dorsal ectoderm to a neural fate (Ozair et al., 2013; Rogers et al., 2009; Stern, 2006). These signals are antagonists of bone morphogenetic proteins (BMPs), antagonists of wingless/integrated proteins (Wnts), and fibroblast growth factors (FGFs). The ventral ectoderm, where these signals are absent, is committed to a non-neural fate by BMP signaling (Fig. 1.2).

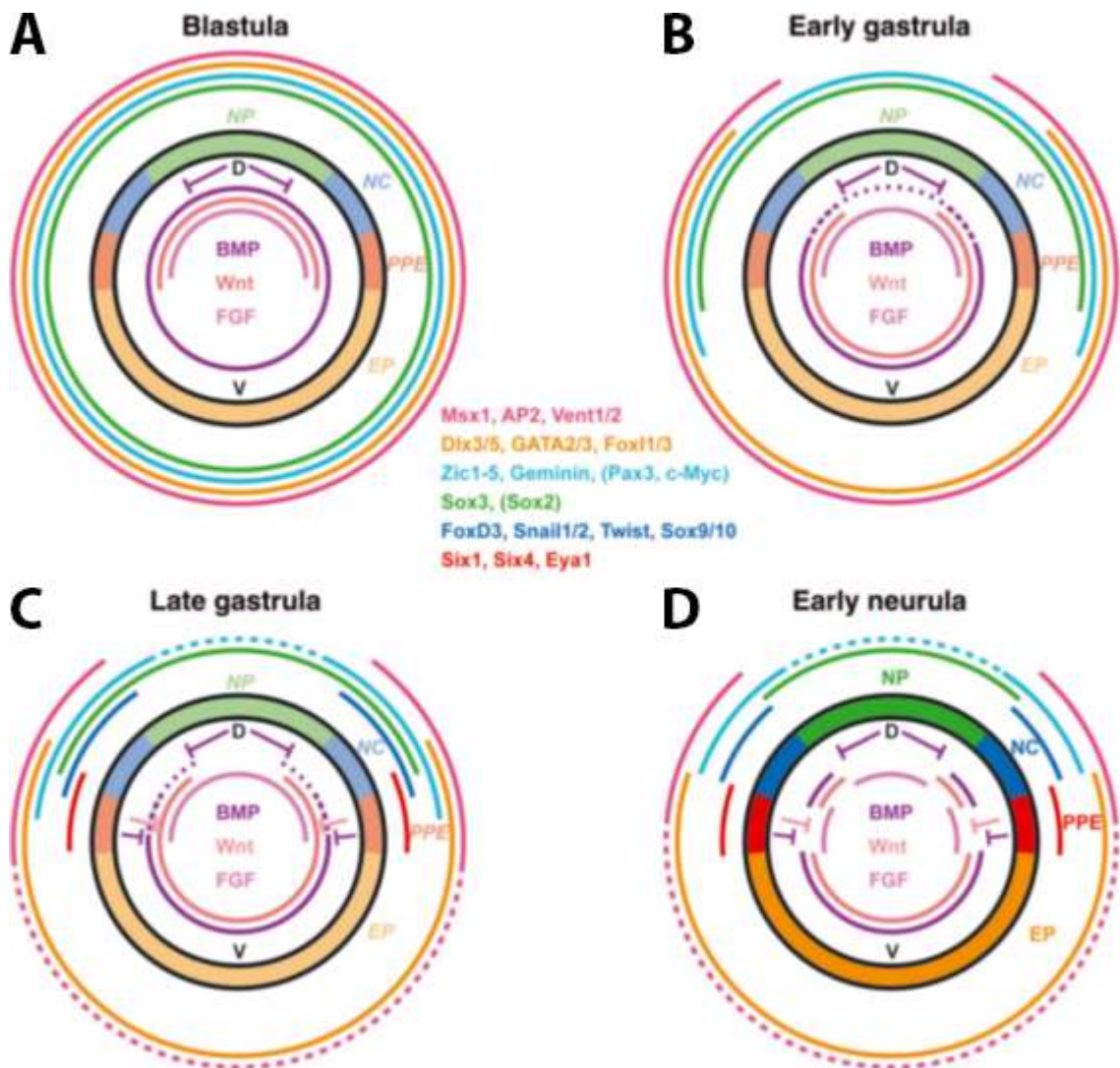
As a result of this dorsal signaling, transcription factors that were initially expressed in the entire ectoderm of the blastula, have their expression domains progressively restricted to the dorsal or ventral side during gastrulation. The dorsal transcription factors include *Sox2*, *Sox3*, *Geminin*, and *Zic1-5*, whose expression is repressed by BMP, while BMP induces the expression of *Dlx3/5*, *GATA2/3*, *Foxl1/3*, *Msx1*, *AP2*, and *Vent1/2* on the ventral side (Feledy et al., 1999; Friedle and Knochel, 2002; Kwon et al., 2010; Mizuseki et al., 1998; Suzuki et al., 1997).

As gastrulation proceeds, the region of overlap between the dorsal and ventral transcription factors becomes progressively smaller, and will become the so-called neural plate border region, which is flanked dorsally/medially by the neural plate (defined by *sox2/sox3* expression), and ventrally/laterally by the epidermis (reviewed in Grocott et al., 2012; Saint-Jeannet and Moody, 2014; Schlosser, 2010).

Within the neural plate border region, the most medial territory, expressing *zic* genes, will display the neural competence characteristic of the dorsal ectoderm and form the neural crest (Pieper et al., 2012). Active Wnt signaling, low level BMP signaling and FGF

signaling are required to establish this territory. Other transcription factors, like Pax3 and c-Myc, will be upregulated there, and finally neural crest specifiers (FoxD3, Snail1/2, Twist, Sox9/10) will be induced (Bellmeyer et al., 2003; Hong and Saint-Jeannet, 2007; Milet et al., 2013; Monsoro-Burq et al., 2005; Sato et al., 2005).

The most lateral territory of the neural plate border region is also influenced by Wnt and BMP inhibition, and FGF signaling. While this territory, which will form the PPE, requires FGF like the medially adjacent neural crest, it is repressed by BMP and Wnt signaling in contrast to the neural crest territory. Similar to the laterally adjacent epidermis, the PPE expresses *dlx*, *gata* and *foxl* genes and displays non-neural competence (Ahrens and Schlosser, 2005; Brugmann et al., 2004; Hong and Saint-Jeannet, 2007; Litsiou et al., 2005; Matsuo-Takasaki et al., 2005; Pieper et al., 2012). Retinoic acid (RA) signaling also intervenes to restrict the posterior boundary of the PPE, which as opposed to the neural crest, is confined to the head region (Dubey et al., 2018). The PPE is characterized by the expression of genes coding for Six1/4 and their cofactors of the Eya family.



**Fig. 1.2.** Establishment of ectodermal territories in early development. Schematic cross sections through the cranial region of *Xenopus* embryos (D, dorsal; V, ventral). The regions that will give rise to neural plate (NP), neural crest (NC), preplacodal ectoderm (PPE), and epidermis (EP) are shown as fate map for blastula and gastrula stages (a–c: faint colors) and as specified territories for early neurula stages (d: strong colors). Expression domains of transcription factors are represented as colored lines around the cross sections. Hatched lines represent downregulations. Transcription factors in parentheses only get upregulated in the respectively colored domains during gastrulation (Pax3 and c-Myc: lateral part of the turquoise domain; Sox2: green domain). Colored lines inside the schematic cross sections show the BMP, Wnt and FGF signaling activities along the dorsoventral axis, with graded activity of BMP and position of sources of BMP inhibitors and Wnt inhibitors indicated (bars) (adapted from Schlosser, 2014).

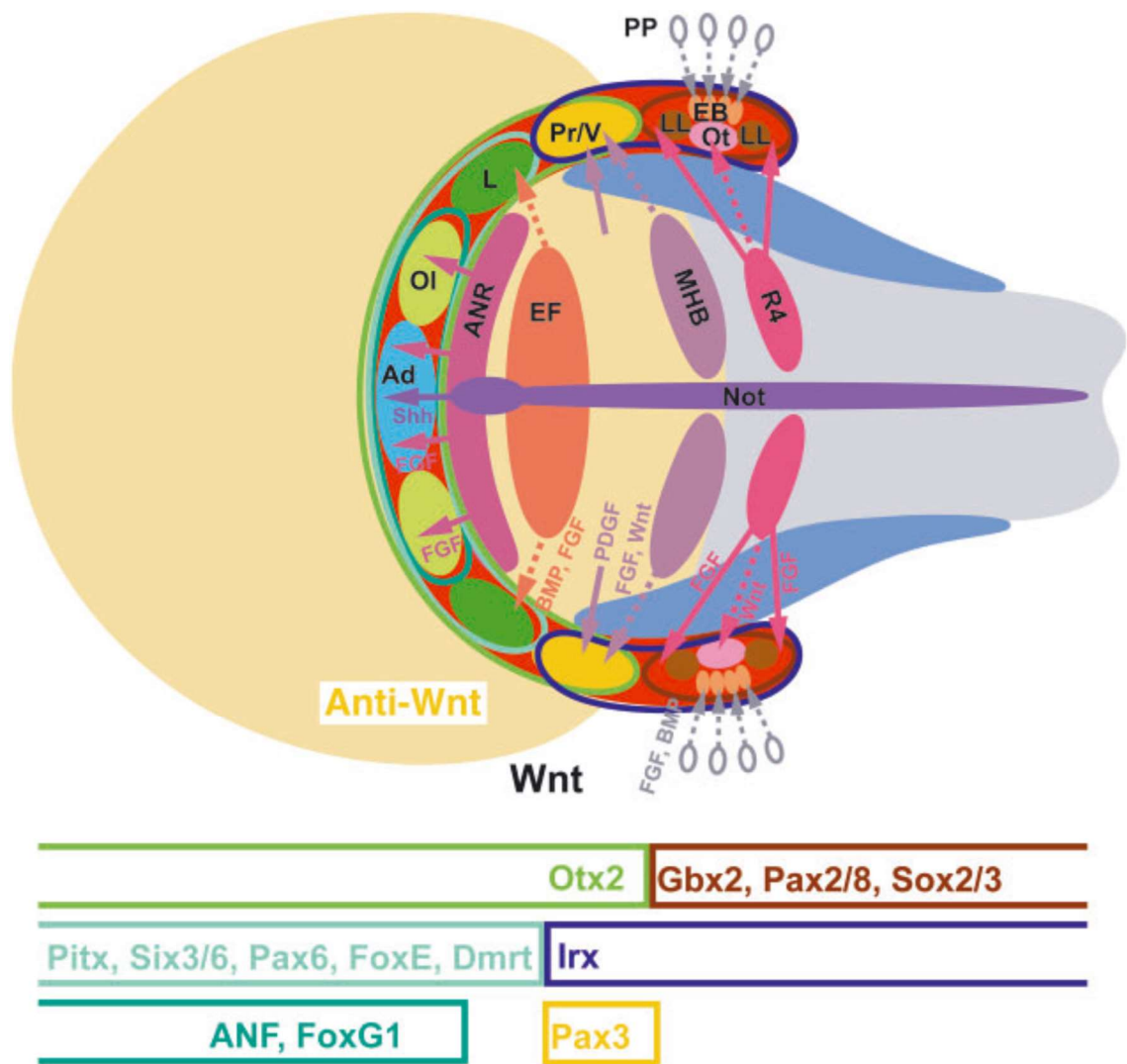
## 1.4. Placode segregation

As mentioned in (1.3), in neural plate stage *dlx*, *gata* and *foxl* genes are expressed in the most lateral territory of the neural plate border, that gives rise to the PPE. However, these genes are not specific to the PPE, being also expressed in more ventral ectodermal territories. On the other hand the expression of genes of the *eya* family and genes of the *six1/2* and *six4/5* subfamilies is restricted to the PPE, and is maintained in all placodes as their development proceeds (Bessarab et al., 2004; Chen et al., 2009; Ikeda et al., 2007; Konishi et al., 2006; Schlosser and Ahrens, 2004; Zou et al., 2004). Moreover placode development is compromised after mutation or knockdown of genes of the *eya* and *six* families (see section 1.5). *Eya* and *six* genes seem to establish the PPE as the common ground state for all placodes, conferring to the derivatives of this area general placodal properties (morphogenetic movements of epithelia, high levels of proliferation, ability for the cells to change shape, delaminate and migrate, neurogenicity). From that common ground, placodes will subsequently progressively segregate and specialize (reviewed in Grocott et al., 2012; Saint-Jeannet and Moody, 2014; Schlosser, 2010).

First an anterior-posterior regionalization of the PPE is driven by differential Wnt, FGF and RA signaling, promoting the expression of transcription factor genes like *gbx2* and *irx1* in the posterior region, while the anterior PPE expresses *otx2* and *fezf* (Braun et al., 2003; Kiecker and Niehrs, 2001; Lecaudey et al., 2005; Li et al., 2009; Niehrs, 2010; Nordstrom et al., 2006; Petersen and Reddien, 2009; Schlosser, 2006). Mutual cross-repression between these anterior and posterior transcription factors sharpens the border between these two regions. *Otx2* has been shown to be required for the development of anterior placodes (olfactory, lens and trigeminal placodes), while *Gbx2* is required for the development of the more posterior otic and epibranchial placodes (Steventon et al., 2012).

The PPE is then further subdivided by signals from the adjacent endomesoderm and neural plate. An extended anterior placodal area is induced by neuropeptides (somatostatin, nociceptin) (Lleras-Forero et al., 2013) and defined by the expression of *pitx*, *six3/6*, *pax6*, *foxE*, *dmrt*, *anf* and *foxg1*. Within this area, Shh, FGF and BMP signaling will induce the formation of the adenohipophyseal, olfactory and lens placodes,

respectively (Schlosser, 2006, 2010; Toro and Varga, 2007). The posterior placodal area, expressing *pax2/8* and *sox2/3*, is the territory of the presumptive otic, lateral line and epibranchial placodes, induced by differential Wnt, FGF and BMP signaling (Ladher et al., 2010; Schlosser, 2006). Finally, between the anterior and posterior placodal areas, Wnt, FGF and PDGF signaling will induce the development of the profundal placode, defined by *pax3* expression, and the trigeminal placode (Canning et al., 2008; Lassiter et al., 2007; McCabe and Bronner-Fraser, 2008).



**Fig. 1.3.** Signaling pathways and transcription factors involved in placode specification at neural plate stage. The PPE is represented by the red area; within the PPE colored outlines demarcate multiplacodal areas, and colored ovals indicate individual placodes. The expression areas of some transcription factors are represented below. Their expression is induced by signals (arrows) coming mostly from the mesoderm and neural plate. Hatched arrows: signaling events occurring post-neural stage. Ad, adenohipophyseal placode; ANR, anterior neural ridge; EB, epibranchial placodes; EF, eye field; L, lens placode; LL, lateral line placodes; MHB, midbrain–hindbrain boundary; Not, notochord; Ol, olfactory placode; Ot, otic placode; PP, pharyngeal pouches; Pr/V, profundal/trigeminal placode; R4, rhombomere 4. (From Schlosser, 2014) (modified from Schlosser, 2014).

## 1.5. Six1 and Eya1

Six1 and its cofactor Eya1 are essential for the establishment and maintenance of the PPE, and they are of particular importance in coordinating the subsequent development of placodes, including in the regulation of the balance between cell proliferation and neuronal/sensory differentiation.

### 1.5.1. Six1

*Six* genes code for evolutionarily conserved transcription factors bearing a DNA binding homeodomain, and a N-terminal Six domain involved in protein-protein interactions with transcriptional coactivators (e.g. proteins of the Eya family) or corepressors (e.g. Dach and Groucho) (Fig. 1.4) (Brugmann et al., 2004; Christensen et al., 2008; Ikeda et al., 2002; Kawakami et al., 2000; Kobayashi et al., 2001; Kumar, 2009; Lopez-Rios et al., 2003; Ohto et al., 1999; Patrick et al., 2013; Pignoni et al., 1997; Silver et al., 2003; Weasner et al., 2007; Zhu et al., 2002). Several *six* genes, namely *six1/2* and *six4/5*, are expressed in the PPE, and their expression is maintained in all placodes (except the lens placode in *Xenopus*) as development proceeds (Cvekl and Duncan, 2007; Ghanbari et al., 2001; Kumar, 2009; Pandur and Moody, 2000; Schlosser, 2006; Zuber et al., 2003).

*Six1* is the most studied gene of this family, and its role in the formation of the PPE and in placode development is best understood. Its homologue in *Drosophila*, *sine oculis (so)*, is the first *six* gene whose mutations have been identified and characterized, and is crucial for compound eye development. Interactions between Six and cofactors such as members of Eya, Dach and Groucho families have been reported in *Drosophila* as well as in vertebrates, and the conserved Pax-Six-Eya-Dach gene regulatory network is studied for its roles in cell proliferation and movements, in developmental contexts as well as in cancer (Chen et al., 1997; Cheyette et al., 1994; Fabrizio et al., 2003; Halder et al., 1998; Hanson, 2001; Kawakami et al., 2000; Kozmik et al., 2007; Kumar and Moses, 2001; Niimi et al., 1999; Pappu et al., 2005; Pignoni et al., 1997; Punzo et al., 2002).

In *Xenopus*, knockdown of *six1* results in a reduction of the PPE, concomitant with an expansion of the neural plate, neural crest and epidermis, while *six1* overexpression

leads to an expansion of the PPE and a reduction of the neural crest and epidermis (Brugmann et al., 2004). It has been shown that Six1 transcriptionally represses neural crest (*foxd3*) and epidermal genes (*keratin*), and activates PPE genes (*eya1*, *sox11*), which indicates that Six1 promotes a placodal fate in its expression domain, at the expense of the other ectodermal territories (Brugmann et al., 2004).

### 1.5.2. Eya1

Like *six1*, *eya* genes were first identified and studied in *Drosophila*, in which *eya* (*eyes absent*) is an essential gene for eye formation, that controls cell survival and differentiation in the developing eye, and is able to induce ectopic eyes when ectopically expressed (Bonini et al., 1997; Bonini et al., 1993; Renfranz and Benzer, 1989).

Eya proteins bear an N-terminal transactivation domain, and a C-terminal Eya domain that binds transcription factors, most notably members of the Six1/2 and Six4/5 families in vertebrates. The N-terminal and C-terminal domains also display a threonine- and tyrosine phosphatase activity, respectively (Fig. 1.4) (Jemc and Rebay, 2007; Li et al., 2017; Merk et al., 2020; Rayapureddi et al., 2003; Rebay et al., 2005; Tadjuidje and Hegde, 2013; Tootle et al., 2003).

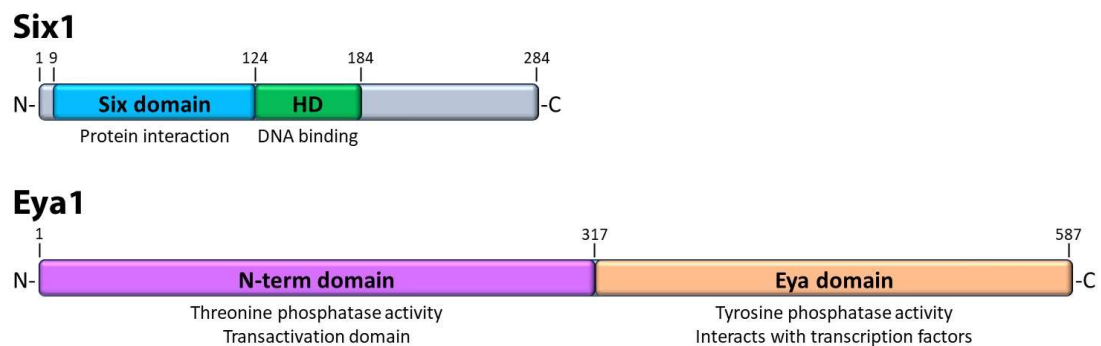
In *Xenopus* *eya1* is the most studied *eya* gene. It is expressed in the PPE, playing important roles for its induction and for subsequent placode development in conjunction with *six1*. Like *six1* its expression is maintained in placodal derivatives (David et al., 2001) (reviewed in Jemc and Rebay, 2007; Schlosser, 2006, 2010).

Eya1 has been shown to be translocated in the nucleus by Six1, where it acts as its transcriptional co-activator (Ohto et al., 1999; Zhang et al., 2004); when Eya1 is associated with non-Six cofactors, its tyrosine phosphatase activity may modulate their transcriptional activity. For example Dach acts as a strong repressor when only associated with Six, but seems to act as an activator when associated with Eya1 in a Six-Eya-Dach complex (Li et al., 2003).

Eya proteins play additional roles in the cytoplasm, mediated by their phosphatase activity (Jemc and Rebay, 2007; Tadjuidje and Hegde, 2013). For instance cytoplasmic

EYA4 plays a role in innate immunity in mice (Okabe et al., 2009), and cytoplasmic EYA3 promotes cell motility (Pandey et al., 2010). Cytoplasmic Eya1 has been shown to play roles in cell division, by controlling cell polarity and coordinating spindle orientation, via its interaction with aPKC and Gαi (El-Hashash et al., 2011; Merk et al., 2020).

In humans, mutations of *EYA1* (or *SIX1*) can impair the development of placodal derivatives, and lead to branchio-oto-renal (BOR) syndrome, characterized by hearing loss and chronic kidney failure caused by craniofacial and renal malformations (Abdelhak et al., 1997; Kochhar et al., 2007; Ruf et al., 2004).



**Fig. 1.4.** Domain structures of Six1 and Eya1 (*Xenopus laevis*). Numbers represent the amino acid number. C, C-terminus; N, N-terminus; HD: homeodomain.

### 1.5.3. Roles in placode development

It is known that Six1 and Eya1 are important for inducing and conferring general placodal properties to the PPE, and for subsequent placode development, however their mode of action is not fully understood. *six1* and *eya1* expression in the PPE is required for the expression and maintenance of the other PPE genes. However, ectopic expression of *six1* or *eya1* in the non-neural ectoderm can trigger the expression of some, but not all PPE markers, indicating that Six1 and Eya1 are not sufficient for PPE formation and other factors are also at play (Brugmann et al., 2004; Christophorou et al., 2009).

Beyond their role in PPE specification and maintenance, Six1 and Eya1 have the ability to confer generic placodal properties to the PPE derivatives, related to morphogenesis, cell survival, proliferation, and neuronal and sensory differentiation. Indeed the

morphogenetic properties of placodes (invagination of epithelia, and delamination of neurons) are impaired after *six1* or *eya1* loss of function (Bosman et al., 2009; Chen et al., 2009; Friedman et al., 2005; Johnson et al., 1999; Kozlowski et al., 2005; Laclef et al., 2003; Li et al., 2003; Ozaki et al., 2004; Xu et al., 1999; Zheng et al., 2003; Zou et al., 2008; Zou et al., 2004; Zou et al., 2006), while elevated levels of *six1* or *eya1* expression have been associated with increases in EMT, cell movement, and formation of metastases in some cancers (Farabaugh et al., 2012; McCoy et al., 2009; Micalizzi et al., 2009; Pandey et al., 2010; Patrick et al., 2013; Yu et al., 2006; Yu et al., 2004). Concerning cell survival, it has been shown with loss-of-function experiments that SIX1 and EYA1 display an anti-apoptotic role in placodes, and it has been suggested that for EYA1, this anti-apoptotic activity is mediated by its ability to dephosphorylate the histone variant H2AX, which indirectly promotes DNA damage repair (Cook et al., 2009; Krishnan et al., 2009).

The roles of Six1 and Eya in proliferation and differentiation will be discussed more extensively in section 1.6.3.

## 1.6. Regulation of placodal neurogenesis

Even though the nervous system of vertebrates is composed of many different cell types that are intricately organized, the general features of neuronal and sensory differentiation are largely shared between different types of neurons or sensory cells, and they rely on a generic neuronal core network with SoxB1 and proneural bHLH transcription factors as key actors, both in the central and peripheral nervous systems. In this section I will overview the roles of SoxB1 and proneural bHLH factors, then I will focus on how Six1 and Eya1 regulate the generic neuronal core network in the specific context of placodal neurogenesis.

### 1.6.1. SoxB1 transcription factors

In vertebrates, SoxB1 transcription factors, which include Sox1, Sox2 and Sox3, are a subfamily of HMG-box containing transcription factors that bias (for Sox2 and Sox3) the prospective neural plate towards a neural fate during gastrulation, and are subsequently downregulated in the differentiating neurons of the central nervous system (CNS) during neurulation, while their expression is maintained in neural progenitor cells (Bergsland et al., 2011; Mizuseki et al., 1998; Okuda et al., 2010; Pieper et al., 2012; Rogers et al., 2009). The same happens in the PPE, where *sox2* and *sox3* are expressed: their expression is maintained in the placodal proliferating progenitors, but not in the differentiating neurons and sensory cells (Abu-Elmagd et al., 2001; Donner et al., 2007; Hernandez et al., 2007; Ishii et al., 2001; Kawauchi et al., 2004; Nikaido et al., 2007; Rex et al., 1997; Riddiford and Schlosser, 2017; Schlosser and Ahrens, 2004; Schlosser et al., 2008; Sun et al., 2007; Wood and Episkopou, 1999). Whether in the developing CNS or in the PPE and its derivatives, SoxB1 proteins play two central roles: they keep cells in which they are expressed in a proliferative and undifferentiated progenitor state, inhibiting their differentiation, and concurrently they bias their ultimate differentiation towards a neuronal or sensory fate (reviewed in Julian et al., 2017; Kondoh and Kamachi, 2010; Maucksch et al., 2013; Miyagi et al., 2009; Pevny and Placzek, 2005; Pevny and Nicolis, 2010; Sarkar and Hochedlinger, 2013; Shimosaki, 2014; Wegner, 2010; Wegner and Stolt, 2005; Zhang and Cui, 2014). This differentiation can occur only after *soxB1* genes are downregulated. It must be noted that *soxB1* genes are not expressed in the neural crest, and that the differentiation of neural crest cells thus depends on other factors.

SoxB1 transcription factors seem to have the ability to maintain cells in a progenitor state by two ways. First, they can directly activate the expression of genes involved in the maintenance of a progenitor state. These comprise *cyclinD1*, a key actor of the cell cycle progression; components of the Shh and EGFR signaling pathways; and other genes known to play a role in progenitor maintenance, including *sox2* itself (Aguirre et al., 2010; Bergsland et al., 2011; Chen et al., 2008; Favaro et al., 2009; Hagey and Muhr, 2014; Holmberg et al., 2008; Hu et al., 2010; Rogers et al., 2009; Shimosaki et al., 2012; Surzenko et al., 2013; Takanaga et al., 2009; Tomioka et al., 2002). Second, SoxB1 factors

can also directly promote the expression of genes involved in the Notch signaling pathway (the Notch receptor, its ligands and/or Hes proteins), thus inhibiting neuronal differentiation (Agathocleous et al., 2009; Bani-Yaghoub et al., 2006; Bergsland et al., 2011; Matsushima et al., 2011; Panaliappan et al., 2018; Surzenko et al., 2013; Takanaga et al., 2009; Taranova et al., 2006; Zhou et al., 2016).

SoxB1 factors have also been shown to be required for the acquisition of neuronal and sensory fates in the CNS as well as in placodes. Several different mechanisms are at play: thanks to their chromatin remodeling capabilities, SoxB1 factors act as pioneer factors, making the regulatory regions of neural genes accessible for other transcription factors (Bergsland et al., 2011); they also directly promote the expression of bHLH factors (Ahmed et al., 2012a; Ahmed et al., 2012b; Amador-Arjona et al., 2015; Bergsland et al., 2011; Neves et al., 2012; Zhou et al., 2016) (see section 1.6.2); and they modulate the activity of signaling pathways (Kuwabara et al., 2009; Zhou et al., 2016).

These are general modes of action of the SoxB1 factors, but their activity is highly context-specific. Not all cells expressing *soxB1* genes will become neurons or sensory cells, indicating that cooperation with other factors is crucial for biasing cells towards their specific fates (Dee et al., 2008; Puligilla et al., 2010; Rogers et al., 2009; Schlosser et al., 2008). The effects of SoxB1 factors are also dosage-dependent: in the mouse brain, retina, and otic placode, it has been shown that different levels of SoxB1 correspond to different roles, with the highest levels promoting neural stem cells with low proliferation rates, lower levels promoting high proliferation and favouring early stages of differentiation, and the lowest levels characterizing differentiated cells (Cavallaro et al., 2008; Dabdoub et al., 2008; Hagey and Muhr, 2014; Taranova et al., 2006). This can account, at least partially, for how the transition between the distinct roles of SoxB1 factors in proliferation versus differentiation is controlled.

The interplay between the pioneering abilities of the different Sox factors, their differential chromatin remodeling and DNA binding abilities, and the context-dependent availability of cofactors, could also partially account for how the transition is regulated, as different sets of genes are sequentially activated according to how accessible their regulatory region is made for the transcriptional machinery, and which factors are present. It has been shown for instance that the activation of genes expressed in the

embryonic stem cells, neural progenitors and differentiating neurons is correlated with the sequential binding of Sox2, Sox3 and Sox11, respectively, to their regulatory regions, in association with histone modifications (Bergslund et al., 2011). However the precise requirements for this orderly sequential activation of genes are still poorly understood.

### 1.6.2. Proneural bHLH transcription factors

Basic helix-loop-helix (bHLH) factors are subdivided into six phylogenetic groups, from A to F (Ledent et al., 2002). Proneural bHLH factors belong to group A, and bind to hexameric sequences called E-boxes (CANNTG) (Murre et al., 1989). In cranial placodes several of them are often expressed, in different combinations depending on the placode (Begbie et al., 2002; Nieber et al., 2009; Schlosser and Northcutt, 2000). Gain and loss of function experiments have shown that proneural bHLH factors are key actors of neuronal and sensory differentiation, being both required and sufficient for it. Indeed differentiation is blocked by knockout mutations of particular proneural bHLH factors in the regions where they are normally expressed (Andermann et al., 2002; Bermingham et al., 1999; Cau et al., 2002; Cau et al., 1997; Chen et al., 2002; Fode et al., 1998; Guillemot and Joyner, 1993; Ma et al., 2000; Ma et al., 1998; Ma et al., 1996; Millimaki et al., 2007; Murray et al., 2003; Sarrazin et al., 2006; Woods et al., 2004). Conversely, overexpression of proneural factors is often sufficient to trigger neuronal or sensory differentiation in regions of ectopic expression or may even change the fate of differentiated cells (although at a low rate if a single proneural factor is overexpressed) (Berninger et al., 2007; Brulet et al., 2017; Chanda et al., 2014; Guo et al., 2014; Masserdotti et al., 2015; Vierbuchen et al., 2010; Woods et al., 2004; Zhang et al., 2013; Zheng and Gao, 2000). For example, *Ascl1*, *Neurog1/2* or *Neurod1/4* in *Xenopus* embryos can convert non-neural ectoderm into neurons (Lee et al., 1995; Ma et al., 1996; Perron et al., 1999; Talikka et al., 2002).

Several different mechanisms are at play in the ability of proneural bHLH factors to promote neuronal or sensory differentiation. First, they activate the differentiation genes coding for the proteins that are characteristic for neurons or sensory cells (Bertrand et al., 2002; Cau et al., 1997; Chae et al., 2004; Cho and Tsai, 2004; Fode et al.,

1998; Ma et al., 1998; Ma et al., 1996). Some proneural factors can act as pioneer factors, allowing other transcription factors to bind once chromatin is made accessible and directly activate the neuronal or sensory cell genes (Alsina, 2020; Aydin et al., 2019). Second, proneural bHLH factors promote cell cycle exit (Alvarez-Rodriguez and Pons, 2009; Farah et al., 2000; Lacomme et al., 2012; Mizuguchi et al., 2001; Novitch et al., 2001; Ochocinska and Hitchcock, 2009; Politis et al., 2007; Yi et al., 2008), and inhibit the expression of *soxB1* genes (Bylund et al., 2003; Dabdoub et al., 2008; Evsen et al., 2013). Third, by a process called lateral inhibition, they repress neuronal and sensory differentiation in the neighboring cells: proneural bHLH factors activate the expression of ligands of the Notch signaling pathway, that will instruct the adjacent cells to express genes coding for Hes1 and Hes5, which are group D bHLH factors that directly repress the expression of *ascl1*, *neurog1/2* or other proneural genes (Cau et al., 2000; Chen et al., 1997; Davis and Turner, 2001; Dhanesh et al., 2016; Hatakeyama et al., 2004; Ishibashi et al., 1995; Kageyama et al., 2008; Kobayashi and Kageyama, 2014; Ohtsuka et al., 1999; Sasai et al., 1992). As a result, some cells will maintain high levels of proneural proteins and will differentiate into neurons, while their neighbors will maintain a progenitor state. Fourth, beyond their role in promoting the expression of genes coding for the generic neuronal or sensory proteins, proneural factors promote the differentiation of different subtypes of neurons or sensory cells, by driving the activation of different sets of genes (reviewed in Allan and Thor, 2015; Bertrand et al., 2002; Huang et al., 2014). This differential activation is due to different affinities to different E-boxes (Aydin et al., 2019), combined with cooperation with other transcription factors, typically other bHLH proteins or homeodomain proteins (Andersson et al., 2007; Berninger et al., 2007; Cho et al., 2014; Jeong et al., 2006; Lee et al., 2012; Lee and Pfaff, 2003; Ma et al., 1999; Ma et al., 2008; Mazzoni et al., 2013; Mizuguchi et al., 2001; Novitch et al., 2001; Scardigli et al., 2001).

### 1.6.3. Roles of Six1 and Eya1 in cell proliferation and neuronal differentiation

In cranial placodes specifically, the generic neuronal core network is regulated by Six and Eya family members, in particular Six1 and its cofactor Eya1 (reviewed in Grocott et al., 2012; Moody and LaMantia, 2015; Schlosser, 2010; Singh and Groves, 2016; Streit,

2018; Wong et al., 2013; Xu, 2013). A recent screen indicates that *soxB1* genes (*sox2*, *sox3*), proneural genes (*atoh1*, *neurog1*), genes promoting neuronal or sensory differentiation (*pou4f1*, *islet2*, *gfi1*, *tlx1*) and genes encoding Hes repressors (*hes8*, *hes2*, *hes9*) are putative direct targets of Six1 and Eya1 (Riddiford and Schlosser, 2016). Other proneural or neuronal/sensory differentiation genes have also been shown to be direct Six1 targets (Ahmed et al., 2012a; Li et al., 2020).

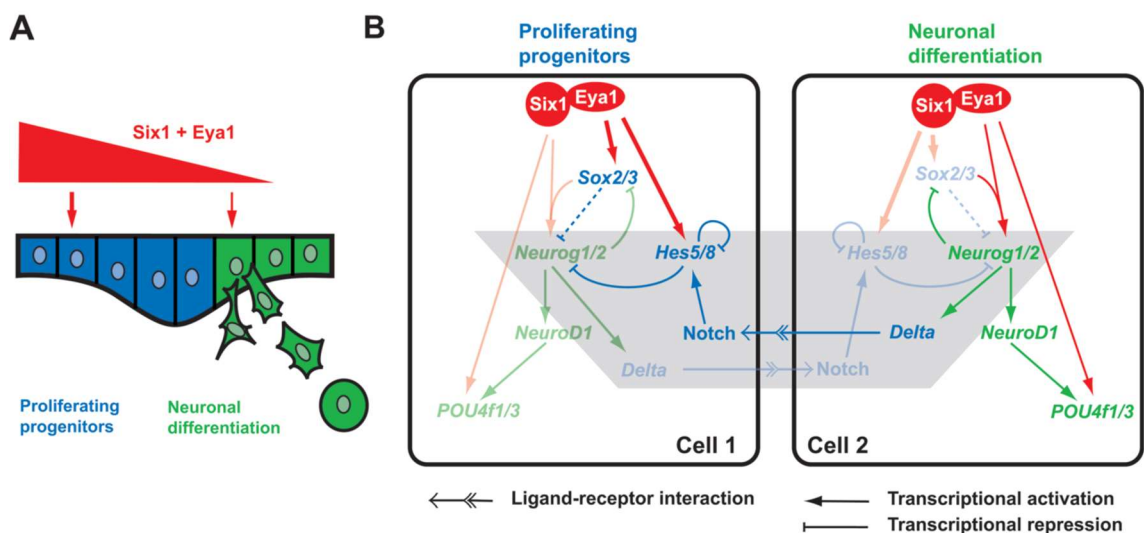
Even though the expression of *soxB1* genes in placodes depends on Six1 and Eya1, *soxB1* genes are not expressed in the entire PPE, but in two subregions: an anterior subregion corresponding to the adenohipophyseal and olfactory placodes, and a posterior subregion corresponding to the profundal/trigeminal, otic, lateral line, and epibranchial placodes. This indicates that additional factors are necessary to activate the expression of *soxB1* genes in the PPE (Schlosser and Ahrens, 2004).

Six1 and Eya1 thus perform two seemingly contradictory functions, promoting progenitor maintenance and neuronal/sensory differentiation in placodes. It has been shown that these effects are strongly dosage dependent (Fig. 1.5): in *Xenopus*, gain and loss of function experiments have shown that high levels of Six1 and Eya1 promote the expression of progenitor genes (*soxB1*, *hes*) and proliferation, while lower levels promote the expression of proneural genes and neuronal differentiation (Riddiford and Schlosser, 2017; Schlosser et al., 2008). This is consistent with what is observed during normal development: *six1* and *eya1* are highly expressed in proliferating, *soxB1*-expressing cells, and their expression level declines in cells that migrate away from placodes and express neuronal differentiation genes (Chen et al., 2009; Schlosser et al., 2008; Zou et al., 2008). However the mechanistic aspects of these dosage dependent effects still have to be elucidated.

Like SoxB1 factors, and in combination with them, Six1 and Eya1 may promote cell proliferation by directly activating cell cycle control genes, such as *cyclin A1*, *cyclin D1* and *c-myc* (Coletta et al., 2004; Coletta et al., 2008; Ford et al., 1998; Li et al., 2003; McCoy et al., 2009; Miller et al., 2010; Pandey et al., 2010; Yu et al., 2006; Zhang et al., 2005). Like SoxB1 factors again, Six1 may act as a pioneer factor: Six1 has been shown to occupy enhancers of its target genes before they are expressed, and it is able to recruit SWI/SNF chromatin remodeling complexes (Ahmed et al., 2012b; Li et al., 2020).

Since Six1 binds to enhancers of differentiation genes for several different placodal cell types prior to their expression, it could act as a competence factor, allowing cells to differentiate into multiple sensory or neuronal cell types, depending on the availability of different cofactors.

Indeed, it has been shown that the ability of Six1 and Eya1 to promote different cell fates is determined by their interaction with different cofactors: Six1-Eya1-Sox2 interactions promote the activation of *atoh1* and otic hair cell development (Ahmed et al., 2012a); Six1-Eya1-Sox2 interactions with the SWI/SNF chromatin remodeling complex promote neuronal differentiation in the inner ear by activating the transcription of *neurog1* and *neurod1* (Ahmed et al., 2012b); Six1 can also interact with many other proteins, including proteins encoded by its own target genes (e.g. Atoh1, Pou4f3, Gfi1, Gata3, Rxf) (Li et al., 2020).



**Fig. 1.5.** Model for regulation of progenitor maintenance and neuronal differentiation in placodal neurogenesis. (A) High levels of Six1 and Eya1 first promote a proliferating progenitor state. When cells migrate away from placodes, declining levels of Six1 and Eya1 promote neuronal differentiation. (B) Six1 and Eya1 interact with genes and proteins involved in progenitor maintenance and neuronal differentiation. In proliferating progenitors, neuronal differentiation genes (green) are repressed by Sox2/3 and Hes5/8 transcription factors (hatched line: indirect repression; solid line: direct repression). In differentiating neurons, Neurog1/2 activate NeuroD1 and POU4f1, promoting neuronal differentiation. Neurog1/2 also activate Delta, which upon binding to a Notch receptor of an adjacent cell, represses neuronal differentiation in that neighbour cell (lateral inhibition pathway, gray area). While high levels of Six1/Eya1 are necessary to activate the target genes that promote progenitor maintenance (thick red arrows), low levels are sufficient to activate the target genes that promote neuronal differentiation (thin red arrows). Sox2/3 alone inhibits neuronal differentiation upstream and downstream (not shown) of Neurog1/2. Sox2/3 in conjunction with Six1/Eya1 poises Neurog1/2 for activation. (Modified from Riddiford and Schlosser, 2017).

## 1.7. *Xenopus laevis* as a model for the study of placodal biology

*Xenopus laevis* is a particularly well-suited animal model for the purpose of studying the development of vertebrate embryonic structures like placodes: similarly to more conventional vertebrate models like mouse and chicken, its genome has been fully sequenced. Moreover it is a robust species, easy to maintain, and capable of producing a large number of embryos on demand. The embryos themselves are large, and develop externally; they are thus easy to manipulate, graft, and inject for gain- and loss-of-function experiments, and their development can be monitored precisely (Wheeler and Brandli, 2009). Because of its long generation time (1-2 years) however, generating transgenic lines is unpractical, and *Xenopus laevis* pseudotetraploid genome can be problematic in terms of gene function redundancy (Beck and Slack, 2001).

## 1.8. Aim of the project

Six1 and its cofactor Eya1 are key regulators of sensory neurogenesis in placodes, where they affect the balance between progenitor maintenance, cell proliferation and neuronal/sensory differentiation, and modulate the generic neuronal core network constituted by *soxB1* and other progenitor promoting genes, as well as proneural *bhlh* genes. However very little is currently known about how Eya1 exerts its different functions during sensory neurogenesis and how the important balancing act between progenitor maintenance and differentiation is regulated. The aim of my project is to investigate whether and how potential Eya1 cofactors contribute to its different functions for sensory neurogenesis in the placodes, possibly helping to control the balance between proliferation and differentiation that is regulated by Eya1/Six1.

The first part of this project, presented in Chapter 3, consists in a yeast two-hybrid screening analysis, from which promising potential Eya1 cofactors will be selected. The expression patterns of these candidates were characterized by *in situ* hybridization in *Xenopus laevis* embryos at various developmental stages, in order to determine whether Eya1 and its candidate partners are expressed in overlapping and/or contiguous area, and as a first step in assessing their potential functions.

In the second part of the project (chapter 4), a confirmation of the physical interaction between some of these candidates and Eya1 were attempted, by several methods. First, co-immunoprecipitations followed by western blotting were performed on protein extracts from *Xenopus laevis* embryos co-injected with mRNAs coding for Eya1 and for tagged versions of candidate partners. Second, one-by-one yeast two-hybrid solid growth tests between Eya1 and two candidate interaction partners, Pias4 and Smarce1, were performed to confirm the interactions identified in the two-hybrid screening. Third, the outcome of a co-immunoprecipitation involving Eya1 and the same two candidates followed by mass spectrometry were presented.

In the third part of the project (chapter 5), the roles of these two candidates in sensory neurogenesis were investigated by gain- and loss-of-function experiments. The phenotypes of embryos injected with either mRNAs coding for Pias4 or Smarce1, or with morpholinos preventing their translation, were analysed by *in situ* hybridization, using placodal (*eya1*, *six1*, *sox3*), neural crest (*foxd3*) and neuronal differentiation markers (*neurog1*, *neurog2*, *hes5.4*, *neurod1*, *tubb2b*).

## Chapter 2. Materials and Methods

### 2.1. Animals

The African clawed frog *Xenopus laevis* was my model organism for this study. Frogs were purchased from either Nasco (Fort Atkinson, WI, USA) or the European Xenopus Resource Centre (EXRC, Portsmouth, UK). Animal experiments were conducted in accordance with Irish and European legislations, approved by the NUI Galway Animal Care Research Ethics Committee (ACREC) and covered under the project license (AE19125/P098) to Dr Gerhard Schlosser.

#### 2.1.1. Induction of egg laying

Egg laying was induced by injection of human Chorionic Gonadotropin (hCG) into the dorsal lymph sac of female frogs. Each female was primed with 50 units hCG 5 to 15 days prior to egg laying, injected with 700 units approximately 16 hours prior to egg laying, and housed individually overnight in tank water at 16.5 °C until egg laying.

#### 2.1.2. In vitro fertilization

The next morning, females were transferred to 1x MBSH at room temperature, and eggs were collected regularly into large Petri dishes. Males were anaesthetised in 0.1% tricaine methanesulfonate (MS222) diluted in tap water (pH brought to around 7) for 5 minutes, then testes were collected and stored in MBSH at 4 °C (for up to two weeks), and the cadaver was frozen. Small pieces of testes were macerated with forceps and incubated with eggs for 10 minutes, then sperm were activated by the addition of 0.1x MBS to the Petri dish. After about 20 minutes, once the eggs were fertilised (as indicated by upward-facing pigmented animal poles), jelly coats were removed by a cysteine treatment (2% in 0.1x MBS, pH 8) for 6-8 minutes, then cysteine was removed by 5 washes in 0.1x MBS. Embryos were then incubated on a cold plate at 14 °C and let develop up to the appropriate developmental stage.

## 2.2. Molecular methods

Recipes for solutions are listed in Appendix A.

### 2.2.1. RNA extraction

RNA was extracted from fresh embryos at stages 13, 19, 23, 28 or 33-34 using RNeasy mini kit (Qiagen; cat. no.: 74104), according to manufacturer's instructions.

For each RNA extraction, 5 embryos were homogenised by pipetting in 300 to 700  $\mu$ l buffer RLT. The homogenate was centrifuged at 13,000 rpm for 3 minutes, and the supernatant was transferred to a new tube, and mixed by pipetting after addition of an equivalent volume of 70% ethanol. The mixture was then transferred to an RNeasy spin column placed in a 2 ml collection tube, and centrifuged for 15 seconds at 13,000 rpm. The flow-through was discarded and 700  $\mu$ l of buffer RW1 was added to the column. After another centrifugation for 15 seconds at 13,000 rpm, the flow-through was discarded and 500  $\mu$ l of buffer RPE was added to the column, before a 2 minutes centrifugation at 13,000 rpm. The flow-through was discarded and the column was placed in a new 2 ml collection tube. Then 30  $\mu$ l of RNase free water was added to the column, followed by a one minute centrifugation at 13,000 rpm. The RNA concentration of the extract was then measured photometrically using a NanoDrop, and the extract was stored at -20 °C.

### 2.2.2. cDNA generation

Using RNA extracted from the embryos as template, reverse transcription was performed using QuantiTect reverse transcription kit (Qiagen; cat. no.: 205311), according to manufacturer's instructions.

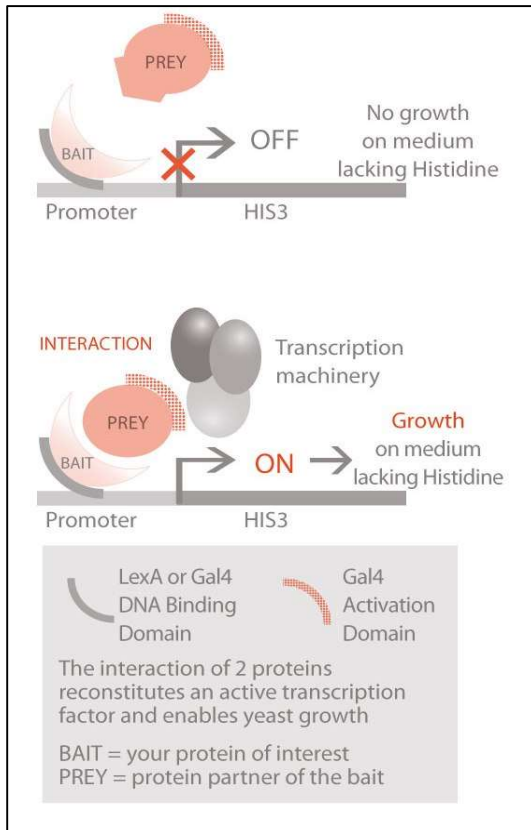
First, the genomic DNA was eliminated from the RNA extractions: 1  $\mu$ g of RNA extraction was placed in a tube with 2  $\mu$ l of gDNA wipeout buffer 7x and RF water to a volume of 14  $\mu$ l. The mixture was incubated at 42 °C for 2 minutes and placed on ice.

A reverse transcription mix was then prepared, made of 1  $\mu$ l of reverse transcriptase, 4  $\mu$ l of reverse transcription buffer and 1  $\mu$ l of reverse transcription primer mix. The 14  $\mu$ l of template RNA prepared in the former step was added to it and the mixture was incubated for 30 minutes at 42 °C, then at 95 °C for 3 minutes to inactivate the reverse transcriptase.

### 2.2.3. Yeast two-hybrid screening

Yeast two-hybrid (Y2H) screening was performed by Hybrigenics (<https://www.hybrigenics-services.com>) using a *Xenopus laevis* cDNA library generated in our lab. The principle of the Hybrigenics ULTImate Y2H™ screening method is as follows: a vector coding for a fragment of the bait protein (in our case the residues 316 to 587 of *Xenopus laevis* Eya1- $\alpha$ , corresponding to the Eya domain known to be involved in protein interactions), fused with a LexA DNA binding domain, is pretransformed into bait yeast cells (sex type:  $\alpha$ ), and vectors coding for protein fragments from the *Xenopus laevis* embryo library, fused with an activation domain, are pretransformed into library yeast cells (sex type:  $\alpha$ ).

In the subsequent screen, pretransformed bait cells are mated with pretransformed library cells, and the mating leads to the production of diploid cells, expressing both the bait and one of the preys. In these cells, if the bait fragment and the prey fragment interact, the LexA DNA binding domain fused with the bait and the Gal4 activation domain fused with the prey come in close proximity and reconstitute a functional transcription factor that activates the expression of the HIS3 reporter gene, allowing the cells to grow on a medium lacking histidine (Fig. 2.1). The DNA of the positive clones is then sequenced by Hybrigenics, allowing the identification of the protein partners.



**Fig. 2.1.** Hybrigenics ULTimate Y2H™ yeast two-hybrid screening method.

Each predicted interaction partner gets a Predicted Biological Score (PBS). The PBS is a statistical confidence score computed as an e-value, that represents the probability of an interaction to be non-specific. This score is primarily established by comparing the number of independent prey fragments found for an interaction, and the chance of finding them at random. Information about these interactions from other screens performed at Hybrigenics is also taken into account (Formstecher et al., 2005).

Thresholds have been defined in order to rank the results in 4 categories from A (very high confidence in the interaction) to D (moderate confidence in the interaction). The interactions ranked in the D category involve one unique prey fragment or multiple identical ones, and are either false positives or interactions hardly detectable by the Y2H technique (due to low representation of the mRNA in the library, prey folding, or prey toxicity in the yeast cells). Highly connected prey domains and established technical false positives are ranked in distinct categories, E and F, respectively.

#### 2.2.4. PCR primers design

PCR primers were designed such that the generated amplicons would bear appropriate restriction sites, tags or linkers before being subcloned into pCS2+ or pcDNA3-EGFP vectors (see Appendix B). The primers were used to generate these inserts from a cDNA template or from an existing plasmid containing the sequence of interest.

For the amplification of some difficult genes, two pairs of primers were designed: the first pair allowed a preliminary amplification of the sequence of interest, and the second pair was used on this first amplicon (nested PCR) to add the restriction sites and tags.

The primers were ordered from the company biomers.net and received lyophilized. They were resuspended in nuclease free water to a concentration of 100  $\mu$ M, heated for 3 minutes at 55 °C, vortexed, spun and stored at -20 °C. This master stock was used to prepare 10  $\mu$ M aliquots that were used for the PCRs.

#### 2.2.5. PCR amplification

Gradient PCRs were performed using Phusion High-Fidelity DNA polymerase (NEB; cat. no.: M0530S). Elongation times were adapted according to the size of the amplicons to be generated. PCR reaction mix and PCR program are provided in Appendix B.

#### 2.2.6. Agarose gel electrophoresis

To prepare agarose gels, 0.5 g of agarose were mixed with 50 ml of 1x TAE buffer. The mixture was boiled in a microwave and 5  $\mu$ l of Sybr Safe (Thermo Fisher; cat. no.: S33102) was added once the bottle cooled enough to be held. The mixture was then poured in a gel cast with a comb for the wells and let to solidify before being used for electrophoresis.

The 20  $\mu$ l samples were mixed with 4  $\mu$ l of 6x loading dye and loaded in the wells. 6  $\mu$ l of protein ladder (NEB; cat. no.: P7719S) were loaded in a well. The electrophoresis was then run at 75V for about 30 minutes, and either pictured under UV or used for DNA extraction using blue light.

### 2.2.7. Agarose gel DNA extraction

After the PCR products were submitted to electrophoresis, the agarose gel was placed on UV light in order to visualise the DNA. Bands corresponding to amplicons of the appropriate size were excised from the gel with a razor blade, and the gel slices were placed in tubes and weighted.

The DNA was then extracted using a QIAquick gel extraction kit (Qiagen; cat. no.: 28704) according to manufacturers instructions, eluted in 30 µl ultrapure water, and DNA concentration was measured photometrically using a NanoDrop.

### 2.2.8. Subcloning

Amplicons and plasmids were digested using the appropriate restriction enzymes (see Appendix B). Amplicons to be subcloned in pCS2+ plasmids were cut with XhoI/XbaI (except Msh6-C-term-flag, cut with AsuII/XbaI). Amplicons to be subcloned in pcDNA3-EGFP plasmids were cut with KpnI/NotI (except Pias4-C-term, cut with EcoRI/NotI).

Restriction digestions were carried out in 50 µl reactions: 1 µg plasmid or amplicon, 10 µl buffer, 5 µl restriction enzyme 1, 5 µl restriction enzyme 2, and dH<sub>2</sub>O to 50 µl. The mix was incubated at 37 °C for several hours or overnight (or according to manufacturer's instructions; Thermo Fisher restriction enzymes). The restricted DNA was then purified using QIAquick PCR purification kit (Qiagen; cat. no.: 28104) to a final volume of 30 µl.

Restricted plasmids and inserts were ligated in 10 µl ligation reactions, using T4 DNA ligase (Thermo Fisher; cat. no.: EL0011) according to the manufacturer's instructions (using x times 50 ng insert for 50 ng plasmid for an insert x times smaller than the plasmid).

### 2.2.9. Bacterial transformation

2.5 % Luria Broth (LB) was prepared in dH<sub>2</sub>O in 100 ml Erlenmeyer flasks, sealed with aluminium foil and autoclaved. Agar plates were prepared from freshly autoclaved 3.7% LB agar in dH<sub>2</sub>O, and supplemented with an appropriate antibiotic (e.g. ampicillin 100

µg/ml) when cold enough to touch. Plates were then poured and allowed to cool at RT and stored upside down at 4 °C.

100 µl XL1-Blue competent cells (Agilent; cat. no.: 200249) were thawed on ice and transformed with 2.5 µl ligation reaction, according to manufacturer's instructions. Bacterial cells were concentrated following recovery by centrifugation for 8 minutes at 6000 rpm and the bottom 10% (100 µl) of the resulting cell suspension was plated onto 37 °C LB agar plates using a flame sterilized tool. Plates were sealed and bred upside down at 37 °C overnight.

#### 2.2.10. Miniprep

4 single colonies were incubated in 10 ml LB with ampicillin and cultured overnight at 37 °C on shaker.

For each culture, 1.5 ml was taken and centrifuged 5' at 5000 rpm. The supernatant was removed and the pellet was resuspended in 100 µl TELT buffer. 10 µl of lysozyme at 10 mg/ml was added and the mix was incubated for 10 minutes at room temperature.

The mix was then boiled at 100 °C for 2 minutes, put on ice for 2 minutes, and centrifuged for 10' at 13000 rpm. The supernatant was transferred into a new tube and 100 µl of isopropanol was added. After 10 minutes, the sample was centrifuged for 10 minutes at 13000 rpm, the supernatant was removed and the pellet was washed in 0.5 ml EtOH and centrifuged for 5 minutes at 13000 rpm. The supernatant was removed again and the pellet was let to dry and resuspended in 50 µl ultrapure water.

#### 2.2.11. Restriction test digest

For each different colony restriction test digests were prepared by mixing 5 µl of eluate from miniprep, 1 µl of each restriction enzyme, 1 µl of restriction buffer and 2 µl of dH<sub>2</sub>O. The mix was left at 37 °C for several hours or overnight. DNA Loading buffer was added and the mix was run on agarose gel.

One of the colonies presenting the right restriction profile was then cultured by inoculating an Erlenmeyer containing 50 ml LB medium with ampicillin. The culture was grown at 37 °C overnight on shaker and midiprep.

#### 2.2.12. Midiprep

A small amount of culture coming from a single colony was put in 100 ml LB medium supplemented with ampicillin, and bacteria were let to grow at 37 °C overnight on shaker. Midiprep was performed on this culture using NucleoBond Xtra Midi kit (Thermo Fisher; cat. no.: 12798402) according to manufacturer's instructions.

#### 2.2.13. Plasmid linearization

Plasmids were linearized for either mRNA transcription or probe transcription, by mixing 10 µg of plasmid from midiprep, 5 µl of the appropriate restriction enzyme (see Tables 2.1 and 2.2), 5 ul of restriction buffer, and dH<sub>2</sub>O to a total volume of 50 µl.

The mix was left at 37 °C for at least two hours or overnight. DNA was then purified using QIAquick PCR purification kit (Qiagen; cat. no.: 28104) according to manufacturer's instructions, to be eluted in a final volume of 30 µl RNase-free H<sub>2</sub>O.

#### 2.2.14. mRNA synthesis for microinjection

SP6 or T7 (see Table 2.1) mRNA transcription was performed from 1 µg of plasmid, using mMessage mMachine SP6 (Thermo Fisher; cat. no.: AM1340) or T7 (Thermo Fisher; cat. no.: AM1344) transcription kits, according to manufacturer's instructions. mRNA was then diluted to a final concentration of 500 ng/µl in RNase free H<sub>2</sub>O.

The mRNA was then purified using RNeasy mini kit (Qiagen; cat. no.: 74104) according to the manufacturer's instructions, and diluted to a final concentration of 500 ng/µl in RNase free water.

**Table 2.1.** Vector and mRNA synthesis information.

| Plasmid                             | Linearisation | Transcription | Published                    |
|-------------------------------------|---------------|---------------|------------------------------|
| <b>Eya1/pCS2+</b>                   | NotI          | SP6           | (Ahrens and Schlosser, 2005) |
| <b>LacZ/pCS2+</b>                   | NotI          | SP6           |                              |
| <b>N-term-flag-Six1/pCS2+</b>       | NotI          | SP6           |                              |
| <b>N-term-Strep-Pias4/pCS2+</b>     | NotI          | SP6           |                              |
| <b>pcDNA3-EGFP</b>                  | SmaI          | T7            | (Amiri et al., 2007)         |
| <b>pCMT-eGFP</b>                    | NotI          | SP6           | (Gougnard et al., 2016)      |
| <b>Pias4/pCS2+</b>                  | NotI          | SP6           | (Daniels et al., 2004)       |
| <b>Pias4-C-term-eGFP/pcDNA3</b>     | SmaI          | T7            |                              |
| <b>Pias4-C-term-flag/pCS2+</b>      | NotI          | SP6           |                              |
| <b>Pias4-C-term-Strep/pCS2+</b>     | NotI          | SP6           |                              |
| <b>Pias4-C-term-TwinStrep/pCS2+</b> | NotI          | SP6           |                              |
| <b>Six1-C-term-eGFP/pcDNA3</b>      | StuI          | T7            |                              |
| <b>Six1-C-term-flag/pCS2+</b>       | NotI          | SP6           |                              |
| <b>Smarce1-C-term-eGFP/pcDNA3</b>   | SmaI          | T7            |                              |
| <b>Smarce1-C-term-HA/pCS2+</b>      | NotI          | SP6           | (Domingos et al., 2002)      |
| <b>Sox11-C-term-eGFP/pcDNA3</b>     | SmaI          | T7            |                              |
| <b>Sox11-C-term-flag/pCS2+</b>      | NotI          | SP6           |                              |
| <b>Zmym3-C-term-flag/pCS2+</b>      | NotI          | SP6           |                              |

#### 2.2.15. RNA probes synthesis for *in situ* hybridization

RNA probes were synthesized by T3 or T7 transcription (see Table 2.2) from linearized plasmid using a Dig RNA labeling kit (Merck; cat. no.: 11175025910) according to the manufacturer's instructions. The probes were purified using RNeasy mini kit (Qiagen; cat. no.: 74104) according to the manufacturer's instructions, diluted to a final concentration of 100 µg/ml in hybridization buffer, and stored at -20 °C.

**Table 2.2.** Vector and probe synthesis information.

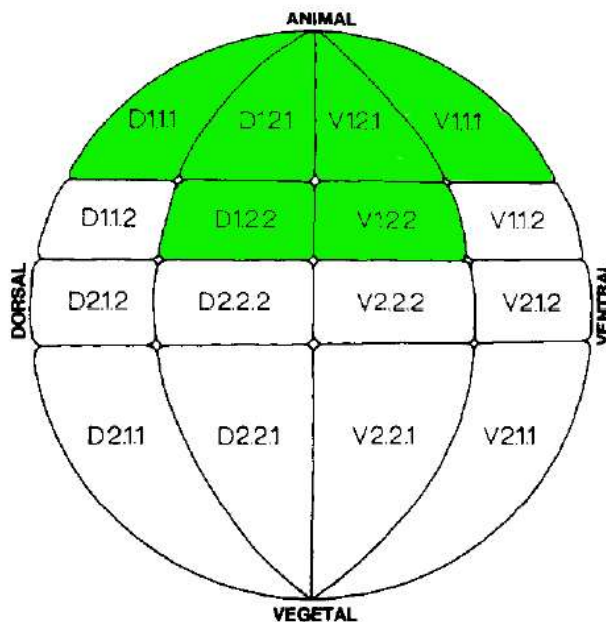
| <b>Plasmid</b>                         | <b>Linearisation (sense)</b> | <b>Transcription (sense)</b> | <b>Linearisation (antisense)</b> | <b>Transcription (antisense)</b> | <b>Published</b>                |
|--|------------------------------|------------------------------|----------------------------------|----------------------------------|---------------------------------|
| <b>Eya1-<math>\alpha</math>/pT-Adv</b> | /                            | /                            | BamHI                            | T7                               | (David et al., 2001)            |
| <b>FoxD3 pBS-SK(-) 99A</b>             | /                            | /                            | EcoRI                            | T7                               | (Sasai et al., 2001)            |
| <b>Hes5.4 pCS2+</b>                    | /                            | /                            | BamHI                            | T7                               | (Riddiford and Schlosser, 2016) |
| <b>pCS2P+ Neurog1</b>                  | /                            | /                            | EcoRI                            | T7                               | (Nieber et al., 2009)           |
| <b>pBS-X-ngnr-1b</b>                   | /                            | /                            | EcoRI                            | T7                               | (Ma et al., 1996)               |
| <b>pBSII-SK(+) NeuroD</b>              | /                            | /                            | XbaI                             | T7                               | (Lee et al., 1995)              |
| <b>pBSII-SK XSix1</b>                  | /                            | /                            | NotI                             | T7                               | (Pandur and Moody, 2000)        |
| <b>pBK-CMV Sox3</b>                    | /                            | /                            | EcoRI                            | T7                               | (Penzel et al., 1997)           |
| <b>Tubb2b/pCS2+</b>                    | /                            | /                            | BamHI                            | T3                               | (Oschwald et al., 1991)         |
| <b>Garre1-C-term-flag/pCS2+</b>        | XbaI                         | SP6                          | Clal                             | T3                               |                                 |
| <b>Msh6-C-term-flag/pCS2+</b>          | XbaI                         | SP6                          | Clal                             | T3                               |                                 |
| <b>Pias4-C-term-flag/pCS2+</b>         | NotI                         | SP6                          | Clal                             | T3                               |                                 |
| <b>Smarce1-C-term-HA/pCS2+</b>         | NotI                         | SP6                          | Clal                             | T3                               |                                 |
| <b>Zmym3-C-term-flag/pCS2+</b>         | XbaI                         | SP6                          | Clal                             | T3                               |                                 |

#### 2.2.16. Microinjection of mRNA or morpholino antisense oligonucleotides

The constructs to be injected were freshly prepared before each injection. Embryos to be used for protein extractions were injected at 2-cell stage, in both cells, with mRNAs at a concentration of 100 ng/ $\mu$ l. When no mRNA coding for an eGFP-tagged protein was part of the injected mix, mRNA coding for MT-eGFP was added to it (at a concentration

of 50 ng/μl), in order to allow for subsequent selection of successfully injected embryos by fluorescence microscopy.

Embryos to be used for GOF/LOF experiments were injected with mRNAs or morpholino oligonucleotides (MO) at varying concentrations (*pias4.L* MO: 50 μM; *smarce1.LS* MOs: 250 μM; Control MO: 100 μM; *pias4* mRNA: 50 ng/μl; *smarce1-HA* mRNA: 100 ng/μl). They were also injected with *lacZ* mRNA (50 ng/μl), in order to allow for subsequent visualization of the injected side by X-gal staining. Those embryos were injected at 16- to 64-cell stage, targeting specifically, when possible, one of the blastomeres that were shown to contribute significantly to cranial placodes and/or ganglia (Moody, 1987) (Fig. 2.2).



**Fig. 2.2.** Blastomere nomenclature in the 32-cell stage *Xenopus* embryo. For GOF/LOF experiments, embryos were injected in one of the blastomeres contributing significantly to cranial placodes and/or ganglia (highlighted in green). (Adapted from Moody, 1987).

Morpholino oligonucleotides (Table 2.3) were purchased from Gene Tools, and *Pias4.L* MO was previously used in (Daniels et al., 2004). *Smарce1.LS* MO1 and *smarce1.LS* MO2 were designed for this study, and *smarce1.LS* MO2 efficacy was confirmed by western blotting from protein extracts of embryos injected with *smarce1-eGFP* mRNA (see Chapter 5). The use of *smарce1.LS* MO1 and *smарce1.LS* MO2 lead to similar phenotypes. A standard control MO obtained from Gene Tools was used in control injections.

**Table 2.3.** Morpholino oligonucleotide sequences and sequences of mRNA parts they bind to. Start codon is in red.

| Morpholino            | MO sequence (5' to 3')   |
|-----------------------|--------------------------|
| <i>pias4.L MO</i>     | CCGCCATCTGGCTTCCAGCGTCCC |
| <i>smarce1.LS MO1</i> | TTGCAGCTTTCTTTGGTTCAGAC  |
| <i>smarce1.LS MO2</i> | TGAGGGTCGTTTGGACAT       |
| control MO            | CCTCTTACCTCAGTTACAATTATA |

| mRNA                  | Bound mRNA sequence (5' to 3')              |
|-----------------------|---|
| <i>pias4.L mRNA</i>   | GGGACGCTGGAAGCCAAGATGGCGG                   |
| <i>smarce1.S mRNA</i> | GTCTGAACCAAAGAAATCTGCAAACATGTCGAAACGACCCTCA |
| <i>smarce1.L mRNA</i> | GTCTGAATAAAACAAGCTGCAAAAATGTCCAAGCGACCATCA  |

Microneedles were prepared from glass capillaries (Narishige; cat. no.: GD-1) on a microneedle puller (Narishige; cat. no.: PN-31) using the following settings: heat 98.1; sub magnet 22.0; main magnet 94.1. The needle was mounted on a microinjector (Narishige; cat. no.: IM-300) and the solution to be injected was transferred on a slide covered with parafilm before being drawn into the needle. The injection was calibrated by injecting into a drop of mineral oil on a micro ruler, and adjusting the diameter of the injected droplet to 0.2-0.22 mm (5 nl).

Embryos were transferred to an agar dish 4% bearing individual wells and containing 5% Ficoll in 0.1x MBS (around 200 embryos per dish). The liquid was removed before injection. Embryos to be used for protein extractions were injected in two cells, at 2- to 4-cell stage; embryos to be used in GOF/LOF experiments were injected in one cell, at 32- to 64-cell stage. After injection the embryos were transferred into a small Petri dish filled with 5% Ficoll, and let on a cold plate at 14 °C overnight. They were transferred into a small plate filled with 0.1x MBS the following morning, until collection at the desired stage.

The next morning embryos were transferred into 0.1x MBS and kept at the desired temperature until they reached the appropriate developmental stage (Nieuwkoop and Faber [NF] staging table). Dead embryos were removed regularly from the dishes and embryos were washed with fresh 0.1x MBS when needed.

### 2.2.17. Embryo fixation and X-gal staining

Recipes for solutions used for X-gal staining can be found in Appendix A.2. Embryos to be used for *in situ* hybridizations were collected at the desired developmental stage (NF stage 14-18, 22, 27 or 34) and fixed in Paraformaldehyde (PFA) solution, 4% in PBS (Thermo Fisher; cat. no.: 15670799) for 30 minutes. Embryos were rinsed 2x 10 minutes in 0.1M PB, then incubated at 37 °C in X-gal staining solution until blue staining was apparent (up to 3h). Embryos were rinsed 2x 5 minutes in 0.1M PB, post-fixed for one more hour in PFA 4%, rinsed 2x 10 minutes in 0.1M PB, 10 minutes in 50% ethanol, and finally stored in 70% ethanol at 4 °C.

### 2.2.18. Whole mount *in situ* hybridization

Recipes for stock solutions can be found in Appendix A.2.

#### First day:

All solutions used on the first day were prepared with DEPC-H<sub>2</sub>O to ensure RNase free conditions. Embryos were rehydrated for 5 minutes in 50% ethanol followed by 5 minutes in 30% ethanol. They were then washed in PTW (PBS + 0.1% Tween-20) for 3x 5 minutes and treated with proteinase K solution (10 µg/ml in PTW) for 1 minute.

They were then rinsed 2x 5 minutes in 0.1M TEA (last rinse in 4 ml). Then 0.5 ml TEA/acetic anhydride (250 µl acetic anhydride in 10 ml 0.1M TEA) was added and the tubes were occasionally gently shaken for 5 minutes, before adding another 0.5 ml of TEA/acetic anhydride and shaking for another 5 minutes.

Embryos were then washed 2x 5 minutes in PTW and refixed in MEMFA for 20 minutes, followed by 5x 5 minutes washes in PTW; embryos were transferred into 24-well plates during the last wash. 1 ml of PTW was then added.

500 µl of hybridization buffer were added and embryos were allowed to settle. All the hybridization buffer was removed and replaced by 500 µl hybridization buffer, and embryos were left to incubate at 60 °C for 10 minutes.

The hybridization buffer was then replaced again (500 µl) and embryos were incubated for 6 hours at 60 °C. The hybridization buffer was replaced by 500 µl of probe solution (hybridization buffer with 1 µg/ml of probe) and embryos were incubated overnight at 60 °C.

#### Second day:

The probe solution was saved for further hybridizations (up to 5 times) and replaced with 500 µl hybridization buffer, before a 10 minutes incubation at 60 °C. Embryos were then washed for 3x 20 minutes in 2x SSC at 60 °C before RNase treatment in RNase solution for 30 minutes at 37 °C (RNase A 20 µg/ml and RNase T1 20 units/ml in 2x SSC)

Embryos were washed in 2x SSC for 10 minutes at room temperature, and in 0.2x SSC for 2x 30 minutes at 60 °C. They were then washed for 2x 5 minutes in MAB, and in 2% BBR in MAB for 1h, before incubation in 1ml MAB + 2% BBR + 20% HIGS for 1 hour. This solution was then replaced by MAB + 2% BBR + 20% HIGS + 1:1000 anti-digoxigenin antibody coupled with alkaline phosphatase (Merck; cat. no.: 11093274910), and the embryos were stored overnight at 4 °C.

#### Third day:

The antibody solution was removed and embryos were washed for 5x 1 hour in MAB. Embryos were then washed for 2x 5 minutes in AP buffer, and incubated in the dark in staining solution made of AP buffer + NBT (4.5 µl [100 mg/ml] in 10 ml AP buffer) + BCIP (35 µl [50 mg/ml] in 10 ml AP buffer) at room temperature until staining was apparent. If staining was not sufficient after 3-4 hours, the staining solution was replaced and embryos were stored at 4 °C overnight before staining was reassessed. Upon sufficient staining, the reaction was stopped with 3x 5 minutes MAB washes, and embryos were refixed overnight (2.5 ml formaldehyde, 0.5 ml glacial acetic acid, 7 ml dH<sub>2</sub>O).

#### Fourth day:

Background staining was removed with 2x 30 minutes 100% ethanol washes. After additional washes in 70% ethanol and 50% ethanol (5 minutes each) embryos were bleached for several hours to several days in bleaching solution. Embryos were then rinsed in SSC for 5 minutes and 50% ethanol for 5 minutes, and stored at 4 °C in 70% ethanol.

#### 2.2.19. TnT *in vitro* transcription and translation

In vitro transcriptions and translations were performed using either TNT coupled reticulocyte lysate SP6 kit (Promega; cat. no.: L4600) or TNT wheat germ extract SP6 kit (Promega; cat. no.: L4130), according to manufacturer's instructions. 20 to 25 µl TnT reactions were prepared, using 1 µg of plasmid DNA template per reaction. Once the reaction was complete, samples were stored at -20 °C.

#### 2.2.20. Protein extraction

Embryos were collected in a 2 ml tube around NF stage 14 and used directly for protein extraction, or frozen at -70 °C for later extraction. For protein extraction on 100 embryos, 250 µl to 1 ml ice-cold extraction buffer (see Appendix A.3) was added to the tube. Embryos were lysed by pipetting until the lysate was homogeneous. A 1:1 volume of freon was added to the tube before vortexing and centrifugation for 3 minutes at 13000 rpm. After centrifugation the upper phase containing the proteins was collected, avoiding the interface containing the yolk. The protein extract was then used directly for co-immunoprecipitation, or frozen at -70 °C.

### 2.2.21. Co-immunoprecipitation

#### Using GFP-catcher beads:

Each sample was prepared from protein extracts of 50 embryos lysed in 500 µl extraction buffer. 52 µl of extract were saved to be used as the crude extract for western blot analysis, and the rest was used for the following co-immunoprecipitation procedure.

GFP-catcher beads (Antibodies-online; cat. no.: ABIN5311508) are 4% cross-linked agarose beads covalently bound to anti-GFP antibody. 25 µl of GFP-catcher beads slurry were transferred in a tube. Beads were equilibrated by 500 µl washes with extraction buffer, pelleted by centrifugation for 5 minutes at 2500 g, and the supernatant was removed, three times. The lysate was then added to the beads and incubated on a rotator overnight at 4 °C.

The next day the beads were washed three times with extraction buffer, and transferred to a new tube during the last wash. After the supernatant was removed, beads were resuspended in 20 µl LDS sample buffer 4x (Merck, cat. no.: MPSB-10ML), 8 µl DTT 1M, and 52 µl extraction buffer, for a total volume of 80 µl eluate. The mix was then heated at 70 °C for 10 minutes, and after centrifugation the supernatant was collected and used for polyacrylamide gel electrophoresis (PAGE). Similarly, 20 µl LDS sample buffer 4x and 8 µl DTT 1M were added to the 52 µl of extract saved as the non-bound fraction, for a total volume of 80 µl, and the mix was heated at 70 °C for 10 minutes before use for PAGE.

#### Using Protein A/G magnetic beads:

Each protein extract was made from 50 embryos lysed in 500 µl extraction buffer. 52 µl of extract was saved to be used as the crude extract for western blot analysis, and the rest was used for the following co-immunoprecipitation procedure.

2 µl of rabbit anti-GFP antibody (Abcam; cat. no.: ab290) or 2 µl of guinea pig anti-Eya1 antibody (Ahrens and Schlosser, 2005) were added to the extract, before incubation on a rotator overnight at 4 °C.

Pierce Protein G magnetic beads (Thermo Fisher; cat. no.: 88848) were used with anti-GFP antibody, while Pierce Protein A magnetic beads (Thermo Fisher; cat. no.: 888485) were used with anti-Eya1 antibody. 25  $\mu$ l of beads slurry were transferred in a tube. Beads were washed with 175  $\mu$ l wash buffer (see Appendix A.3) (or with extraction buffer when lower stringency washes were desired, for the rest of the procedure). The tube was gently vortexed, the tube was placed in a magnetic stand in order to separate the beads from the solution, the supernatant was removed and the beads were washed again in 1 ml wash buffer. The tube was inverted several times for one minute, the supernatant removed, and the protein extract was added to the beads and incubated at RT for one hour with mixing. The supernatant was discarded, and 3x500  $\mu$ l washes were performed with wash buffer. The beads were transferred to a new tube during the last wash. The beads were washed with 500  $\mu$ l ultrapure H<sub>2</sub>O, and the tube was gently mixed before the supernatant was discarded.

Beads were resuspended in 20  $\mu$ l LDS sample buffer 4x, 8  $\mu$ l DTT 1M, and 52  $\mu$ l extraction buffer, for a total volume of 80  $\mu$ l eluate. The mix was then heated at 70 °C for 10 minutes, and after centrifugation the supernatant was collected and used for PAGE. Similarly, 20  $\mu$ l LDS sample buffer 4x and 8  $\mu$ l DTT 1M were added to the 52  $\mu$ l of extract saved as the non-bound fraction, for a total volume of 80  $\mu$ l, and the mix was heated at 70 °C for 10 minutes before use for PAGE.

#### 2.2.22. Polyacrylamide gel electrophoresis (PAGE)

mPAGE 4-12% Bis-Tris Precast gels (Merck; cat. no.: MP41G12 and MP41G15) were used for the PAGE procedure. After the gel chamber was installed, it was filled with running buffer (Appendix A.4), and wells were loaded with 35 to 40  $\mu$ l of protein sample. The electrophoresis was run at 120 V for about one hour. The gel was loaded and migration was run at 150 V for about one hour.

#### 2.2.23. Western blotting

The blotting chamber was filled with borate transfer buffer (BTB, Appendix A.4). After PAGE migration the gel was placed on a PVDF membrane that had been activated by a

30-second immersion in methanol. A transfer sandwich was prepared by stacking a foam pad, a layer of Whatman paper, the PVDF membrane, the gel, another layer of Whatman paper, and another foam pad. The sandwich was then pressed between two plastic layers and placed in the blotting chamber, with the gel side facing the negative electrode and the membrane side facing the positive electrode. The blotting was run overnight at 24 V and 370 mA.

After the blotting, the membrane was blocked in blocking solution (TBST + 3% bovine serum albumin) for one hour on a shaker, then incubated with the primary antibody solution (1:5000 antibody in 1 ml blocking solution) in a sealed plastic bag for one hour. The primary antibody was either rabbit anti-GFP (Abcam; cat. no.: ab290) or guinea pig anti-Eya1 (Ahrens and Schlosser, 2005).

This incubation was followed by 3x 15 minutes TBST washes, and a second incubation with the secondary antibody solution (1:5000 antibody in 1 ml TBST) for one hour. Depending on the primary antibody used, the secondary antibody was either anti-rabbit HRP (Thermo Fisher: cat. no.: 65-6120) or anti-guinea pig HRP (Abcam; cat. no.: 6771). The membrane was then washed 3x 15 minutes in TBST, and 3x 5 minutes in TBS, on shaker.

The membrane was then imaged in a FluorChem FC2 imager, after 1.5 ml of chemiluminescent substrate (Thermo Fisher; cat. no.: 34580) was applied.

### 2.3. Microscopy

Embryos were observed using an Olympus SZX7 stereomicroscope. GFP screening was performed using an Olympus SZX16 equipped with a DP71 camera with fluorescent illumination capabilities. Wholemount photography was performed on a Leica M165 FC stereomicroscope equipped with a Leica DFC7000 T camera. Images were adjusted for brightness and contrast with Adobe Photoshop.

## 2.4. Data analysis

### 2.4.1. DAVID

The predicted Eya1 interaction partners identified in the Y2H screen were subjected to gene ontology enrichment analyses using DAVID (<https://david.ncicrf.gov>) (Huang et al., 2007). DAVID is a gene ontology tool that allows to highlight the most relevant functional annotation terms associated with a list of genes provided by the user. DAVID generates annotation charts that include, for each annotation term, the gene count and an EASE Score (a modified Fisher Exact P-value) indicating the level of enrichment of the associated annotation term (the smaller, the more enriched) in a defined gene population background (in our case *Xenopus laevis*).

The DAVID functional annotation clustering function allows the grouping of similar, redundant annotation terms in order to provide a better visualization of the categories of biological functions or properties that are enriched in the list of analysed genes. Each cluster has an enrichment score that is based on the EASE scores of each term members (the higher, the more enriched).

### 2.4.2. Panther

The Panther online tool (<https://www.pantherdb.org>). was used for the visualization of the functions or properties of the predicted Eya1 interaction partners as a bar chart. As the Panther tool does not allow for the analysis of *Xenopus laevis* genes, I used their *Xenopus tropicalis* homologs. 25 genes were examined (no information is available in Panther for the gene *myg1*, and the *Xenopus tropicalis* version of *six4* accounts for the two homeologs *six4.S* and *six4.L* in *Xenopus laevis*).

# Chapter 3. Candidate Protein Interaction Partners of Eya1: Identification and Expression

## 3.1. Yeast two-hybrid screening

As a first step in identifying novel protein partners of Eya1, a protein interaction screen was performed in collaboration with the company Hybrigenics. A *Xenopus laevis* cDNA library was generated in our lab by reverse transcription of RNA extracted from early tailbud stage embryos. This library was used by the company to perform their ULTimate Y2H™ yeast two-hybrid screening method using the Eya domain of *Xenopus* Eya1 as bait.

The sequencing results for each hit were blasted against the *X. laevis* database in order to identify the corresponding genes. After eliminating the redundancies, I identified 28 candidate interactants (listed in Table 3.1), including the transcription factor Six1, which is a well-established Eya1 protein partner. Except for *ccdc96.S* (89.29% identity) and *smg1.S* (94.39% identity), all 28 candidates displayed >99% identity with the NCBI database sequences.

**Table 3.1.** Candidate *X. laevis* Eya1 interactants identified by yeast two-hybrid screening, and their *X. tropicalis* homologs.

| Official symbol<br>( <i>X. laevis</i> ) | Official full name<br>( <i>X. laevis</i> )                    | Entrez<br>Gene ID ( <i>X.<br/>laevis</i> ) | Official symbol<br>( <i>X. tropicalis</i> ) | Entrez<br>Gene ID ( <i>X.<br/>tropicalis</i> ) | Global<br>PBS |
|---|---|--|---|--|---------------|
| ( <i>LOC108695548</i> )                 | ( <i>uncharacterized LOC108695548</i> )                       | 108695548                                  | <i>XB5896327</i>                            | 100486056                                      | A             |
| ( <i>LOC108709310</i> )                 | ( <i>RB-associated KRAB zinc finger protein</i> )             | 108709310                                  | <i>znf630</i>                               | 548734   | D             |
| ( <i>LOC108716064</i> )                 | ( <i>gastrula zinc finger protein XICGF26.1-like</i> )        | 108716064                                  | <i>LOC105946211</i>                         | 105946211                                      | D             |
| <i>ankfy1.S</i>                         | <i>ankyrin repeat and FYVE domain containing 1 S homeolog</i> | 108709660                                  | <i>ankfy1</i>                               | 780349   | D             |
| <i>ccdc15.S</i>                         | <i>coiled-coil domain containing 15 S homeolog</i>            | 735233                                     | <i>ccdc15</i>                               | 100038036                                      | D             |
| <i>ccdc96.S</i>                         | <i>coiled-coil domain containing 96 S homeolog</i>            | 108706532                                  | <i>ccdc96</i>                               | 100489589                                      | D             |
| <i>exosc10.L</i>                        | <i>exosome component 10 L homeolog</i>                        | 431865                                     | <i>exosc10</i>                              | 407941   | D             |
| <i>garre1.L</i>                         | <i>granule associated Rac and RHO G effector 1 L homeolog</i> | 108714109                                  | <i>garre1</i>                               | 100493490                                      | D             |

|                  |   |           |                |           |   |
|------------------|---|-----------|----------------|-----------|---|
| <i>iars1.S</i>   | <i>isoleucyl-tRNA synthetase 1 S homeolog</i>   | 403361    | <i>iars1</i>   | 100036668 | B |
| <i>klhl41.L</i>  | <i>kelch like family member 41 L homeolog</i>   | 398449    | <i>klhl41</i>  | 394822    | D |
| <i>kmt2a.S</i>   | <i>lysine methyltransferase 2A S homeolog</i>   | 108705229 | <i>kmt2a</i>   | 100135006 | D |
| <i>msh6.L</i>    | <i>mutS homolog 6 L homeolog</i>  | 734294    | <i>msh6</i>    | 100145639 | D |
| * <i>myg1.L</i>  | <i>MYG1 exonuclease L homeolog</i>  | 443610    | * <i>myg1</i>  | 594885    | D |
| <i>myg1.S</i>    | <i>MYG1 exonuclease S homeolog</i>  | 496075    | * <i>myg1</i>  | 594885    | D |
| <i>pax3.S</i>    | <i>paired box 3 S homeolog</i>  | 496376    | <i>pax3</i>    | 448464    | C |
| <i>pi4ka.S</i>   | <i>phosphatidylinositol 4-kinase, catalytic, alpha S homeolog</i>   | 446720    | <i>pi4ka</i>   | 100127709 | D |
| <i>pias4.S</i>   | <i>protein inhibitor of activated STAT 4 S homeolog</i>   | 398703    | <i>pias4</i>   | 496945    | D |
| <i>ppard.S</i>   | <i>peroxisome proliferator activated receptor delta S homeolog</i>  | 397768    | <i>ppard</i>   | 100038152 | D |
| <i>six1.L</i>    | <i>SIX homeobox 1 L homeolog</i>  | 398185    | <i>six1</i>    | 100101702 | C |
| <i>six4.L</i>    | <i>SIX homeobox 4 L homeolog</i>  | 108698825 | <i>six4</i>    | 100498150 | A |
| <i>six4.S</i>    | <i>SIX homeobox 4 S homeolog</i>  | 108699752 | <i>six4</i>    | 100498150 | D |
| <i>smarce1.S</i> | <i>SWI/SNF related, matrix associated, actin dependent regulator of chromatin, subfamily e, member 1 S homeolog</i> | 108702475 | <i>smarce1</i> | 448018    | A |
| <i>smg1.S</i>    | <i>SMG1 phosphatidylinositol 3-kinase-related kinase S homeolog</i>   | 108703118 | <i>smg1</i>    | 100145499 | D |
| <i>sox11.L</i>   | <i>SRY-box 11 L homeolog</i>  | 100216330 | <i>sox11</i>   | 493415    | D |
| <i>sox7.L</i>    | <i>SRY-box 7 L homeolog</i>   | 378665    | <i>sox7</i>    | 549080    | D |
| <i>tmtc3.L</i>   | <i>transmembrane and tetratricopeptide repeat containing 3 L homeolog</i>   | 108711051 | <i>tmtc3</i>   | 100145573 | D |
| <i>zmym3.L</i>   | <i>zinc finger MYM-type containing 3 L homeolog</i>   | 108698328 | <i>zmym3</i>   | 100495745 | C |
| <i>znf319.S</i>  | <i>zinc finger protein 319 S homeolog</i>   | 108715459 | <i>znf319</i>  | 100491476 | D |

\* Not analysed through gene ontology online tools (not recognized).

### 3.2. Candidate Eya1 interactants ontology and selection

In order to get an overview of the nature and functions of the identified candidates, I analysed them with the gene ontology tools DAVID (<https://david.ncifcrf.gov>) and Panther (<https://www.pantherdb.org>).

Functional annotations were associated by DAVID to 27 out of the 28 candidate genes (no information was available for *myg1.l*). Three clusters showed a high level of enrichment (>2) (see Table 3.2). A first cluster grouped terms associated with the presence of a HMG box, a second cluster grouped terms associated with DNA binding,

transcription factor activity, cell differentiation and developmental function, and a third cluster grouped terms associated with DNA binding, transcription factor activity, and the presence of a homeobox.

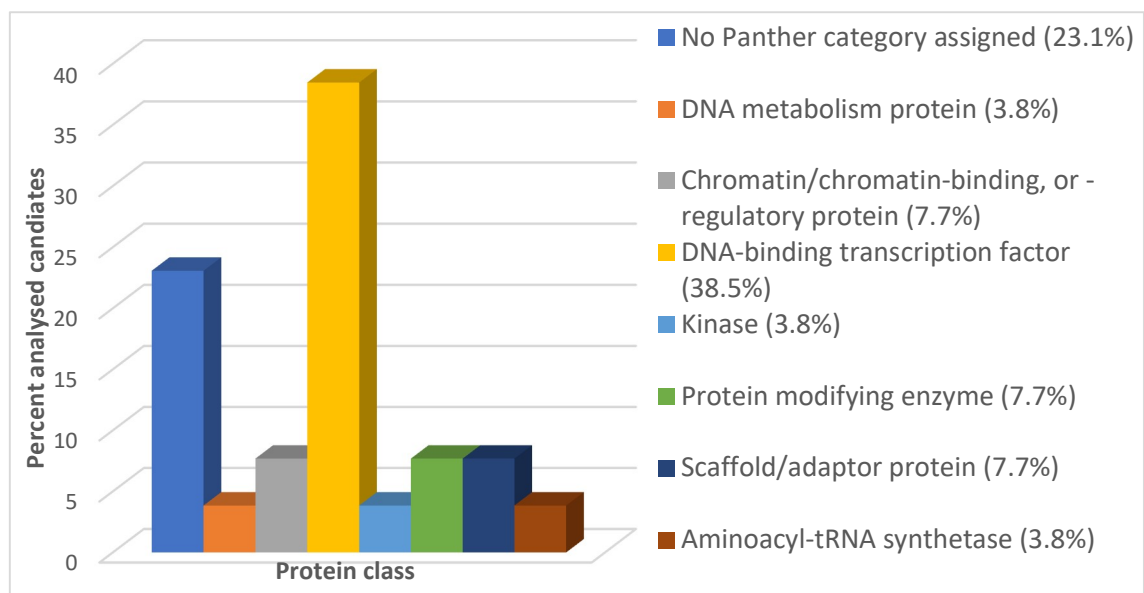
**Table 3.2.** Functional annotation clusters generated by DAVID from the list of candidates identified by yeast two-hybrid screening, displaying an enrichment score >2.

| <b>Annotation cluster 1</b> |  | <b>Enrichment score: 2.53</b> |         |
|-----------------------------|--|-------------------------------|---------|
| Annotation category         | Annotation term  | Gene count                    | P-value |
| UP_SEQ_FEATURE              | DOMAIN:HMG box   | 3                             | 2.2E-3  |
| UP_SEQ_FEATURE              | DNA_BIND:HMG   | 3                             | 2.2E-3  |
| INTERPRO                    | High mobility group (HMG) box domain   | 3                             | 2.5E-3  |
| SMART                       | HMG  | 3                             | 6.0E-3  |
| <b>Annotation cluster 2</b> |  | <b>Enrichment score: 2.3</b>  |         |
| Annotation category         | Annotation term  | Gene count                    | P-value |
| UP_KW_MOLECULAR_FUNCTION    | DNA-binding  | 8                             | 6.1E-5  |
| GOTERM_MF_DIRECT            | DNA binding  | 9                             | 2.5E-4  |
| UP_KW_CELLULAR_COMPONENT    | Nucleus  | 8                             | 3.5E-4  |
| GOTERM_CC_DIRECT            | Nucleus  | 9                             | 8.9E-4  |
| UP_KW_MOLECULAR_FUNCTION    | Activator  | 4                             | 3.9E-4  |
| GOTERM_MF_DIRECT            | RNA polymerase II transcription factor activity, sequence-specific DNA binding | 4                             | 7.3E-3  |
| UP_KW_BIOLOGICAL_PROCESS    | Transcription regulation   | 5                             | 1.5E-2  |
| UP_KW_BIOLOGICAL_PROCESS    | Transcription  | 5                             | 1.8E-2  |
| UP_KW_MOLECULAR_FUNCTION    | Developmental protein  | 4                             | 2.7E-2  |
| UP_KW_MOLECULAR_FUNCTION    | Developmental protein  | 4                             | 2.7E-2  |
| UP_KW_BIOLOGICAL_PROCESS    | Differentiation  | 3                             | 2.9E-2  |
| GOTERM_BP_DIRECT            | cell differentiation   | 3                             | 3.5E-2  |
| GOTERM_MF_DIRECT            | sequence-specific DNA binding  | 3                             | 4.6E-2  |
| <b>Annotation cluster 3</b> |  | <b>Enrichment score: 2.06</b> |         |
| Annotation category         | Annotation term  | Gene count                    | P-value |
| GOTERM_MF_DIRECT            | DNA binding  | 9                             | 2.5E-4  |
| GOTERM_CC_DIRECT            | nucleus  | 9                             | 8.9E-4  |
| GOTERM_BP_DIRECT            | regulation of transcription, DNA-templated                                     | 6                             | 4.2E-3  |
| UP_SEQ_FEATURE              | DOMAIN:Homeobox  | 4                             | 4.9E-3  |
| UP_SEQ_FEATURE              | DNA_BIND:Homeobox  | 4                             | 5.1E-3  |
| GOTERM_MF_DIRECT            | RNA polymerase II transcription factor activity, sequence-specific DNA binding | 4                             | 7.3E-3  |
| INTERPRO                    | Homeobox, conserved site   | 3                             | 3.8E-2  |
| INTERPRO                    | Homeodomain  | 3                             | 5.3E-2  |
| INTERPRO                    | Homeodomain-like   | 3                             | 6.7E-2  |
| SMART                       | HOX  | 3                             | 1.1E-1  |

The analysis of the enrichment of protein class terms using Panther (Fig. 3.1) showed that a large proportion of the candidates (10 out of 25) were transcription factors, either HMG box transcription factors (Sox11 and Sox7), homeodomain transcription factors

(Pax3, Six1 and Six4), or zinc finger transcription factors (LOC105946211, Ppard, Zmym3, Znf319 and Znf630). This is consistent with the annotation terms clustering generated by DAVID.

Among the other candidates, two have chromatin-binding or chromatin-regulatory properties (Kmt2a and Smarce1), two are protein-modifying enzymes (the ubiquitin-protein ligase Pias4 and the serine/threonine protein kinase Smg1), two are scaffold/adaptor proteins (Ankfy1 and Khl41) and three are alone in their categories: Msh6 (involved in DNA metabolism), Pi4ka (kinase) and lars1 (aminoacyl-tRNA synthetase). The remaining candidates (Ccdc15, Ccdc96, Exosc10, Garre1, Tmtc3, and XB5896327) were not classified by Panther.



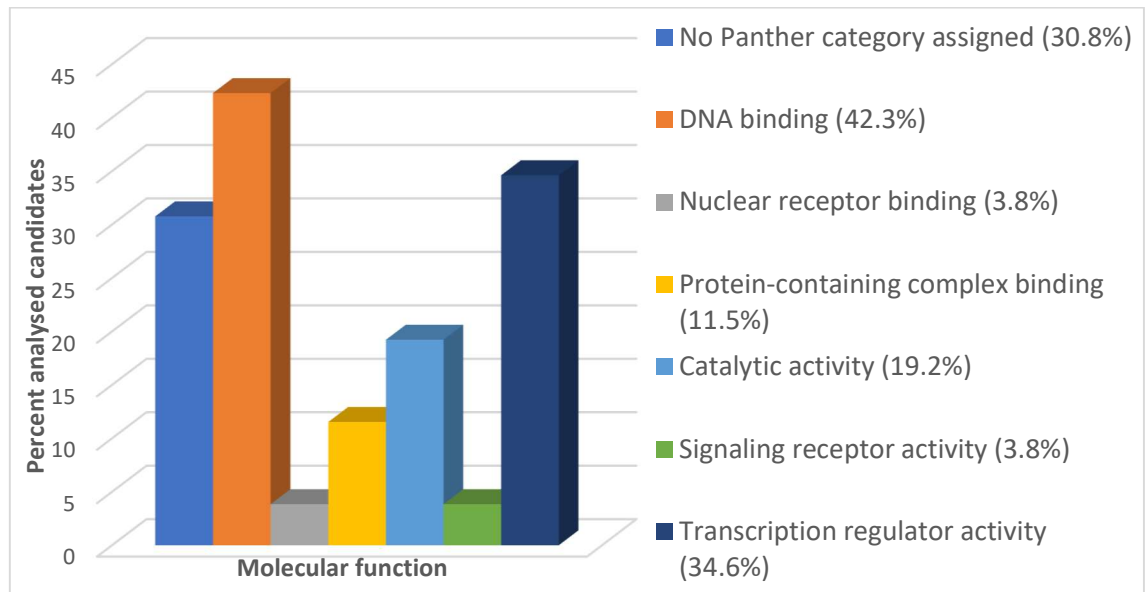
**Fig. 3.1.** Classification by protein class terms of the *Xenopus tropicalis* homologs of the list of candidates identified by yeast two-hybrid screening, generated by Panther.

When considering the molecular function terms (Fig. 3.2), the Panther analysis showed a large proportion of DNA-binding proteins (11 candidates: LOC105946211, Msh6, Pax3, Ppard, Six1, Six4, Smarce1, Sox11, Sox7, Znf319, Znf630), most of which also displaying a transcription factor activity, except Msh6, Smarce1 and Znf319.

Smarce1 is present in the nuclear receptor binding and nucleosome binding categories, while Garre1 and Znf319 bind to other protein-containing complexes. Ppard acts as a signaling receptor.

Five candidates display a catalytic activity: lars1 (acting on RNA), Pias4 and Smg1 (SUMO transferases), Kmt2a (histone H3K4 methyltransferase) and Pi4ka. Among these five proteins, Smg1 also acts as a serine/threonine kinase, while Pias4 has a transcription coregulator activity.

The unclassified candidates included Ankfy1, Ccdc15, Ccdc96, Exosc10, Klhl41, Tmtc3, XB5896327 and Zmym3.



**Fig. 3.2.** Classification by molecular function terms of the *Xenopus tropicalis* homologs of the list of candidates identified by yeast two-hybrid screening, generated by Panther.

### Candidates selection:

The gene ontology analysis showed that the proteins identified by two-hybrid screening as Eya1 protein partners are largely involved in transcription regulation and/or protein modification, which is consistent with the idea that they could perform regulatory functions in conjunction with the transcriptional coactivator Eya1. I selected 9 candidates out of the list of 28 for further characterization, based on whether their known molecular functions were compatible with a potential role in the regulation of neuronal cell proliferation and/or cell differentiation.

Transcription factors are natural candidates for performing regulatory functions. I selected Pax3, Sox7 and Sox11, that are known to play roles in nervous system development and whose known expression patterns in the embryo would be consistent

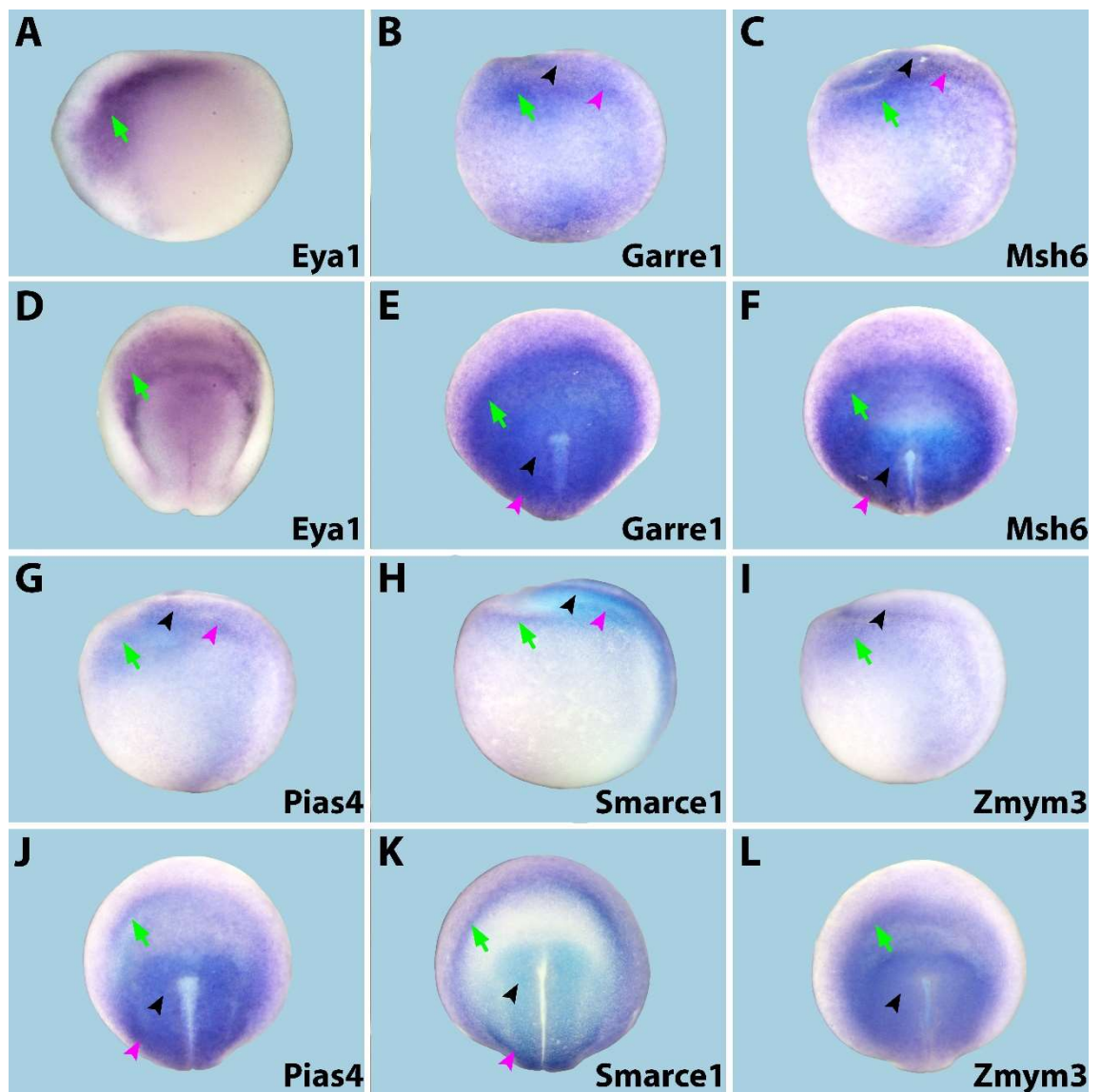
with roles performed in conjunction with Eya1 (Fawcett and Klymkowsky, 2004; Hyodo-Miura et al., 2002; Maczkowiak et al., 2010; Plouhinec et al., 2014), and Zmym3 whose function in the nervous system is unknown. I also selected both candidates identified as chromatin-regulatory proteins, which therefore could play a role in the regulation of Eya1-mediated gene expression: Kmt2a and Smarce1. The E3 SUMO protein ligase Pias4 was also selected as I hypothesized based on a previous study that Pias4-mediated Eya1 SUMOylation could modulate its activity (Alkuraya et al., 2006). Msh6, involved in DNA mismatch repair, and Garre1, which associates with the Ccr4-Not complex that contributes to gene expression regulation (Youn et al., 2018), were also selected.

### 3.3. Candidate Eya1 interactants expression patterns

In order to confirm that Eya1 and its candidate interaction partners are expressed in overlapping areas, and to visualize their expression dynamics, *in situ* hybridization was performed on embryos at four different developmental stages (neurula, NF stage 14-18; early tailbud, NF stage 22; mid tailbud, NF stage 27; late tailbud, NF stage 34). I characterized the expression patterns of *eya1*, *garre1*, *msh6*, *pias4*, *smarce1* and *zmym3*. As a negative control, *in situ* hybridization using sense probes was systematically performed in parallel, at each stage and for each candidate (illustrated for stage 27 in Appendix C).

The expression of *kmt2a* could not be characterized, since I could not successfully amplify that gene from cDNA and thus could not generate a probe for it. The expression of *pax3*, *sox7* and *sox11* has already been extensively characterized and was not studied here.

### 3.3.1. Stage 14-18



**Fig. 3.3.** Expression patterns of *eya1* and its candidate interaction partners in whole-mount *Xenopus laevis* embryos at stage 14-18, in lateral views (A, B, C, G, H, I - anterior is to the left) and dorsal views (D, E, F, J, K, L - anterior is up). Green arrows indicate expression in the preplacodal ectoderm; black and magenta arrowheads indicate expression in the neural plate and neural crest, respectively.

#### *Eya1*:

*Eya1* expression during *X. laevis* development has been previously characterized (David et al., 2001; Schlosser and Ahrens, 2004). I provide here a redescription of *eya1* expression patterns for the purpose of comparing them with the expression patterns of the candidate interactants.

At neurula stages, *eya1* is expressed in a crescent-shaped domain of ectoderm surrounding the anterior neural plate and neural crest, called the preplacodal ectoderm (PPE), from which cranial placodes will arise (Fig 3.3 A-B). As the neural folds elevate, the anterior placodal domain, which will give rise to the adenohipophysial and olfactory placodes, progressively gets separated from the parts of the placodal domain that are lateral to the neural folds. *Eya1* is subsequently downregulated in the prospective lens placode area.

#### Candidate interactants:

Similarly to *eya1*, all candidates exhibited expression in the PPE at neurula stages. In addition, they were expressed in the neural ectoderm (neural plate and neural crest) (Fig 3.3 C to L) as described in detail in the following sections.

#### *Garre1:*

At neurula stages *garre1* was expressed in the preplacodal ectoderm, in the whole neural ectoderm (neural plate and neural crest), and in an undefined population of cells in the ventral area of the embryo (Fig 3.3 C-D).

#### *Msh6:*

Very similarly to *garre1*, *msh6* was expressed in the preplacodal ectoderm, neural plate and neural crest, as well as in a ventral area of the embryo adjacent to the posterior neural plate (Fig 3.3 E-F).

#### *Pias4:*

At neurula stages *pias4* expression was detected in the preplacodal ectoderm. Expression was stronger in the neural plate and neural crest (Fig 3.3 G-H).

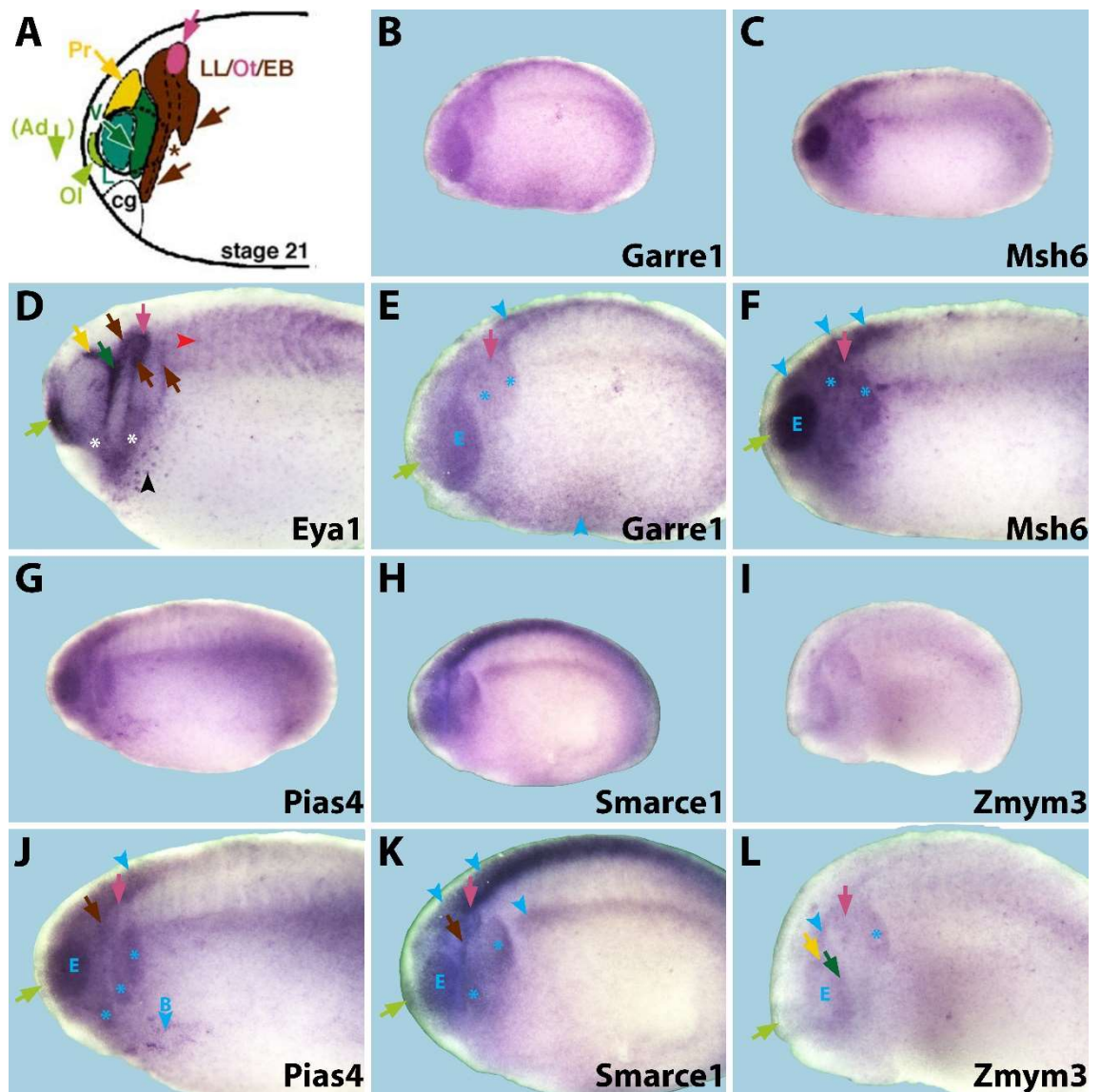
*Smarce1:*

*Smarce1* was present in the neural plate, the neural crest and at the border between the preplacodal ectoderm and the epidermis (Fig 3.3 I-J).

*Zmym3:*

*Zmym3* expression was visible in an area encompassing the preplacodal ectoderm, neural plate, and probably neural crest (Fig 3.3 K-L).

### 3.3.2. Stage 22



**Fig. 3.4.** Expression patterns of *eya1* and its candidate interaction partners in whole-mount *Xenopus laevis* embryos at stage 22, in lateral views (anterior is to the left). The schematic drawing (A) shows the distribution of placodes in an early tailbud stage embryo. Arrows indicate expression in placodes and display the colour code used in the drawing, arrowheads and asterisks indicate other areas of expression. Red arrowhead in D indicates *eya1* expression in the somites, white asterisks indicate expression in the pharyngeal pouches, and black arrowhead indicates expression in the anteroventral noradrenergic cells. Blue asterisks (neural crest streams) and arrowheads indicate expression in areas where *eya1* is not expressed. Pictures E, F, J, K and L are magnifications of pictures B, C, G, H and I, respectively. Abbreviations: Ad, adenohipophysial placode; B, blood islands; cg, cement gland; E, prospective eye, including overlying lens (L) placode; LL/Ot/EB: posterior placodal area, from which lateral line (LL), otic (Ot), and epibranchial (EB) placodes develop; Ol, olfactory placode; Pr, profundal placode; V, trigeminal placode. Schematic drawing from (Schlosser and Ahrens, 2004).

### *Eya1:*

Except for the lens placode area, *eya1* continues to be expressed in all areas derived from the preplacodal ectoderm (Fig. 3.4 C). They include the adenohipophyseal and olfactory placodes, and the ectodermal domain lateral to the neural tube that has separated into two distinct areas: the profundal/trigeminal area, and the posterior placodal area comprising the otic placode and two ventral extensions, that will give rise to the lateral line and epibranchial placodes. At stage 22 *eya1* expression is also observed in the endoderm of the developing pharyngeal pouches, in the somites, and in an anteroventral population of cells which probably are neural crest-derived noradrenergic cells (Wylie et al., 2015).

### *Garre1:*

At stage 22, *garre1* expression was present at the level of the olfactory and otic placodes. Unlike *eya1*, *garre1* was also expressed in the prospective eye, in the brain, along the spinal cord, and in migrating neural crest cells. An undefined population of cells in the ventral area of the embryo also exhibited *garre1* expression (Fig 3.4 C-D).

### *Msh6:*

*Msh6* exhibited strong expression in the prospective eye, and expression in the brain and migrating neural crest cells. The otic placode, and possibly the olfactory placode, also displayed *msh6* expression (Fig 3.4 E-F).

### *Pias4:*

At stage 22 *pias4* expression could be observed in the prospective eye, in the olfactory placode and posterior placodal area, in migrating neural crest cells, and in the brain and spinal cord. *Pias4* was also present in a ventral population of cells, presumably ventral blood islands (Fig 3.4 G-H).

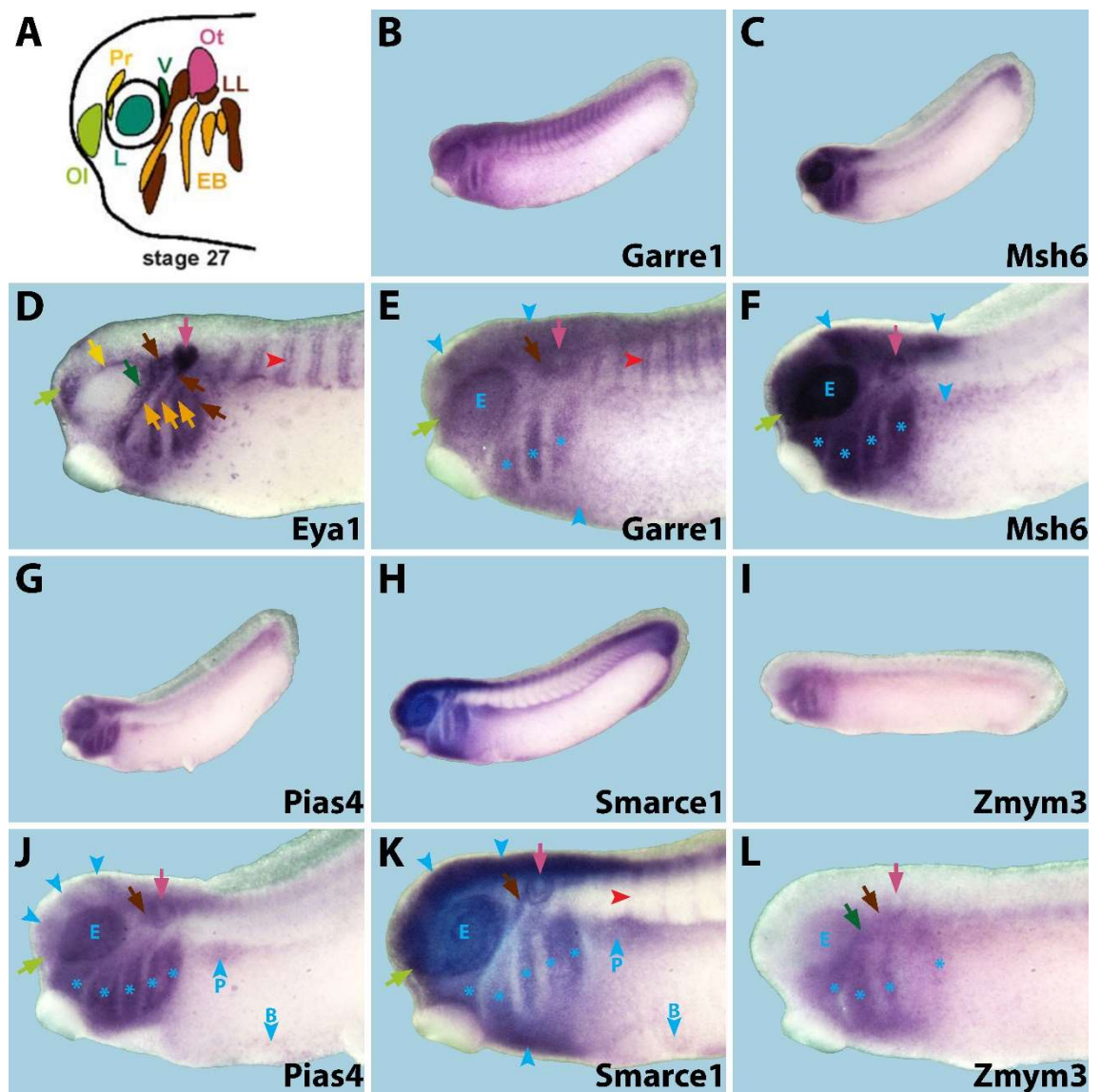
*Smarce1:*

At stage 22 *smarce1* was expressed in the prospective eye, in the olfactory placode and posterior placodal area, in migrating neural crest cells, and in the hindbrain and spinal cord. *Smarce1* expression was also visible at the level of the intermediate mesoderm (Fig 3.4 I-J).

*Zmym3:*

*Zmym3* expression could be seen in the prospective eye, the migrating neural crest cells and the posterior placodal area. The profundal and trigeminal placodes possibly displayed *zmym3* expression, as well as the olfactory placode. Expression was also visible in the floor of the anterior neural tube (Fig 3.4 K-L).

### 3.3.3. Stage 27



**Fig. 3.5.** Expression patterns of *eya1* and its candidate interaction partners in whole-mount *Xenopus laevis* embryos at stage 27, in lateral views (anterior is to the left). The schematic drawing (A) shows the distribution of placodes in a mid tailbud stage embryo. Arrows indicate expression in placodes and display the colour code used in the drawing, arrowheads and asterisks indicate other areas of expression. Red arrowheads indicate expression in the somites, and white asterisks indicate expression in the pharyngeal pouches. Blue asterisks (neural crest streams) and arrowheads indicate expression in areas where *eya1* is not expressed. Pictures E, F, J, K and L are magnifications of pictures B, C, G, H and I, respectively. Abbreviations: B, blood islands; E, prospective eye, including lens (L) placode; EB, epibranchial placodes; LL, lateral line placodes; Ol, olfactory placode; Ot, otic placode; P, pronephros; Pr, profundal placode; V, trigeminal placode. Schematic drawing from (Schlosser and Ahrens, 2004).

### Eya1:

At stage 27, *eya1* maintains its presence in the derivatives of expression areas mentioned for stage 22 (Fig 3.5 B). They include the adenohipophysial and olfactory placodes, the profundal and trigeminal placodes (which sizes have now decreased), the otic placode invaginating to form the otic vesicle, and the now more individualised lateral line and epibranchial placodes. *Eya1* expression is also maintained in the endoderm of the pharyngeal pouches and in the somites. Expression is strong in the most posterior somites, and extends further posteriorly down to the proctodeum.

### Garre1:

The olfactory and otic placodes continued to show *garre1* expression at stage 27, and similarly to *eya1*, expression had appeared in the somites and tailbud, and possibly in the anterodorsal lateral line placode (apposed anteriorly to the otic placode). Other areas of maintained expression included the prospective eye, neural crest cells that had now migrated ventrally within the branchial arches, the brain (with stronger expression in the hindbrain and part of the midbrain), spinal cord, and a population of cells in the ventral area (Fig 3.5 C-D).

### Msh6:

At stage 27 *msh6* continued to be expressed in the prospective eye, the brain, migrating neural crest cells, the otic placode and possibly the olfactory placode. In the brain expression was clearly stronger in two distinct areas: the posterior hindbrain, and possibly the midbrain-hindbrain boundary. Expression was also observed in a cell population located posteriorly to the branchial arches and ventrally to the somites, and in the tailbud (Fig 3.5 E-F).

#### *Pias4:*

At mid-tailbud stage *pias4* expression was maintained in the eye, in the olfactory, otic and lateral line placodes, in the neural crest cells, and in the brain and spinal cord. *Pias4* was still present in what could be the ventral blood islands, and was now observed in the tailbud and in the developing pronephros. At the level of the brain, *pias4* expression was stronger in the posterior rhombencephalon, and in three discrete areas in the forebrain, midbrain and presumably the midbrain-hindbrain boundary (Fig 3.5 G-H).

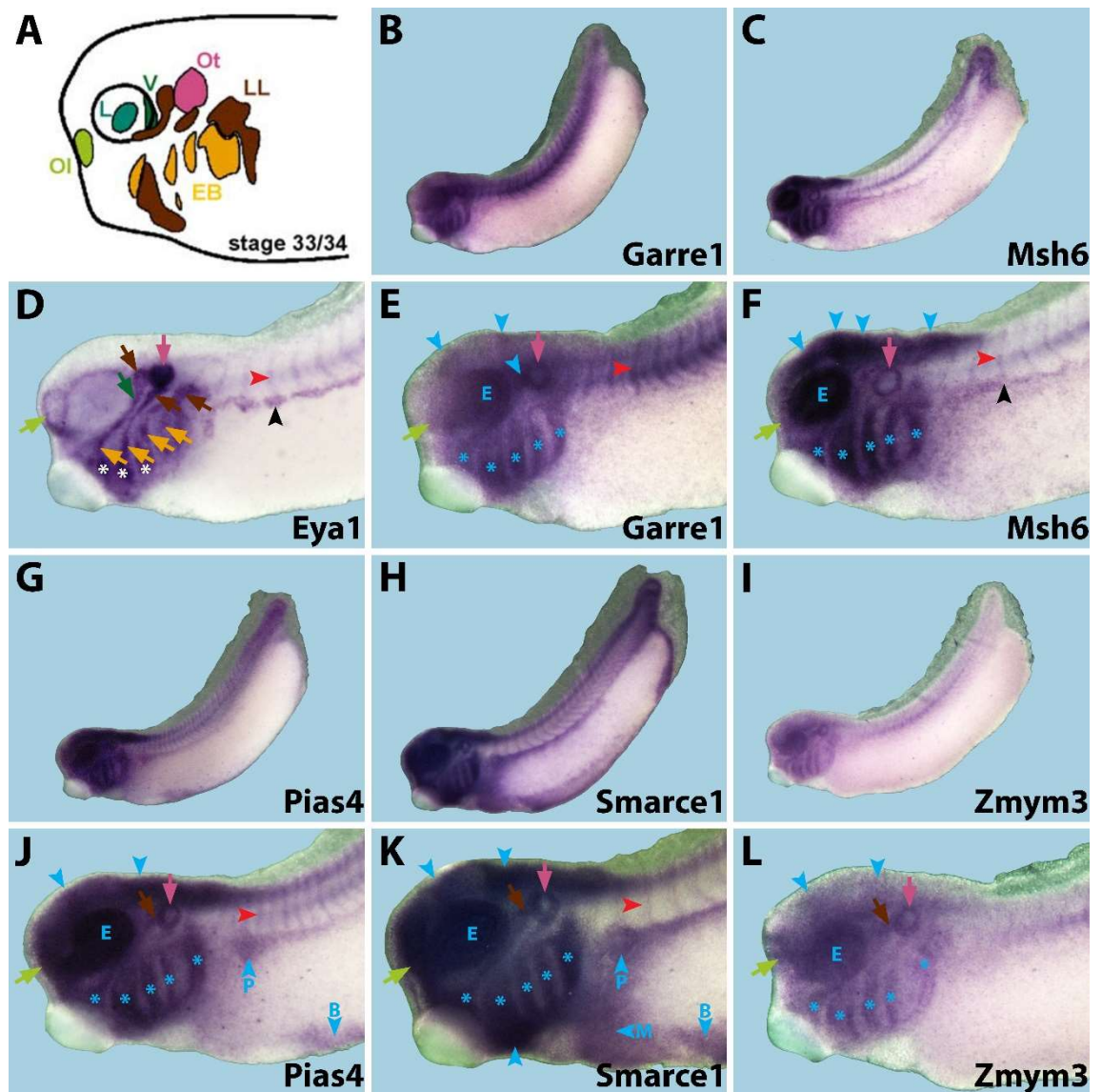
#### *Smarce1:*

*Smarce1* expression at stage 27 was observed in the eye, the olfactory placode and posterior placodal area, in neural crest cells, and in the brain (with stronger expression in midbrain and hindbrain) and spinal cord. In addition, *smarce1* expression could be found in the somites and tailbud, in the proctodeum, at the level of the intermediate mesoderm and/or its derivatives (possibly the developing pronephros and posterior cardinal vein), as well as in presumed blood islands, and in populations of cells in the ventral branchial region, and posteriorly to the branchial region (Fig 3.5 I-J).

#### *Zmym3:*

At stage 27 *zmym3* expression was still visible in the eye, the otic vesicle and the anterodorsal lateral line placode, as well as in the neural crest cells within the pharyngeal arches. Expression was possibly maintained in the trigeminal placode (Fig 3.5 K-L).

### 3.3.4. Stage 34



**Fig. 3.6.** Expression patterns of *eya1* and its candidate interaction partners in whole-mount *Xenopus laevis* embryos at stage 34, in lateral views (anterior is to the left). The schematic drawing (A) shows the distribution of placodes in a late tailbud stage embryo. Arrows indicate expression in placodes and display the colour code used in the drawing, arrowheads and asterisks indicate other areas of expression. Red arrowheads indicate expression in the somites, black arrowheads indicate expression in the hypaxial muscle precursors, and white asterisks indicate expression in the pharyngeal pouches. Blue asterisks (neural crest streams) and arrowheads indicate expression in areas where *eya1* is not expressed. Pictures E, F, J, K and L are magnifications of pictures B, C, G, H and I, respectively. Abbreviations: B, blood islands; E, prospective eye, including lens (L) placode; EB, epibranchial placodes; LL, lateral line placodes; M, lateral plate mesoderm; Ol, olfactory placode; Ot, otic placode; P, pronephros; V, trigeminal placode. Schematic drawing from (Schlosser and Ahrens, 2004).

### *Eya1:*

At stage 34 the placodal derivatives continue to express *eya1* (Fig 3.6 B). The profundal placode has disappeared and the trigeminal placode continues to shrink. Expression is maintained in the endoderm of the pharyngeal pouches and in the somites, and is strong at the base of the tailbud, but is no longer present in the proctodeum. *Eya1* is now also observed in the hypaxial muscle precursors.

### *Garre1:*

*Garre1* kept being expressed in the areas mentioned at stage 27: the eye, the otic vesicle, the olfactory and anterodorsal lateral line placodes, as well as the brain, spinal cord, neural crest cells populating the branchial arches, somites and tailbud. In the brain the expression was still stronger in part of the midbrain, but the area of strong expression in the hindbrain now seemed restricted to one rhombomere (Fig 3.6 C-D).

### *Msh6:*

*Msh6* expression at stage 34 was maintained in the eye, the brain (with stronger expression in the posterior hindbrain and possibly the midbrain-hindbrain boundary, similarly to what was observed at stage 27), the otic vesicle, the olfactory placode, and the neural crest cells populating the branchial arches. Expression was also still present in the somites, tailbud, in the hypaxial muscle precursors, and in an area posterior to the branchial arches and ventral to the somites (Fig 3.6 E-F).

### *Pias4:*

At stage 34 *pias4* expression was maintained in the areas mentioned at stage 27: the eye, the otic vesicle, the olfactory and lateral line placodes, the neural crest cells populating the branchial arches, the brain and spinal cord, the tailbud, and hypothetically the pronephros and ventral blood islands, all exhibit *pias4* expression. In

the brain expression was stronger in the hindbrain and in parts of the midbrain. *Pias4* could now also be observed in the somites (Fig 3.6 G-H).

#### *Smarce1*:

At stage 34, the eye, the olfactory, otic and anterodorsal lateral line placodes, the brain (with stronger expression in the hindbrain) and spinal cord, and the neural crest cells, maintained their *smarce1* expression, as well as the somites, tailbud, proctodeum, intermediate mesoderm/pronephros area, presumed blood islands, and cells located ventrally and posteriorly to the branchial area (Fig 3.6 I-J).

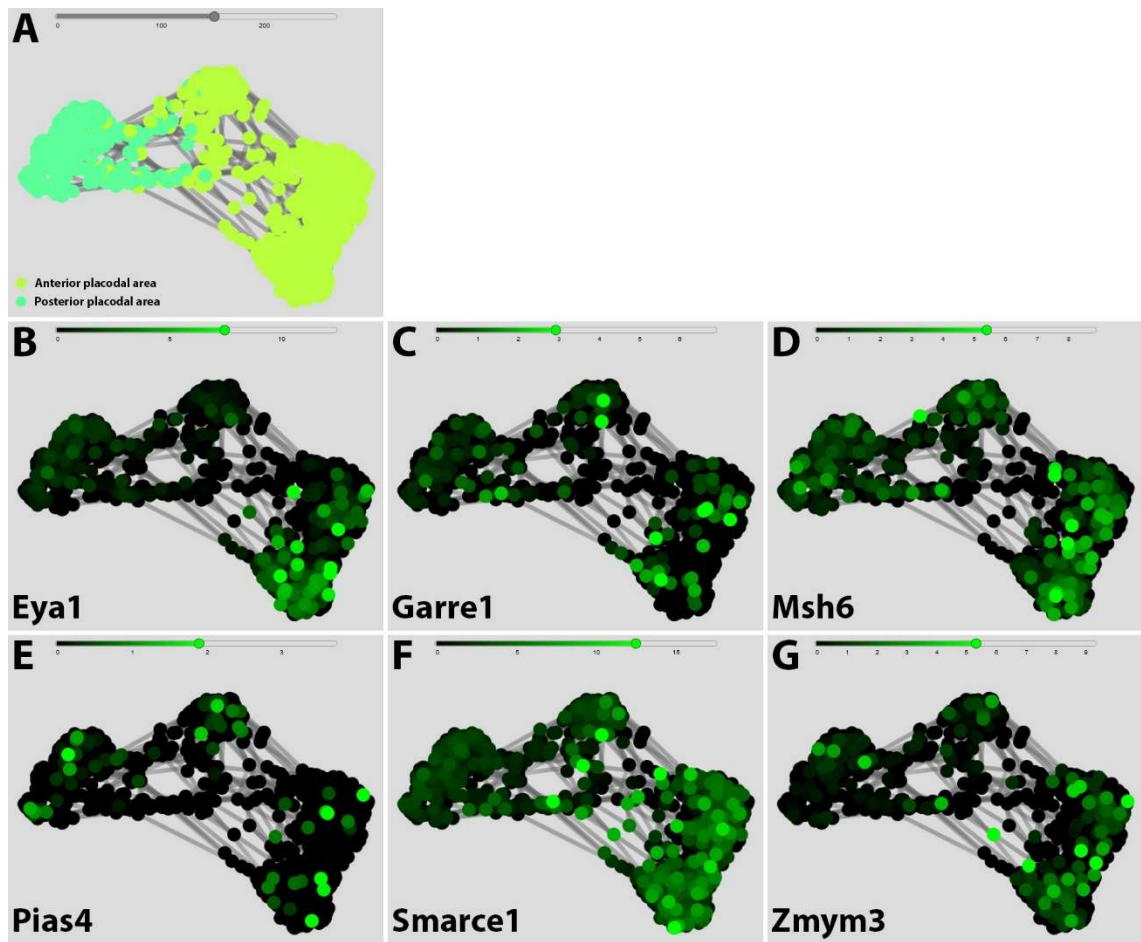
#### *Zmym3*:

*Zmym3* expression was observed in the olfactory epithelium, and was maintained in the eye, the otic vesicle, the anterodorsal lateral line placode and the neural crest cells. Expression was also visible in the brain, and was stronger in two areas located in the midbrain and anterior hindbrain (Fig 3.6 K-L).

### 3.4. Candidate *Eya1* interactants single cell atlas data

The *in situ* experiments confirmed that *eya1* and its candidate interacting partners are expressed in overlapping areas in the developing embryo. I then examined their colocalisation at the cellular level, by consulting single cell data available from the Harvard *Xenopus tropicalis* embryo cell atlas (Briggs et al., 2018; Petrova et al., 2024), focusing on placodal areas at stage 14 (Fig. 3.7).

Single cell data confirmed that the five selected candidate genes, along with *eya1*, are all expressed in anterior and posterior placodal cells, and showed that they all colocalise with *eya1* in at least some of the individual cells. While the expressions of *msh6* and *smarce1* are rather ubiquitous in the placodal area, *garre1* and *zmym3* (similarly to *eya1*) are comparatively expressed in slightly fewer cells, and *pias4* expression displays a more salt and pepper distribution.



**Fig. 3.7.** Single cell expression data from the Harvard *Xenopus* Embryo Cell Atlas (Petrova et al., 2024), for *eya1* and its candidate interactants, in the placodal area of stage 14 *Xenopus tropicalis* embryos. (A) The anterior and posterior placodal cell subpopulations were selected. (B) *Eya1* is expressed in most placodal cells. (C-G) Genes coding for the five selected candidate *Eya1* interactants are all expressed as well in placodal cells, including in at least some of the individual cells expressing *eya1*.

### 3.5. Conclusion

A yeast two-hybrid screening conducted by Hybrigenics from a *Xenopus laevis* cDNA library generated in our lab, lead to the identification of 28 candidate *Eya1* interactants. The gene ontology analysis of these 28 candidates showed that they were mostly involved in transcription regulation and/or protein modification, as was expected for proteins acting in conjunction with the transcriptional coactivator *Eya1*.

The embryonic expression profiles of five of these candidates (*garre1*, *msh6*, *pias4*, *smarce1*, *zmym3*) were analysed by *in situ* hybridization, from neurula stage to late tailbud stage (NF stages 14-18, 22, 27, 34), in order to confirm that they are expressed

in areas overlapping *eya1* expression areas. At all stages considered, these expression profiles overlapped at least partially with that of *eya1*, with all five candidates notably being expressed in the preplacodal ectoderm and some of its derivatives. Contrary to *eya1*, the candidates were also expressed to varying degrees in the neural plate, neural crest, and their derivatives. Data from the Harvard *Xenopus tropicalis* embryo cell atlas confirm that the five candidates are expressed in placodal areas, and all colocalise with *eya1* in at least some of the individual cells.

Overall in this chapter, I provided a characterization of the embryonic expression profiles of *garre1*, *msh6*, *pias4*, *smarce1* and *zmym3* in *Xenopus laevis*, and I showed that these expression profiles are consistent with a function involving an interaction with Eya1.

## Chapter 4. Validation of Interaction between Eya1 and Candidate Cofactors

### 4.1. Co-immunoprecipitation of Eya1 and candidate cofactors

Since the genes *garre1*, *msh6*, *pax3*, *pias4*, *smarce1*, *sox11*, *sox7* and *zmym3* displayed expression patterns that are compatible with a role in sensory neurogenesis in conjunction with *eya1*, and since they code for proteins that were identified as Eya1 interaction partners by the Hybrigenics yeast two-hybrid screen, I attempted to further strengthen the evidence for the interaction of each of these candidates with Eya1 by co-immunoprecipitation, in order to select the most reliable candidates for subsequent functional studies.

My strategy consisted in injecting mRNA coding for tagged versions of the candidate proteins along with *eya1* mRNA in *X. laevis* embryos, and performing co-immunoprecipitations on protein extracts from these embryos, followed by SDS-PAGE and western blotting. Eya1 detection was performed using a reliable Eya1 antibody (Almasoudi and Schlosser, 2021), and the detection of candidate interaction partners was enabled by using protein fusion constructs with a common tag, allowing us to label any candidate via a single commercial antibody.

#### 4.1.1. Flag-tagged candidates

I attempted to generate pCS2+ expression vectors coding for C-term flag-tagged versions of the eight selected candidates. cDNA for their coding sequence was generated by reverse transcription from total embryonic mRNA, and the flag tag was added to the sequence by PCR.

Three of the candidates were successfully cloned, sequenced and used for mRNA transcription and embryo injection (*Pias4*-flag, *Sox11*-flag, *Zmym3*-flag), but all attempts to detect these proteins in embryo extracts using anti-flag antibodies failed (even

though I could detect flag-tagged versions of Six1), making it impossible to use these constructs for co-immunoprecipitation experiments.

#### 4.1.2. (Twin-)Strep-tagged Pias4

Since I could not detect the flag-tagged candidate proteins by western blotting, I tested whether using another type of tag would lead to better results.

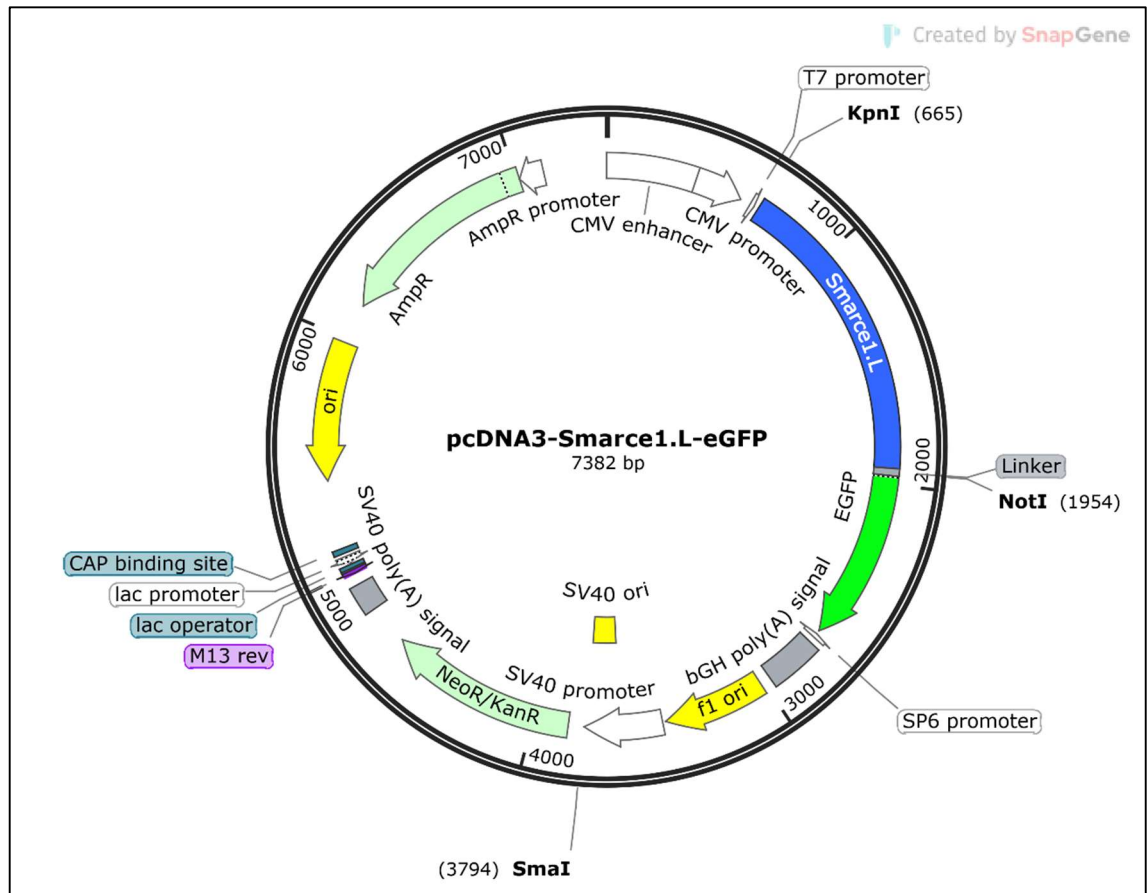
Strep-tag II has a high affinity for Strep-Tactin (an engineered version of streptavidin), and proteins tagged with Strep-tagII can be efficiently purified using Strep-Tactin affinity columns, and detected by western blotting using Strep-tactin conjugated with horseradish peroxidase (HRP). As a proof of concept I generated and tested expression vectors coding for C-term and N-term Strep-tagged versions of one of the candidates, Pias4, as well as an expression vector coding for a C-term Twin-Strep-tagged version of Pias4 (the Twin-Strep tag binds to Strep-Tactin with even higher affinity than the Strep-tagII). These Strep-tag constructs were generated in a similar fashion to the flag-tag constructs: the Strep-tags were added to the candidate sequences by PCR, and the resulting amplicons were cloned into pCS2+ vectors.

Again the use of these constructs was largely unsuccessful: on one occasion I could detect the C-term tagged version of Pias4, that I generated using an in vitro transcription/translation system and in which the lysine residues were biotinylated, which enhanced the detection of the protein since biotin, like Strep-tagII, also has a strong affinity for Strep-Tactin-HRP. On one occasion I could also detect the Twin-Strep-tagged version of Pias4. However I could not reproduce these results, and did not proceed further with the generation or use of Strep-tagged constructs.

#### 4.1.3. eGFP-tagged candidates

My third approach was to generate eGFP-tagged constructs, by cloning the coding sequence of candidates into a pcDNA3-eGFP expression vector (see Fig. 4.1). A GSGSGSRPLE linker was inserted between the protein of interest and the C-term eGFP tag to ensure flexibility and mitigate potential misfolding.

Three candidates (Pias4.S, Smarce1.L and Sox11.S) were successfully tagged and their presence in whole protein extracts from injected embryos was consistently detected by western blotting using an anti-GFP antibody, which was a necessary condition before any co-immunoprecipitation experiment could be undertaken. I also generated an expression vector coding for an eGFP-tagged version of Six1.L, that I used in these co-immunoprecipitation experiments as a positive control for interaction with Eya1.

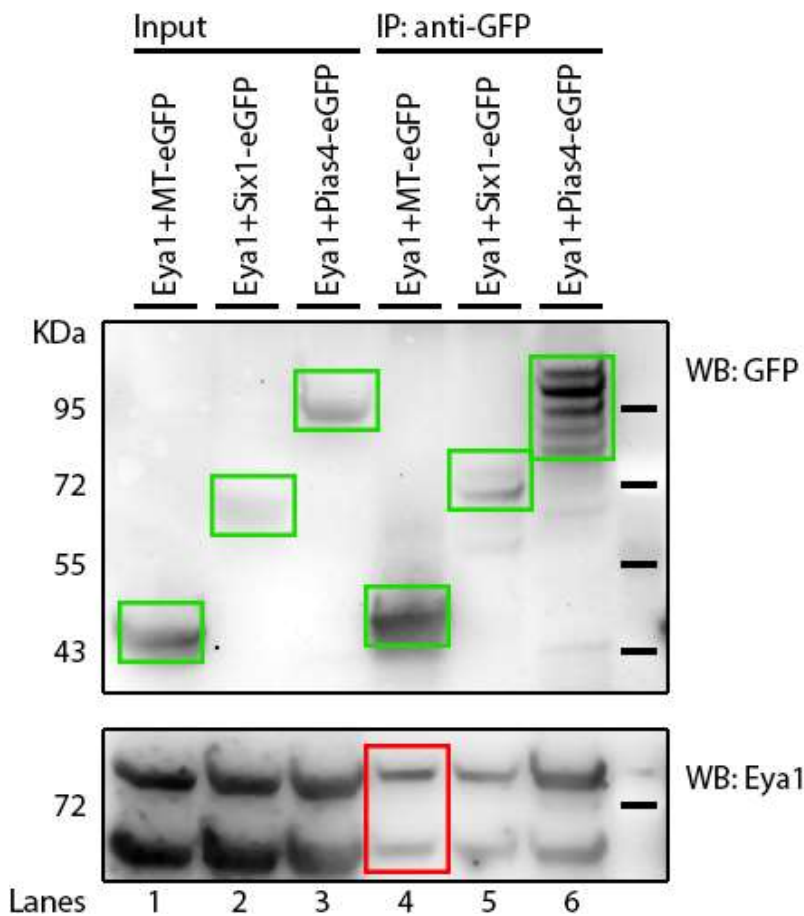


**Fig. 4.1.** Map displaying the main features of the pcDNA3-Smarce1.L-eGFP expression vector. The coding sequence of Smarce1.L was cloned between KpnI and NotI restriction sites. The vector was linearized with SmaI prior to T7 in vitro transcription. All eGFP fusion protein constructs were generated in a similar fashion.

#### 4.1.4. Co-immunoprecipitation experiments

Once I ensured that the eGFP-tagged proteins were detectable by western blotting, I could perform co-immunoprecipitation experiments on protein extracts containing both Eya1 and an eGFP-tagged candidate partner. Six1-eGFP was used as a positive control for interaction with Eya1, and MT-eGFP as a negative control.

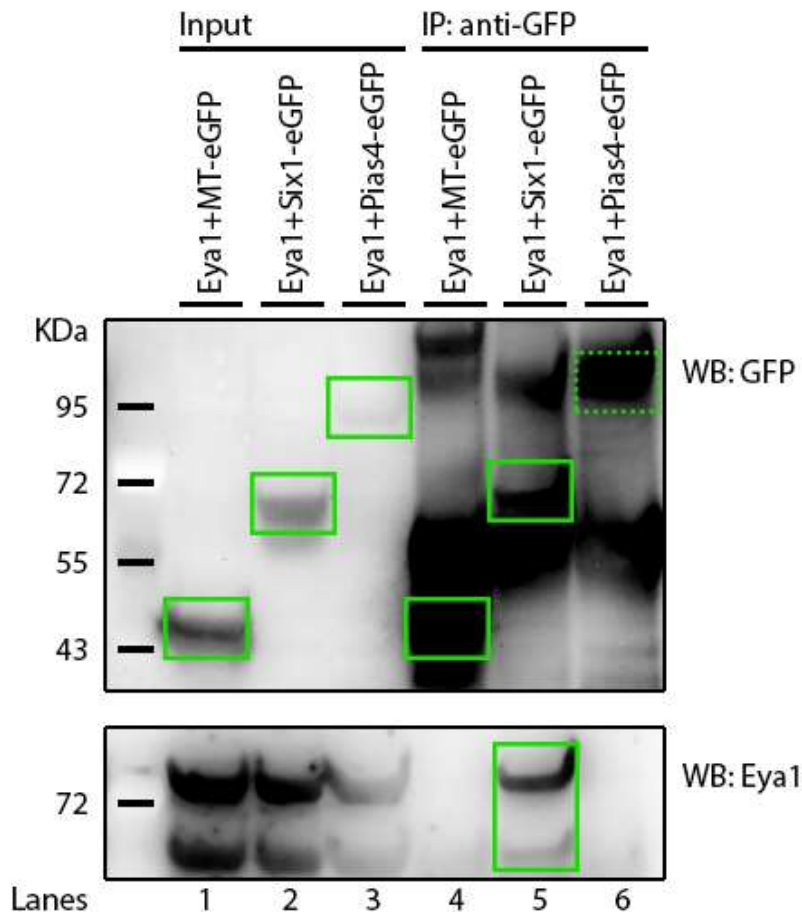
I first attempted co-immunoprecipitations on samples containing Eya1 and Pias4-eGFP, using commercial agarose beads covalently linked to an anti-GFP antibody (GFP-Catcher beads). While those beads were able to pull down the eGFP-tagged proteins (Fig. 4.2, lanes 4 to 6), Eya1 was also present in the eluates of each sample, including the negative control (Fig. 4.2, lane 4), indicating that the beads were non-specifically binding Eya1. Therefore no reliable co-immunoprecipitation result could be obtained using the GFP-Catcher beads.



**Fig. 4.2.** Western blot analysis of protein co-immunoprecipitation using GFP-catcher beads, on total protein extracts from embryos co-injected with mRNA coding for Eya1 and MT-eGFP (negative control), Six1-eGFP (positive control) or Pias4-eGFP. Eya1 and the eGFP-tagged proteins were present in the total protein extracts (lanes 1 to 3). The eGFP-tagged proteins were immunoprecipitated (lanes 4 to 6). Eya1 was also present in every eluate, including the negative control sample eluate (lane 4), indicating non-specific binding to the beads.

Co-immunoprecipitations were then carried out using Protein G magnetic beads, that I coupled with an anti-GFP antibody (Fig. 4.3). MT-eGFP and Six1-eGFP were successfully pulled down (Fig. 4.3, lanes 4-5). I assume that Pias4-eGFP was pulled down as well, since a band corresponding approximately to the expected size of Pias4-eGFP could be seen (Fig. 4.3, lane 6). However the band was very broad and background staining could be seen at the same level in the other IP lanes, therefore I cannot be certain that Pias4-eGFP was immunoprecipitated. Since I used the same anti-GFP antibody for bead coupling and for eGFP immunodetection, this background staining was likely due to the fact that upon elution, the anti-GFP antibodies themselves were eluted from the beads along with the proteins they were bound to, and subsequently produced a signal on western blots. To circumvent this problem, I tried using other anti-GFP antibodies for immunodetections, but they did not produce a signal on blots.

Despite the caveat of high background staining, using these beads improved the reliability of the co-immunoprecipitations. Unlike the GFP-Catcher beads, the Protein G beads did not bind Eya1 unspecifically: Eya1 was absent in the negative control eluate, and was pulled down in the Six1-eGFP-containing sample only (Fig. 4.3, lanes 4-5). However Eya1 was also absent in the Pias4-eGFP sample eluate, either because Pias4-eGFP was not or insufficiently immunoprecipitated, because the Eya1-Pias4 interaction was disrupted by inadequate stringency conditions, or because Eya1 and Pias4 generally do not interact.

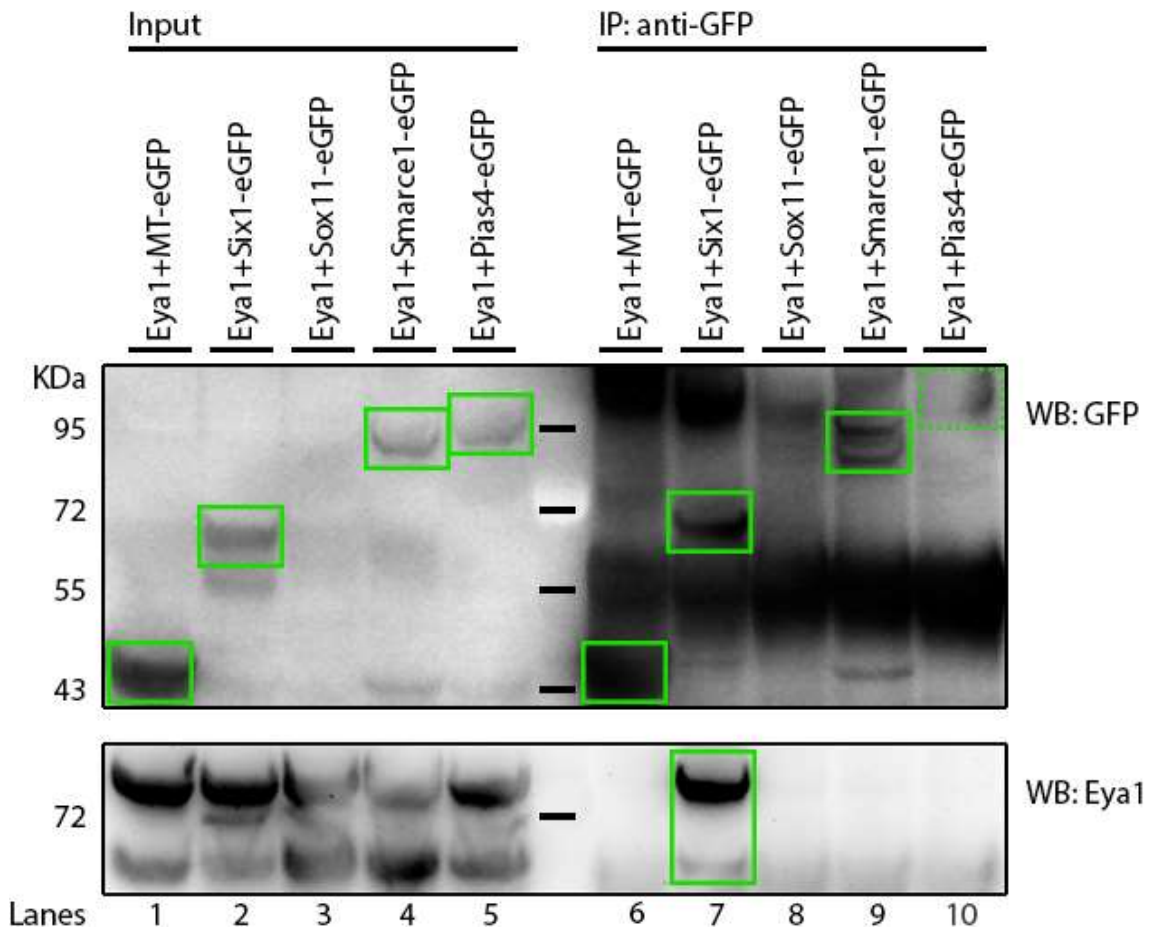


**Fig. 4.3.** Western blot analysis of protein co-immunoprecipitation using Protein G beads coupled with anti-GFP antibody, on total protein extracts from embryos co-injected with mRNA coding for Eya1 and MT-eGFP (negative control), Six1-eGFP (positive control) or Pias4-eGFP. Eya1 and the eGFP-tagged proteins were present in the total protein extracts (lanes 1 to 3). Eya1-MT-eGF, Six1-eGFP, and possibly Pias4-eGFP, were immunoprecipitated (lanes 4 to 6). Eya1 was co-immunoprecipitated in the positive control sample only (lane 5).

I continued using Protein G beads coupled with anti-GFP antibody for subsequent co-immunoprecipitation experiments, and tested for interaction with Eya1 eGFP-tagged versions of Sox11 and Smarce1 in addition to Pias4. With the exception of Sox11-eGFP, these proteins were detected at their respective approximate expected sizes in the input samples (Fig. 4.4, lanes 1 to 5), as well as in the corresponding bead eluates (Fig. 4.4, lanes 6 to 10), indicating proper pull down (at the possible exception of Pias4-eGFP, whose presumptive signal is weak in the eluate).

Again, Eya1 was not pulled down in the negative control sample, and was properly pulled down by Six1-eGFP (Fig. 4.4, lanes 6-7). However this experiment still did not provide

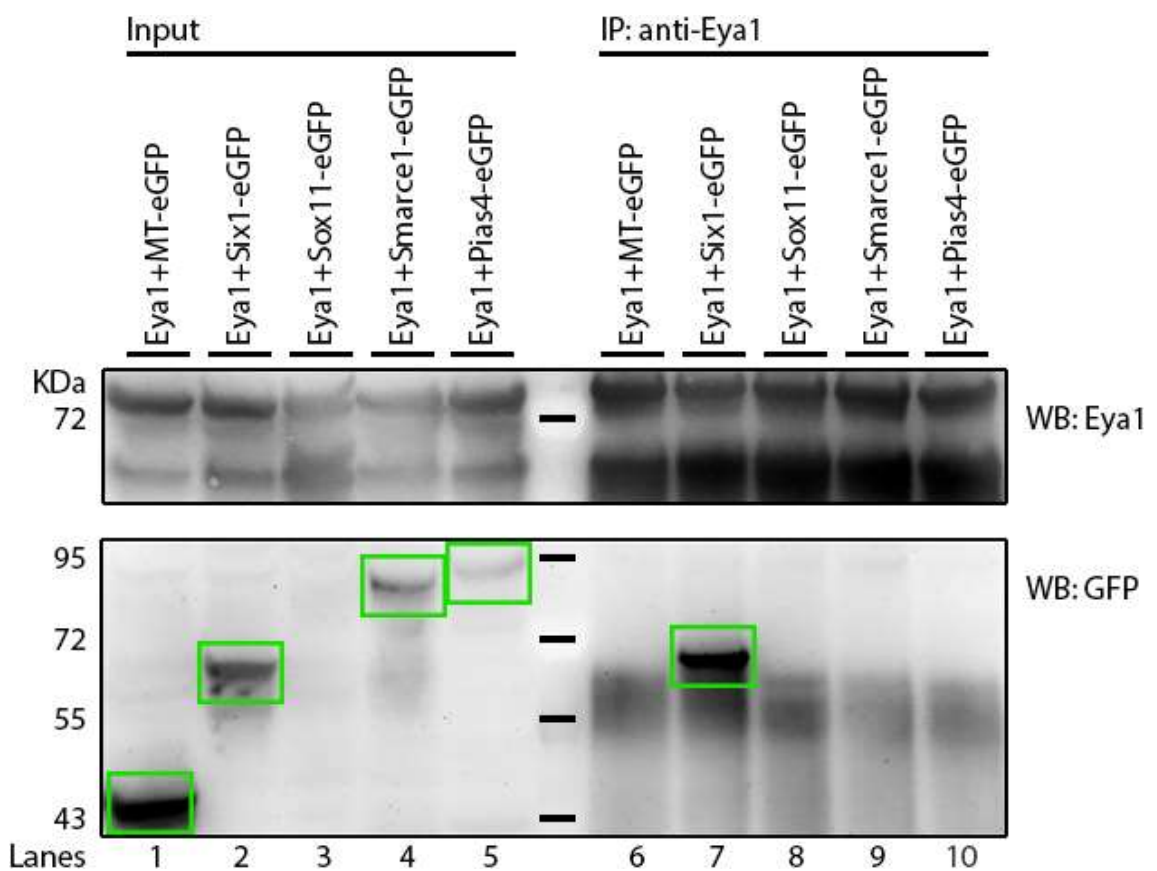
evidence for interaction between Eya1 and the three tested candidates, since none of them immunoprecipitated Eya1 (Fig. 4.4, lanes 8 to 10).



**Fig. 4.4.** Western blot analysis of protein co-immunoprecipitation using Protein G beads coupled with anti-GFP antibody, on total protein extracts from embryos co-injected with mRNA coding for Eya1 and MT-eGFP (negative control), Six1-eGFP (positive control), Sox11-eGFP, Smarce1-eGFP or Pias4-eGFP. Eya1 and all eGFP-tagged proteins except Sox11-eGFP were present in the total protein extracts (lanes 1-2-4-5). Eya1-MT-eGF, Six1-eGFP, Smarce1-eGFP, and possibly Pias4-eGFP, were immunoprecipitated (lanes 6-7-9-10). Eya1 was co-immunoprecipitated in the positive control sample only (lane 7).

I then carried out a reverse co-immunoprecipitation, using Protein A magnetic beads that I coupled with our anti-Eya1 antibody. An advantage of reverse co-immunoprecipitations was that, the anti-Eya1 antibody and the anti-GFP antibody being raised in different species, the anti-Eya1 antibodies present in the bead eluates did not produce a parasitic signal that would mask the signal emitted by eGFP-tagged proteins on anti-GFP immunoblots.

I tested again the three previously tested candidates for interaction with Eya1. Eya1 was detected in each input sample, as well as in each bead eluate, meaning that Eya1 was successfully pulled down by the beads (Fig. 4.5, lanes 1 to 10). With the exception of Sox11-eGFP, all the eGFP-tagged proteins were also detected in the input samples (Fig. 4.5, lanes 1 to 5). MT-eGFP was not present in the eluate, confirming that eGFP does not bind unspecifically to the Protein A beads, and Six1-eGFP was pulled down by Eya1 as expected (Fig. 4.5, lanes 6-7). However once again, Sox11-eGFP, Smarce1-eGFP and Pias4-eGFP were not pulled down (Fig. 4.5, lanes 8 to 10).



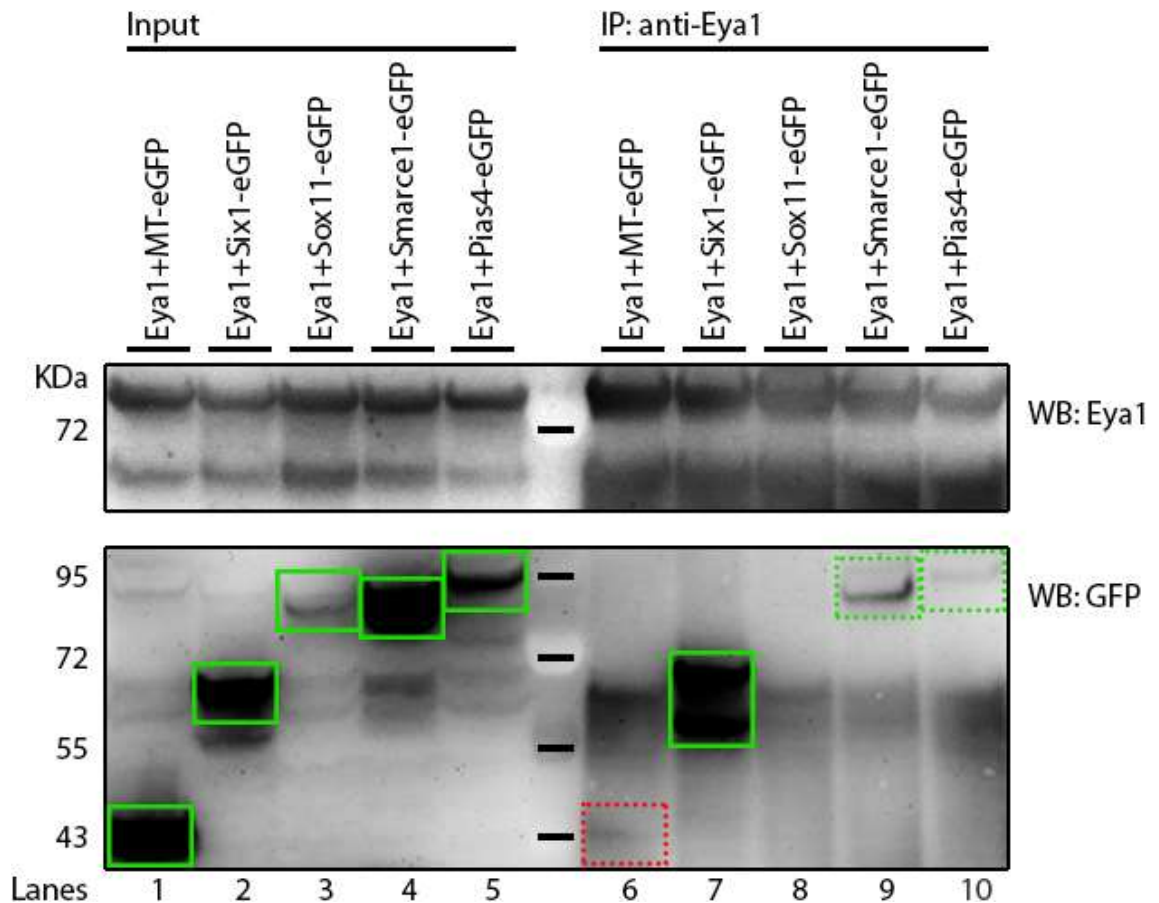
**Fig. 4.5.** Western blot analysis of protein co-immunoprecipitation using Protein A beads coupled with anti-Eya1 antibody, on total protein extracts from embryos co-injected with mRNA coding for Eya1 and MT-eGFP (negative control), Six1-eGFP (positive control), Sox11-eGFP, Smarce1-eGFP or Pias4-eGFP. Eya1 and all eGFP-tagged proteins except Sox11-eGFP were present in the total protein extracts (lanes 1-2-4-5). Eya1 was immunoprecipitated in all samples (lanes 6 to 10). Among the eGFP-tagged proteins, only the positive control Six1-eGFP was co-immunoprecipitated (lane 7).

In co-immunoprecipitations the stringency of the buffer used to wash the beads after antigen binding is an important factor: a less stringent buffer is less likely to prevent non-specific protein binding, while a more stringent buffer is more likely to disrupt the specific protein interactions that we want to detect (Trinkle-Mulcahy et al., 2008). Therefore finding the right balance is critical, especially if we want to detect weak or transient protein-protein interactions.

Since the stringency of the wash buffer that was used in the previous co-immunoprecipitation experiments was quite high, I hypothesized that this high stringency could have been the cause for the failure to detect interactions between Eya1 and its candidate interactants, if these interactions are weak or transient.

Therefore I repeated the same reverse co-immunoprecipitation experiment, using a less stringent wash buffer. Eya1 and each eGFP-tagged protein, this time including Sox11-eGFP, were detected in the input samples (Fig. 4.6, lanes 1 to 5). The beads pulled down Eya1 in each sample (Fig. 4.6, lanes 6 to 10), and as expected, Six1-eGFP was pulled down by Eya1 (Fig. 4.6, lane 7). Smarce1-eGFP, and more weakly Pias4-eGFP, were detected in the eluate, suggesting that they were immunoprecipitated by Eya1 (Fig. 4.6, lanes 9-10) under these low-stringency conditions. Sox11-eGFP was not present in the eluate, suggesting that it is not immunoprecipitated by Eya1, although this negative finding could also have resulted from a low amount of this protein present in the input, as observed in lane 3.

As a caveat, a very weak band was also observed in the MT-eGFP eluate (Fig. 4.6, lane 6), casting some doubt on the reliability of the positive results obtained for Smarce1-eGFP and Pias4-eGFP. However, the MT-eGFP signal was very faint, suggesting that non-specific protein binding on the beads was minimal.



**Fig. 4.6.** Western blot analysis of protein co-immunoprecipitation using Protein A beads coupled with anti-Eya1 antibody and a mild wash buffer, on total protein extracts from embryos co-injected with mRNA coding for Eya1 and MT-eGFP (negative control), Six1-eGFP (positive control), Sox11-eGFP, Smarce1-eGFP or Pias4-eGFP. Eya1 and all eGFP-tagged proteins were present in the total protein extracts (lanes 1 to 5). Eya1 was immunoprecipitated in all samples (lanes 6 to 10). The positive control Six1-eGFP was co-immunoprecipitated (lane 7). Smarce1-eGFP and Pias4-eGFP were also co-immunoprecipitated (lanes 9 and 10), but MT-eGFP was weakly detectable in the negative control eluate as well (lane 6).

In summary, after trying many other approaches to confirm protein-protein interactions, I successfully established the co-IP method by using eGFP-tagged candidates and anti-GFP antibodies coupled with protein-G magnetic beads (or alternatively anti-Eya1 antibodies coupled with protein-A magnetic beads). I generated eGFP-tagged versions of Pias4, Smarce1, Sox11, and Six1 (positive control) that were consistently detectable by western blotting. The Eya1-Six1 interaction was consistently detected, but while I obtained some evidence for Eya1-Pias4 and Eya1-Smarce1 interactions, my findings are not entirely conclusive, because of some weak unspecific binding remaining in my control sample.

## 4.2. One-by-one validation by solid growth tests (by Hybrigenics)

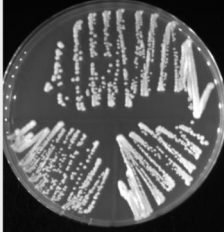

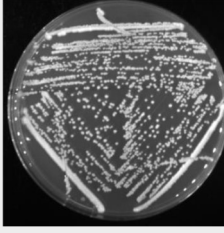
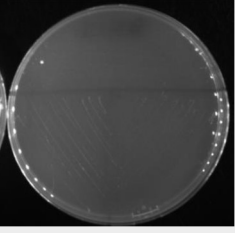
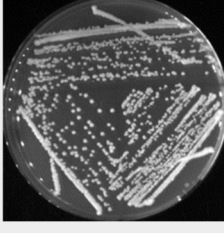
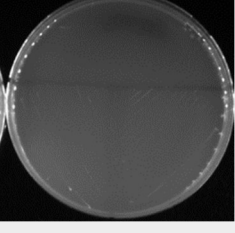
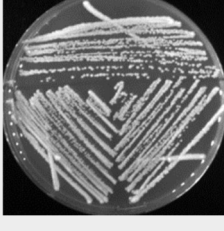
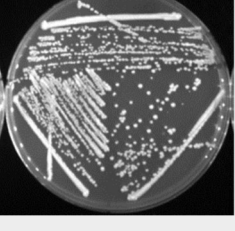
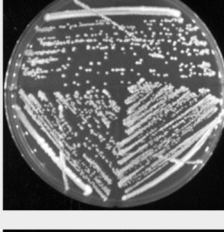
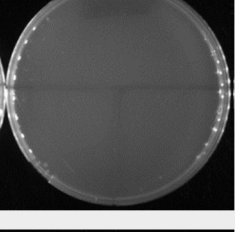
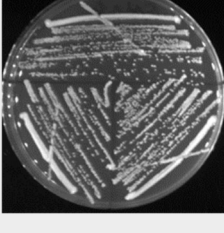
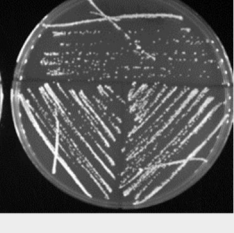
To further confirm the interaction between Eya1 and Pias4 and/or Smarce1, one-by-one yeast two-hybrid tests were performed by Hybrigenics. These tests were based on the same principle as the two-hybrid screening (see chapter 3): a vector coding for the prey fragment (Eya1) fused to a DNA binding domain (DBD), and a vector coding for the bait fragment (Pias4 or Smarce1) fused to an activation domain (AD), were co-transformed into yeast cells. If the prey fragment and the bait fragment interact, their DBD and AD domains reconstitute a transcription factor allowing the growth of the yeast cells on a medium lacking histidine.

These cells were either grown on a medium lacking tryptophane and leucine (DO-2), selective for the presence of both DBD and AD fusions, or on a medium lacking tryptophane, leucine and histidine (DO-3), selective for the interaction between the DBD and AD fusions. The one-by-one test included negative controls, with Eya1 and the empty AD vector as well as the empty DBD vector with the preys, and a positive control with bait and prey vectors coding for two known interactants, SMAD and SMURF, respectively (Fig. 4.7).

On the solid growth tests performed for Pias4 and Smarce1 (see Fig. 4.7), we could observe that, while cells co-transformed with the Eya1 pB27 vector and the empty pP7 vector could grow on DO-2 medium (indicating that both the DBD and the AD domains were present), they could not do so on DO-3 medium, which confirmed that DBD and AD domains do not spontaneously interact if they are not fused to interacting bait and prey fragments. Similarly, pP6 vectors bearing sequences coding for Pias4 or Smarce1, co-transformed with the empty pB27 vector, allowed growth of the transformed cells on DO-2 only.

When the Eya1 pB27 vector was co-transformed with either the Pias4 pP6 or the Smarce1 pP6 vector, however, the transformed cells could grow on both types of medium, indicating that Eya1 was indeed interacting with these candidates.

These solid growth test positive results were in line with the two-hybrid screening results for Pias4 and Smarce1, and seem to reinforce the evidence provided by the co-immunoprecipitation experiments that these candidates are indeed cofactors of Eya1.

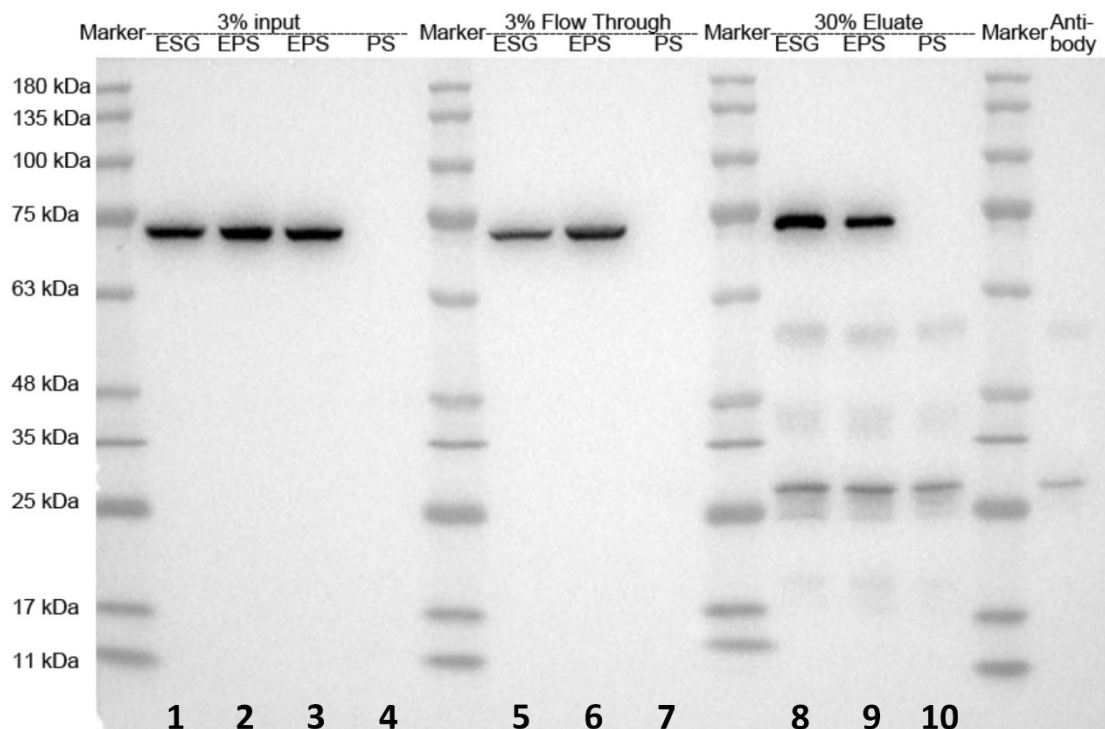
| Interaction Matrix |                  |                 | Selection Medium   |   |
|--------------------|------------------|-----------------|--|---|
| Type               | Bait             | Prey            | DO-2   | DO-3  |
| Positive control   | SMAD             | SMURF           |    |    |
| Negative control   | Eya1             | pP7 $\emptyset$ |    |    |
| Negative control   | pB27 $\emptyset$ | Smarce1         |  |  |
| Interaction        | Eya1             | Smarce1         |  |  |
| Negative control   | pB27 $\emptyset$ | Pias4           |  |  |
| Interaction        | Eya1             | Pias4           |  |  |

**Fig. 4.7.** One-by-one yeast two-hybrid solid growth tests results, provided by Hybrigenics. Baits were expressed in a LexA DNA-Binding-Domain vector (pB27), preys were expressed in a Gal4 Activation Domain vector (pP6 or pP7). Yeast cells that were co-transformed with vectors coding for fragments of Eya1 + Smarce1, and with vectors coding for fragments of Eya1 + Pias4, were able to grow on a medium lacking histidine, indicating a physical interaction between these two protein fragments. DO-2: selective medium without tryptophane and leucine; DO-3: selective medium without tryptophane, leucine and histidine; pB27 $\emptyset$ : empty pB27 vector; pP7 $\emptyset$ : empty pP7 vector.

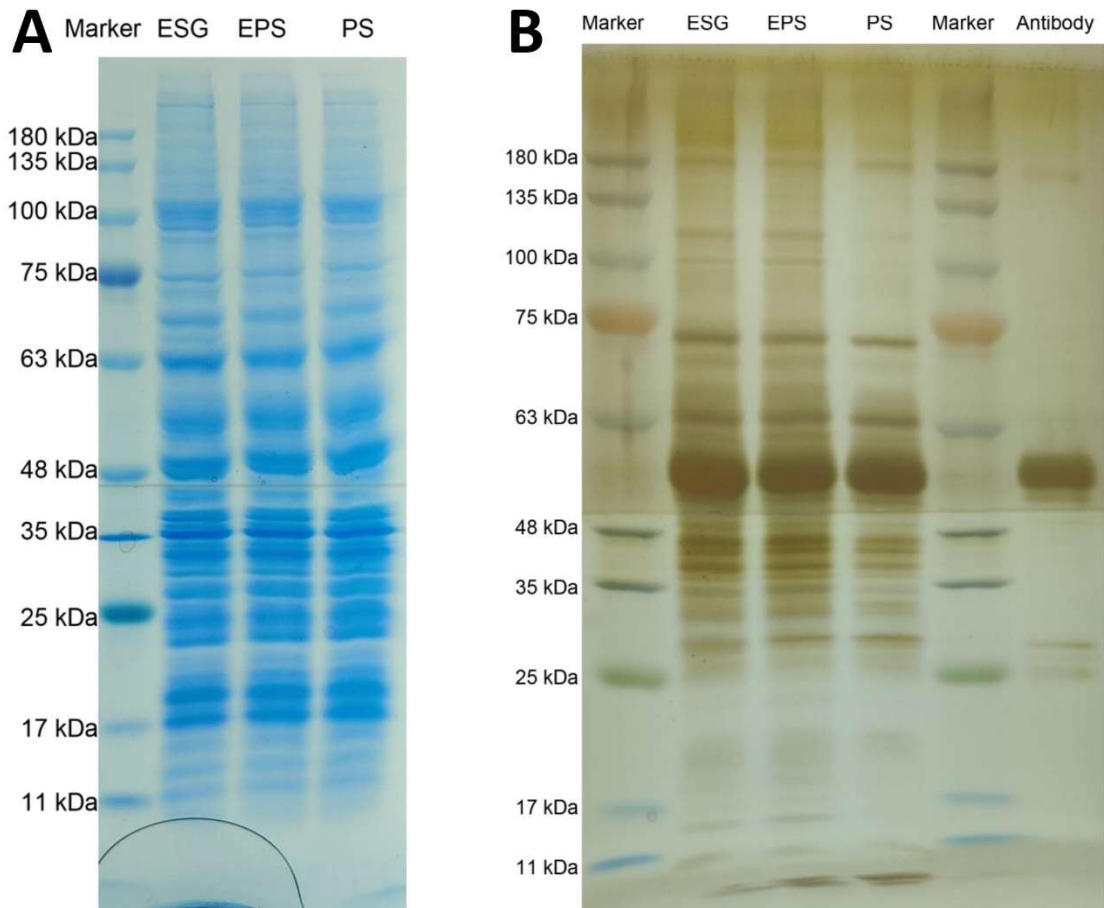
### 4.3. Mass spectrometry

As a fourth way of confirming that Pias4 and Smarce1 are Eya1 interactants, I solicited the company Creative Proteomics to conduct a co-immunoprecipitation using our Eya1 antibody followed by mass spectrometry, on protein lysates from embryos injected with mRNAs coding for either Eya1 + N-term-flag-Six1 + eGFP (ESG - positive control), Eya1 + Pias4 + Smarce1-C-term-HA (EPS), and Pias4 + Smarce1-C-term-HA (PS - negative control).

The success of Eya1 immunoprecipitation was confirmed by western blotting (Fig. 4.8), and a comparison of total protein stainings performed before and after co-immunoprecipitation, confirmed that some amount of Eya1 interactants were captured along with Eya1 (Fig. 4.9).



**Fig. 4.8.** Western blot anti-Eya1 performed by Creative Proteomics, confirming the success of Eya1 immunoprecipitation. ESG: Eya1-Six1-eGFP samples (positive controls); EPS: Eya1-Pias4-Smarce1 samples; PS: Pias4-Smarce1 samples (negative controls). Eya1 is detected in the expected whole lysates (lanes 1 to 3) and immunoprecipitation eluates (lanes 8-9). Eya1 is also detected in the flow throughs (lanes 5-6) indicating that the high quantity of Eya1 in the whole lysates exceeds the capture capacity of the beads. All negative controls are negative (lanes 4-7-10).



**Fig. 4.9.** Total protein stainings on blots performed by Creative Proteomics, confirming the capture of Eya1 interactants by co-immunoprecipitation. (A) Total protein staining corresponding to the whole lysates. All three samples display similar staining profiles. (B) Total protein staining corresponding to the co-immunoprecipitation eluates. While the eluates of samples containing Eya1 (ESG and EPS) have similar staining profiles, less staining is visible for the eluate of the PS sample. The proteins present in ESG and EPS, but not in PS, should correspond to the proteins that were captured by Eya1. ESG: Eya1-Six1-eGFP samples (positive controls); EPS: Eya1-Pias4-Smarce1 samples; PS: Pias4-Smarce1 samples (negative controls).

After the co-immunoprecipitation was established, Liquid Chromatography Tandem Mass Spectrometry (LC-MS/MS) was performed by Creative Proteomics on the co-immunoprecipitation eluates. The expectations were that, aside from Eya1, Six1 would

show an enrichment in the ESG eluate, and to a lesser extent in the EPS eluate (endogenous Six1), compared to the PS eluate. If Pias4 or Smarce1 interact with Eya1, one could similarly expect an enrichment in the EPS eluate. More generally, all other proteins interacting with Eya1 should ideally show an enrichment in the ESG and EPS eluates compared to the PS eluate. For those proteins, the ESG and EPS samples could be considered as duplicates.

The mass spectrometry produced a total of 1494 protein hits. Two parameters were considered when analyzing these hits: the scores, and the LFQ intensities.

Scores were calculated for each protein, derived from peptide posterior error probabilities (PEP). The PEP of a peptide is the probability of that peptide being wrongly identified. The protein score is the product of peptide PEPs (one for each sequence). A higher score means a higher probability that the protein was correctly identified.

The LFQ (Label-Free Quantification) intensities provide a normalized, relative quantification of proteins across the different samples, allowing to compare abundances between samples.

I compared the LFQ intensities relative to my three different samples (ESG, EPS, PS). First I examined these values for Eya1, Six1, Pias4 and Smarce1 (Table 4.1). The expectations were met for Eya1, whose LFQ intensities were much higher in the ESG and EPS samples than in the PS sample, reflecting a successful immunoprecipitation and MS/MS identification. However Six1 was virtually absent from the ESG sample, in which its concentration should have been the highest. As for Pias4, it was only present in the PS sample (negative control for co-immunoprecipitation), and its score was relatively low, rendering its identification dubious. Smarce1 was not detected in any sample. Thus these MS/MS results did not allow to draw any conclusion regarding the interaction between Eya1 and the candidates Pias4 and Smarce1.

**Table 4.1.** MS/MS identity scores and LFQ intensities for Eya1 and its known (Six1) or candidate (Pias4, Smarce1) protein partners.

|         | Score    | LFQ ESG    | LFQ EPS    | LFQ PS   |
|---------|----------|------------|------------|----------|
| Eya1    | 323.31   | 3765200000 | 8840900000 | 5494700  |
| Six1    | 163      | 0          | 955310000  | 55002000 |
| Pias4   | 13.904   | 0          | 0          | 10209000 |
| Smarce1 | (absent) | /          | /          | /        |

I also paid particular attention to the candidates previously identified in the two-hybrid screening (see Chapter 3) (Table 4.2). Only two of these candidates were present in the MS/MS dataset. The lars1.S hit seemed reliable: it had a high score and its LFQ intensities in the Eya1 samples were both more than twice the LFQ intensity in the negative control, indicating significant enrichment when Eya1 is present. The Msh6 result was less reliable, the identity score being low and the LFQ intensity being zero in the ESG sample.

**Table 4.2.** Eya1 candidate protein partners previously identified by two-hybrid screening and present in the MS/MS dataset.

|         | Score  | LFQ ESG  | LFQ EPS  | LFQ PS   | LFQ ESG/PS | LFQ EPS/PS |
|---------|--------|----------|----------|----------|------------|------------|
| lars1.S | 76.331 | 91482000 | 71084000 | 32925000 | 2.78       | 2.16       |
| Msh6.L  | 14.154 | 0        | 5612600  | 0        | /          | /          |

The rest of the hits was then examined. In order to sort out relevant candidates from the dataset, presenting high probabilities for both identity and interaction with Eya1, I selected the proteins with a score  $\geq 50$  (457/1494 proteins), and within this sublist I selected the proteins with a LFQ  $(\text{ESG} + \text{EPS}) / (2 * \text{PS}) \geq 2$  (in other words, proteins that were at least two times more enriched in the ESG and EPS samples than in the PS sample).

The resulting final list comprises 73 proteins (Table 4.3). As expected Eya1 is the most enriched protein, being on average more than 1000 times more abundant in the Eya1

samples compared to the PS sample. An unidentified, Ig-like domain-containing protein also appears among the most enriched proteins; this could correspond to the anti-Eya1 antibody used for co-immunoprecipitation prior to mass spectrometry.

Endogenous Six1 from the EPS sample showed a high enrichment (17x) but astonishingly, Six1 is virtually absent from the ESG sample, in which it should have been the most abundant. This could be due to the injection of a wrong or degraded version of Six1 mRNA in the embryos used for the ESG sample preparation, although this wouldn't account for the complete absence of Six1, since at least the endogenous Six1 should be present. This will be discussed further in Chapter 6.

Strikingly, the majority of the other proteins were either: cytoskeletal proteins or proteins involved in processes relative to cytoskeleton, vesicular transport or transport to the nucleus; proteins involved in DNA replication; tRNA synthetases; or ribosomal proteins. With the exception of lars1.S, none of those proteins were identified in the two-hybrid screening; this is not necessarily surprising, since the two-hybrid method only identifies direct interactants, while protein complexes can be pulled down by co-immunoprecipitation. However the above-mentioned types of proteins are particularly prone to generate false positives in co-immunoprecipitations (see Chapter 6).

#### 4.4. Conclusion

Co-immunoprecipitation experiments did provide some support for but did not allow to conclusively confirm the Eya1-Pias4 and Eya1-Smarce1 interactions, since some level of unspecific binding was also observed for the negative control MT-eGFP. Growth tests performed individually for the Eya1-Pias4 and Eya1-Smarce1 interactions did lead to positive results, in line with the two-hybrid screen results. However since the growth tests are based on the same technology than the two-hybrid screening, they don't really constitute an independent way of confirming these interactions.

Attempting to detect these interactions by mass spectrometry proved unfruitful: Pias4 and Smarce1 did not appear on the list of selected potential Eya1 interaction partners; although this certainly does not invalidate the possibility of an interaction, since with

the exception of *Iars1.S*, none of the candidates identified in the two-hybrid screen appear in that list either.

Overall, although the results obtained by yeast two-hybrid assays (whether screening or one-by-one) were positive, the co-IP-based experiments (western blotting or mass spectrometry) did not allow to conclusively confirm the *Eya1-Pias4* or *Eya1-Smarce1* interactions.

**Table 4.3.** List of Eya1 candidate protein partners identified by MS/MS, presenting high identity scores and high enrichments.

| Protein symbol                             | Protein name  | Score | LFQ intensity<br>EPS | LFQ intensity<br>ESG | LFQ intensity<br>PS | LFQ<br>EPS/PS | LFQ<br>ESG/PS | (EPS+ESG)<br>/2*PS |
|--|---|-------|----------------------|----------------------|---------------------|---------------|---------------|--------------------|
| <b>Tbcd.L</b>                              | tubulin folding cofactor D                              | 71,95 | 13216000             | 20082000             | 0                   | (LFQ PS = 0)  | (LFQ PS = 0)  | (LFQ PS = 0)       |
| <b>Eya1.L</b>                              | EYA transcriptional coactivator and phosphatase 1       | 71,16 | 0                    | 17985000             | 0                   | (LFQ PS = 0)  | (LFQ PS = 0)  | (LFQ PS = 0)       |
| <b>LOC443608</b>                           | granulin 2  | 50,13 | 84464000             | 187220000            | 0                   | (LFQ PS = 0)  | (LFQ PS = 0)  | (LFQ PS = 0)       |
| <b>Eya1.L</b>                              | EYA transcriptional coactivator and phosphatase 1       | 323,3 | 8840900000           | 3765200000           | 5494700             | 1608,987      | 685,242       | 1147,114           |
| <b>(Ig-like domain-containing protein)</b> | (Ig-like domain-containing protein)                     | 58,51 | 9394600000           | 8072400000           | 606800000           | 15,482        | 13,303        | 14,393             |
| <b>Six1.L</b>                              | SIX homeobox 1  | 163   | 955310000            | 0                    | 55002000            | 17,369        | 0,000         | 8,684              |
| <b>Ipo7.S</b>                              | importin 7  | 89,59 | 75405000             | 97505000             | 17064000            | 4,419         | 5,714         | 5,067              |
| <b>Tubal3.S</b>                            | tubulin alpha like 3 gene 1                             | 71,08 | 474280000            | 566730000            | 119930000           | 3,955         | 4,726         | 4,340              |
| <b>Kpnb1.S</b>                             | karyopherin (importin) beta 1                           | 247,4 | 615190000            | 1011700000           | 201560000           | 3,052         | 5,019         | 4,036              |
| <b>Dlat.L</b>                              | dihydrolipoamide S-acetyltransferase                    | 63,02 | 212800000            | 46168000             | 32406000            | 6,567         | 1,425         | 3,996              |
| <b>Tubb4a.S</b>                            | tubulin beta 4A class Iva                               | 50,46 | 77845000             | 81715000             | 20266000            | 3,841         | 4,032         | 3,937              |
| <b>Eif2s2.S</b>                            | eukaryotic translation initiation factor 2 subunit beta | 62,57 | 120760000            | 180720000            | 38483000            | 3,138         | 4,696         | 3,917              |
| <b>Lrp1.S</b>                              | LDL receptor related protein 1                          | 143,2 | 143090000            | 89694000             | 30286000            | 4,725         | 2,962         | 3,843              |
| <b>Gfpt1.S</b>                             | glutamine--fructose-6-phosphate transaminase 1          | 123,2 | 63444000             | 114130000            | 27148000            | 2,337         | 4,204         | 3,270              |
| <b>Copa.L</b>                              | COPI coat complex subunit alpha                         | 112,7 | 98627000             | 150420000            | 38265000            | 2,577         | 3,931         | 3,254              |

|                     |  |       |            |           |           |       |       |       |
|---------------------|--|-------|------------|-----------|-----------|-------|-------|-------|
| <b>Rps10.S</b>      | ribosomal protein S10  | 133,5 | 548520000  | 881400000 | 224010000 | 2,449 | 3,935 | 3,192 |
| <b>Rps5.S</b>       | ribosomal protein S5   | 129,3 | 1208000000 | 983300000 | 346460000 | 3,487 | 2,838 | 3,162 |
| <b>Cltc.L</b>       | clathrin, heavy chain (Hc)   | 323,3 | 781390000  | 922010000 | 271520000 | 2,878 | 3,396 | 3,137 |
| <b>Cse1L.S</b>      | CSE1 chromosome segregation 1-like   | 256,3 | 508700000  | 766420000 | 204220000 | 2,491 | 3,753 | 3,122 |
| <b>Dync1h1.L</b>    | dynein cytoplasmic 1 heavy chain 1   | 183,6 | 169900000  | 239430000 | 66108000  | 2,570 | 3,622 | 3,096 |
| <b>Mcm7.L</b>       | minichromosome maintenance complex component 7                                   | 134,3 | 91078000   | 136290000 | 37885000  | 2,404 | 3,597 | 3,001 |
| <b>Ipo9.S</b>       | importin 9   | 103,4 | 128210000  | 171550000 | 49985000  | 2,565 | 3,432 | 2,998 |
| <b>Cad.L</b>        | carbamoyl-phosphate synthetase 2, aspartate transcarbamylase, and dihydroorotase | 110,6 | 60690000   | 126400000 | 31392000  | 1,933 | 4,027 | 2,980 |
| <b>Ipo5.S</b>       | importin 5   | 141,9 | 196060000  | 238220000 | 77101000  | 2,543 | 3,090 | 2,816 |
| <b>Cand1.S</b>      | cullin-associated and neddylation-dissociated 1                                  | 239,3 | 339450000  | 477540000 | 148520000 | 2,286 | 3,215 | 2,750 |
| <b>Tuba1c.S</b>     | tubulin alpha 1c   | 112   | 432920000  | 623620000 | 197410000 | 2,193 | 3,159 | 2,676 |
| <b>Mcm5.L</b>       | minichromosome maintenance complex component 5                                   | 107,8 | 120200000  | 182410000 | 56938000  | 2,111 | 3,204 | 2,657 |
| <b>Copg1.L</b>      | COPI coat complex subunit gamma 1  | 98,56 | 66005000   | 110200000 | 33797000  | 1,953 | 3,261 | 2,607 |
| <b>Usp5.S</b>       | ubiquitin specific peptidase 5   | 135,2 | 177620000  | 196420000 | 72976000  | 2,434 | 2,692 | 2,563 |
| <b>LOC108706570</b> | 60S ribosomal protein L9   | 59,37 | 551310000  | 531710000 | 215140000 | 2,563 | 2,471 | 2,517 |
| <b>Lars1.L</b>      | leucyl-tRNA synthetase 1   | 96,54 | 122060000  | 154650000 | 55146000  | 2,213 | 2,804 | 2,509 |
| <b>Myh9.S</b>       | myosin, heavy chain 9, non-muscle  | 223,3 | 180890000  | 186080000 | 73541000  | 2,460 | 2,530 | 2,495 |
| <b>Rpl38.L</b>      | ribosomal protein L38  | 58,14 | 196180000  | 263930000 | 92653000  | 2,117 | 2,849 | 2,483 |
| <b>Mcm4.L</b>       | minichromosome maintenance complex component 4                                   | 106,2 | 125910000  | 157780000 | 57378000  | 2,194 | 2,750 | 2,472 |
| <b>Iars1.S</b>      | isoleucyl-tRNA synthetase 1  | 76,33 | 71084000   | 91482000  | 32925000  | 2,159 | 2,778 | 2,469 |

|                   |  |       |            |            |           |       |       |       |
|-------------------|--|-------|------------|------------|-----------|-------|-------|-------|
| <b>Eif3a.S</b>    | eukaryotic translation initiation factor 3 subunit A     | 304,9 | 941460000  | 572220000  | 307900000 | 3,058 | 1,858 | 2,458 |
| <b>Pold2.L</b>    | polymerase (DNA directed), delta 2, accessory subunit    | 66,46 | 28006000   | 32956000   | 12459000  | 2,248 | 2,645 | 2,447 |
| <b>Tubb4b.L</b>   | tubulin beta 4B class Ivb                                | 323,3 | 509330000  | 701460000  | 249470000 | 2,042 | 2,812 | 2,427 |
| <b>Myh10.S</b>    | myosin, heavy chain 10, non-muscle                       | 66,84 | 23496000   | 13426000   | 7659300   | 3,068 | 1,753 | 2,410 |
| <b>Tubal3.L</b>   | tubulin alpha like 3 gene 1                              | 314,5 | 511130000  | 759150000  | 265910000 | 1,922 | 2,855 | 2,389 |
| <b>Usp10.S</b>    | ubiquitin specific peptidase 10                          | 67,64 | 73474000   | 82300000   | 32731000  | 2,245 | 2,514 | 2,380 |
| <b>Amdhd1.L</b>   | amidohydrolase domain containing 1                       | 132,7 | 191910000  | 215860000  | 87174000  | 2,201 | 2,476 | 2,339 |
| <b>Dnmt1.L</b>    | DNA methyltransferase 1                                  | 58,27 | 43112000   | 54216000   | 20815000  | 2,071 | 2,605 | 2,338 |
| <b>Abcf1.L</b>    | ATP binding cassette subfamily F member 1                | 52,49 | 11177000   | 43937000   | 11809000  | 0,946 | 3,721 | 2,334 |
| <b>Eif2s3.L</b>   | eukaryotic translation initiation factor 2 subunit gamma | 144   | 306210000  | 479110000  | 169770000 | 1,804 | 2,822 | 2,313 |
| <b>Rpl10a.S</b>   | ribosomal protein L10a                                   | 173,7 | 109230000  | 186720000  | 642520000 | 1,700 | 2,906 | 2,303 |
| <b>Copb1.S</b>    | COPI coat complex subunit beta 1                         | 56,65 | 43303000   | 77303000   | 26248000  | 1,650 | 2,945 | 2,297 |
| <b>Cul1.S</b>     | cullin 1   | 88,49 | 73513000   | 75122000   | 32411000  | 2,268 | 2,318 | 2,293 |
| <b>Pdcd6ip.L</b>  | programmed cell death 6 interacting protein              | 207,5 | 262830000  | 411770000  | 147740000 | 1,779 | 2,787 | 2,283 |
| <b>Lta4h.L</b>    | leukotriene A4 hydrolase                                 | 197,3 | 763630000  | 810360000  | 348690000 | 2,190 | 2,324 | 2,257 |
| <b>Pfkm.S</b>     | phosphofructokinase, muscle                              | 231,8 | 338230000  | 426130000  | 169380000 | 1,997 | 2,516 | 2,256 |
| <b>Eif3a.L</b>    | eukaryotic translation initiation factor 3 subunit A     | 61,96 | 98700000   | 36093000   | 30206000  | 3,268 | 1,195 | 2,231 |
| <b>Eif3b.S</b>    | eukaryotic translation initiation factor 3 subunit B     | 165,9 | 655200000  | 430840000  | 243400000 | 2,692 | 1,770 | 2,231 |
| <b>Tubal3.2.L</b> | tubulin alpha like 3, gene 2                             | 74,71 | 529390000  | 744640000  | 286200000 | 1,850 | 2,602 | 2,226 |
| <b>Myh9.L</b>     | myosin, heavy chain 9, non-muscle                        | 323,3 | 1194300000 | 1153400000 | 528910000 | 2,258 | 2,181 | 2,219 |

|                   |  |       |            |            |            |       |       |       |
|-------------------|--|-------|------------|------------|------------|-------|-------|-------|
| <b>MGC82602</b>   | MGC82602 protein   | 116   | 4926200000 | 5786500000 | 2433500000 | 2,024 | 2,378 | 2,201 |
| <b>Mars1.L</b>    | methionyl-tRNA synthetase 1  | 65,5  | 55863000   | 64668000   | 27496000   | 2,032 | 2,352 | 2,192 |
| <b>Mcm6.2.L</b>   | minichromosome maintenance complex component 6 gene 2                  | 183,9 | 184220000  | 241920000  | 97334000   | 1,893 | 2,485 | 2,189 |
| <b>Pygl.S</b>     | phosphorylase, glycogen, liver   | 323,3 | 2937200000 | 4612900000 | 1739400000 | 1,689 | 2,652 | 2,170 |
| <b>Rnpep.L</b>    | arginyl aminopeptidase (aminopeptidase B)                              | 65,96 | 63423000   | 82474000   | 33622000   | 1,886 | 2,453 | 2,170 |
| <b>Rack1.S</b>    | receptor for activated C kinase 1                                      | 259,9 | 1134000000 | 1488700000 | 604950000  | 1,875 | 2,461 | 2,168 |
| <b>Gfus.L</b>     | GDP-L-fucose synthase  | 136,4 | 420130000  | 625030000  | 241480000  | 1,740 | 2,588 | 2,164 |
| <b>Mcm2.S</b>     | minichromosome maintenance complex component 2                         | 185,7 | 300320000  | 330730000  | 147950000  | 2,030 | 2,235 | 2,133 |
| <b>Eprs1.L</b>    | glutamyl-prolyl-tRNA synthetase 1                                      | 176,8 | 342060000  | 413070000  | 179140000  | 1,909 | 2,306 | 2,108 |
| <b>Eif3c.L</b>    | eukaryotic translation initiation factor 3 subunit C                   | 190   | 499800000  | 444960000  | 225030000  | 2,221 | 1,977 | 2,099 |
| <b>Atp6v1b2.S</b> | ATPase, H <sup>+</sup> transporting, lysosomal 56/58kDa, V1 subunit B2 | 225,8 | 745020000  | 632630000  | 332760000  | 2,239 | 1,901 | 2,070 |
| <b>Rpl28.S</b>    | ribosomal protein L28  | 105,7 | 499340000  | 731250000  | 297330000  | 1,679 | 2,459 | 2,069 |
| <b>Rpl21.L</b>    | ribosomal protein L21  | 52,25 | 263840000  | 362920000  | 152120000  | 1,734 | 2,386 | 2,060 |
| <b>Rpl13a.S</b>   | ribosomal protein L13a   | 52,08 | 514250000  | 649430000  | 283670000  | 1,813 | 2,289 | 2,051 |
| <b>Rrm2.L</b>     | ribonucleotide reductase M2, gene 1                                    | 58,17 | 91672000   | 80858000   | 42314000   | 2,166 | 1,911 | 2,039 |
| <b>Huwe1.L</b>    | HECT, UBA and WWE domain containing E3 ubiquitin protein ligase 1      | 133,2 | 79074000   | 109040000  | 46268000   | 1,709 | 2,357 | 2,033 |
| <b>Abce1.S</b>    | ATP binding cassette subfamily E member 1                              | 92,29 | 136690000  | 212820000  | 86300000   | 1,584 | 2,466 | 2,025 |
| <b>Tkt.L</b>      | transketolase  | 156,5 | 423780000  | 701940000  | 279270000  | 1,517 | 2,513 | 2,015 |

# Chapter 5. Roles of Pias4 and Smarce1 in Sensory Neurogenesis

## 5.1. Introduction

In neural plate – neural fold stage *Xenopus laevis* embryos (stage 14-18), different ectodermal territories are clearly defined and can be visualized by specific markers. The PPE is characterized by the expression of both *eya1* and *six1* (Schlosser and Ahrens, 2004). *Sox3* is expressed in the neural plate, in the anterior placodal area (prospective adenohypophyseal and olfactory placodes) and in a subpopulation of cells in the posterior placodal area which will develop into the otic, lateral line and epibranchial placodes (Schlosser and Ahrens, 2004). In between the neural plate and the posterior placodal area, the expression domain of *foxd3* delimitates the neural crest (Sasai et al., 2001).

At that stage the neuronal determination factor *neurog1* is expressed in three bilateral stripes in the posterior neural plate, corresponding to three domains of primary neurogenesis that will give rise to motoneurons (medial), interneurons (intermediate) and sensory neurons (lateral) (Nieber et al., 2009). *Neurog1* is also expressed in a horseshoe-shaped domain in the anterior neural plate, that will give rise to the ventral midbrain, and in the trigeminal/profundal placode area.

*Neurog2* expression area is broader than that of *neurog1* in the posterior neural plate, encompassing the intermediate and lateral stripes of *neurog1* expression; but *neurog1* expression extends further anteriorly in the neural plate compared to *neurog2* (Ma et al., 1996; Nieber et al., 2009). Similarly to *neurog1*, *neurog2* is expressed in the trigeminal/profundal placode area; in addition it is expressed in the olfactory placode area.

*Hes5.4* represses *neurog1* expression, thus keeping progenitor cells in an undifferentiated state (Riddiford and Schlosser, 2017). Quite similarly to neurogenins, it is expressed in stripes of cells in the posterior neural plate, in a horseshoe-shaped

domain in the anterior neural plate, in the anterior placodal region, and in the trigeminal/profundal placode area (Riddiford and Schlosser, 2016).

*Neurog1* and *neurog2* activate the neuronal differentiation factor *neurod1* (Cau et al., 2002; Fode et al., 1998; Ma et al., 1998; Ma et al., 1996). At neural plate – neural fold stage *neurod1* thus displays a similar, but less extended expression pattern than that of its activators, in the neural plate as well as in the trigeminal/profundal placode area (Ma et al., 1996). *Neurod1* itself is upstream of *tubb2b* (Lee et al., 1995), which marks differentiated neurons and is present in similar areas at that stage.

In order to explore the roles of *Pias4* and *Smarce1* in sensory neurogenesis, I performed gain- and loss-of-function experiments, followed by *in situ* hybridizations using probes for the marker genes mentioned above. *Xenopus laevis* embryos were injected with mRNA or morpholino oligonucleotides corresponding to *pias4* or *smarce1*. The embryos were injected at 16- to 64-cell stage, which allowed us to better target the injection site and minimize gastrulation defects (see Chapter 2). *LacZ* mRNA was coinjected to allow for the identification of the injected side by X-gal staining, and *in situ* hybridizations were performed on neural plate – neural fold stage embryos.

## 5.2. Morpholinos specificity and efficacy

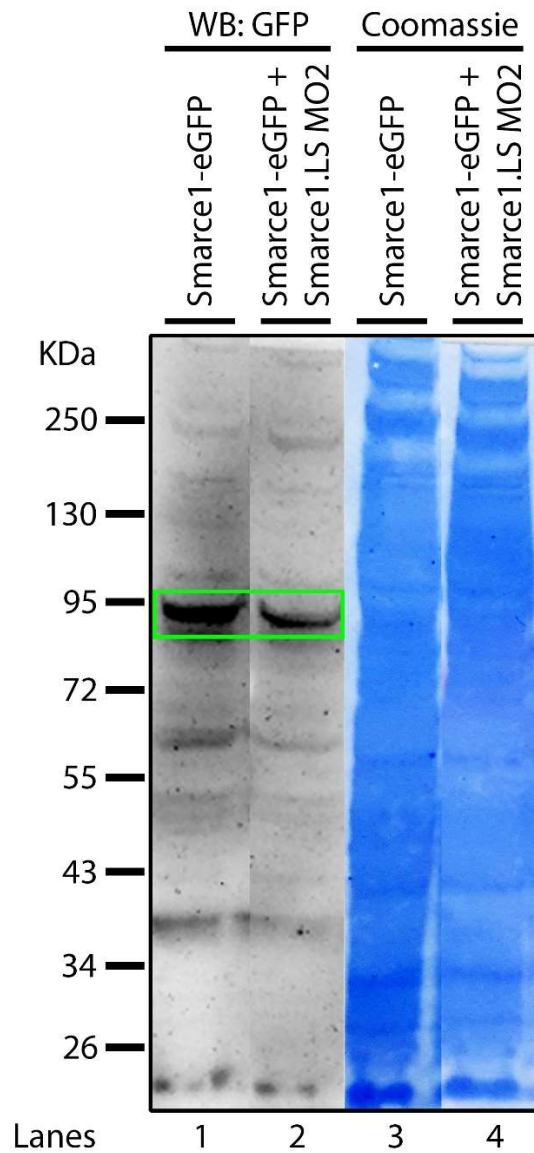
### 5.2.1. *Pias4.L* morpholino

The *pias4.L* morpholino sequence sits partly on the 5'UTR of *pias4.L* mRNA sequence, and partly on its CDS (see Chapter 2). Its efficacy and specificity have been established in another study (Daniels et al., 2004), and were not tested here.

### 5.2.2. *Smarce1.LS* morpholinos

Two different morpholinos have been used for the *smarce1* loss-of-function experiments. Both have been designed to target both *smarce1* homeologs (*smarce1.L* and *smarce1.S*), but while *smarce1.LS* MO1 targets their 5'UTR, *smarce1.LS* MO2 targets their CDS.

The efficacy of *smarce1.LS* MO2 has been confirmed by western blotting, from protein extracts of embryos injected with *smarce1-eGFP* mRNA: indeed Smarce1 protein levels were reduced in embryos co-injected with *smarce1.LS* MO2, compared to embryos solely injected with *smarce1-eGFP* mRNA (Fig. 5.1). Both morpholinos have been used separately and lead to similar phenotypes at similar frequencies, suggesting that their effects are not off-target, but are specifically due to the inactivation of *smarce1* mRNA.



**Fig. 5.1.** *Smarce1.LS* MO2 efficacy test. Western blot analysis on total protein extracts from embryos injected with *smarce1-eGFP* mRNA (lane 1) or co-injected with *smarce1-eGFP* + *smarce1.LS* MO2 (lane 2). The extract from co-injected embryos displays a lower amount of Smarce1-eGFP protein. Coomassie staining performed on the same blot (lanes 3-4) shows that the total protein input is equivalent between both lanes.

### 5.3. Effects of *pias4* gain- and loss-of-function in sensory neurogenesis

The effects of *pias4* morpholino or mRNA injection on the expression of placodal (*eya1*, *six1*, *sox3*), neural crest (*foxd3*) and neuronal differentiation (*hes5.4*, *neurog1*, *neurog2*, *neurod1*, *tubb2b*) markers, in the non-neural and in the neural ectoderm, are quantified in table 5.1. Sections 5.2.1 and 5.2.2 provide a description of the observed phenotypes after *pias4* morpholino or mRNA injection, respectively.

**Table 5.1.** Changes in marker gene expression in non-neural and neural ectoderm after injection of various *pias4*-related constructs.

| Injection             | control MO<br>100 µM |          | <i>pias4</i> MO <sup>a</sup><br>50 µM |          | <i>pias4</i> mRNA<br>50 ng/µl |          |
|-----------------------|----------------------|----------|---------------------------------------|----------|-------------------------------|----------|
|                       | Non-neural           | Neural   | Non-neural                            | Neural   | Non-neural                    | Neural   |
| Phenotype             | %<br>(n)             | %<br>(n) | %<br>(n)                              | %<br>(n) | %<br>(n)                      | %<br>(n) |
| <b><i>eya1</i></b>    |                      |          |                                       |          |                               |          |
| Reduced               | 8.5                  | n/a      | 30*                                   | n/a      | 66.0                          | n/a      |
| Increased/ectopic     | 1.7                  | 0        | 0                                     | 0        | 2.1                           | 0        |
|                       | (59)                 | (59)     | (30)                                  | (30)     | (47)                          | (47)     |
| <b><i>six1</i></b>    |                      |          |                                       |          |                               |          |
| Reduced               | 13.9                 | n/a      | 41.7**                                | n/a      | 58.1                          | n/a      |
| Increased/ectopic     | 1.4                  | 0        | 0                                     | 0        | 4.8                           | 0        |
|                       | (72)                 | (72)     | (36)                                  | (36)     | (62)                          | (62)     |
| <b><i>sox3</i></b>    |                      |          |                                       |          |                               |          |
| Reduced               | 8.7                  | 0        | 21.2                                  | 0        | 12.7                          | 43.8     |
| Increased/ectopic     | 2.9                  | 2.9      | 57.6***                               | 0        | 70.9                          | 0        |
| Broader np            | n/a                  | 14.5     | n/a                                   | 0        | n/a                           | 0        |
|                       | (69)                 | (69)     | (33)                                  | (33)     | (55)                          | (48)     |
| <b><i>foxd3</i></b>   |                      |          |                                       |          |                               |          |
| Reduced               | n/a                  | 7.7      | n/a                                   | 20.4*    | n/a                           | 61.4     |
| Increased/ectopic     | 0                    | 3.3      | 0                                     | 16.7**   | 0                             | 5.7      |
|                       | (91)                 | (91)     | (54)                                  | (54)     | (70)                          | (70)     |
| <b><i>hes5.4</i></b>  |                      |          |                                       |          |                               |          |
| Reduced               | 14.7                 | 3.7      | 58.8***                               | 21.4     | 62.7                          | 25.7     |
| Increased/ectopic     | 0                    | 0        | 0                                     | 0        | 6.7                           | 0        |
|                       | (34)                 | (27)     | (34)                                  | (28)     | (75)                          | (74)     |
| <b><i>neurog1</i></b> |                      |          |                                       |          |                               |          |
| Reduced               | 14.7                 | 7.9      | 33.3                                  | 18.5     | 54.7                          | 53.1     |
| Increased/ectopic     | 0                    | 1.3      | 7.4                                   | 3.7      | 4.7                           | 3.1      |
|                       | (75)                 | (76)     | (27)                                  | (27)     | (64)                          | (64)     |

|                   |      |      |         |      |      |      |
|-------------------|------|------|---------|------|------|------|
| <b>neurog2</b>    |      |      |         |      |      |      |
| Reduced           | 7.3  | 5.1  | 35.3*** | 14.7 | 60.4 | 20.8 |
| Increased/ectopic | 2.4  | 0    | 11.8    | 2.9  | 7.5  | 0    |
|                   | (83) | (78) | (34)    | (34) | (53) | (53) |
| <b>neurod1</b>    |      |      |         |      |      |      |
| Reduced           | 20.0 | 14.9 | 52.0**  | 24.0 | 68.5 | 65.4 |
| Increased/ectopic | 0    | 0    | 0       | 0    | 3.7  | 0    |
|                   | (55) | (47) | (25)    | (25) | (54) | (52) |
| <b>tubb2b</b>     |      |      |         |      |      |      |
| Reduced           | 20.4 | 11.4 | 46.2*   | 25.6 | 62.3 | 39.3 |
| Increased/ectopic | 0    | 0    | 2.6     | 0    | 3.3  | 0    |
|                   | (49) | (79) | (39)    | (39) | (61) | (61) |

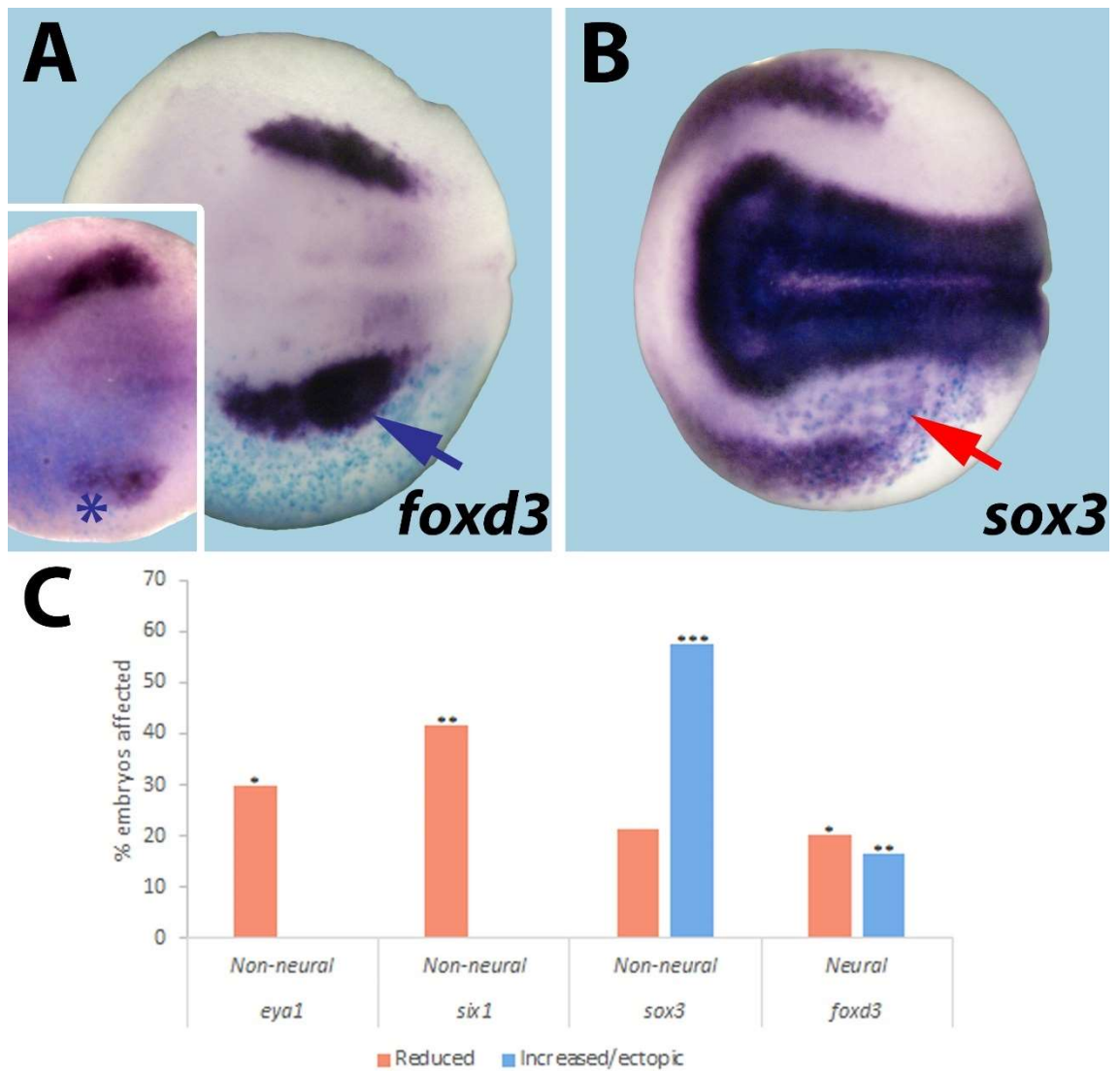
n: number of embryos analyzed at neural plate (stage 14-18) stage.

<sup>a</sup> Significant differences (Fisher's exact test, two-tailed; \*: p<0.05, \*\*: p<0.01; \*\*\*: p<0.001) to control MO injections are indicated.

### 5.3.1. *Pias4* loss of function

Upon *pias4* morpholino injection, embryos at neural plate stage frequently displayed a reduction in the size of the preplacodal area, indicated by a decrease in the expression of *eya1* (30% of the embryos) and *six1* (41.7%). Interestingly, *sox3* expression in the PPE was reduced at a lower rate compared to that of *eya1* and *six1* (21.2%, doesn't reach significance), whereas ectopic *sox3* expression in the non-neural ectoderm was very frequent on the site of injection (57.6%, Fig. 5.2, B). The width of the neural plate was not affected by *pias4* morpholino injection, as indicated by the unchanged *sox3* expression in this area, suggesting that the reduction of *eya1* and *six1* expression domains in the PPE were not due to a broadening of the neural plate at the expense of these territories.

The effects of *pias4* loss of function on neural crest were ambivalent: *foxd3* expression was sometimes reduced (20.4% of the embryos), sometimes increased (16.7%) (Fig. 5.2, A).

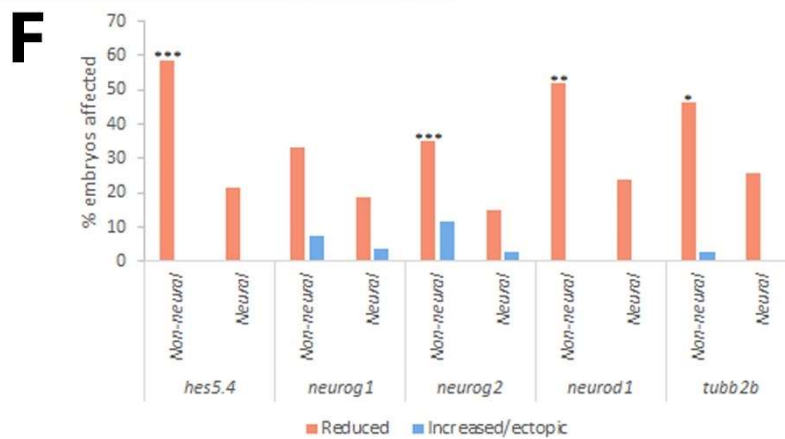
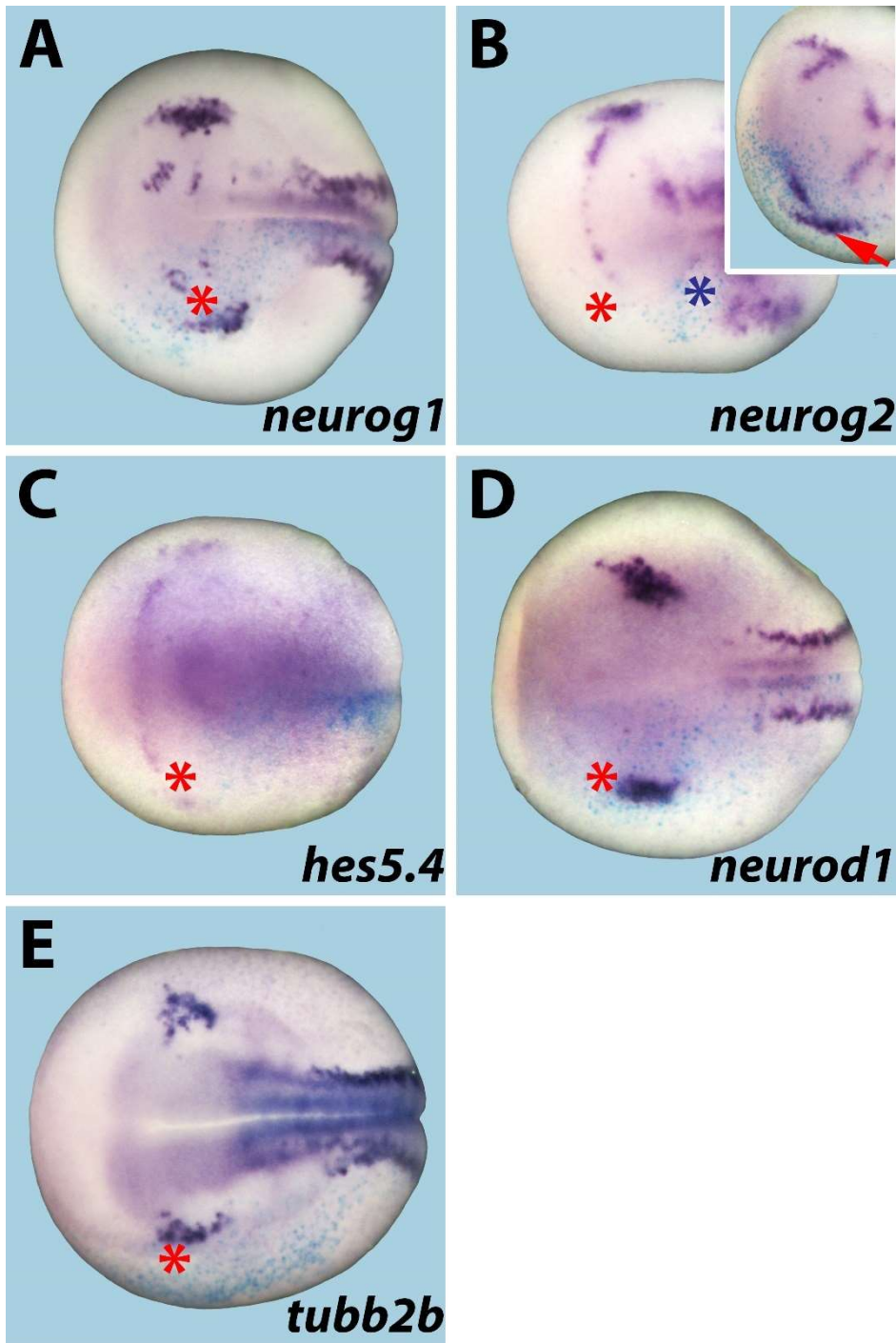


**Fig. 5.2.** Effects of *pias4* knockdown on placodal and neural crest markers. Neural plate stage embryos after unilateral injection of *pias4.L* MO. Embryos were injected at 16- to 64-cell stage in a blastomere contributing to cranial placodes and/or ganglia. *LacZ* mRNA was co-injected as a lineage tracer and X-gal staining (blue) marks the injected side (lower half). (A) Blue arrow and blue asterisk respectively mark increased and decreased expressions of the neural crest marker *foxd3*. (B) Red arrow marks increased *sox3* expression in non-neural ectoderm. (C) Percentages of injected embryos showing a reduction and/or an increase in the expression of *eya1*, *six1*, *sox3* (non-neural ectoderm) and *foxd3* (neural ectoderm) (see Table 5.1 for numbers). Significant differences (Fisher's exact test, two-tailed; \*:  $p < 0.05$ , \*\*:  $p < 0.01$ , \*\*\*:  $p < 0.001$ ) to control MO injections are indicated.

A majority of embryos (58.8%) showed a decrease in *hes5.4* expression in the anterior and trigeminal/profundal placodal areas (Fig 5.3, C). In these placodal areas a decrease in expression was also frequent for the neuronal determination markers *neurog1* (although not significant, 33.3%) and *neurog2* (35.3%) (Fig 5.3, A, B). As illustrated in Fig

5.3 B, *neurog2* expression domain was also sometimes extended in these areas, although at a frequency that was not significantly different from control morpholinos (11.8%). Expressions of *neurod1* (52%) and *tubb2b* (46.2%) were reduced in the trigeminal/profundal placodes in about half of the embryos (Fig. 5.3, D, E). This suggests that *Pias4* is required for initial stages of neurogenesis (*neurog1*, *neurog2*, *hes5.4*) as well as for neuronal differentiation (*neurod1*, *tubb2b*) in the developing placodes.

In the neural ectoderm, only non-significant reductions of *Hes5.4* (21.4%), *neurog1* (18.5%), *neurog2* (14.7%), *neurod1* (24%) and *tubb2b* (25.6%) were observed.

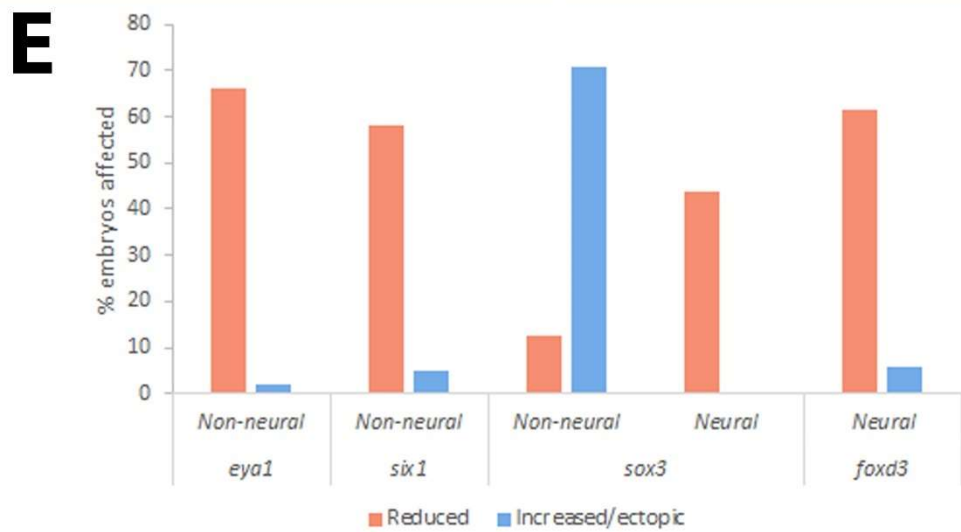
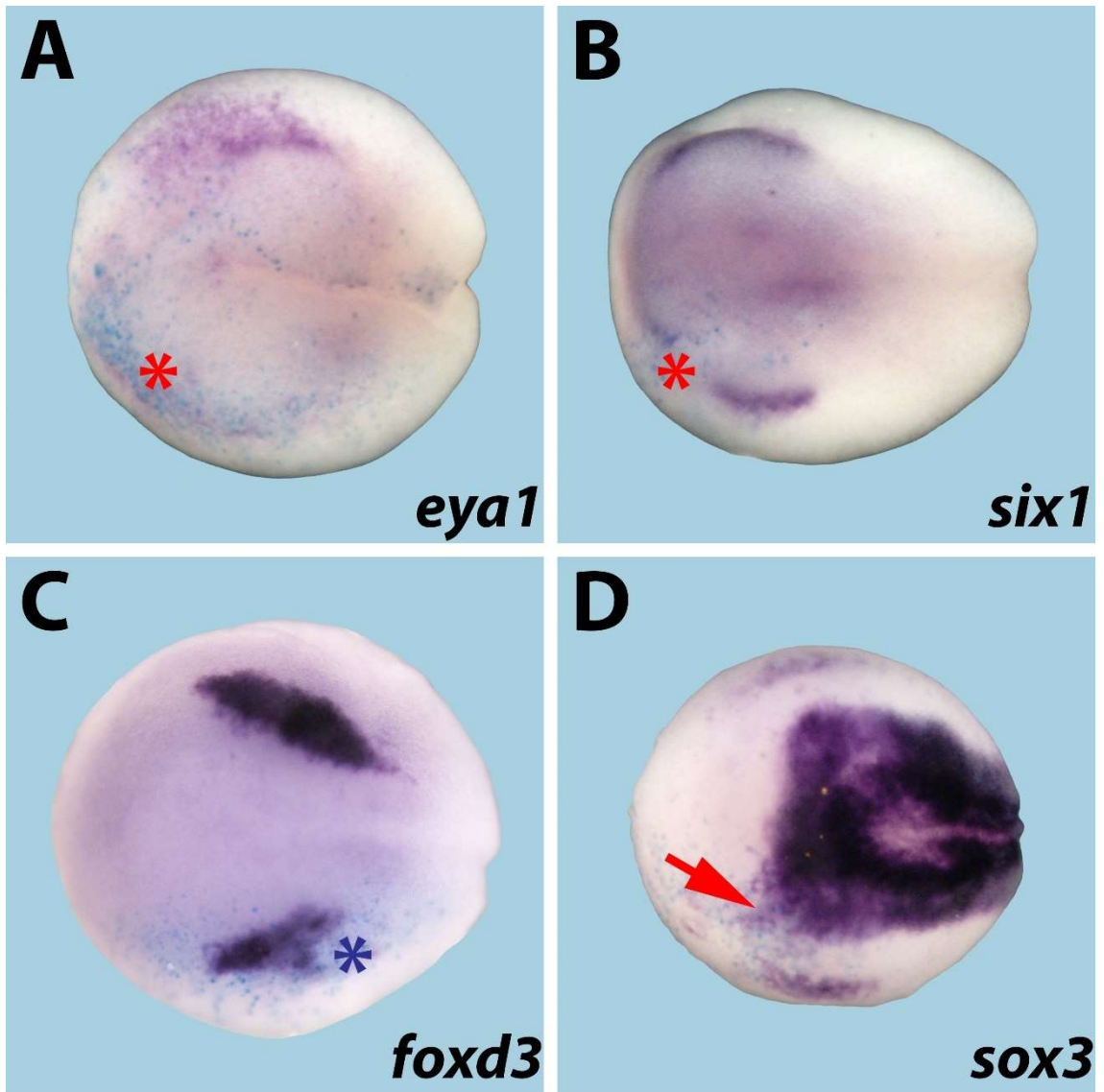


**Fig. 5.3.** Effects of *pias4* knockdown on neuronal differentiation markers. Neural plate stage embryos after unilateral injection of *pias4.L* MO. Embryos were injected at 16- to 64-cell stage in a blastomere contributing to cranial placodes and/or ganglia. *LacZ* mRNA was co-injected as a lineage tracer and X-gal staining (blue) marks the injected side (lower half). For all markers (A to E), red asterisks mark decreased expression in non-neural ectoderm. *Neurog1* (A) and *neurog2* (B) expressions are reduced in both the olfactory and the profundal/trigeminal placodes. *Hes5.4* (C), *neurod1* (D) and *tubb2b* (E) expressions are reduced in the profundal/trigeminal placodal areas. In (B), blue asterisk marks decreased *neurog2* expression in neural ectoderm, and red arrow marks increased *neurog2* expression in non-neural ectoderm. (F) Percentages of injected embryos showing a reduction and/or an increase in the expression of *hes5.4*, *neurog1*, *neurog2*, *neurod1*, and *tubb2b*, in the non-neural and neural ectoderms (see Table 5.1 for numbers). Significant differences (Fisher's exact test, two-tailed; \*:  $p < 0.05$ , \*\*:  $p < 0.01$ ; \*\*\*:  $p < 0.001$ ) to control MO injections are indicated.

### 5.3.2. *Pias4* gain of function

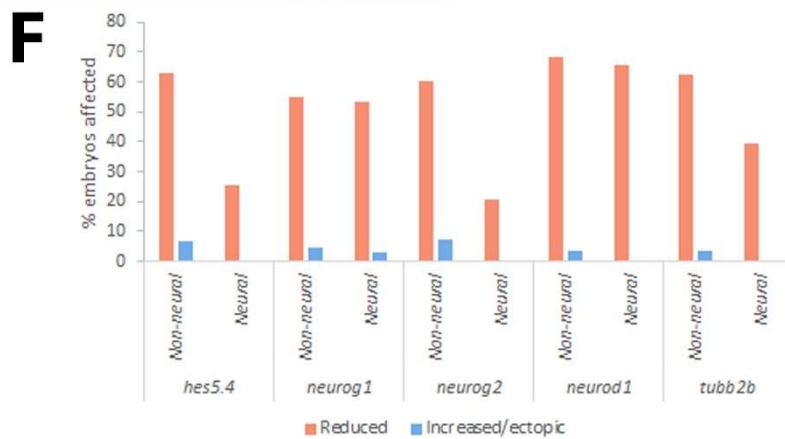
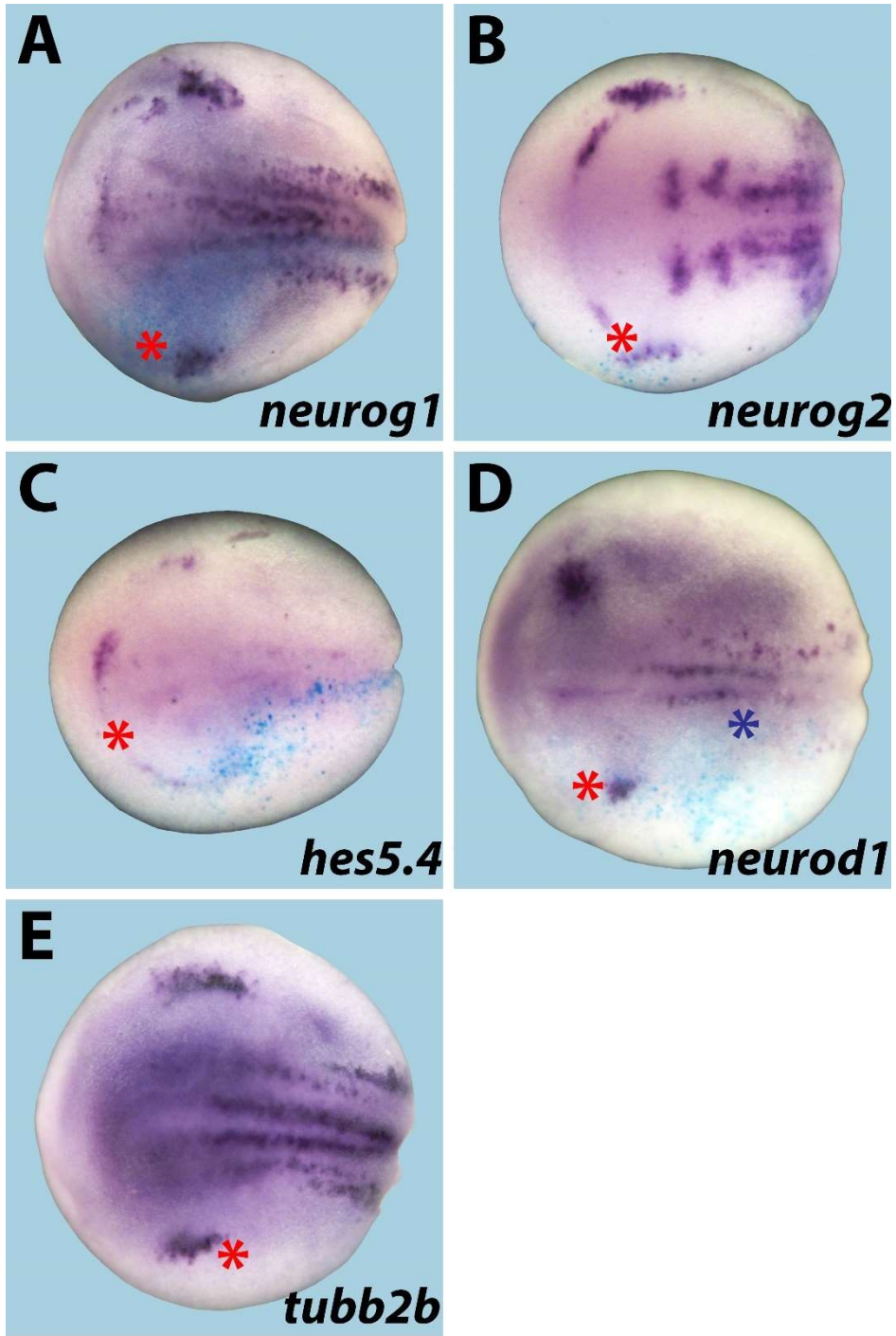
Similarly to what was observed in the loss of function experiments, injection of *pias4* mRNA lead to a decrease in the size of the PPE: *eya1* expression was reduced in 66% of the embryos, and *six1* in 58.1% (Fig. 5.4, A, B). Ectopic *sox3* expression in the non-neural ectoderm could also be observed on the site of injection in most of the embryos (70.9%, Fig 5.4, D). Unlike what was observed after *pias4* loss-of-function, *sox3* expression was decreased in the neural plate in 43.8% of the embryos.

The effects on the neural crest domain were also distinct: while the effects of *pias4* MO injection on *foxd3* expression were ambivalent, the *foxd3* expression domain was predominantly reduced upon *pias4* mRNA injection (61.4%, Fig 5.4, C).



**Fig. 5.4.** Effects of *pias4* overexpression on placodal and neural crest markers. Neural plate stage embryos after unilateral injection of *pias4.S* mRNA. Embryos were injected at 16- to 64-cell stage in a blastomere contributing to cranial placodes and/or ganglia. *LacZ* mRNA was co-injected as a lineage tracer and X-gal staining (blue) marks the injected side (lower half). Red asterisks mark decreased expressions of the placodal markers *eya1* (A) and *six1* (B). Blue asterisk in (C) marks decreased expression of the neural crest marker *foxd3*. Red arrow in (D) marks ectopic *sox3* expression in non-neural ectoderm. (E) Percentages of injected embryos showing a reduction and/or an increase in the expression of *eya1*, *six1* (non-neural ectoderm), *sox3* (non-neural and neural ectoderm), and *foxd3* (neural ectoderm) (see Table 5.1 for numbers).

*Hes5.4* expression was reduced in the anterior and trigeminal/profundal placodal regions (62.7%, Fig 5.5, C), *neurog1* (54.7%) and *neurog2* (60.4%) expressions were reduced in the olfactory and trigeminal/profundal placodal areas (Fig 5.5, A, B), and *neurod1* (68.5%) and *tubb2b* (62.3%) were both frequently reduced in the trigeminal/profundal placodes (Fig 5.5, D, E). Expression in the neural ectoderm was frequently affected as well, particularly for *neurog1* (reduced in 53.1% of the embryos), *neurod1* (65.4%, Fig 5.5, D) and *tubb2b* (39.3%). This reduction in the expression of neuronal determination and differentiation markers was similar to what could be observed after *pias4* knockdown, and shows that the injection of *pias4* mRNA seemed to interfere with neurogenesis as well.



**Fig. 5.5.** Effects of *pias4* overexpression on neuronal differentiation markers. Neural plate stage embryos after unilateral injection of *pias4.S* mRNA. Embryos were injected at 16- to 64-cell stage in a blastomere contributing to cranial placodes and/or ganglia. *LacZ* mRNA was co-injected as a lineage tracer and X-gal staining (blue) marks the injected side (lower half). For all markers (A to E), red asterisks mark decreased expression in non-neural ectoderm. *Neurog1* (A) and *neurog2* (B) expressions are reduced in both the olfactory and the profundal/trigeminal placodes. *Hes5.4* (C), *neurod1* (D) and *tubb2b* (E) expressions are reduced in the profundal/trigeminal placodal areas. In (D), blue asterisk marks decreased *neurod1* expression in neural ectoderm. (F) Percentages of injected embryos showing a reduction and/or an increase in the expression of *hes5.4*, *neurog1*, *neurog2*, *neurod1*, and *tubb2b*, in the non-neural and neural ectoderms (see Table 5.1 for numbers).

### 5.3.3. *Pias4* gain- and loss-of-function: summary

The effects of *pias4* gain- and loss-of-function were unexpectedly similar, with both types of injection leading to a decrease in the size of the PPE, as demonstrated by decreased *eya1* and *six1* expressions. Both GOF and LOF also lead to ectopic *sox3* expression in the non-neural ectoderm, although only *pias4* GOF resulted in decreased *sox3* expression in the neural plate.

The neural crest was differentially affected: while *foxd3* expression could be either reduced or increased upon *pias4* LOF, it was predominantly reduced after *pias4* mRNA injection.

*Pias4* GOF and LOF had similar effects as well on the expression of neuronal determination/differentiation markers, with *hes5.4*, *neurog1*, *neurog2*, *neurod1* and *tubb2b* having their expression reduced.

## 5.4. Effects of *smarce1* gain- and loss-of-function in sensory neurogenesis

The effects of *smarce1* morpholino or mRNA injection on the expression of placodal (*eya1*, *six1*, *sox3*), neural crest (*foxd3*) and neuronal differentiation (*hes5.4*, *neurog1*, *neurog2*, *neurod1*, *tubb2b*) markers, in the non-neural and in the neural ectoderm, are quantified in table 5.2. Sections 5.3.1 and 5.3.2 provide a description of the observed phenotypes after *smarce1* morpholino or mRNA injection, respectively.

**Table 5.2.** Changes in marker gene expression in non-neural and neural ectoderm after injection of various *smarce1*-related constructs.

| Injection             | control MO<br>100 $\mu$ M |          | <i>smarce1</i> MO1 <sup>a</sup><br>250 $\mu$ M |          | <i>smarce1</i> MO2 <sup>a</sup><br>250 $\mu$ M |          | <i>smarce1</i> mRNA<br>100 ng/ $\mu$ l |          |
|-----------------------|---------------------------|----------|--|----------|--|----------|--|----------|
|                       | Non-<br>neural            | Neural   | Non-<br>neural                                 | Neural   | Non-<br>neural                                 | Neural   | Non-<br>neural                         | Neural   |
| Phenotype             | %<br>(n)                  | %<br>(n) | %<br>(n)                                       | %<br>(n) | %<br>(n)                                       | %<br>(n) | %<br>(n)                               | %<br>(n) |
| <b><i>eya1</i></b>    |                           |          |  |          |  |          |  |          |
| Reduced               | 8.5                       | n/a      | 44.9***  | n/a      | 54.5***  | n/a      | 16.7                                   | n/a      |
| Increased/ectopic     | 1.7                       | 0        | 6.1  | 0        | 1.8  | 0        | 0                                      | 0        |
|                       | (59)                      | (59)     | (49)   | (49)     | (55)   | (55)     | (54)                                   | (54)     |
| <b><i>six1</i></b>    |                           |          |  |          |  |          |  |          |
| Reduced               | 13.9                      | n/a      | 58.3***  | n/a      | 45.3***  | n/a      | 27.1                                   | n/a      |
| Increased/ectopic     | 1.4                       | 0        | 0  | 0        | 1.6  | 0        | 0                                      | 0        |
|                       | (72)                      | (72)     | (36)   | (36)     | (64)   | (64)     | (96)                                   | (96)     |
| <b><i>sox3</i></b>    |                           |          |  |          |  |          |  |          |
| Reduced               | 8.7                       | 0        | 4.8  | 0        | 11.7   | 0        | 16.5                                   | 0        |
| Increased/ectopic     | 2.9                       | 2.9      | 59.5***  | 0        | 40.8***  | 0        | 1.1                                    | 0        |
| Broader np            | n/a                       | 14.5     | n/a  | 21.4     | n/a  | 29.1*    | n/a                                    | 14.3     |
|                       | (69)                      | (69)     | (42)   | (42)     | (103)  | (103)    | (91)                                   | (91)     |
| <b><i>foxd3</i></b>   |                           |          |  |          |  |          |  |          |
| Reduced               | n/a                       | 7.7      | n/a  | 32.0***  | n/a  | 41.1***  | n/a                                    | 29.3     |
| Increased/ectopic     | 0                         | 3.3      | 0  | 6.0      | 0  | 2.7      | 0                                      | 2.2      |
|                       | (91)                      | (91)     | (50)   | (50)     | (112)  | (112)    | (92)                                   | (92)     |
| <b><i>hes5.4</i></b>  |                           |          |  |          |  |          |  |          |
| Reduced               | 14.7                      | 3.7      | 72.7***  | 39.1**   | 51.4***  | 24.6*    | 35.4                                   | 19.2     |
| Increased/ectopic     | 0                         | 0        | 0  | 0        | 2.9  | 0        | 2.1                                    | 0        |
|                       | (34)                      | (27)     | (33)   | (33)     | (70)   | (69)     | (48)                                   | (52)     |
| <b><i>neurog1</i></b> |                           |          |  |          |  |          |  |          |
| Reduced               | 14.7                      | 7.9      | 40.5**   | 16.2     | 56.8***  | 28.4*    | 18.1                                   | 11.8     |
| Increased/ectopic     | 0                         | 1.3      | 0  | 0        | 1.4  | 0        | 4.2                                    | 0        |
|                       | (75)                      | (76)     | (37)   | (37)     | (74)   | (81)     | (72)                                   | (76)     |
| <b><i>neurog2</i></b> |                           |          |  |          |  |          |  |          |
| Reduced               | 7.3                       | 5.1      | 34.9***  | 18.6*    | 52.6***  | 28.4***  | 36.0                                   | 9.6      |
| Increased/ectopic     | 2.4                       | 0        | 7.0  | 0        | 2.1  | 0        | 10.7                                   | 0        |
|                       | (83)                      | (78)     | (43)   | (43)     | (94)   | (88)     | (75)                                   | (73)     |
| <b><i>neurod1</i></b> |                           |          |  |          |  |          |  |          |
| Reduced               | 20.0                      | 14.9     | 52.5**   | 32.5     | 56.1***  | 36.8*    | 29.8                                   | 14.0     |
| Increased/ectopic     | 0                         | 0        | 5.0  | 0        | 3.5  | 0        | 9.3                                    | 0        |
|                       | (55)                      | (47)     | (40)   | (40)     | (57)   | (57)     | (54)                                   | (57)     |
| <b><i>tubb2b</i></b>  |                           |          |  |          |  |          |  |          |
| Reduced               | 20.4                      | 11.4     | 57.9***  | 50.0***  | 58.2***  | 47.2***  | 42.9                                   | 27.4     |
| Increased/ectopic     | 0                         | 0        | 0  | 0        | 3.0  | 1.1      | 0                                      | 0        |
|                       | (49)                      | (79)     | (38)   | (44)     | (67)   | (89)     | (28)                                   | (73)     |

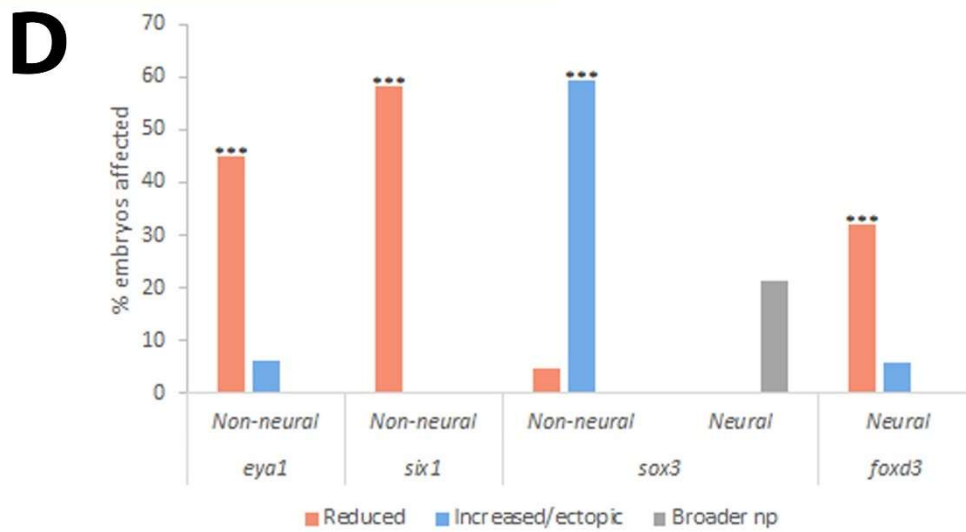
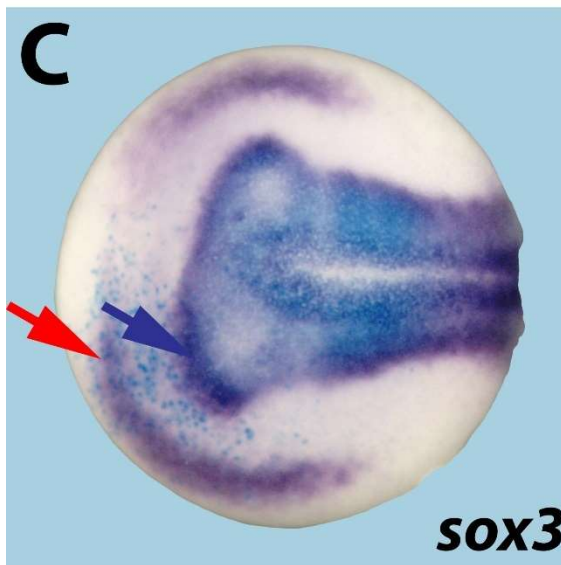
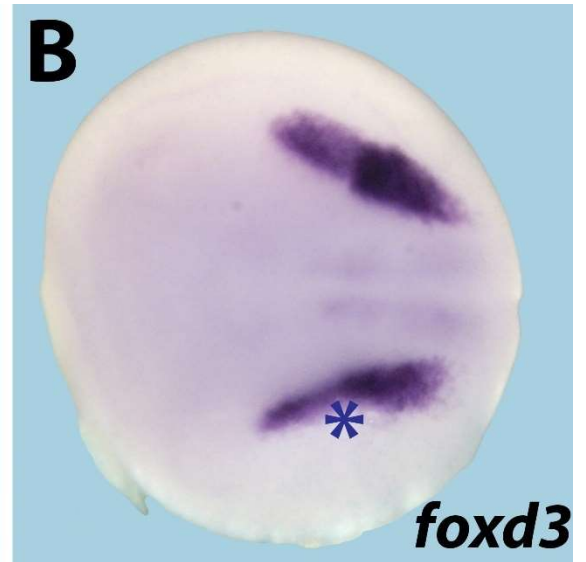
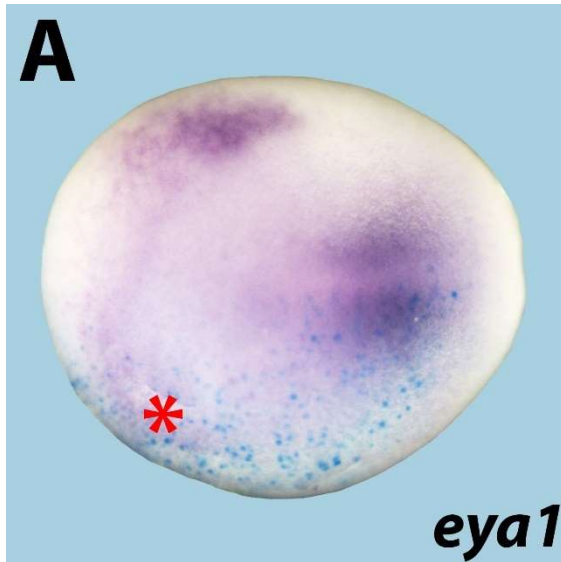
n: number of embryos analyzed at neural plate (stage 14-18) stage.

<sup>a</sup> Significant differences (Fisher's exact test, two-tailed; \*: p<0.05, \*\*: p<0.01; \*\*\*: p<0.001) to control MO injections are indicated.

#### 5.4.1. *Smarce1* loss of function

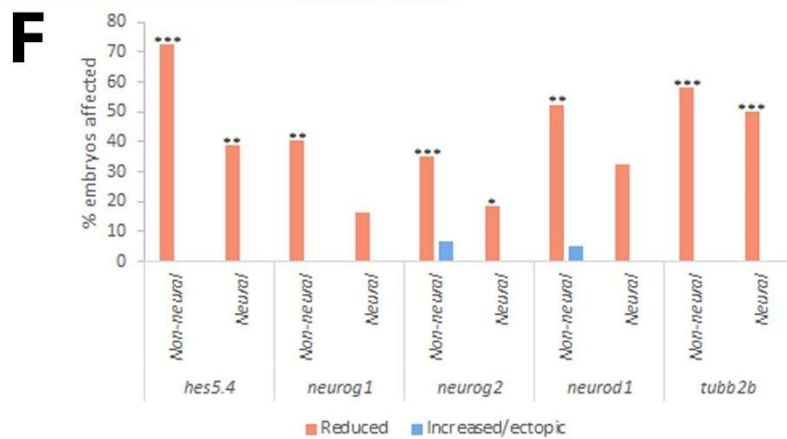
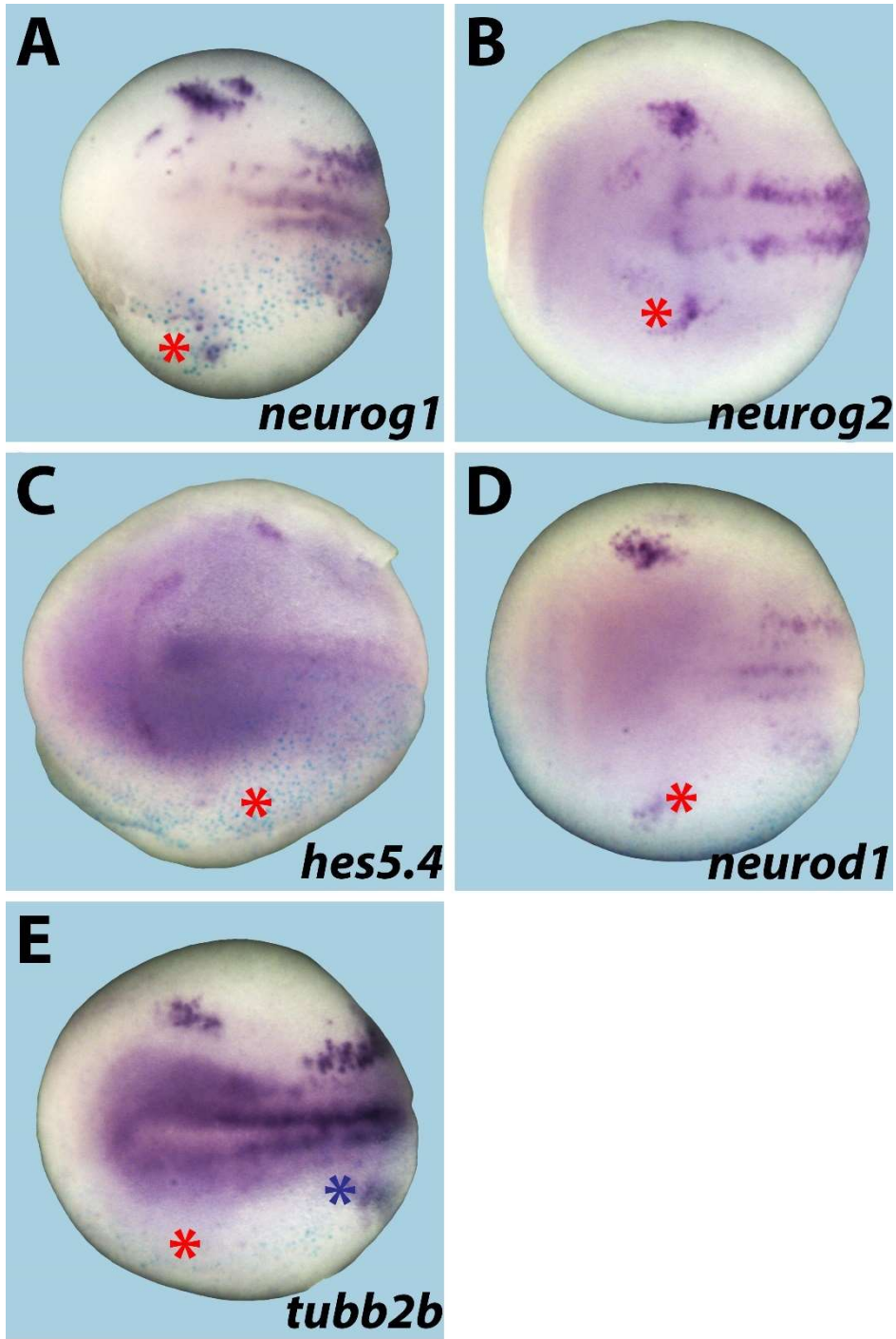
Two different morpholinos, *smarce1.LS* MO1 and *smarce1.LS* MO2, were used for the *smarce1* loss of function experiments. Both were designed to target both the *smarce1.S* and *smarce1.L* homeologs; *smarce1.LS* MO1 targets their 5'UTR, while *smarce1.LS* MO2 targets their CDS (see Chapter 2). The efficacy of *smarce1.LS* MO2 was confirmed by western blotting (see section 5.1.2), and *smarce1.LS* MO1 was successfully used as a specificity control: the use of one morpholino or the other indeed lead to similar phenotypes.

Upon *smarce1* morpholino injection, the size of the preplacodal area was often reduced in neural plate stage embryos: *eya1* expression was reduced (44.9% and 54.5% of the embryos with MO1 and MO2, respectively) (Fig 5.6, A), as well as *six1* expression (58.3% - 45.3%). Interestingly, the opposite is true for *sox3*, which frequently showed increased/ectopic expression in the non-neural ectoderm (59.5% for MO1, 40.8% for MO2). *Smarce1* loss of function also lead to a broadening of the neural plate (21.4% - 29.1%, Fig 5.6, D), which was not observed upon *pias4* loss of function. This may reflect a role of *Smarce1* in either gastrulation (since broader neural plates often result from gastrulation defects and compromised convergent extension), or in early patterning of neural plate border fates. As for *foxd3*, a reduction of its expression was regularly observed (32% - 41.1%) (Fig 5.6, C).



**Fig. 5.6.** Effects of *smarce1* knockdown on placodal and neural crest markers. Neural plate stage embryos after unilateral injection of *smarce1.LS* MO1. Embryos were injected at 16- to 64-cell stage in a blastomere contributing to cranial placodes and/or ganglia. *LacZ* mRNA was co-injected as a lineage tracer and X-gal staining (blue) marks the injected side (lower half). (A) Red asterisk marks decreased expression of the placodal marker *eya1*. (B) Blue asterisk marks decreased expression of the neural crest marker *foxd3*. (C) Red arrow marks increased *sox3* expression in non-neural ectoderm, and blue arrow marks a broadening of the neural plate. (D) Percentages of injected embryos showing a reduction and/or an increase in the expression of *eya1*, *six1* (non-neural ectoderm), *sox3* (non-neural and neural ectoderm) and *foxd3* (neural ectoderm) (see Table 5.2 for numbers). Significant differences (Fisher's exact test, two-tailed; \*:  $p < 0.05$ , \*\*:  $p < 0.01$ ; \*\*\*:  $p < 0.001$ ) to control MO injections are indicated.

The effects of *smarce1* loss of function on neuronal determination and differentiation were similar to those observed upon *pias4* loss of function but more severe. In the anterior and trigeminal/profundal placodal regions, the expressions of *Hes5.4* (72.7% with MO1 - 51.4% with MO2), *neurog1* (40.5% - 56.8%), and *neurog2* (34.9% - 52.6%) were frequently reduced (Fig 5.7, A to C). In the trigeminal/profundal placodal area, *neurod1* (52.5% - 56.1%) and *tubb2b* (57.9% - 58.2%) also displayed a frequent decrease (Fig 5.7, D, E). It should be noted that these frequencies were much higher than the observed neural plate broadening frequencies. This suggests that, at least in some embryos, the reduced expressions of these neuronal determination and differentiation markers reflect a disruption of neurogenesis itself, rather than being a side effect of gastrulation or early patterning defects. The expression of these markers was significantly reduced in the neural ectoderm as well (*hes5.4* 39.1% - 24.6%; *neurog1* 16.2% - 28.4%; *neurog2* 18.6% - 28.4%; *neurod1* 32.5% - 36.8%; *tubb2b* 50% - 47.2%) (Fig. 5.7 D, E) suggesting that *Smarce1* also plays a role for neurogenesis in the neural plate.

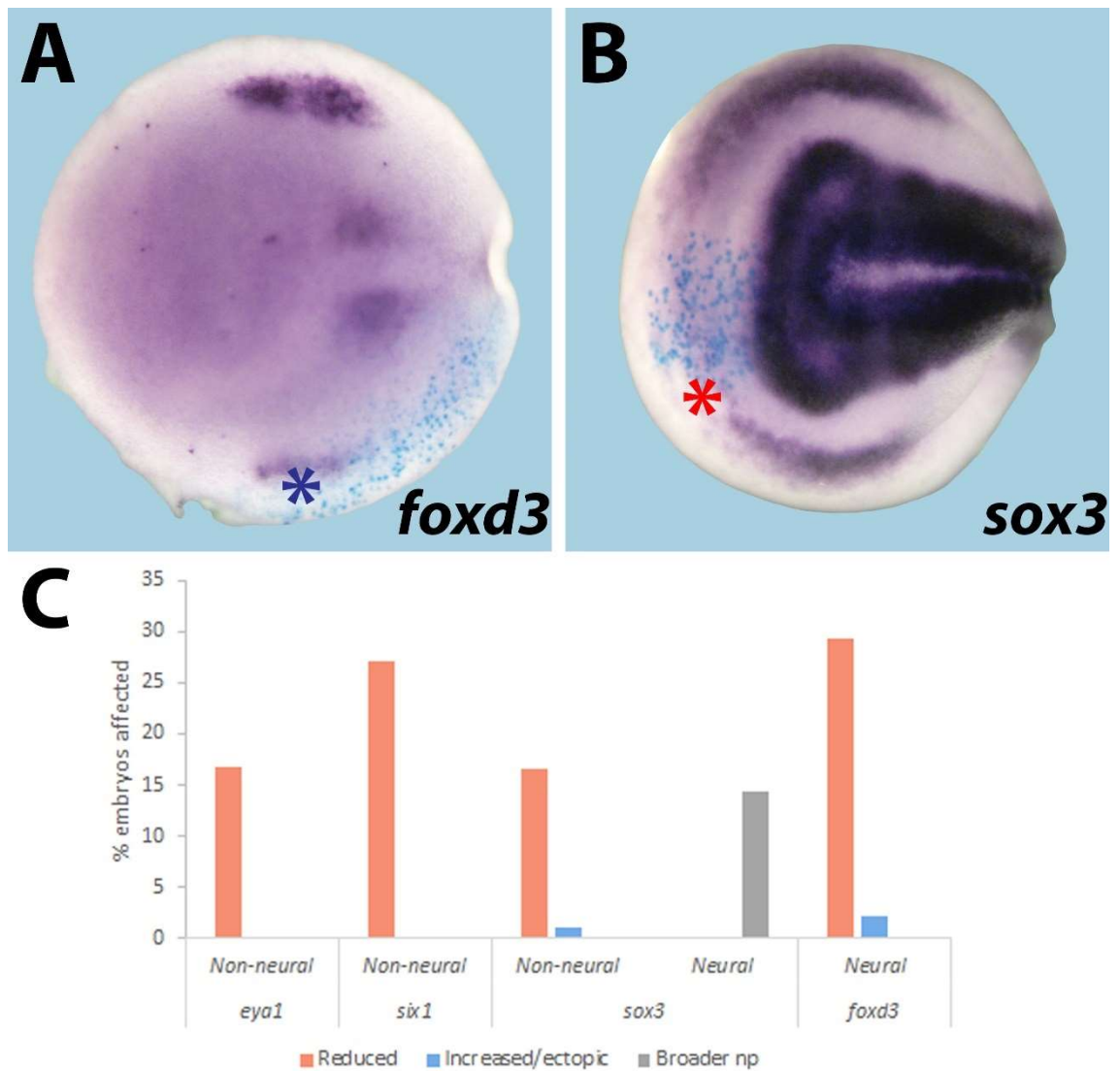


**Fig. 5.7.** Effects of *smarce1* knockdown on neuronal differentiation markers. Neural plate stage embryos after unilateral injection of *smarce1.LS* MO1. Embryos were injected at 16- to 64-cell stage in a blastomere contributing to cranial placodes and/or ganglia. *LacZ* mRNA was co-injected as a lineage tracer and X-gal staining (blue) marks the injected side (lower half). For all markers (A to E), red asterisks mark decreased expression in non-neural ectoderm. *Neurog1* (A) and *neurog2* (B) expressions are reduced in both the olfactory and the profundal/trigeminal placodes. *Hes5.4* (C), *neurod1* (D) and *tubb2b* (E) expressions are reduced in the profundal/trigeminal placodal areas. In (E), blue asterisk marks decreased *tubb2b* expression in neural ectoderm. (F) Percentages of injected embryos showing a reduction and/or an increase in the expression of *hes5.4*, *neurog1*, *neurog2*, *neurod1*, and *tubb2b*, in the non-neural and neural ectoderms (see Table 5.2 for numbers). Significant differences (Fisher's exact test, two-tailed; \*:  $p < 0.05$ , \*\*:  $p < 0.01$ ; \*\*\*:  $p < 0.001$ ) to control MO injections are indicated.

#### 5.4.2. *Smrce1* gain of function

Injection of *smarce1* mRNA did not seem to affect the preplacodal ectoderm much: the reduction rates of *eya1* (16.7%), *six1* (27.1%) and *sox3* (16.5%, Fig 5.8, B) were modest. Also, contrary to what can be seen upon *pias4* mRNA injection, ectopic *sox3* expression in the non-neural ectoderm was almost never present (1.1%). The neural plate was occasionally broadened (14.3% of the embryos), suggesting a mild effect of *smarce1* gain of function on gastrulation and/or early patterning of neural plate border fates, similar to the effect already observed after *smarce1* loss of function. This could explain the observed reductions in the expressions of preplacodal markers, which occurred at comparable rates.

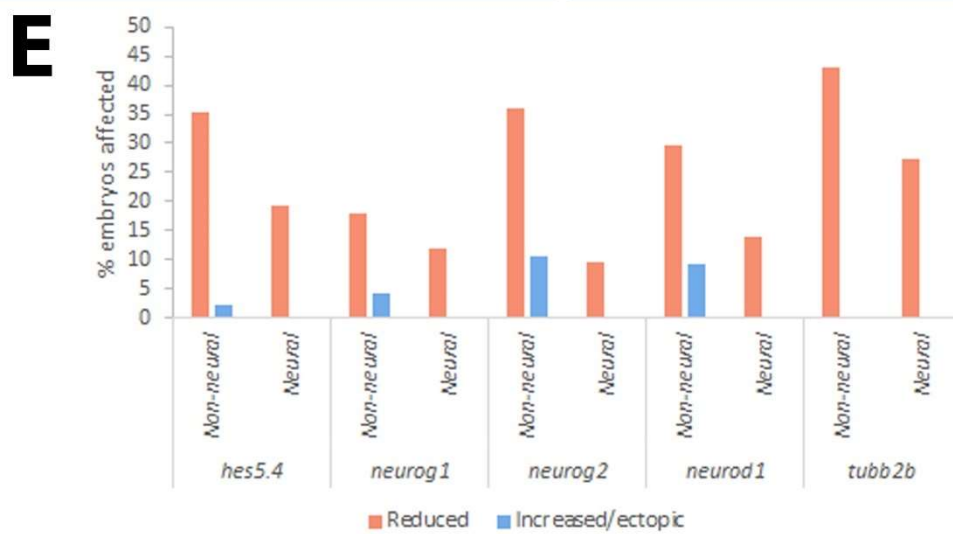
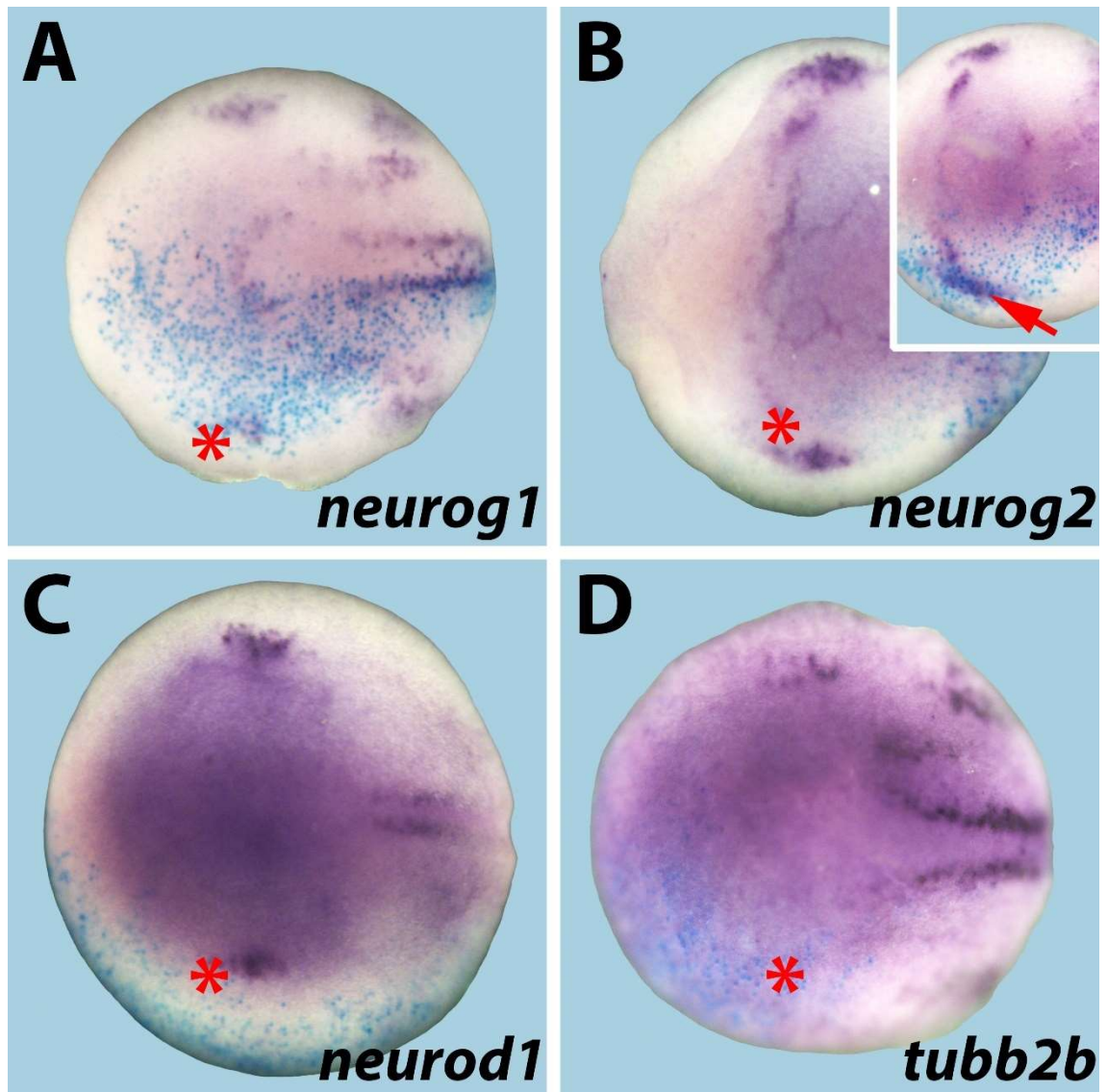
The neural crest domain was reduced quite often, as indicated by a decrease in *foxd3* expression in 29.3% of the embryos (Fig 5.8, A). Again, the effect was very similar to that observed after *smarce1* loss of function.



**Fig. 5.8.** Effects of *smarce1* overexpression on placodal and neural crest markers. Neural plate stage embryos after unilateral injection of *smarce1.L-HA* mRNA. Embryos were injected at 16- to 64-cell stage in a blastomere contributing to cranial placodes and/or ganglia. *LacZ* mRNA was co-injected as a lineage tracer and X-gal staining (blue) marks the injected side (lower half). In (A), blue asterisk marks decreased expression of the neural crest marker *foxd3*. In (B), red asterisk marks decreased *sox3* expression in non-neural ectoderm. (C) Percentages of injected embryos showing a reduction and/or an increase in the expression of *eya1*, *six1* (non-neural ectoderm), *sox3* (non-neural and neural ectoderm), and *foxd3* (neural ectoderm) (see Table 5.2 for numbers).

In the anterior and trigeminal/profundal placodal areas, decreases in *hes5.4* expression (35.4%) occurred frequently. The decrease rates were similar for *neurog2* (36%) but lower for *neurog1* (18.1%) (Fig 5.9, A, B). In the profundal/trigeminal placodes, *neurod1* (29.8%) and *tubb2b* (42.9%) were frequently decreased as well (Fig 5.9, C, D). This suggests that *smarce1* mRNA injection somehow interfered with the normal expression

of these genes. In the neural ectoderm, the reduction rates were lower: only *tubb2b* (27.4%) was decreased in more than 20% of the embryos.



**Fig. 5.9.** Effects of *smarce1* overexpression on neuronal differentiation markers. Neural plate stage embryos after unilateral injection of *smarce1.L-HA* mRNA. Embryos were injected at 16- to 64-cell stage in a blastomere contributing to cranial placodes and/or ganglia. *LacZ* mRNA was co-injected as a lineage tracer and X-gal staining (blue) marks the injected side (lower half). For all markers (A to D), red asterisks mark decreased expression in non-neural ectoderm. *Neurog1* (A) and *neurog2* (B) expressions are reduced in both the olfactory and the profundal/trigeminal placodes. Red arrow in (B) marks increased *neurog2* expression in non-neural ectoderm. *Neurod1* (C) and *tubb2b* (D) expressions are reduced in the profundal/trigeminal placodal areas. (E) Percentages of injected embryos showing a reduction and/or an increase in the expression of *hes5.4*, *neurog1*, *neurog2*, *neurod1*, and *tubb2b*, in the non-neural and neural ectoderms (see Table 5.2 for numbers).

#### 5.4.3. *Smarce1* gain- and loss-of-function: summary

Both *smarce1* GOF and LOF lead to decreases in the size of the PPE, although the reduction rates were modest upon GOF. Both types of injection also lead to a broadening of the neural plate; this was more frequent after *smarce1* LOF, and ectopic *sox3* expression could be frequently observed in the non-neural ectoderm, which was not the case upon *smarce1* GOF.

Both GOF and LOF lead to similar decreases in *foxd3* expression, and both lead to decreased expressions of neuronal determination/differentiation markers *hes5.4*, *neurog1*, *neurog2*, *neurod1* and *tubb2b*. These reductions were more frequent upon *smarce1* LOF, including in the neural ectoderm.

## 5.5. Conclusion

In the PPE, knocking down either *pias4* or *smarce1* lead to reductions in *eya1* and *six1* expressions in 30 to 60% of the embryos. These reductions were not due to a broadening of the neural plate at the expense of the PPE: in the case of *pias4* LOF, these reductions were not accompanied by a broadening of the neural plate, and in the case of *smarce1* LOF, the broadening of the neural plate was much less frequent than the reduction of *eya1* and *six1* expressions. This suggests that both *pias4* and *smarce1* play a role for the proper expression of *eya1* and *six1* in the PPE.

Intriguingly, *pias4* or *smarce1* GOF also lead to reductions in *eya1* and *six1* expressions in the PPE. In the case of *pias4* GOF, the neural plate was not concomitantly broadened

suggesting a dosage dependent requirement of *Pias4* upstream of *eya1* and *six1*. As for *smarce1* GOF, the decreases in *eya1* and *six1* were less frequent and could be due to the broadening of the neural plate, since they occurred at a similar rate.

With the exception of *smarce1* mRNA, injection of any of the constructs lead to frequent ectopic *sox3* expression in the non-neural ectoderm. Injection of any construct also lead to reductions of the neural crest domain, which could indicate either disruptions of the neural plate border patterning and/or dysregulation of *foxd3* expression. When comparing the respective effects of each construct, the reduction rates of *eya1/six1* expressions in the PPE were similar to the disruption rates of *foxd3* expression in the NC; this could be indicative of a role of *Pias4* and *Smarce1* in coordinating the patterning of both regions. It should be noted that *pias4* LOF sometimes lead to increases in *foxd3* expression.

Finally injection of any of the constructs lead to reductions of all the neuronal determination and differentiation markers in their placodal areas and in the neural ectoderm, to varying degrees. This striking reduction of markers for early stages of neurogenesis (*neurog1*, *neurog2*, *hes5.4*) as well as of markers for neuronal differentiation (*neurod1*, *tubb2b*) after both LOF and GOF of *pias4* and *smarce1* suggests that both of these genes play important roles for neurogenesis in a dosage dependent way, similar to what has been previously described for *eya1* and *six1* (Riddiford and Schlosser, 2017; Schlosser et al., 2008). Alternatively, one cannot exclude that decreases in the size of the PPE domain in the injected embryos were one of the main factors leading to decreases in the subsequent number of differentiating neurons in the placodal areas, although neuronal differentiation was also affected in the neural ectoderm.

## Chapter 6. Discussion

### 6.1. Introduction

The aim of my project was to investigate whether potential Eya1 cofactors could be involved in the modulation of the balance between proliferating progenitors and differentiating sensory neurons that is regulated by Eya1. Specifically, it was planned to (1) identify putative interaction partners of Eya1 in a yeast two hybrid screen; (2) validate their interactions with Eya1; and (3) investigate their role in sensory neurogenesis in gain and loss of function studies. While several candidate interaction partners could be identified, none of these could be conclusively validated in follow-up studies. However, several of the candidates identified are expressed in patterns compatible with a role in sensory neurogenesis and for two of the candidates, Pias4 and Smarce1, such a role could be confirmed in functional studies. In the following, I will discuss first the potential pitfalls in confirming Eya1 interaction partners (6.2). I will then comment on the expression (6.3) and potential function (6.4) of putative Eya1 interaction partners. Finally, I will discuss the roles of Pias4 and Smarce1 in sensory neurogenesis as revealed by the functional studies presented here (6.5).

### 6.2. Confirming Eya1 interaction partners

After I obtained a list of 28 candidate Eya1 interactants by yeast two-hybrid (Y2H) screening, my attempts to confirm the interaction between Eya1 and selected candidate partners were made using three different methods: solid growth tests (based, like the screening, on Y2H technology), and co-immunoprecipitation (co-IP) followed by protein identification/detection, either by western blotting or by mass spectrometry.

The results obtained by co-IP based methods lead to negative or dissimilar results compared to those obtained by Y2H. The possible reasons for this discrepancy are discussed below.

### 6.2.1. Solid growth tests

The solid growth tests results using Pias4 and Smarce1 prey fragments were in line with the screening results. These tests are based on the same technology as the two-hybrid screening, therefore the positive results obtained for Pias4 and Smarce1 don't provide conclusive evidence for an interaction between these proteins and Eya1. Still, conducting these tests was of interest: had the results been negative, they would have indicated that the screening results for these two proteins were false positives, and that they were not worth investigating further.

### 6.2.2. Co-IP followed by western blotting

Whereas the use of eGFP tags ultimately allowed us to consistently detect candidates by western blotting, my initial attempts to detect Flag- and Strep-tagged candidates with antibodies were largely unsuccessful although Six1-flag constructs, which were used as positive controls, were successfully detected with anti-flag antibodies. A lack of accessibility of the tag to the antibody due to protein conformation is unlikely to be the cause of this, since PAGE was performed in denaturing conditions. Plasmids were fully sequenced and size and integrity of injected mRNAs were checked before use. A proteolytic cleavage of the flag- or strep- tags could be an explanation, even though protease inhibitors were used during the sample preparation process, and one would expect that the same problem should occur with eGFP tags, but this has not been the case. I can think of no satisfactory explanation for the failure to detect these tagged proteins.

The problem was solved through the use of eGFP tags but initially, non-specific binding to the agarose beads made the co-IP experiments with Eya1 impracticable. Using Protein A/G magnetic beads alleviated the issue to some extent, but I could not convincingly confirm the interaction between Eya1 and the tested candidates Pias4, Smarce1 and Sox11: using high stringency buffers allowed Eya1-Six1 co-IP, but prevented any co-IP of Eya1 with the candidates; while lowering the stringency resulted in slight non-specific binding of the negative control (eGFP) along with binding – specific or not – of Pias4 and Smarce1.

These results do not rule out the possibility that Pias4 and Smarce1 are partners of Eya1, but the results obtained do not allow us to confirm this conclusively. Capturing protein-protein interactions, especially low-affinity or transient ones, by co-IP can be challenging, and requires finding adequate stringency conditions which may differ from one pair of partners to the other. Stabilizing protein complexes by cross-linking is an option, but its optimization can be equally challenging. Cross-linking can lead to gel migration problems and increases the likelihood of generating false positives, which is counterproductive when the objective is to obtain a reliable confirmation of interaction.

### 6.2.3. Co-IP followed by mass spectrometry

To validate interactions between candidates and Eya1 in a different way, I therefore attempted to combine co-IP with mass spectrometry. However, this strategy did not yield more conclusive results and I, therefore, did not pursue it further with additional replicates. None of the overexpressed protein – Six1, Pias4 or Smarce1 – was detected by mass spectrometry, although Six1 is well established as an Eya1 interaction partner (Li et al., 2003; Ohto et al., 1999), which was confirmed by the Co-IP data presented here (and surprisingly also in our mass spectrometry analysis of embryos, not injected with Six1). Moreover, with the exception of Iars1.S and Six1.L, none of the proteins identified as potential Eya1 interactants by mass spectrometry was detected by the yeast two-hybrid screen. This discrepancy could be explained by several factors, and lead us to consider overall that these mass spectrometry results are not reliable.

First, agarose beads were used for the co-immunoprecipitation assays performed by Creative Proteomics, and (Trinkle-Mulcahy et al., 2008) showed that some classes of proteins bind non-specifically to sepharose beads and constitute common contaminants in immunoprecipitation assays. They usually are abundant proteins, and they include cytoskeletal, structural and/or motility proteins, DEAD box proteins, translation elongation and initiation factors, heat shock proteins, histones, hnRNP proteins, and ribosomal proteins. Out of our list of 73 hits (70 when the Eya1 antibody and the double Eya1 hit are subtracted), at least 37 belong to these classes of proteins, or were

individually identified as being common contaminants, and are thus likely to be false positives (see Appendix D).

Second, since I overexpressed Eya1 in the ESG and EPS samples in order to ensure that Eya1 would be pulled down in a sufficient amount, Eya1 was not expressed near physiological levels, and proteins in excess tend to associate with chaperones and can lead to improper intracellular localization (Gingras et al., 2007). This can contribute to the generation of false positives.

Third, co-immunoprecipitation followed by mass spectrometry tends to capture more stable, more abundant interactors, or the ones with highest affinity. For this reason, the real but less abundant Eya1 partners could be underrepresented in the data, and the fact that Eya1 was overexpressed may have exacerbated this effect. In addition, co-IP conditions can easily be too harsh and disrupt or prevent weak or transient interactions, and flag and GFP tags can also potentially disrupt protein-protein interactions. All these factors could explain why almost none of the candidates identified in the two-hybrid screen appeared in the mass spectrometry results.

Fourth, in addition to potentially preventing protein-protein interaction, it should be noted that protein tags can also generate their own false positives. This could be part of the explanation for the discrepancies between our different samples: even though the EPS and ESG samples could be considered as replicates for native proteins that were not overexpressed, they overexpress different constructs, and these or the tags of these constructs could affect the interactions of other proteins in different ways.

The factors mentioned above could also account for the paradoxical failure to detect Six1 after Co-IP by mass spectrometry in the ESG sample, in which Six1 was specifically overexpressed: one, Six1 overexpression could affect its intracellular localization, and prevent it from interacting with Eya1; two, the overexpressed Six1 bears a flag tag, which could disrupt normal interactions and/or favour interactions with other proteins over Eya1; three, the ESG sample is the only sample overexpressing eGFP, which could affect protein-protein interactions in its own ways.

Finally, I only relied on two samples (EPS and ESG) and a negative control (PS), used in a single MS experiment. Using more replicates would allow to rule out experimental errors as a cause for some of the observations that were made.

With these caveats in mind, some of the proteins identified after Co-IP mass spectrometry (white in Table 6.1) may in fact be actual Eya1 interactants. The known functions of some candidates could make them worth investigating: Cse1l, Kpnb1 and the importins Ipo5-7-9, involved notably in nucleocytoplasmic transport of transcription factors and/or other regulatory proteins (Baas et al., 2016; Chen et al., 2011a; Kutay et al., 1997; Palma et al., 2019; Sun et al., 2016); the DNA methyltransferase Dnmt1 (Kikuchi et al., 2022); and Cul1, Huwe1, Pold2, Usp5 and Usp10, involved in (de)ubiquitination and/or DNA repair (Bhattacharya et al., 2020; Cong et al., 2022; Furukawa et al., 2000; Gao et al., 2024; Kao et al., 2018).

#### 6.2.4. Y2H-based vs co-IP-based results

Apart from potential technical problems discussed in the last section, there may be other reasons for a discrepancy between putative interactants identified by mass spectrometry and those identified by the Y2H screen. While Y2H-based methods identify direct interactants, co-IP-based methods pull down indiscriminately direct interactants and members of interacting protein complexes.

Overall, it seems that we can be more confident about the yeast two-hybrid-based data than about those obtained by mass spectrometry: in the Y2H screen each candidate is tested for interaction with Eya1 individually, and the problematic aspects of co-IP + MS (contamination, weak and transient interactions not detected, stability/degradation of proteins, positive results “drowned” by interactions between Eya1 and more abundant proteins) are less prevalent, even though Y2H assays are not immune to false positives, mostly because proteins that would normally not be expressed in the same cells in *Xenopus* are artificially expressed in the same yeast cell. Also, the rate of false negatives in Y2H screens can be quite high, because fused proteins are used, because fragments instead of full-length proteins are used, and because the interactions occur in yeast cells

and not in their natural environment (hence potential folding problems, different post-translational modifications, and proteins potentially toxic for yeast cells).

Nonetheless, the gene ontology of the putative Eya1 interactants identified by Y2H screening seems overall consistent with a role of these candidates in collaboration with Eya1, and some of the candidates belong to protein families that are known to act in conjunction with the Six and Eya families: of course Six1 and Six4 (Ohto et al., 1999); Sox7 and Sox11 (the functions of Eya1-Six1 and Sox2 are closely linked) (Ahmed et al., 2012b; De Lope et al., 2019), Pax3 (Pax-Six-Eya-Dach network) (Kingsbury et al., 2019; Pappu and Mardon, 2004), and Zmym3 (Zmym2 has been shown to interact with Six4, and Zmym4 is suspected to interact with Six1) (Connaughton et al., 2020; Jourdeuil et al., 2023). As shown by previous studies or by *in situ* hybridization in this present thesis, the expression patterns of many candidates is also consistent with a function involving an interaction with Eya1.

### 6.3. Developmental expression of selected candidate Eya1 interactants

#### 6.3.1. Expression patterns: previous data and updates

I characterized the developmental expression patterns of five candidate Eya1 partners, from neurula to late tailbud stages. For some of the candidates (Pias4, Smarce1, Zmym3), embryonic expression data already existed to some extent, in *Xenopus* or in other organisms, and was part of the reasons why I selected those candidates to test the interaction with Eya1. Still, existing data was fragmentary, and in this thesis I provide a more complete description of the developmental expression patterns in *Xenopus*.

##### 6.3.1.1. *Garre1* and *msh6*:

To my knowledge, *garre1* developmental expression was never characterized in any animal model, and *msh6* embryonic expression was only partially described in mouse by (Corradi et al., 1996) at later developmental stages (Theiler stages 17 to 27) than the ones I considered in this thesis. The authors emphasized the proliferative state of tissues

and areas where they observed *msh6* expression: in the ventricular zone throughout the CNS, in the highly proliferative external germinal layer in the developing cerebellum, and in the hippocampus. While I did not examine later stages at which the hippocampus and cerebellum develop, I also observed widespread expression in the CNS at tailbud stages, with higher expression in part of the midbrain and in one anterior rhombomere, which could prefigure later *garre1* cerebellar expression.

#### 6.3.1.2. *Zmym3*:

Some information about developmental expression in *Xenopus* was available for *zmym3*: (Chen et al., 2011b) provide a picture of an *in situ* hybridization against *zmym3* on a *Xenopus laevis* embryo at stage 32, showing broad expression throughout the brain, in the eye, and in the pharyngeal arches area, that is consistent with my late tailbud stage observations. I described with more details the expression pattern in the head at late tailbud stage, by showing that *zmym3* is specifically expressed in the olfactory epithelium, the eye, the otic and anterodorsal lateral line placodes, the neural crest, and in the brain, where expression is stronger in two areas located in the midbrain and anterior hindbrain. I also provided the first characterization of *zmym3* expression from neurula stage to early tailbud stage.

#### 6.3.1.3. *Pias4*:

The first description of *pias4* embryonic expression profile was provided by (Sturm et al., 2000) in mouse. At Theiler stages 13-19 *pias4* is detected in the neural tube, the neuroepithelium of the forebrain and the hindbrain, the eye and branchial arches. Later in development, *pias4* is notably detected in the epithelium of the olfactory system, and in the retina. It is also present in the vibrissa hair follicle, the piriform cortex, and the habenula.

In *Xenopus*, *pias4* developmental expression was described by (Daniels et al., 2004) and (Burn et al., 2011), and was in line with my own observations. At blastula stage, maternal *pias4* mRNA is present at the animal pole. At neurula stage, *pias4* is present in the neural ectoderm and the PPE, with stronger expression in the anterior neural plate. Expression in neural tissues is maintained at later stages at least until stage 37/38. Burn et al more

specifically describe a strong expression in the brain, spinal cord, eyes, olfactory and otic placodes, and migrating neural crest cells at tailbud stage.

I presented a more detailed description of *pias4* expression profile at tailbud stage. In addition to Burn's observations, I identified lateral line placodes as areas of *pias4* expression, as well as tailbud, somites, pronephros and presumably ventral blood islands. I also found that within the brain, expression is strongest in the posterior rhombencephalon, and in three discrete areas corresponding to forebrain, midbrain and presumably midbrain-hindbrain boundary.

#### 6.3.1.4. *Smarce1*:

The developmental expression of *smarce1* in *Xenopus laevis* has been examined previously by (Domingos et al., 2002). At neurula stage they report *smarce1* expression in the neural plate and in what they identify as the border between the neural plate and epidermal ectoderm. I similarly observed expression in the neural plate, neural crest, and a stripe of stronger expression at the border between the PPE and the epidermis. At tailbud stage, they report expression throughout the CNS, in the forebrain, midbrain and hindbrain and with weaker expression in the posterior spinal cord, as well as in the eye, otic vesicle, branchial arches and tail bud, and in vascular structures: the posterior cardinal vein, intersomitic vessels, and vascular vitelline network. My observations were in line with those, and in addition I reported expression in the olfactory and anterodorsal lateral line placodes, and in the proctodeum.

Whether or not their expression was previously characterized, we can observe that overall these five genes are expressed in strikingly similar areas at the stages I examined, and these areas are relevant for a function involving interaction with *Eya1* and with neurogenesis in general.

#### 6.3.2. Expression in the PPE and its derivatives

Crucially, like *eya1*, all five candidates are expressed in the PPE at neurula stages (with the possible exception of *smarce1* whose expression at the PPE level seems limited to a

thin strip between PPE and epidermis). Contrary to *eya1* though, whose expression is downregulated in the prospective lens placode as development proceeds (David et al., 2001; Schlosser and Ahrens, 2004), expression of the five candidates is maintained in the eye up to late tailbud stage, presumably in the prospective lens placode although one cannot rule out that they are also, or exclusively, expressed in the retina.

The candidates continue to be expressed in placodal derivatives up to late tailbud stage, with some minor differences: all five genes maintain their expression in the olfactory and otic placodes, and with the exception of *msh6*, expression is also maintained in lateral line placode. In the case of *zmym3*, expression is also possibly maintained in the profundal/trigeminal placodal area up to stage 27.

### 6.3.3. Expression in other areas of *eya1* expression

Similarities between the candidates and *eya1* expressions are not limited to placodal derivatives, suggesting that their potential interactions might play other roles beyond sensory development. They also display expression in the somites (although this expression appears later than the *eya1* expression) and in the tailbud. *Eya1* and *msh6* also share common expression in the hypaxial muscle precursors, and *eya1* and *smarce1* are both expressed in the proctodeum (David et al., 2001; Schlosser and Ahrens, 2004).

### 6.3.4. Expression in areas with no *eya1* expression

Contrary to *eya1*, all candidates are also expressed in the neural plate and neural crest at neurula stages, and their expression is maintained to varying degrees in the brain and/or spinal cord, and in migrating cranial neural crest cells as development proceeds. This widespread expression in the developing nervous system, from neurula stages to late tailbud stage, suggests that these genes could have core roles in neurogenesis processes, from proliferation to differentiation.

Finally, both *pias4* and *smarce1* show expression in intermediate mesoderm and its derivatives, presumably in the pronephros and ventral blood islands. Even though *eya1* is not expressed in the *Xenopus* pronephros (David et al., 2001), it plays roles in later

nephrogenesis (Xu et al., 2014) (leading to kidney defects affecting branchio-oto-renal syndrome patients, in which *eya1* is mutated) (Abdelhak et al., 1997; Zhang et al., 2004), that may or may not be performed in conjunction with Pias4 and/or Smarce1.

## 6.4. The known functions of candidate Eya1 interactants are interconnected

Not only do the five candidates described here display overall similar expression patterns, they also (with the exception of *Garre1*) intervene in common processes that participate in the regulation of cell proliferation and differentiation. In this section I will show how their known functions are interconnected with each other and with *Eya1*.

### 6.4.1. Pias E3 ligases and SUMOylation: general functions

SUMOylation is a post-translational protein modification process similar to ubiquitination, by which small SUMO (small ubiquitin-like modifier) polypeptides are covalently linked to target proteins. Five SUMO paralogs have been described in vertebrates, and at least three of them (SUMO1, 2, 3) can be conjugated to proteins.

The SUMOylation pathway involves four types of enzymes: the E1 enzyme SAE1/UBA2 activates mature SUMO, which is transferred to the conjugating E2 enzyme UBC9. Then SUMO is transferred from UBC9 to the target protein, frequently (but not necessarily) with the contribution of an E3 SUMO ligase, typically of the Pias family (Pias1 to 4 in vertebrates).

SUMOylation is reversible, and SUMO proteases, typically of the SENP family, are involved in both maturation of SUMO before activation by the E1 enzyme, and SUMO deconjugation from target proteins (Lara-Urena et al., 2022).

Protein SUMOylation can affect protein activity, stability, localization and interaction with other proteins, and intervenes in a large variety of cellular processes, notably in cell cycle regulation, DNA damage repair and replication, and transcriptional regulation. In

various contexts SUMO proteins provide a binding platform for the recruitment of proteins and the formation of protein complexes, and Pias proteins often mediate the assembly of these proteins, through their SUMO E3 ligase activity, but also through their ability to interact themselves with SUMO and with DNA (reviewed in Rytinki et al., 2009). In the context of neural development, SUMOylation of transcription factors and their cofactors has been shown to be important in regulating their activity, affecting the balance between proliferation, differentiation, and survival of neural stem cells (reviewed in Queiroz et al., 2024).

In favor of the hypothesis of an interaction between Eya1 and Pias proteins, it has been shown that Eya1 can be SUMOylated, and that Eya1 SUMOylation can inhibit its transcriptional activity (Sun et al., 2015). Interestingly, developmental defects observed in *Eya1*-deficient mice include a cleft palate (Xu et al., 1999), a defect that is shared by mouse mutants for *SUMO1*, and (Alkuraya et al., 2006) showed that the penetrance of this phenotype is increased in compound heterozygous mutants for *SUMO1* and *Eya1*. This result must be considered carefully though, since in other studies, *SUMO1* mutants do not exhibit a cleft palate, seemingly because SUMO2/3 compensate the lack of SUMO1 (Evdokimov et al., 2008; Zhang et al., 2008).

#### 6.4.2. Pias, SUMOylation of transcription factors and regulation of signaling pathways

Pias (protein inhibitor of activated STAT) proteins are called so because they were first identified as proteins binding to activated Stat transcription factors, inhibiting Stat-mediated gene activation (Chung et al., 1997; Liu et al., 1998). Specifically, Pias4, in cooperation with Pias1, is a corepressor of Stat1 and NF- $\kappa$ B (Liu et al., 2001; Tahk et al., 2007). Smad4 SUMOylation is increased in the presence of Pias4, suggesting a role for Pias4 in TGF- $\beta$  signaling (Lee et al., 2003). Pias4 also inhibits mesoderm induction by downregulating Smad2 transcriptional activity (Daniels et al., 2004).

Six1 and Eya1 also participate in both Stat and TGF- $\beta$  signaling: they have been shown to induce cell proliferation via activation of STAT3 signaling in thyroid carcinoma (Kong et al., 2019), and Six1 and Eya2 activate TGF- $\beta$  signaling in mammary carcinoma cells

(Farabaugh et al., 2012; Micalizzi et al., 2009) but whether these roles are linked to Pias function or SUMOylation has not been established.

Pias4 is involved in the regulation of Wnt signaling via interaction with and SUMOylation of LEF1 (Sachdev et al., 2001) and TCF-4 (Yamamoto et al., 2003). In line with this, cytokine and Wnt signaling are affected in Pias4-deficient mice (Roth et al., 2004), and injection of *pias4* mRNA enhances the induction of the direct targets of Wnt signaling in *Xenopus* embryos (Burn et al., 2011). Wnt-dependent ZIC SUMOylation modulates its activity and promotes expression of the neural crest specifier *foxd3* (Ali et al., 2021; Bellchambers et al., 2021). Fox transcription factors are commonly involved in Wnt/ $\beta$ -catenin signaling, and FoxD1 has recently been shown to directly interact with Pias4 (Moparhi and Koch, 2023).

Eya1 and Six1 are also linked with Wnt signaling: in mouse, activated  $\beta$ -catenin promotes otic placodal fate rather than epidermal fate in Pax2+ cells (Ohyama et al., 2006), but then sets boundaries within the otic vesicle by down-regulating *eya1* and *six1* expression (Freyer and Morrow, 2010). Cell proliferation/survival and neurogenesis are altered in the otic placode of  $\beta$ -catenin GOF mutants, as shown by a decrease in *eya1*, *six1* and *ngn1* expressions (Freyer and Morrow, 2010).

Pias proteins have been shown to interact with and regulate the activity of a number of other transcription factors, such as p53 and androgen receptor (Gross et al., 2001; Kotaja et al., 2000; Nelson et al., 2001). As explained in the next section, SUMOylation can also modulate Sox proteins activity in neural development contexts.

#### 6.4.3. Pias, SUMOylation, Sox and neuronal differentiation

As mentioned in Chapter 1, Sox proteins are part of the neuronal core network that establishes embryonic stem cells identity and regulates maintenance of multipotency in neural and placodal territories, in conjunction with Eya1 and Six1 (Schlosser, 2010).

SUMOylation can regulate the DNA binding ability, protein interaction and transcriptional activity of Sox proteins and their partners: Sox1 potential SUMOylation sites have been identified (Ahmad et al., 2020), and SUMOylation has been shown to

modulate the activity of Sox2 and its partner Oct4 (Tsuruzoe et al., 2006; Wu et al., 2012), Sox3 (Savare et al., 2005), Sox6 (Fernandez-Lloris et al., 2006), Sox9 (Hattori et al., 2006) and Sox10 (Taylor and Labonne, 2005), often with the involvement of Pias proteins, including Pias4 (Tolkunova et al., 2007). Overall neurogenesis has been associated with net deSUMOylation (Juarez-Vicente et al., 2016), but SUMOylation can increase or decrease transcriptional activity, and promote or suppress neuronal differentiation in a context-dependent way (Bernstock et al., 2019).

#### 6.4.4. Pias, SUMOylation, Msh6, Zmym3 and DNA repair

Msh6 (mutS homolog 6) is a member of the mutS family of proteins, homologs of the *Escherichia coli* mismatch-binding protein MutS. It is involved in DNA mismatch repair by heterodimerizing with Msh2 to form an evolutionarily conserved mismatch-binding complex (MutS $\alpha$ ) in eukaryotes (Drummond et al., 1995; Iaccharino et al., 1996; Palombo et al., 1995). Msh6 is part of the BASC complex, that includes tumor suppressors and other DNA damage repair proteins and that coordinates the maintenance of genomic integrity during replication (Wang et al., 2000). In this complex Msh6 interacts with BRCA1, an E3 ubiquitin ligase involved in the regulation of DNA repair by homologous recombination through histone H2A ubiquitylation (Kalb et al., 2014).

Strikingly, the zinc-finger protein Zmym3 is a histone- and DNA-binding DNA damage response factor that also facilitates BRCA1 recruitment to damaged chromatin (Leung et al., 2017), and Pias1 and Pias4 have been shown to promote the recruitment of BRCA1 to double-strand break sites as well (Han et al., 2022). A wide range of SUMOylated factors are involved in double-strand break repair response (reviewed in Garvin and Morris, 2017).

As mentioned in Chapter 1, Eya1 and Eya3 are also involved in the regulation of DNA damage repair through chromatin modification: Eya-dependent dephosphorylation of histone H2AX allows recruitment of repair complexes (Cook et al., 2009; Krishnan et al., 2009). While there is no evidence that this regulation is made in direct conjunction with the candidates involved in DNA damage repair and chromatin modification, this does

constitute one more context in which Eya1 and the candidate partners are susceptible to collaborate.

#### 6.4.5. Smarce1, Zmym, SUMOylation and chromatin modification

The SWI/SNF complexes, or BAF complexes, are chromatin modifiers that play central roles in gene regulation during development, including neural development, with many different BAF subunits combinations regulating different developmental processes (Chohra et al., 2023; Sokpor et al., 2017). During neural development specifically, it has been shown that a switch in subunit composition of the BAF complexes correlates with the global chromatin changes that accompany the transition between neural stem cells and committed neuronal lineages (Lessard et al., 2007).

Smarce1, also called BAF57, was first identified by (Wang et al., 1998) as a HMG domain-containing, DNA-binding subunit present in all BAF complexes in higher eukaryotes. Smarce1 plays a key role in the control of the composition of the BAF complexes, which affects cell cycle progression. In Hela cells, it has been shown that SMARCE1 is important for the recruitment of the BRM/BRG1 subunits of the BAF complex to the promoters of G2-M-related genes, and knocking down *SMARCE1* leads to a decrease in cell proliferation (Hah et al., 2010). Through its interactions with estrogen and androgen receptors (Garcia-Pedrero et al., 2006; Link et al., 2005) and their p160 coactivators (Belandia et al., 2002), SMARCE1 is also able to stimulate nuclear receptor-mediated cell proliferation. It can also play anti-proliferative roles, mediating cell cycle arrest or apoptosis (Wang et al., 2005).

SMARCE1 is not found outside the BAF complexes, but it is able to interact with many protein partners outside of them, notably with the LSD1-CoREST-HDAC1/2 histone demethylase/deacetylase complex during the repression of neuronal genes in non-neuronal cells (Battaglioli et al., 2002; Lomeli and Castillo-Robles, 2016). Interestingly, the protein HMG20B, also called SMARCE1r because of its structural similarity with SMARCE1 (Wattler et al., 1999), is a subunit of this CoREST complex, and HMG20B SUMOylation is required for the repression of neuronal-specific genes by that complex (Ceballos-Chavez et al., 2012).

ZMYM3 also interacts with the transcriptional co-repressor complex LSD1-coREST-HDAC1/2 to stabilize it on specific promoters (Gocke and Yu, 2008; Hakimi et al., 2003); its MYM type zinc fingers confer to ZMYM3 a SUMO-binding activity (Guzzo et al., 2014), and SUMOylation of HDAC1 has been shown to stimulate its binding to ZMYM3. Similarly, (Aguilar-Martinez et al., 2015) showed that ZMYM2 recruitment to chromatin is mediated by its ability to bind SUMOylated proteins. Interestingly, (Connaughton et al., 2020) showed that ZMYM2 is a proximity interactor of PIAS proteins (namely PIAS1, PIAS2 and PIAS4) and many zinc finger protein, including ZMYM3. Similarly to ZMYM3, ZMYM2 interacts with HDAC1 and other components of repressor complexes (Giurgiu et al., 2019; Joshi et al., 2013).

In mouse otic development, it was shown that EYA1 and SIX1 may recruit the BAF complex (of which SMARCE1 is a core subunit) to induce the expression of *neurog1* and *neurod1* and drive neurogenesis, in cooperation with SOX2 (Ahmed et al., 2012b). EYA1 and SIX1 directly interact with the BAF complex subunits SMARCC2/BAF170, and SMARCA4/BRG1. Another study showed that EYA1 and SIX2 directly interact with the BAF complex and with BRG1 to modulate self-renewal and differentiation of nephron progenitor cells (Li et al., 2021).

Because *zmym4* is expressed in branchial arches, neural crest and cranial placodes, and shows structural similarities with the Six1 cofactor Sobp (Neilson et al., 2010; Tavares et al., 2021), a previous study investigated whether Zmym4 directly interacts with Six1 (Jourdeuil et al., 2023). Even though no direct Zmym4-Six1 interaction could be detected, altering Zmym4 levels in *Xenopus* embryo was shown to affect cranial neural crest and preplacodal gene expression. Zmym2 has been shown to interact with Six4 and to play roles in renal development (Connaughton et al., 2020).

## 6.5. Garre1 and the CCR4-NOT deadenylase complex

In animal cells, processing bodies (or P-bodies) are a type of RNA granules, spatially restricted cytosolic protein assemblies involved in the regulation of mRNA processing, translation and degradation (reviewed in Luo et al., 2018). A previous study found that

GARR1 interacts with components of the CCR4-NOT deadenylase complex (Youn et al., 2018), which is part of the P-bodies and is responsible for the mRNA deadenylation that initiates the cellular 5'-to-3' mRNA decay pathway (Jonas and Izaurralde, 2015). This decay process is important for mRNA turnover and fine-tuning of gene expression, and RNA-binding proteins present in RNA granules have been linked to control of gene expression in developmental processes (Dash et al., 2020) (reviewed in Dash et al., 2016 for eye development).

GARRE1 also interacts with the Argonaute AGO2 and GW182 proteins, required for miRNA-mediated gene silencing (Jonas and Izaurralde, 2015). The CCR4-NOT complex can also be located in the nucleus, and is involved in cell cycle regulation, cell proliferation, chromatin modification, activation and inhibition of transcription initiation, control of transcription elongation, RNA export, nuclear RNA surveillance, and DNA damage response (Chalabi Hagkarim and Grand, 2020).

The role of Garre1, whether in relation to P-bodies or hypothetically in the nucleus, is unknown, and Garre1 shares no obvious function or known direct interaction with the other candidate Eya1 interactants. GARRE1 (granule associated RAC and RHOG effector 1) was named so after (Bagci et al., 2020) discovered that it is a direct binding partner of RAC1, specifically recruited by its active form. RAC1, along with RAC2, RAC3 and RHOG, is a member of the Rac subfamily within the Rho family of GTPases, which are signaling proteins that act as molecular switches for the regulation of many cellular processes, notably associated with the cytoskeleton (reviewed in El Masri and Delon, 2021). (Serres et al., 2023) have shown that Garre1 also binds the GTPases Rac1 and Rab35 in zebrafish and controls actin cytoskeleton and membrane trafficking for ciliogenesis.

## 6.6. Roles of Pias4 and Smarce1 in sensory neurogenesis

Although Pias4 and Smarce1 could not be conclusively validated as Eya1 interaction partners, the gain and loss of function studies presented here show them to be important regulators of sensory neurogenesis with some interesting parallels to Eya1.

Knockdown of both *pias4* and *smarce1* show significant reductions of all genes expressed during specification and differentiation of cranial sensory neurons (*neurog1*, *neurog2*, *hes5.4*, *neurod1* and *tubb2b*), suggesting that both of these genes, like *eya1* (Riddiford and Schlosser, 2017; Schlosser et al., 2008) are required for these processes. Also similar to what has previously been reported for *eya1* and *six1* (Riddiford and Schlosser, 2017; Schlosser et al., 2008), overexpression of *pias4* and *smarce1* results in the reductions of these neuronal specification/differentiation genes. This suggests that like Eya1, Pias4 and Smarce 1 may play dosage-dependent roles in sensory neurogenesis, although this requires confirmation in further studies.

Interestingly, the gain and loss of function studies reported here show that Pias4 and Smarce1 also play important roles for the regulation of Eya1 and Six1 themselves, since the latter are reduced after both gain and loss of Pias4 and Smarce1. This raises the possibility that the effects of Pias4 and Smarce1 on neuronal specification/differentiation may be indirect and could be mediated by Eya1 and Six1. However, as discussed below, the effects of Pias4 and Smarce1 on other markers (in particular *sox3*) is different from Eya1, making it unlikely that all of the effects of these genes on neurogenesis are mediated by Eya1. Clearly, further studies will be needed to clarify the precise epistatic relationships between the *eya1*, *pias4* and *smarce1* genes.

In previous studies, the ability of high doses of Eya1 to repress neuronal differentiation has been attributed at least partly to the ability of the Eya1-Six1 coactivator complex to promote a neuronal progenitor fate by activating *soxB1* transcription factors like *sox2* and *sox3* (Ahmed et al., 2012b; Riddiford and Schlosser, 2017; Schlosser et al., 2008). Interestingly, *pias4* overexpression is shown here to also upregulate *sox3* in the non-neural ectoderm. This could suggest that it may promote neuronal progenitor states in the non-neural ectoderm similar to (and again either upstream or in parallel to) Eya1. However, unlike *eya1* knockdown *pias4* knockdown does not lead to a reduction in non-neural *sox3* expression (Schlosser et al., 2008), but instead also results in ectopic expression of *sox3*. This indicates that Pias4 is required at some stage or under some conditions to suppress *sox3* in the non-neural ectoderm. It currently remains puzzling how the two functions of Pias4 in promoting and repressing *sox3* can be reconciled. The observation that neural crest (*foxd3*) and panplacodal markers (*eya1*, *six1*) are reduced

after *pias4* overexpression, while *sox3* is reduced in neural but increased in non-neural ectoderm lends some support to the hypothesis that in addition to its role in sensory neurogenesis, Pias4 may have some earlier function for patterning of the neural plate border (NPB). Additional experiments are required to determine whether this hypothesis is correct and to dissect the potentially different roles of Pias4 for NPB patterning and sensory neurogenesis.

Knockdown of *smarce1* like knockdown of *pias4* also results in an increase of *sox3* in the non-neural ectoderm as well as in a reduction of NPB genes (*foxd3*, *eya1*, *six1*) suggesting that Smarce1 may have a potentially similar role in NPB patterning. However, in distinction to *pias4* and *eya1*, *smarce1* overexpression does not upregulate *sox3* in the non-neural ectoderm. This suggests that Smarce1, unlike Pias4 and Eya1, may not be involved in the promotion of neuronal progenitor fates. Again, further experiments will be required to further clarify the mechanism of Smarce1 function for NPB formation and neurogenesis. In particular, rescue experiments (co-injection of morpholino and of non MO-targeted mRNA to replace the depleted transcripts) would be useful to confirm that the phenotypes observed after *pias4* and *smarce1* morpholino injections are due to the knockdown of these genes, and not to morpholino off-target effects.

## 6.7. Summary and Conclusion

Even though a direct interaction between Eya1 and its five candidate partners could not be confirmed, the developmental expression profiles of these candidates and their known functions in other contexts is compatible with the possibility that they may play important roles in the development of cranial sensory neurons, possibly in cooperation and/or interaction with Eya1. For two of these candidates, Pias4 and Smarce1, the gain and loss of function studies presented here indeed reveal important and hitherto undescribed functions in sensory neurogenesis with both proteins being required for the differentiation of sensory neurons and Pias4 potentially playing an additional role in neuronal progenitor formation. However, further studies are needed to further elucidate the position of these proteins in the regulatory network controlling sensory neurogenesis; to conclusively show whether the Pias4 and Smarce1 proteins physically

interact with Eya1; and to clarify their context-dependent roles in neurogenesis versus NPB formation.

## Bibliography

Abdelhak, S., Kalatzis, V., Heilig, R., Compain, S., Samson, D., Vincent, C., Weil, D., Cruaud, C., Sahly, I., Leibovici, M., Bitner-Glindzicz, M., Francis, M., Lacombe, D., Vigneron, J., Charachon, R., Boven, K., Bedbeder, P., Van Regemorter, N., Weissenbach, J., Petit, C., 1997. A human homologue of the *Drosophila* eyes absent gene underlies branchio-oto-renal (BOR) syndrome and identifies a novel gene family. *Nat Genet* 15, 157-164.

Abu-Elmagd, M., Ishii, Y., Cheung, M., Rex, M., Le Rouedec, D., Scotting, P.J., 2001. cSox3 expression and neurogenesis in the epibranchial placodes. *Dev Biol* 237, 258-269.

Agathocleous, M., Iordanova, I., Willardsen, M.I., Xue, X.Y., Vetter, M.L., Harris, W.A., Moore, K.B., 2009. A directional Wnt/beta-catenin-Sox2-proneural pathway regulates the transition from proliferation to differentiation in the *Xenopus* retina. *Development* 136, 3289-3299.

Aguilar-Martinez, E., Chen, X., Webber, A., Mould, A.P., Seifert, A., Hay, R.T., Sharrocks, A.D., 2015. Screen for multi-SUMO-binding proteins reveals a multi-SIM-binding mechanism for recruitment of the transcriptional regulator ZMYM2 to chromatin. *Proc Natl Acad Sci U S A* 112, E4854-4863.

Aguirre, A., Rubio, M.E., Gallo, V., 2010. Notch and EGFR pathway interaction regulates neural stem cell number and self-renewal. *Nature* 467, 323-327.

Ahmad, A., Strohbuecker, S., Scotti, C., Tufarelli, C., Sottile, V., 2020. In Silico Identification of SOX1 Post-Translational Modifications Highlights a Shared Protein Motif. *Cells* 9.

Ahmed, M., Wong, E.Y., Sun, J., Xu, J., Wang, F., Xu, P.X., 2012a. Eya1-Six1 interaction is sufficient to induce hair cell fate in the cochlea by activating Atoh1 expression in cooperation with Sox2. *Dev Cell* 22, 377-390.

Ahmed, M., Xu, J., Xu, P.X., 2012b. EYA1 and SIX1 drive the neuronal developmental program in cooperation with the SWI/SNF chromatin-remodeling complex and SOX2 in the mammalian inner ear. *Development* 139, 1965-1977.

Ahrens, K., Schlosser, G., 2005. Tissues and signals involved in the induction of placodal Six1 expression in *Xenopus laevis*. *Dev Biol* 288, 40-59.

Ali, R.G., Bellchambers, H.M., Warr, N., Ahmed, J.N., Barratt, K.S., Neill, K., Diamand, K.E.M., Arkell, R.M., 2021. WNT-responsive SUMOylation of ZIC5 promotes murine neural crest cell development, having multiple effects on transcription. *J Cell Sci* 134.

Alkuraya, F.S., Saadi, I., Lund, J.J., Turbe-Doan, A., Morton, C.C., Maas, R.L., 2006. SUMO1 haploinsufficiency leads to cleft lip and palate. *Science* 313, 1751.

Allan, D.W., Thor, S., 2015. Transcriptional selectors, masters, and combinatorial codes: regulatory principles of neural subtype specification. *Wiley Interdiscip Rev Dev Biol* 4, 505-528.

Almasoudi, S.H., Schlosser, G., 2021. Eya1 protein distribution during embryonic development of *Xenopus laevis*. *Gene Expr Patterns* 42, 119213.

Alsina, B., 2020. Mechanisms of cell specification and differentiation in vertebrate cranial sensory systems. *Curr Opin Cell Biol* 67, 79-85.

Alsina, B., Giraldez, F., Pujades, C., 2009. Patterning and cell fate in ear development. *Int J Dev Biol* 53, 1503-1513.

Alvarez-Rodriguez, R., Pons, S., 2009. Expression of the proneural gene encoding Mash1 suppresses MYCN mitotic activity. *J Cell Sci* 122, 595-599.

Amador-Arjona, A., Cimadamore, F., Huang, C.T., Wright, R., Lewis, S., Gage, F.H., Terskikh, A.V., 2015. SOX2 primes the epigenetic landscape in neural precursors enabling proper gene activation during hippocampal neurogenesis. *Proc Natl Acad Sci U S A* 112, E1936-1945.

Amiri, A., Noei, F., Feroz, T., Lee, J.M., 2007. Geldanamycin anisimycins activate Rho and stimulate Rho- and ROCK-dependent actin stress fiber formation. *Mol Cancer Res* 5, 933-942.

Andermann, P., Ungos, J., Raible, D.W., 2002. Neurogenin1 defines zebrafish cranial sensory ganglia precursors. *Dev Biol* 251, 45-58.

Andersson, E.K., Irvin, D.K., Ahlsio, J., Parmar, M., 2007. Ngn2 and Nurr1 act in synergy to induce midbrain dopaminergic neurons from expanded neural stem and progenitor cells. *Exp Cell Res* 313, 1172-1180.

Aydin, B., Kakumanu, A., Rossillo, M., Moreno-Estelles, M., Garipler, G., Ringstad, N., Flames, N., Mahony, S., Mazzoni, E.O., 2019. Proneural factors Ascl1 and Neurog2 contribute to neuronal subtype identities by establishing distinct chromatin landscapes. *Nat Neurosci* 22, 897-908.

Ayer-Le Lievre, C.S., Le Douarin, N.M., 1982. The early development of cranial sensory ganglia and the potentialities of their component cells studied in quail-chick chimeras. *Dev Biol* 94, 291-310.

Baas, R., Sijm, A., van Teeffelen, H.A., van Es, R., Vos, H.R., Marc Timmers, H.T., 2016. Quantitative Proteomics of the SMAD (Suppressor of Mothers against Decapentaplegic) Transcription Factor Family Identifies Importin 5 as a Bone Morphogenic Protein Receptor SMAD-specific Importin. *J Biol Chem* 291, 24121-24132.

Bagci, H., Sriskandarajah, N., Robert, A., Boulais, J., Elkholi, I.E., Tran, V., Lin, Z.Y., Thibault, M.P., Dube, N., Faubert, D., Hipfner, D.R., Gingras, A.C., Cote, J.F., 2020. Mapping the proximity interaction network of the Rho-family GTPases reveals signalling pathways and regulatory mechanisms. *Nat Cell Biol* 22, 120-134.

Baker, C.V., Bronner-Fraser, M., 2001. Vertebrate cranial placodes I. Embryonic induction. *Dev Biol* 232, 1-61.

Bani-Yaghoub, M., Tremblay, R.G., Lei, J.X., Zhang, D., Zurakowski, B., Sandhu, J.K., Smith, B., Ribocco-Lutkiewicz, M., Kennedy, J., Walker, P.R., Sikorska, M., 2006. Role of Sox2 in the development of the mouse neocortex. *Dev Biol* 295, 52-66.

Battaglioli, E., Andres, M.E., Rose, D.W., Chenoweth, J.G., Rosenfeld, M.G., Anderson, M.E., Mandel, G., 2002. REST repression of neuronal genes requires components of the hSWI.SNF complex. *J Biol Chem* 277, 41038-41045.

Beck, C.W., Slack, J.M., 2001. An amphibian with ambition: a new role for *Xenopus* in the 21st century. *Genome Biol* 2, REVIEWS1029.

Begbie, J., Ballivet, M., Graham, A., 2002. Early steps in the production of sensory neurons by the neurogenic placodes. *Mol Cell Neurosci* 21, 502-511.

Belandia, B., Orford, R.L., Hurst, H.C., Parker, M.G., 2002. Targeting of SWI/SNF chromatin remodelling complexes to estrogen-responsive genes. *EMBO J* 21, 4094-4103.

Bellchambers, H.M., Barratt, K.S., Diamand, K.E.M., Arkell, R.M., 2021. SUMOylation Potentiates ZIC Protein Activity to Influence Murine Neural Crest Cell Specification. *Int J Mol Sci* 22.

Bellmeyer, A., Krase, J., Lindgren, J., LaBonne, C., 2003. The protooncogene c-myc is an essential regulator of neural crest formation in *xenopus*. *Dev Cell* 4, 827-839.

Bergsland, M., Ramskold, D., Zaouter, C., Klum, S., Sandberg, R., Muhr, J., 2011. Sequentially acting Sox transcription factors in neural lineage development. *Genes Dev* 25, 2453-2464.

Bermingham, N.A., Hassan, B.A., Price, S.D., Vollrath, M.A., Ben-Arie, N., Eatock, R.A., Bellen, H.J., Lysakowski, A., Zoghbi, H.Y., 1999. Math1: an essential gene for the generation of inner ear hair cells. *Science* 284, 1837-1841.

Berninger, B., Costa, M.R., Koch, U., Schroeder, T., Sutor, B., Grothe, B., Gotz, M., 2007. Functional properties of neurons derived from in vitro reprogrammed postnatal astroglia. *J Neurosci* 27, 8654-8664.

Bernstock, J.D., Peruzzotti-Jametti, L., Leonardi, T., Vicario, N., Ye, D., Lee, Y.J., Maric, D., Johnson, K.R., Mou, Y., Van Den Bosch, A., Winterbone, M., Friedman, G.K., Franklin, R.J.M., Hallenbeck, J.M., Pluchino, S., 2019. SUMOylation promotes survival and integration of neural stem cell grafts in ischemic stroke. *EBioMedicine* 42, 214-224.

Bertrand, N., Castro, D.S., Guillemot, F., 2002. Proneural genes and the specification of neural cell types. *Nat Rev Neurosci* 3, 517-530.

Bessarab, D.A., Chong, S.W., Korzh, V., 2004. Expression of zebrafish six1 during sensory organ development and myogenesis. *Dev Dyn* 230, 781-786.

Bhattacharya, U., Neizer-Ashun, F., Mukherjee, P., Bhattacharya, R., 2020. When the chains do not break: the role of USP10 in physiology and pathology. *Cell Death Dis* 11, 1033.

Bok, J., Chang, W., Wu, D.K., 2007. Patterning and morphogenesis of the vertebrate inner ear. *Int J Dev Biol* 51, 521-533.

Bonini, N.M., Bui, Q.T., Gray-Board, G.L., Warrick, J.M., 1997. The *Drosophila* eyes absent gene directs ectopic eye formation in a pathway conserved between flies and vertebrates. *Development* 124, 4819-4826.

Bonini, N.M., Leiserson, W.M., Benzer, S., 1993. The eyes absent gene: genetic control of cell survival and differentiation in the developing *Drosophila* eye. *Cell* 72, 379-395.

Bosman, E.A., Quint, E., Fuchs, H., Hrabe de Angelis, M., Steel, K.P., 2009. Catweasel mice: a novel role for Six1 in sensory patch development and a model for branchio-oto-renal syndrome. *Dev Biol* 328, 285-296.

- Braun, M.M., Etheridge, A., Bernard, A., Robertson, C.P., Roelink, H., 2003. Wnt signaling is required at distinct stages of development for the induction of the posterior forebrain. *Development* 130, 5579-5587.
- Briggs, J.A., Weinreb, C., Wagner, D.E., Megason, S., Peshkin, L., Kirschner, M.W., Klein, A.M., 2018. The dynamics of gene expression in vertebrate embryogenesis at single-cell resolution. *Science* 360.
- Brugmann, S.A., Pandur, P.D., Kenyon, K.L., Pignoni, F., Moody, S.A., 2004. Six1 promotes a placodal fate within the lateral neurogenic ectoderm by functioning as both a transcriptional activator and repressor. *Development* 131, 5871-5881.
- Brulet, R., Matsuda, T., Zhang, L., Miranda, C., Giacca, M., Kaspar, B.K., Nakashima, K., Hsieh, J., 2017. NEUROD1 Instructs Neuronal Conversion in Non-Reactive Astrocytes. *Stem Cell Reports* 8, 1506-1515.
- Buck, L.B., 2004. Olfactory receptors and odor coding in mammals. *Nutr Rev* 62, S184-188; discussion S224-141.
- Burn, B., Brown, S., Chang, C., 2011. Regulation of early *Xenopus* development by the PIAS genes. *Dev Dyn* 240, 2120-2126.
- Bylund, M., Andersson, E., Novitch, B.G., Muhr, J., 2003. Vertebrate neurogenesis is counteracted by Sox1-3 activity. *Nat Neurosci* 6, 1162-1168.
- Canning, C.A., Lee, L., Luo, S.X., Graham, A., Jones, C.M., 2008. Neural tube derived Wnt signals cooperate with FGF signaling in the formation and differentiation of the trigeminal placodes. *Neural Dev* 3, 35.
- Cau, E., Casarosa, S., Guillemot, F., 2002. Mash1 and Ngn1 control distinct steps of determination and differentiation in the olfactory sensory neuron lineage. *Development* 129, 1871-1880.
- Cau, E., Gradwohl, G., Casarosa, S., Kageyama, R., Guillemot, F., 2000. Hes genes regulate sequential stages of neurogenesis in the olfactory epithelium. *Development* 127, 2323-2332.
- Cau, E., Gradwohl, G., Fode, C., Guillemot, F., 1997. Mash1 activates a cascade of bHLH regulators in olfactory neuron progenitors. *Development* 124, 1611-1621.

Cavallaro, M., Mariani, J., Lancini, C., Latorre, E., Caccia, R., Gullo, F., Valotta, M., DeBiasi, S., Spinardi, L., Ronchi, A., Wanke, E., Brunelli, S., Favaro, R., Ottolenghi, S., Nicolis, S.K., 2008. Impaired generation of mature neurons by neural stem cells from hypomorphic Sox2 mutants. *Development* 135, 541-557.

Ceballos-Chavez, M., Rivero, S., Garcia-Gutierrez, P., Rodriguez-Paredes, M., Garcia-Dominguez, M., Bhattacharya, S., Reyes, J.C., 2012. Control of neuronal differentiation by sumoylation of BRAF35, a subunit of the LSD1-CoREST histone demethylase complex. *Proc Natl Acad Sci U S A* 109, 8085-8090.

Chae, J.H., Stein, G.H., Lee, J.E., 2004. NeuroD: the predicted and the surprising. *Mol Cells* 18, 271-288.

Chalabi Hagkarim, N., Grand, R.J., 2020. The Regulatory Properties of the Ccr4-Not Complex. *Cells* 9.

Chanda, S., Ang, C.E., Davila, J., Pak, C., Mall, M., Lee, Q.Y., Ahlenius, H., Jung, S.W., Sudhof, T.C., Wernig, M., 2014. Generation of induced neuronal cells by the single reprogramming factor ASCL1. *Stem Cell Reports* 3, 282-296.

Chen, B., Kim, E.H., Xu, P.X., 2009. Initiation of olfactory placode development and neurogenesis is blocked in mice lacking both Six1 and Six4. *Dev Biol* 326, 75-85.

Chen, H., Thiagalingam, A., Chopra, H., Borges, M.W., Feder, J.N., Nelkin, B.D., Baylin, S.B., Ball, D.W., 1997. Conservation of the *Drosophila* lateral inhibition pathway in human lung cancer: a hairy-related protein (HES-1) directly represses achaete-scute homolog-1 expression. *Proc Natl Acad Sci U S A* 94, 5355-5360.

Chen, J., Liu, M.Y., Parish, C.R., Chong, B.H., Khachigian, L., 2011a. Nuclear import of early growth response-1 involves importin-7 and the novel nuclear localization signal serine-proline-serine. *Int J Biochem Cell Biol* 43, 905-912.

Chen, P., Johnson, J.E., Zoghbi, H.Y., Segil, N., 2002. The role of Math1 in inner ear development: Uncoupling the establishment of the sensory primordium from hair cell fate determination. *Development* 129, 2495-2505.

- Chen, Y., Ding, Y., Zhang, Z., Wang, W., Chen, J.Y., Ueno, N., Mao, B., 2011b. Evolution of vertebrate central nervous system is accompanied by novel expression changes of duplicate genes. *J Genet Genomics* 38, 577-584.
- Chen, Y., Shi, L., Zhang, L., Li, R., Liang, J., Yu, W., Sun, L., Yang, X., Wang, Y., Zhang, Y., Shang, Y., 2008. The molecular mechanism governing the oncogenic potential of SOX2 in breast cancer. *J Biol Chem* 283, 17969-17978.
- Cheyette, B.N., Green, P.J., Martin, K., Garren, H., Hartenstein, V., Zipursky, S.L., 1994. The *Drosophila sine oculis* locus encodes a homeodomain-containing protein required for the development of the entire visual system. *Neuron* 12, 977-996.
- Cho, H.H., Cargnin, F., Kim, Y., Lee, B., Kwon, R.J., Nam, H., Shen, R., Barnes, A.P., Lee, J.W., Lee, S., Lee, S.K., 2014. *Isl1* directly controls a cholinergic neuronal identity in the developing forebrain and spinal cord by forming cell type-specific complexes. *PLoS Genet* 10, e1004280.
- Cho, J.H., Tsai, M.J., 2004. The role of BETA2/NeuroD1 in the development of the nervous system. *Mol Neurobiol* 30, 35-47.
- Chohra, I., Chung, K., Giri, S., Malgrange, B., 2023. ATP-Dependent Chromatin Remodellers in Inner Ear Development. *Cells* 12.
- Chow, R.L., Lang, R.A., 2001. Early eye development in vertebrates. *Annu Rev Cell Dev Biol* 17, 255-296.
- Christensen, K.L., Patrick, A.N., McCoy, E.L., Ford, H.L., 2008. The six family of homeobox genes in development and cancer. *Adv Cancer Res* 101, 93-126.
- Christophorou, N.A., Bailey, A.P., Hanson, S., Streit, A., 2009. Activation of *Six1* target genes is required for sensory placode formation. *Dev Biol* 336, 327-336.
- Chung, C.D., Liao, J., Liu, B., Rao, X., Jay, P., Berta, P., Shuai, K., 1997. Specific inhibition of Stat3 signal transduction by PIAS3. *Science* 278, 1803-1805.
- Coletta, R.D., Christensen, K., Reichenberger, K.J., Lamb, J., Micommonaco, D., Huang, L., Wolf, D.M., Muller-Tidow, C., Golub, T.R., Kawakami, K., Ford, H.L., 2004. The *Six1* homeoprotein stimulates tumorigenesis by reactivation of cyclin A1. *Proc Natl Acad Sci U S A* 101, 6478-6483.

Coletta, R.D., Christensen, K.L., Micalizzi, D.S., Jedlicka, P., Varella-Garcia, M., Ford, H.L., 2008. Six1 overexpression in mammary cells induces genomic instability and is sufficient for malignant transformation. *Cancer Res* 68, 2204-2213.

Cong, F., Long, J., Liu, J., Deng, Z., Yan, B., Liang, C., Huang, X., Liu, J., Tang, W., 2022. An integrative analysis revealing POLD2 as a tumor suppressive immune protein and prognostic biomarker in pan-cancer. *Front Genet* 13, 877468.

Connaughton, D.M., Dai, R., Owen, D.J., Marquez, J., Mann, N., Graham-Paquin, A.L., Nakayama, M., Coyaud, E., Laurent, E.M.N., St-Germain, J.R., Blok, L.S., Vano, A., Klambt, V., Deutsch, K., Wu, C.W., Kolvenbach, C.M., Kause, F., Ottlewski, I., Schneider, R., Kitzler, T.M., Majmundar, A.J., Buerger, F., Onuchic-Whitford, A.C., Youying, M., Kolb, A., Salmanullah, D., Chen, E., van der Ven, A.T., Rao, J., Ityel, H., Seltz, S., Rieke, J.M., Chen, J., Vivante, A., Hwang, D.Y., Kohl, S., Dworschak, G.C., Hermle, T., Alders, M., Bartolomeus, T., Bauer, S.B., Baum, M.A., Brilstra, E.H., Challman, T.D., Zyskind, J., Costin, C.E., Dipple, K.M., Duijkers, F.A., Ferguson, M., Fitzpatrick, D.R., Fick, R., Glass, I.A., Hulick, P.J., Kline, A.D., Krey, I., Kumar, S., Lu, W., Marco, E.J., Wentzensen, I.M., Mefford, H.C., Platzer, K., Povolotskaya, I.S., Savatt, J.M., Shcherbakova, N.V., Senguttuvan, P., Squire, A.E., Stein, D.R., Thiffault, I., Voinova, V.Y., Somers, M.J.G., Ferguson, M.A., Traum, A.Z., Daouk, G.H., Daga, A., Rodig, N.M., Terhal, P.A., van Binsbergen, E., Eid, L.A., Tasic, V., Rasouly, H.M., Lim, T.Y., Ahram, D.F., Gharavi, A.G., Reutter, H.M., Rehm, H.L., MacArthur, D.G., Lek, M., Laricchia, K.M., Lifton, R.P., Xu, H., Mane, S.M., Sanna-Cherchi, S., Sharrocks, A.D., Raught, B., Fisher, S.E., Bouchard, M., Khokha, M.K., Shril, S., Hildebrandt, F., 2020. Mutations of the Transcriptional Corepressor ZMYM2 Cause Syndromic Urinary Tract Malformations. *Am J Hum Genet* 107, 727-742.

Cook, P.J., Ju, B.G., Telese, F., Wang, X., Glass, C.K., Rosenfeld, M.G., 2009. Tyrosine dephosphorylation of H2AX modulates apoptosis and survival decisions. *Nature* 458, 591-596.

Corradi, A., Croci, L., Stayton, C.L., Gulisano, M., Boncinelli, E., Consalez, G.G., 1996. cDNA sequence, map, and expression of the murine homolog of GTBP, a DNA mismatch repair gene. *Genomics* 36, 288-295.

Couly, G.F., Le Douarin, N.M., 1985. Mapping of the early neural primordium in quail-chick chimeras. I. Developmental relationships between placodes, facial ectoderm, and prosencephalon. *Dev Biol* 110, 422-439.

- Cvekl, A., Duncan, M.K., 2007. Genetic and epigenetic mechanisms of gene regulation during lens development. *Prog Retin Eye Res* 26, 555-597.
- Cvekl, A., Zhang, X., 2017. Signaling and Gene Regulatory Networks in Mammalian Lens Development. *Trends Genet* 33, 677-702.
- D'Amico-Martel, A., Noden, D.M., 1983. Contributions of placodal and neural crest cells to avian cranial peripheral ganglia. *Am J Anat* 166, 445-468.
- Dabdoub, A., Puligilla, C., Jones, J.M., Fritzsche, B., Cheah, K.S., Pevny, L.H., Kelley, M.W., 2008. Sox2 signaling in prosensory domain specification and subsequent hair cell differentiation in the developing cochlea. *Proc Natl Acad Sci U S A* 105, 18396-18401.
- Daniels, M., Shimizu, K., Zorn, A.M., Ohnuma, S., 2004. Negative regulation of Smad2 by PIASy is required for proper *Xenopus* mesoderm formation. *Development* 131, 5613-5626.
- Dash, S., Brastrom, L.K., Patel, S.D., Scott, C.A., Slusarski, D.C., Lachke, S.A., 2020. The master transcription factor SOX2, mutated in anophthalmia/microphthalmia, is post-transcriptionally regulated by the conserved RNA-binding protein RBM24 in vertebrate eye development. *Hum Mol Genet* 29, 591-604.
- Dash, S., Siddam, A.D., Barnum, C.E., Janga, S.C., Lachke, S.A., 2016. RNA-binding proteins in eye development and disease: implication of conserved RNA granule components. *Wiley Interdiscip Rev RNA* 7, 527-557.
- David, R., Ahrens, K., Wedlich, D., Schlosser, G., 2001. *Xenopus* Eya1 demarcates all neurogenic placodes as well as migrating hypaxial muscle precursors. *Mech Dev* 103, 189-192.
- Davis, R.L., Turner, D.L., 2001. Vertebrate hairy and Enhancer of split related proteins: transcriptional repressors regulating cellular differentiation and embryonic patterning. *Oncogene* 20, 8342-8357.
- Davis, S.W., Ellsworth, B.S., Perez Millan, M.I., Gergics, P., Schade, V., Foyouzi, N., Brinkmeier, M.L., Mortensen, A.H., Camper, S.A., 2013. Pituitary gland development and disease: from stem cell to hormone production. *Curr Top Dev Biol* 106, 1-47.
- De Lope, C., Martin-Alonso, S., Auzmendi-Iriarte, J., Escudero, C., Mulet, I., Larrasa-Alonso, J., Lopez-Antona, I., Matheu, A., Palmero, I., 2019. SIX1 represses senescence and promotes SOX2-mediated cellular plasticity during tumorigenesis. *Sci Rep* 9, 1412.

Dee, C.T., Hirst, C.S., Shih, Y.H., Tripathi, V.B., Patient, R.K., Scotting, P.J., 2008. Sox3 regulates both neural fate and differentiation in the zebrafish ectoderm. *Dev Biol* 320, 289-301.

Dhanesh, S.B., Subashini, C., James, J., 2016. Hes1: the maestro in neurogenesis. *Cell Mol Life Sci* 73, 4019-4042.

Domingos, P.M., Obukhanych, T.V., Altmann, C.R., Hemmati-Brivanlou, A., 2002. Cloning and developmental expression of Baf57 in *Xenopus laevis*. *Mech Dev* 116, 177-181.

Donner, A.L., Episkopou, V., Maas, R.L., 2007. Sox2 and Pou2f1 interact to control lens and olfactory placode development. *Dev Biol* 303, 784-799.

Drummond, J.T., Li, G.M., Longley, M.J., Modrich, P., 1995. Isolation of an hMSH2-p160 heterodimer that restores DNA mismatch repair to tumor cells. *Science* 268, 1909-1912.

Dubey, A., Rose, R.E., Jones, D.R., Saint-Jeannet, J.P., 2018. Generating retinoic acid gradients by local degradation during craniofacial development: One cell's cue is another cell's poison. *Genesis* 56.

Dupin, E., Calloni, G.W., Coelho-Aguiar, J.M., Le Douarin, N.M., 2018. The issue of the multipotency of the neural crest cells. *Dev Biol* 444 Suppl 1, S47-S59.

El-Hashash, A.H., Al Alam, D., Turcatel, G., Bellusci, S., Warburton, D., 2011. Eyes absent 1 (Eya1) is a critical coordinator of epithelial, mesenchymal and vascular morphogenesis in the mammalian lung. *Dev Biol* 350, 112-126.

El Masri, R., Delon, J., 2021. RHO GTPases: from new partners to complex immune syndromes. *Nat Rev Immunol* 21, 499-513.

elAmraoui, A., Dubois, P.M., 1993. Experimental evidence for the early commitment of the presumptive adenohypophysis. *Neuroendocrinology* 58, 609-615.

Evdokimov, E., Sharma, P., Lockett, S.J., Lualdi, M., Kuehn, M.R., 2008. Loss of SUMO1 in mice affects RanGAP1 localization and formation of PML nuclear bodies, but is not lethal as it can be compensated by SUMO2 or SUMO3. *J Cell Sci* 121, 4106-4113.

Evsen, L., Sugahara, S., Uchikawa, M., Kondoh, H., Wu, D.K., 2013. Progression of neurogenesis in the inner ear requires inhibition of Sox2 transcription by neurogenin1 and neurod1. *J Neurosci* 33, 3879-3890.

- Fabrizio, J.J., Boyle, M., DiNardo, S., 2003. A somatic role for eyes absent (*eya*) and sine oculis (*so*) in *Drosophila* spermatocyte development. *Dev Biol* 258, 117-128.
- Farabaugh, S.M., Micalizzi, D.S., Jedlicka, P., Zhao, R., Ford, H.L., 2012. *Eya2* is required to mediate the pro-metastatic functions of *Six1* via the induction of TGF-beta signaling, epithelial-mesenchymal transition, and cancer stem cell properties. *Oncogene* 31, 552-562.
- Farah, M.H., Olson, J.M., Sucic, H.B., Hume, R.I., Tapscott, S.J., Turner, D.L., 2000. Generation of neurons by transient expression of neural bHLH proteins in mammalian cells. *Development* 127, 693-702.
- Favaro, R., Valotta, M., Ferri, A.L., Latorre, E., Mariani, J., Giachino, C., Lancini, C., Tosetti, V., Ottolenghi, S., Taylor, V., Nicolis, S.K., 2009. Hippocampal development and neural stem cell maintenance require Sox2-dependent regulation of *Shh*. *Nat Neurosci* 12, 1248-1256.
- Fawcett, S.R., Klymkowsky, M.W., 2004. Embryonic expression of *Xenopus laevis* SOX7. *Gene Expr Patterns* 4, 29-33.
- Fekete, D.M., Wu, D.K., 2002. Revisiting cell fate specification in the inner ear. *Curr Opin Neurobiol* 12, 35-42.
- Feledy, J.A., Beanan, M.J., Sandoval, J.J., Goodrich, J.S., Lim, J.H., Matsuo-Takasaki, M., Sato, S.M., Sargent, T.D., 1999. Inhibitory patterning of the anterior neural plate in *Xenopus* by homeodomain factors *Dlx3* and *Msx1*. *Dev Biol* 212, 455-464.
- Fernandez-Lloris, R., Osses, N., Jaffray, E., Shen, L.N., Vaughan, O.A., Girwood, D., Bartrons, R., Rosa, J.L., Hay, R.T., Ventura, F., 2006. Repression of SOX6 transcriptional activity by SUMO modification. *FEBS Lett* 580, 1215-1221.
- Fode, C., Gradwohl, G., Morin, X., Dierich, A., LeMeur, M., Goridis, C., Guillemot, F., 1998. The bHLH protein NEUROGENIN 2 is a determination factor for epibranchial placode-derived sensory neurons. *Neuron* 20, 483-494.
- Ford, H.L., Kabingu, E.N., Bump, E.A., Mutter, G.L., Pardee, A.B., 1998. Abrogation of the G2 cell cycle checkpoint associated with overexpression of HSIX1: a possible mechanism of breast carcinogenesis. *Proc Natl Acad Sci U S A* 95, 12608-12613.
- Formstecher, E., Aresta, S., Collura, V., Hamburger, A., Meil, A., Trehin, A., Reverdy, C., Betin, V., Maire, S., Brun, C., Jacq, B., Arpin, M., Bellaiche, Y., Bellusci, S., Benaroch, P., Bornens, M.,

Chanet, R., Chavrier, P., Delattre, O., Doye, V., Fehon, R., Faye, G., Galli, T., Girault, J.A., Goud, B., de Gunzburg, J., Johannes, L., Junier, M.P., Mirouse, V., Mukherjee, A., Papadopoulo, D., Perez, F., Plessis, A., Rosse, C., Saule, S., Stoppa-Lyonnet, D., Vincent, A., White, M., Legrain, P., Wojcik, J., Camonis, J., Daviet, L., 2005. Protein interaction mapping: a Drosophila case study. *Genome Res* 15, 376-384.

Freyer, L., Morrow, B.E., 2010. Canonical Wnt signaling modulates Tbx1, Eya1, and Six1 expression, restricting neurogenesis in the otic vesicle. *Dev Dyn* 239, 1708-1722.

Friedle, H., Knochel, W., 2002. Cooperative interaction of Xvent-2 and GATA-2 in the activation of the ventral homeobox gene Xvent-1B. *J Biol Chem* 277, 23872-23881.

Friedman, R.A., Makmura, L., Biesiada, E., Wang, X., Keithley, E.M., 2005. Eya1 acts upstream of Tbx1, Neurogenin 1, NeuroD and the neurotrophins BDNF and NT-3 during inner ear development. *Mech Dev* 122, 625-634.

Furukawa, M., Zhang, Y., McCarville, J., Ohta, T., Xiong, Y., 2000. The CUL1 C-terminal sequence and ROC1 are required for efficient nuclear accumulation, NEDD8 modification, and ubiquitin ligase activity of CUL1. *Mol Cell Biol* 20, 8185-8197.

Gans, C., Northcutt, R.G., 1983. Neural crest and the origin of vertebrates: a new head. *Science* 220, 268-273.

Gao, S.T., Xin, X., Wang, Z.Y., Hu, Y.Y., Feng, Q., 2024. USP5: Comprehensive insights into structure, function, biological and disease-related implications, and emerging therapeutic opportunities. *Mol Cell Probes* 73, 101944.

Garcia-Pedrero, J.M., Kiskinis, E., Parker, M.G., Belandia, B., 2006. The SWI/SNF chromatin remodeling subunit BAF57 is a critical regulator of estrogen receptor function in breast cancer cells. *J Biol Chem* 281, 22656-22664.

Garvin, A.J., Morris, J.R., 2017. SUMO, a small, but powerful, regulator of double-strand break repair. *Philos Trans R Soc Lond B Biol Sci* 372.

Ghanbari, H., Seo, H.C., Fjose, A., Brandli, A.W., 2001. Molecular cloning and embryonic expression of Xenopus Six homeobox genes. *Mech Dev* 101, 271-277.

Ghysen, A., Dambly-Chaudiere, C., 2004. Development of the zebrafish lateral line. *Curr Opin Neurobiol* 14, 67-73.

- Gibbs, M.A., 2004. Lateral line receptors: where do they come from developmentally and where is our research going? *Brain Behav Evol* 64, 163-181.
- Gingras, A.C., Gstaiger, M., Raught, B., Aebersold, R., 2007. Analysis of protein complexes using mass spectrometry. *Nat Rev Mol Cell Biol* 8, 645-654.
- Giurgiu, M., Reinhard, J., Brauner, B., Dunger-Kaltenbach, I., Fobo, G., Frishman, G., Montrone, C., Ruepp, A., 2019. CORUM: the comprehensive resource of mammalian protein complexes-2019. *Nucleic Acids Res* 47, D559-D563.
- Glenn Northcutt, R., 2005. The new head hypothesis revisited. *J Exp Zool B Mol Dev Evol* 304, 274-297.
- Gocke, C.B., Yu, H., 2008. ZNF198 stabilizes the LSD1-CoREST-HDAC1 complex on chromatin through its MYM-type zinc fingers. *PLoS One* 3, e3255.
- Gouignard, N., Maccarana, M., Strate, I., von Stedingk, K., Malmstrom, A., Pera, E.M., 2016. Musculocontractural Ehlers-Danlos syndrome and neurocristopathies: dermatan sulfate is required for *Xenopus* neural crest cells to migrate and adhere to fibronectin. *Dis Model Mech* 9, 607-620.
- Grocott, T., Tambalo, M., Streit, A., 2012. The peripheral sensory nervous system in the vertebrate head: a gene regulatory perspective. *Dev Biol* 370, 3-23.
- Gross, M., Liu, B., Tan, J., French, F.S., Carey, M., Shuai, K., 2001. Distinct effects of PIA5 proteins on androgen-mediated gene activation in prostate cancer cells. *Oncogene* 20, 3880-3887.
- Guillemot, F., Joyner, A.L., 1993. Dynamic expression of the murine Achaete-Scute homologue Mash-1 in the developing nervous system. *Mech Dev* 42, 171-185.
- Guo, Z., Zhang, L., Wu, Z., Chen, Y., Wang, F., Chen, G., 2014. In vivo direct reprogramming of reactive glial cells into functional neurons after brain injury and in an Alzheimer's disease model. *Cell Stem Cell* 14, 188-202.
- Guzzo, C.M., Ringel, A., Cox, E., Uzoma, I., Zhu, H., Blackshaw, S., Wolberger, C., Matunis, M.J., 2014. Characterization of the SUMO-binding activity of the myeloproliferative and mental retardation (MYM)-type zinc fingers in ZNF261 and ZNF198. *PLoS One* 9, e105271.

Hagey, D.W., Muhr, J., 2014. Sox2 acts in a dose-dependent fashion to regulate proliferation of cortical progenitors. *Cell Rep* 9, 1908-1920.

Hah, N., Kolkman, A., Ruhl, D.D., Pijnappel, W.W., Heck, A.J., Timmers, H.T., Kraus, W.L., 2010. A role for BAF57 in cell cycle-dependent transcriptional regulation by the SWI/SNF chromatin remodeling complex. *Cancer Res* 70, 4402-4411.

Hakimi, M.A., Dong, Y., Lane, W.S., Speicher, D.W., Shiekhattar, R., 2003. A candidate X-linked mental retardation gene is a component of a new family of histone deacetylase-containing complexes. *J Biol Chem* 278, 7234-7239.

Halder, G., Callaerts, P., Flister, S., Walldorf, U., Kloter, U., Gehring, W.J., 1998. Eyeless initiates the expression of both sine oculis and eyes absent during Drosophila compound eye development. *Development* 125, 2181-2191.

Hamburger, V., 1961. Experimental analysis of the dual origin of the trigeminal ganglion in the chick embryo. *J Exp Zool* 148, 91-123.

Han, M.M., Hirakawa, M., Yamauchi, M., Matsuda, N., 2022. Roles of the SUMO-related enzymes, PIAS1, PIAS4, and RNF4, in DNA double-strand break repair by homologous recombination. *Biochem Biophys Res Commun* 591, 95-101.

Hansen, A., Zeiske, E., 1993. Development of the olfactory organ in the zebrafish, *Brachydanio rerio*. *J Comp Neurol* 333, 289-300.

Hanson, I.M., 2001. Mammalian homologues of the Drosophila eye specification genes. *Semin Cell Dev Biol* 12, 475-484.

Harlow, D.E., Barlow, L.A., 2007. Embryonic origin of gustatory cranial sensory neurons. *Dev Biol* 310, 317-328.

Hatakeyama, J., Bessho, Y., Katoh, K., Ookawara, S., Fujioka, M., Guillemot, F., Kageyama, R., 2004. Hes genes regulate size, shape and histogenesis of the nervous system by control of the timing of neural stem cell differentiation. *Development* 131, 5539-5550.

Hattori, T., Eberspaecher, H., Lu, J., Zhang, R., Nishida, T., Kahyo, T., Yasuda, H., de Crombrughe, B., 2006. Interactions between PIAS proteins and SOX9 result in an increase in the cellular concentrations of SOX9. *J Biol Chem* 281, 14417-14428.

- Hernandez, P.P., Olivari, F.A., Sarrazin, A.F., Sandoval, P.C., Allende, M.L., 2007. Regeneration in zebrafish lateral line neuromasts: expression of the neural progenitor cell marker *sox2* and proliferation-dependent and-independent mechanisms of hair cell renewal. *Dev Neurobiol* 67, 637-654.
- Holmberg, J., Hansson, E., Malewicz, M., Sandberg, M., Perlmann, T., Lendahl, U., Muhr, J., 2008. *SoxB1* transcription factors and Notch signaling use distinct mechanisms to regulate proneural gene function and neural progenitor differentiation. *Development* 135, 1843-1851.
- Hong, C.S., Saint-Jeannet, J.P., 2007. The activity of *Pax3* and *Zic1* regulates three distinct cell fates at the neural plate border. *Mol Biol Cell* 18, 2192-2202.
- Hu, Q., Zhang, L., Wen, J., Wang, S., Li, M., Feng, R., Yang, X., Li, L., 2010. The EGF receptor-*sox2*-EGF receptor feedback loop positively regulates the self-renewal of neural precursor cells. *Stem Cells* 28, 279-286.
- Huang, C., Chan, J.A., Schuurmans, C., 2014. Proneural bHLH genes in development and disease. *Curr Top Dev Biol* 110, 75-127.
- Huang, D.W., Sherman, B.T., Tan, Q., Collins, J.R., Alvord, W.G., Roayaei, J., Stephens, R., Baseler, M.W., Lane, H.C., Lempicki, R.A., 2007. The DAVID Gene Functional Classification Tool: a novel biological module-centric algorithm to functionally analyze large gene lists. *Genome Biol* 8, R183.
- Hyodo-Miura, J., Urushiyama, S., Nagai, S., Nishita, M., Ueno, N., Shibuya, H., 2002. Involvement of *NLK* and *Sox11* in neural induction in *Xenopus* development. *Genes Cells* 7, 487-496.
- Iaccarino, I., Palombo, F., Drummond, J., Totty, N.F., Hsuan, J.J., Modrich, P., Jiricny, J., 1996. *MSH6*, a *Saccharomyces cerevisiae* protein that binds to mismatches as a heterodimer with *MSH2*. *Curr Biol* 6, 484-486.
- Ikeda, K., Ookawara, S., Sato, S., Ando, Z., Kageyama, R., Kawakami, K., 2007. *Six1* is essential for early neurogenesis in the development of olfactory epithelium. *Dev Biol* 311, 53-68.
- Ikeda, K., Watanabe, Y., Ohto, H., Kawakami, K., 2002. Molecular interaction and synergistic activation of a promoter by *Six*, *Eya*, and *Dach* proteins mediated through CREB binding protein. *Mol Cell Biol* 22, 6759-6766.

- Ishibashi, M., Ang, S.L., Shiota, K., Nakanishi, S., Kageyama, R., Guillemot, F., 1995. Targeted disruption of mammalian hairy and Enhancer of split homolog-1 (HES-1) leads to up-regulation of neural helix-loop-helix factors, premature neurogenesis, and severe neural tube defects. *Genes Dev* 9, 3136-3148.
- Ishii, Y., Abu-Elmagd, M., Scotting, P.J., 2001. Sox3 expression defines a common primordium for the epibranchial placodes in chick. *Dev Biol* 236, 344-353.
- Jemc, J., Rebay, I., 2007. The eyes absent family of phosphotyrosine phosphatases: properties and roles in developmental regulation of transcription. *Annu Rev Biochem* 76, 513-538.
- Jeong, J.Y., Einhorn, Z., Mercurio, S., Lee, S., Lau, B., Mione, M., Wilson, S.W., Guo, S., 2006. Neurogenin1 is a determinant of zebrafish basal forebrain dopaminergic neurons and is regulated by the conserved zinc finger protein Tof/Fezl. *Proc Natl Acad Sci U S A* 103, 5143-5148.
- Johnson, K.R., Cook, S.A., Erway, L.C., Matthews, A.N., Sanford, L.P., Paradies, N.E., Friedman, R.A., 1999. Inner ear and kidney anomalies caused by IAP insertion in an intron of the *Eya1* gene in a mouse model of BOR syndrome. *Hum Mol Genet* 8, 645-653.
- Jonas, S., Izaurralde, E., 2015. Towards a molecular understanding of microRNA-mediated gene silencing. *Nat Rev Genet* 16, 421-433.
- Joshi, P., Greco, T.M., Guise, A.J., Luo, Y., Yu, F., Nesvizhskii, A.I., Cristea, I.M., 2013. The functional interactome landscape of the human histone deacetylase family. *Mol Syst Biol* 9, 672.
- Jourdeuil, K., Neilson, K.M., Cousin, H., Tavares, A.L.P., Majumdar, H.D., Alfandari, D., Moody, S.A., 2023. *Zmym4* is required for early cranial gene expression and craniofacial cartilage formation. *Front Cell Dev Biol* 11, 1274788.
- Juarez-Vicente, F., Luna-Pelaez, N., Garcia-Dominguez, M., 2016. The Sumo protease *Senp7* is required for proper neuronal differentiation. *Biochim Biophys Acta* 1863, 1490-1498.
- Julian, L.M., McDonald, A.C., Stanford, W.L., 2017. Direct reprogramming with SOX factors: masters of cell fate. *Curr Opin Genet Dev* 46, 24-36.
- Kageyama, R., Ohtsuka, T., Kobayashi, T., 2008. Roles of *Hes* genes in neural development. *Dev Growth Differ* 50 Suppl 1, S97-103.

Kalb, R., Mallery, D.L., Larkin, C., Huang, J.T., Hiom, K., 2014. BRCA1 is a histone-H2A-specific ubiquitin ligase. *Cell Rep* 8, 999-1005.

Kao, S.H., Wu, H.T., Wu, K.J., 2018. Ubiquitination by HUWE1 in tumorigenesis and beyond. *J Biomed Sci* 25, 67.

Kawakami, K., Sato, S., Ozaki, H., Ikeda, K., 2000. Six family genes--structure and function as transcription factors and their roles in development. *Bioessays* 22, 616-626.

Kawauchi, S., Beites, C.L., Crocker, C.E., Wu, H.H., Bonnin, A., Murray, R., Calof, A.L., 2004. Molecular signals regulating proliferation of stem and progenitor cells in mouse olfactory epithelium. *Dev Neurosci* 26, 166-180.

Kiecker, C., Niehrs, C., 2001. A morphogen gradient of Wnt/beta-catenin signalling regulates anteroposterior neural patterning in *Xenopus*. *Development* 128, 4189-4201.

Kikuchi, A., Onoda, H., Yamaguchi, K., Kori, S., Matsuzawa, S., Chiba, Y., Tanimoto, S., Yoshimi, S., Sato, H., Yamagata, A., Shirouzu, M., Adachi, N., Sharif, J., Koseki, H., Nishiyama, A., Nakanishi, M., Defossez, P.A., Arita, K., 2022. Structural basis for activation of DNMT1. *Nat Commun* 13, 7130.

Kingsbury, T.J., Kim, M., Civin, C.I., 2019. Regulation of cancer stem cell properties by SIX1, a member of the PAX-SIX-EYA-DACH network. *Adv Cancer Res* 141, 1-42.

Klein, S.L., Graziadei, P.P., 1983. The differentiation of the olfactory placode in *Xenopus laevis*: a light and electron microscope study. *J Comp Neurol* 217, 17-30.

Kobayashi, M., Nishikawa, K., Suzuki, T., Yamamoto, M., 2001. The homeobox protein Six3 interacts with the Groucho corepressor and acts as a transcriptional repressor in eye and forebrain formation. *Dev Biol* 232, 315-326.

Kobayashi, T., Kageyama, R., 2014. Expression dynamics and functions of Hes factors in development and diseases. *Curr Top Dev Biol* 110, 263-283.

Kochhar, A., Fischer, S.M., Kimberling, W.J., Smith, R.J., 2007. Branchio-oto-renal syndrome. *Am J Med Genet A* 143A, 1671-1678.

Kondoh, H., 2008. Shedding light on developmental gene regulation through the lens. *Dev Growth Differ* 50 Suppl 1, S57-69.

- Kondoh, H., Kamachi, Y., 2010. SOX-partner code for cell specification: Regulatory target selection and underlying molecular mechanisms. *Int J Biochem Cell Biol* 42, 391-399.
- Kong, D., Li, A., Liu, Y., Cui, Q., Wang, K., Zhang, D., Tang, J., Du, Y., Liu, Z., Wu, G., Wu, K., 2019. SIX1 Activates STAT3 Signaling to Promote the Proliferation of Thyroid Carcinoma via EYA1. *Front Oncol* 9, 1450.
- Konishi, Y., Ikeda, K., Iwakura, Y., Kawakami, K., 2006. Six1 and Six4 promote survival of sensory neurons during early trigeminal gangliogenesis. *Brain Res* 1116, 93-102.
- Koontz, A., Urrutia, H.A., Bronner, M.E., 2023. Making a head: Neural crest and ectodermal placodes in cranial sensory development. *Semin Cell Dev Biol* 138, 15-27.
- Kotaja, N., Aittomaki, S., Silvennoinen, O., Palvimo, J.J., Janne, O.A., 2000. ARIP3 (androgen receptor-interacting protein 3) and other PIAS (protein inhibitor of activated STAT) proteins differ in their ability to modulate steroid receptor-dependent transcriptional activation. *Mol Endocrinol* 14, 1986-2000.
- Kozlowski, D.J., Whitfield, T.T., Hukriede, N.A., Lam, W.K., Weinberg, E.S., 2005. The zebrafish dog-eared mutation disrupts *eya1*, a gene required for cell survival and differentiation in the inner ear and lateral line. *Dev Biol* 277, 27-41.
- Kozmik, Z., Holland, N.D., Kreslova, J., Oliveri, D., Schubert, M., Jonasova, K., Holland, L.Z., Pestarino, M., Benes, V., Candiani, S., 2007. Pax-Six-Eya-Dach network during amphioxus development: conservation in vitro but context specificity in vivo. *Dev Biol* 306, 143-159.
- Krimm, R.F., 2007. Factors that regulate embryonic gustatory development. *BMC Neurosci* 8 Suppl 3, S4.
- Krishnan, N., Jeong, D.G., Jung, S.K., Ryu, S.E., Xiao, A., Allis, C.D., Kim, S.J., Tonks, N.K., 2009. Dephosphorylation of the C-terminal tyrosyl residue of the DNA damage-related histone H2A.X is mediated by the protein phosphatase eyes absent. *J Biol Chem* 284, 16066-16070.
- Kumar, J.P., 2009. The sine oculis homeobox (SIX) family of transcription factors as regulators of development and disease. *Cell Mol Life Sci* 66, 565-583.
- Kumar, J.P., Moses, K., 2001. Expression of evolutionarily conserved eye specification genes during *Drosophila* embryogenesis. *Dev Genes Evol* 211, 406-414.

- Kutay, U., Bischoff, F.R., Kostka, S., Kraft, R., Gorlich, D., 1997. Export of importin alpha from the nucleus is mediated by a specific nuclear transport factor. *Cell* 90, 1061-1071.
- Kuwabara, T., Hsieh, J., Muotri, A., Yeo, G., Warashina, M., Lie, D.C., Moore, L., Nakashima, K., Asashima, M., Gage, F.H., 2009. Wnt-mediated activation of NeuroD1 and retro-elements during adult neurogenesis. *Nat Neurosci* 12, 1097-1105.
- Kwon, H.J., Bhat, N., Sweet, E.M., Cornell, R.A., Riley, B.B., 2010. Identification of early requirements for preplacodal ectoderm and sensory organ development. *PLoS Genet* 6, e1001133.
- Laclef, C., Souil, E., Demignon, J., Maire, P., 2003. Thymus, kidney and craniofacial abnormalities in Six 1 deficient mice. *Mech Dev* 120, 669-679.
- Lacomme, M., Liaubet, L., Pituello, F., Bel-Vialar, S., 2012. NEUROG2 drives cell cycle exit of neuronal precursors by specifically repressing a subset of cyclins acting at the G1 and S phases of the cell cycle. *Mol Cell Biol* 32, 2596-2607.
- Ladher, R.K., O'Neill, P., Begbie, J., 2010. From shared lineage to distinct functions: the development of the inner ear and epibranchial placodes. *Development* 137, 1777-1785.
- Lara-Urena, N., Jafari, V., Garcia-Dominguez, M., 2022. Cancer-Associated Dysregulation of Sumo Regulators: Proteases and Ligases. *Int J Mol Sci* 23.
- Lassiter, R.N., Dude, C.M., Reynolds, S.B., Winters, N.I., Baker, C.V., Stark, M.R., 2007. Canonical Wnt signaling is required for ophthalmic trigeminal placode cell fate determination and maintenance. *Dev Biol* 308, 392-406.
- Le Douarin, N., Kalcheim, C., 1999. *The neural crest*, 2nd ed. Cambridge University Press, Cambridge, UK ; New York, NY, USA.
- Lecaudey, V., Anselme, I., Dildrop, R., Ruther, U., Schneider-Maunoury, S., 2005. Expression of the zebrafish Iroquois genes during early nervous system formation and patterning. *J Comp Neurol* 492, 289-302.
- Ledent, V., Paquet, O., Vervoort, M., 2002. Phylogenetic analysis of the human basic helix-loop-helix proteins. *Genome Biol* 3, RESEARCH0030.

Lee, J.E., Hollenberg, S.M., Snider, L., Turner, D.L., Lipnick, N., Weintraub, H., 1995. Conversion of *Xenopus* ectoderm into neurons by NeuroD, a basic helix-loop-helix protein. *Science* 268, 836-844.

Lee, P.S., Chang, C., Liu, D., Derynck, R., 2003. Sumoylation of Smad4, the common Smad mediator of transforming growth factor-beta family signaling. *J Biol Chem* 278, 27853-27863.

Lee, S., Cuvillier, J.M., Lee, B., Shen, R., Lee, J.W., Lee, S.K., 2012. Fusion protein Isl1-Lhx3 specifies motor neuron fate by inducing motor neuron genes and concomitantly suppressing the interneuron programs. *Proc Natl Acad Sci U S A* 109, 3383-3388.

Lee, S.K., Pfaff, S.L., 2003. Synchronization of neurogenesis and motor neuron specification by direct coupling of bHLH and homeodomain transcription factors. *Neuron* 38, 731-745.

Lessard, J., Wu, J.I., Ranish, J.A., Wan, M., Winslow, M.M., Staahl, B.T., Wu, H., Aebersold, R., Graef, I.A., Crabtree, G.R., 2007. An essential switch in subunit composition of a chromatin remodeling complex during neural development. *Neuron* 55, 201-215.

Leung, J.W., Makharashvili, N., Agarwal, P., Chiu, L.Y., Pourpre, R., Cammarata, M.B., Cannon, J.R., Sherker, A., Durocher, D., Brodbelt, J.S., Paull, T.T., Miller, K.M., 2017. ZMYM3 regulates BRCA1 localization at damaged chromatin to promote DNA repair. *Genes Dev* 31, 260-274.

Li, B., Kuriyama, S., Moreno, M., Mayor, R., 2009. The posteriorizing gene *Gbx2* is a direct target of Wnt signalling and the earliest factor in neural crest induction. *Development* 136, 3267-3278.

Li, J., Rodriguez, Y., Cheng, C., Zeng, L., Wong, E.Y.M., Xu, C.Y., Zhou, M.M., Xu, P.X., 2017. EYA1's Conformation Specificity in Dephosphorylating Phosphothreonine in Myc and Its Activity on Myc Stabilization in Breast Cancer. *Mol Cell Biol* 37.

Li, J., Xu, J., Jiang, H., Zhang, T., Ramakrishnan, A., Shen, L., Xu, P.X., 2021. Chromatin Remodelers Interact with *Eya1* and *Six2* to Target Enhancers to Control Nephron Progenitor Cell Maintenance. *J Am Soc Nephrol* 32, 2815-2833.

Li, J., Zhang, T., Ramakrishnan, A., Fritsch, B., Xu, J., Wong, E.Y.M., Loh, Y.E., Ding, J., Shen, L., Xu, P.X., 2020. Dynamic changes in cis-regulatory occupancy by *Six1* and its cooperative interactions with distinct cofactors drive lineage-specific gene expression programs during progressive differentiation of the auditory sensory epithelium. *Nucleic Acids Res* 48, 2880-2896.

Li, X., Oghi, K.A., Zhang, J., Krones, A., Bush, K.T., Glass, C.K., Nigam, S.K., Aggarwal, A.K., Maas, R., Rose, D.W., Rosenfeld, M.G., 2003. Eya protein phosphatase activity regulates Six1-Dach-Eya transcriptional effects in mammalian organogenesis. *Nature* 426, 247-254.

Link, K.A., Burd, C.J., Williams, E., Marshall, T., Rosson, G., Henry, E., Weissman, B., Knudsen, K.E., 2005. BAF57 governs androgen receptor action and androgen-dependent proliferation through SWI/SNF. *Mol Cell Biol* 25, 2200-2215.

Litsiou, A., Hanson, S., Streit, A., 2005. A balance of FGF, BMP and WNT signalling positions the future placode territory in the head. *Development* 132, 4051-4062.

Liu, B., Gross, M., ten Hoeve, J., Shuai, K., 2001. A transcriptional corepressor of Stat1 with an essential LXXLL signature motif. *Proc Natl Acad Sci U S A* 98, 3203-3207.

Liu, B., Liao, J., Rao, X., Kushner, S.A., Chung, C.D., Chang, D.D., Shuai, K., 1998. Inhibition of Stat1-mediated gene activation by PIAS1. *Proc Natl Acad Sci U S A* 95, 10626-10631.

Lleras-Forero, L., Tambalo, M., Christophorou, N., Chambers, D., Houart, C., Streit, A., 2013. Neuropeptides: developmental signals in placode progenitor formation. *Dev Cell* 26, 195-203.

Lomeli, H., Castillo-Robles, J., 2016. The developmental and pathogenic roles of BAF57, a special subunit of the BAF chromatin-remodeling complex. *FEBS Lett* 590, 1555-1569.

Lopez-Rios, J., Tessmar, K., Loosli, F., Wittbrodt, J., Bovolenta, P., 2003. Six3 and Six6 activity is modulated by members of the groucho family. *Development* 130, 185-195.

Lovicu, F.J., McAvoy, J.W., 2005. Growth factor regulation of lens development. *Dev Biol* 280, 1-14.

Luo, Y., Na, Z., Slavoff, S.A., 2018. P-Bodies: Composition, Properties, and Functions. *Biochemistry* 57, 2424-2431.

Ma, E.Y., Raible, D.W., 2009. Signaling pathways regulating zebrafish lateral line development. *Curr Biol* 19, R381-386.

Ma, Q., Anderson, D.J., Fritsch, B., 2000. Neurogenin 1 null mutant ears develop fewer, morphologically normal hair cells in smaller sensory epithelia devoid of innervation. *J Assoc Res Otolaryngol* 1, 129-143.

- Ma, Q., Chen, Z., del Barco Barrantes, I., de la Pompa, J.L., Anderson, D.J., 1998. neurogenin1 is essential for the determination of neuronal precursors for proximal cranial sensory ganglia. *Neuron* 20, 469-482.
- Ma, Q., Fode, C., Guillemot, F., Anderson, D.J., 1999. Neurogenin1 and neurogenin2 control two distinct waves of neurogenesis in developing dorsal root ganglia. *Genes Dev* 13, 1717-1728.
- Ma, Q., Kintner, C., Anderson, D.J., 1996. Identification of neurogenin, a vertebrate neuronal determination gene. *Cell* 87, 43-52.
- Ma, Y.C., Song, M.R., Park, J.P., Henry Ho, H.Y., Hu, L., Kurtev, M.V., Zieg, J., Ma, Q., Pfaff, S.L., Greenberg, M.E., 2008. Regulation of motor neuron specification by phosphorylation of neurogenin 2. *Neuron* 58, 65-77.
- Maczkowiak, F., Mateos, S., Wang, E., Roche, D., Harland, R., Monsoro-Burq, A.H., 2010. The Pax3 and Pax7 paralogs cooperate in neural and neural crest patterning using distinct molecular mechanisms, in *Xenopus laevis* embryos. *Dev Biol* 340, 381-396.
- Magarinos, M., Contreras, J., Aburto, M.R., Varela-Nieto, I., 2012. Early development of the vertebrate inner ear. *Anat Rec (Hoboken)* 295, 1775-1790.
- Maier, E.C., Saxena, A., Alsina, B., Bronner, M.E., Whitfield, T.T., 2014. Sensational placodes: neurogenesis in the otic and olfactory systems. *Dev Biol* 389, 50-67.
- Masserdotti, G., Gillotin, S., Sutor, B., Drechsel, D., Irmeler, M., Jorgensen, H.F., Sass, S., Theis, F.J., Beckers, J., Berninger, B., Guillemot, F., Gotz, M., 2015. Transcriptional Mechanisms of Proneural Factors and REST in Regulating Neuronal Reprogramming of Astrocytes. *Cell Stem Cell* 17, 74-88.
- Matsuo-Takasaki, M., Matsumura, M., Sasai, Y., 2005. An essential role of *Xenopus* Foxi1a for ventral specification of the cephalic ectoderm during gastrulation. *Development* 132, 3885-3894.
- Matsushima, D., Heavner, W., Pevny, L.H., 2011. Combinatorial regulation of optic cup progenitor cell fate by SOX2 and PAX6. *Development* 138, 443-454.
- Maucksch, C., Jones, K.S., Connor, B., 2013. Concise review: the involvement of SOX2 in direct reprogramming of induced neural stem/precursor cells. *Stem Cells Transl Med* 2, 579-583.

Mazzoni, E.O., Mahony, S., Closser, M., Morrison, C.A., Nedelec, S., Williams, D.J., An, D., Gifford, D.K., Wichterle, H., 2013. Synergistic binding of transcription factors to cell-specific enhancers programs motor neuron identity. *Nat Neurosci* 16, 1219-1227.

McCabe, K.L., Bronner-Fraser, M., 2008. Essential role for PDGF signaling in ophthalmic trigeminal placode induction. *Development* 135, 1863-1874.

McCoy, E.L., Iwanaga, R., Jedlicka, P., Abbey, N.S., Chodosh, L.A., Heichman, K.A., Welm, A.L., Ford, H.L., 2009. Six1 expands the mouse mammary epithelial stem/progenitor cell pool and induces mammary tumors that undergo epithelial-mesenchymal transition. *J Clin Invest* 119, 2663-2677.

Medina-Martinez, O., Jamrich, M., 2007. Foxe view of lens development and disease. *Development* 134, 1455-1463.

Merk, D.J., Zhou, P., Cohen, S.M., Pazyra-Murphy, M.F., Hwang, G.H., Rehm, K.J., Alfaro, J., Reid, C.M., Zhao, X., Park, E., Xu, P.X., Chan, J.A., Eck, M.J., Nazemi, K.J., Harwell, C.C., Segal, R.A., 2020. The Eya1 Phosphatase Mediates Shh-Driven Symmetric Cell Division of Cerebellar Granule Cell Precursors. *Dev Neurosci* 42, 170-186.

Micalizzi, D.S., Christensen, K.L., Jedlicka, P., Coletta, R.D., Baron, A.E., Harrell, J.C., Horwitz, K.B., Billheimer, D., Heichman, K.A., Welm, A.L., Schieman, W.P., Ford, H.L., 2009. The Six1 homeoprotein induces human mammary carcinoma cells to undergo epithelial-mesenchymal transition and metastasis in mice through increasing TGF-beta signaling. *J Clin Invest* 119, 2678-2690.

Milet, C., Maczkowiak, F., Roche, D.D., Monsoro-Burq, A.H., 2013. Pax3 and Zic1 drive induction and differentiation of multipotent, migratory, and functional neural crest in *Xenopus* embryos. *Proc Natl Acad Sci U S A* 110, 5528-5533.

Miller, S.J., Lan, Z.D., Hardiman, A., Wu, J., Kordich, J.J., Patmore, D.M., Hegde, R.S., Cripe, T.P., Cancelas, J.A., Collins, M.H., Ratner, N., 2010. Inhibition of Eyes Absent Homolog 4 expression induces malignant peripheral nerve sheath tumor necrosis. *Oncogene* 29, 368-379.

Millimaki, B.B., Sweet, E.M., Dhasan, M.S., Riley, B.B., 2007. Zebrafish *atoh1* genes: classic proneural activity in the inner ear and regulation by Fgf and Notch. *Development* 134, 295-305.

Miyagi, S., Kato, H., Okuda, A., 2009. Role of SoxB1 transcription factors in development. *Cell Mol Life Sci* 66, 3675-3684.

Mizuguchi, R., Sugimori, M., Takebayashi, H., Kosako, H., Nagao, M., Yoshida, S., Nabeshima, Y., Shimamura, K., Nakafuku, M., 2001. Combinatorial roles of olig2 and neurogenin2 in the coordinated induction of pan-neuronal and subtype-specific properties of motoneurons. *Neuron* 31, 757-771.

Mizuseki, K., Kishi, M., Matsui, M., Nakanishi, S., Sasai, Y., 1998. Xenopus Zic-related-1 and Sox-2, two factors induced by chordin, have distinct activities in the initiation of neural induction. *Development* 125, 579-587.

Monsoro-Burq, A.H., Wang, E., Harland, R., 2005. Msx1 and Pax3 cooperate to mediate FGF8 and WNT signals during Xenopus neural crest induction. *Dev Cell* 8, 167-178.

Moody, S.A., 1987. Fates of the blastomeres of the 32-cell-stage Xenopus embryo. *Dev Biol* 122, 300-319.

Moody, S.A., LaMantia, A.S., 2015. Transcriptional regulation of cranial sensory placode development. *Curr Top Dev Biol* 111, 301-350.

Moparthi, L., Koch, S., 2023. FOX transcription factors are common regulators of Wnt/beta-catenin-dependent gene transcription. *J Biol Chem* 299, 104667.

Murray, R.C., Navi, D., Fesenko, J., Lander, A.D., Calof, A.L., 2003. Widespread defects in the primary olfactory pathway caused by loss of Mash1 function. *J Neurosci* 23, 1769-1780.

Murre, C., McCaw, P.S., Baltimore, D., 1989. A new DNA binding and dimerization motif in immunoglobulin enhancer binding, daughterless, MyoD, and myc proteins. *Cell* 56, 777-783.

Neilson, K.M., Pignoni, F., Yan, B., Moody, S.A., 2010. Developmental expression patterns of candidate cofactors for vertebrate six family transcription factors. *Dev Dyn* 239, 3446-3466.

Nelson, V., Davis, G.E., Maxwell, S.A., 2001. A putative protein inhibitor of activated STAT (PIASy) interacts with p53 and inhibits p53-mediated transactivation but not apoptosis. *Apoptosis* 6, 221-234.

Neves, J., Uchikawa, M., Bigas, A., Giraldez, F., 2012. The prosensory function of Sox2 in the chicken inner ear relies on the direct regulation of Atoh1. *PLoS One* 7, e30871.

- Nieber, F., Pieler, T., Henningfeld, K.A., 2009. Comparative expression analysis of the neurogenins in *Xenopus tropicalis* and *Xenopus laevis*. *Dev Dyn* 238, 451-458.
- Niehrs, C., 2010. On growth and form: a Cartesian coordinate system of Wnt and BMP signaling specifies bilaterian body axes. *Development* 137, 845-857.
- Niimi, T., Seimiya, M., Kloter, U., Flister, S., Gehring, W.J., 1999. Direct regulatory interaction of the eyeless protein with an eye-specific enhancer in the sine oculis gene during eye induction in *Drosophila*. *Development* 126, 2253-2260.
- Nikaido, M., Doi, K., Shimizu, T., Hibi, M., Kikuchi, Y., Yamasu, K., 2007. Initial specification of the epibranchial placode in zebrafish embryos depends on the fibroblast growth factor signal. *Dev Dyn* 236, 564-571.
- Noden, D.M., 1980a. Somatotopic and functional organization of the avian trigeminal ganglion: an HRP analysis in the hatchling chick. *J Comp Neurol* 190, 405-428.
- Noden, D.M., 1980b. Somatotopic organization of the embryonic chick trigeminal ganglion. *J Comp Neurol* 190, 429-444.
- Nordstrom, U., Maier, E., Jessell, T.M., Edlund, T., 2006. An early role for WNT signaling in specifying neural patterns of Cdx and Hox gene expression and motor neuron subtype identity. *PLoS Biol* 4, e252.
- Norris, D.O., Carr, J.A., 2021. *Vertebrate endocrinology, Sixth edition.* ed. Academic Press, an imprint of Elsevier, London, United Kingdom ; San Diego, CA.
- Northcutt, R.G., 2004. Taste buds: development and evolution. *Brain Behav Evol* 64, 198-206.
- Northcutt, R.G., Gans, C., 1983. The genesis of neural crest and epidermal placodes: a reinterpretation of vertebrate origins. *Q Rev Biol* 58, 1-28.
- Northcutt, R.G., Muske, L.E., 1994. Multiple embryonic origins of gonadotropin-releasing hormone (GnRH) immunoreactive neurons. *Brain Res Dev Brain Res* 78, 279-290.
- Novitsch, B.G., Chen, A.I., Jessell, T.M., 2001. Coordinate regulation of motor neuron subtype identity and pan-neuronal properties by the bHLH repressor Olig2. *Neuron* 31, 773-789.

- O'Neill, P., Mak, S.S., Fritsch, B., Ladher, R.K., Baker, C.V., 2012. The amniote paratympanic organ develops from a previously undiscovered sensory placode. *Nat Commun* 3, 1041.
- Ochocinska, M.J., Hitchcock, P.F., 2009. NeuroD regulates proliferation of photoreceptor progenitors in the retina of the zebrafish. *Mech Dev* 126, 128-141.
- Ohto, H., Kamada, S., Tago, K., Tominaga, S.I., Ozaki, H., Sato, S., Kawakami, K., 1999. Cooperation of six and eya in activation of their target genes through nuclear translocation of Eya. *Mol Cell Biol* 19, 6815-6824.
- Ohtsuka, T., Ishibashi, M., Gradwohl, G., Nakanishi, S., Guillemot, F., Kageyama, R., 1999. Hes1 and Hes5 as notch effectors in mammalian neuronal differentiation. *EMBO J* 18, 2196-2207.
- Ohyama, T., Mohamed, O.A., Taketo, M.M., Dufort, D., Groves, A.K., 2006. Wnt signals mediate a fate decision between otic placode and epidermis. *Development* 133, 865-875.
- Okabe, Y., Sano, T., Nagata, S., 2009. Regulation of the innate immune response by threonine-phosphatase of Eyes absent. *Nature* 460, 520-524.
- Okuda, Y., Ogura, E., Kondoh, H., Kamachi, Y., 2010. B1 SOX coordinate cell specification with patterning and morphogenesis in the early zebrafish embryo. *PLoS Genet* 6, e1000936.
- Oschwald, R., Richter, K., Grunz, H., 1991. Localization of a nervous system-specific class II beta-tubulin gene in *Xenopus laevis* embryos by whole-mount in situ hybridization. *Int J Dev Biol* 35, 399-405.
- Ozair, M.Z., Kintner, C., Brivanlou, A.H., 2013. Neural induction and early patterning in vertebrates. *Wiley Interdiscip Rev Dev Biol* 2, 479-498.
- Ozaki, H., Nakamura, K., Funahashi, J., Ikeda, K., Yamada, G., Tokano, H., Okamura, H.O., Kitamura, K., Muto, S., Kotaki, H., Sudo, K., Horai, R., Iwakura, Y., Kawakami, K., 2004. Six1 controls patterning of the mouse otic vesicle. *Development* 131, 551-562.
- Palma, M., Riffo, E.N., Sukanuma, T., Washburn, M.P., Workman, J.L., Pincheira, R., Castro, A.F., 2019. Identification of a nuclear localization signal and importin beta members mediating NUA1 nuclear import inhibited by oxidative stress. *J Cell Biochem* 120, 16088-16107.

Palombo, F., Gallinari, P., Iaccarino, I., Lettieri, T., Hughes, M., D'Arrigo, A., Truong, O., Hsuan, J.J., Jiricny, J., 1995. GTBP, a 160-kilodalton protein essential for mismatch-binding activity in human cells. *Science* 268, 1912-1914.

Panaliappan, T.K., Wittmann, W., Jidigam, V.K., Mercurio, S., Bertolini, J.A., Sghari, S., Bose, R., Patthey, C., Nicolis, S.K., Gunhaga, L., 2018. Sox2 is required for olfactory pit formation and olfactory neurogenesis through BMP restriction and Hes5 upregulation. *Development* 145.

Pandey, R.N., Rani, R., Yeo, E.J., Spencer, M., Hu, S., Lang, R.A., Hegde, R.S., 2010. The Eyes Absent phosphatase-transactivator proteins promote proliferation, transformation, migration, and invasion of tumor cells. *Oncogene* 29, 3715-3722.

Pandur, P.D., Moody, S.A., 2000. Xenopus Six1 gene is expressed in neurogenic cranial placodes and maintained in the differentiating lateral lines. *Mech Dev* 96, 253-257.

Pappu, K.S., Mardon, G., 2004. Genetic control of retinal specification and determination in *Drosophila*. *Int J Dev Biol* 48, 913-924.

Pappu, K.S., Ostrin, E.J., Middlebrooks, B.W., Sili, B.T., Chen, R., Atkins, M.R., Gibbs, R., Mardon, G., 2005. Dual regulation and redundant function of two eye-specific enhancers of the *Drosophila* retinal determination gene *dachshund*. *Development* 132, 2895-2905.

Park, B.Y., Saint-Jeannet, J.P., 2010. *Induction and Segregation of the Vertebrate Cranial Placodes*, San Rafael (CA).

Patrick, A.N., Cabrera, J.H., Smith, A.L., Chen, X.S., Ford, H.L., Zhao, R., 2013. Structure-function analyses of the human SIX1-EYA2 complex reveal insights into metastasis and BOR syndrome. *Nat Struct Mol Biol* 20, 447-453.

Penzel, R., Oswald, R., Chen, Y., Tacke, L., Grunz, H., 1997. Characterization and early embryonic expression of a neural specific transcription factor xSOX3 in *Xenopus laevis*. *Int J Dev Biol* 41, 667-677.

Perron, M., Opdecamp, K., Butler, K., Harris, W.A., Bellefroid, E.J., 1999. X-ngnr-1 and Xath3 promote ectopic expression of sensory neuron markers in the neurula ectoderm and have distinct inducing properties in the retina. *Proc Natl Acad Sci U S A* 96, 14996-15001.

Petersen, C.P., Reddien, P.W., 2009. Wnt signaling and the polarity of the primary body axis. *Cell* 139, 1056-1068.

- Petrova, K., Tretiakov, M., Kotov, A., Monsoro-Burq, A.H., Peshkin, L., 2024. A new atlas to study embryonic cell types in *Xenopus*. *Dev Biol* 511, 76-83.
- Pevny, L., Placzek, M., 2005. SOX genes and neural progenitor identity. *Curr Opin Neurobiol* 15, 7-13.
- Pevny, L.H., Nicolis, S.K., 2010. Sox2 roles in neural stem cells. *Int J Biochem Cell Biol* 42, 421-424.
- Pieper, M., Ahrens, K., Rink, E., Peter, A., Schlosser, G., 2012. Differential distribution of competence for planar and neural crest induction to non-neural and neural ectoderm. *Development* 139, 1175-1187.
- Pignoni, F., Hu, B., Zavitz, K.H., Xiao, J., Garrity, P.A., Zipursky, S.L., 1997. The eye-specification proteins So and Eya form a complex and regulate multiple steps in *Drosophila* eye development. *Cell* 91, 881-891.
- Piotrowski, T., Baker, C.V., 2014. The development of lateral line placodes: taking a broader view. *Dev Biol* 389, 68-81.
- Plouhinec, J.L., Roche, D.D., Pegoraro, C., Figueiredo, A.L., Maczkowiak, F., Brunet, L.J., Milet, C., Vert, J.P., Pollet, N., Harland, R.M., Monsoro-Burq, A.H., 2014. Pax3 and Zic1 trigger the early neural crest gene regulatory network by the direct activation of multiple key neural crest specifiers. *Dev Biol* 386, 461-472.
- Politis, P.K., Makri, G., Thomaidou, D., Geissen, M., Rohrer, H., Matsas, R., 2007. BM88/CEND1 coordinates cell cycle exit and differentiation of neuronal precursors. *Proc Natl Acad Sci U S A* 104, 17861-17866.
- Puligilla, C., Dabdoub, A., Brenowitz, S.D., Kelley, M.W., 2010. Sox2 induces neuronal formation in the developing mammalian cochlea. *J Neurosci* 30, 714-722.
- Punzo, C., Seimiya, M., Flister, S., Gehring, W.J., Plaza, S., 2002. Differential interactions of eyeless and twin of eyeless with the sine oculis enhancer. *Development* 129, 625-634.
- Queiroz, L.Y., Kageyama, R., Cimarosti, H.I., 2024. SUMOylation effects on neural stem cells self-renewal, differentiation, and survival. *Neurosci Res* 199, 1-11.

Rayapureddi, J.P., Kattamuri, C., Steinmetz, B.D., Frankfort, B.J., Ostrin, E.J., Mardon, G., Hegde, R.S., 2003. Eyes absent represents a class of protein tyrosine phosphatases. *Nature* 426, 295-298.

Rebay, I., Silver, S.J., Tootle, T.L., 2005. New vision from Eyes absent: transcription factors as enzymes. *Trends Genet* 21, 163-171.

Renfranz, P.J., Benzer, S., 1989. Monoclonal antibody probes discriminate early and late mutant defects in development of the *Drosophila* retina. *Dev Biol* 136, 411-429.

Rex, M., Orme, A., Uwanogho, D., Tointon, K., Wigmore, P.M., Sharpe, P.T., Scotting, P.J., 1997. Dynamic expression of chicken Sox2 and Sox3 genes in ectoderm induced to form neural tissue. *Dev Dyn* 209, 323-332.

Riddiford, N., Schlosser, G., 2016. Dissecting the pre-placodal transcriptome to reveal presumptive direct targets of Six1 and Eya1 in cranial placodes. *Elife* 5, e17666.

Riddiford, N., Schlosser, G., 2017. Six1 and Eya1 both promote and arrest neuronal differentiation by activating multiple Notch pathway genes. *Dev Biol* 431, 152-167.

Rizzoti, K., Lovell-Badge, R., 2005. Early development of the pituitary gland: induction and shaping of Rathke's pouch. *Rev Endocr Metab Disord* 6, 161-172.

Rogers, C.D., Moody, S.A., Casey, E.S., 2009. Neural induction and factors that stabilize a neural fate. *Birth Defects Res C Embryo Today* 87, 249-262.

Roth, W., Sustmann, C., Kieslinger, M., Gilmozzi, A., Irmer, D., Kremmer, E., Turck, C., Grosschedl, R., 2004. PIASy-deficient mice display modest defects in IFN and Wnt signaling. *J Immunol* 173, 6189-6199.

Rothstein, M., Bhattacharya, D., Simoes-Costa, M., 2018. The molecular basis of neural crest axial identity. *Dev Biol* 444 Suppl 1, S170-S180.

Ruf, R.G., Xu, P.X., Silviu, D., Otto, E.A., Beekmann, F., Muerb, U.T., Kumar, S., Neuhaus, T.J., Kemper, M.J., Raymond, R.M., Jr., Brophy, P.D., Berkman, J., Gattas, M., Hyland, V., Ruf, E.M., Schwartz, C., Chang, E.H., Smith, R.J., Stratakis, C.A., Weil, D., Petit, C., Hildebrandt, F., 2004. SIX1 mutations cause branchio-oto-renal syndrome by disruption of EYA1-SIX1-DNA complexes. *Proc Natl Acad Sci U S A* 101, 8090-8095.

- Rytinki, M.M., Kaikkonen, S., Pehkonen, P., Jaaskelainen, T., Palvimo, J.J., 2009. PIAS proteins: pleiotropic interactors associated with SUMO. *Cell Mol Life Sci* 66, 3029-3041.
- Sachdev, S., Bruhn, L., Sieber, H., Pichler, A., Melchior, F., Grosschedl, R., 2001. PIASy, a nuclear matrix-associated SUMO E3 ligase, represses LEF1 activity by sequestration into nuclear bodies. *Genes Dev* 15, 3088-3103.
- Saint-Jeannet, J.P., Moody, S.A., 2014. Establishing the pre-placodal region and breaking it into placodes with distinct identities. *Dev Biol* 389, 13-27.
- Sarkar, A., Hochedlinger, K., 2013. The sox family of transcription factors: versatile regulators of stem and progenitor cell fate. *Cell Stem Cell* 12, 15-30.
- Sarrazin, A.F., Villablanca, E.J., Nunez, V.A., Sandoval, P.C., Ghysen, A., Allende, M.L., 2006. Proneural gene requirement for hair cell differentiation in the zebrafish lateral line. *Dev Biol* 295, 534-545.
- Sasai, N., Mizuseki, K., Sasai, Y., 2001. Requirement of FoxD3-class signaling for neural crest determination in *Xenopus*. *Development* 128, 2525-2536.
- Sasai, Y., Kageyama, R., Tagawa, Y., Shigemoto, R., Nakanishi, S., 1992. Two mammalian helix-loop-helix factors structurally related to *Drosophila* hairy and Enhancer of split. *Genes Dev* 6, 2620-2634.
- Sato, T., Sasai, N., Sasai, Y., 2005. Neural crest determination by co-activation of Pax3 and Zic1 genes in *Xenopus* ectoderm. *Development* 132, 2355-2363.
- Savare, J., Bonneaud, N., Girard, F., 2005. SUMO represses transcriptional activity of the *Drosophila* SoxNeuro and human Sox3 central nervous system-specific transcription factors. *Mol Biol Cell* 16, 2660-2669.
- Scardigli, R., Schuurmans, C., Gradwohl, G., Guillemot, F., 2001. Crossregulation between Neurogenin2 and pathways specifying neuronal identity in the spinal cord. *Neuron* 31, 203-217.
- Schlosser, G., 2002. Development and evolution of lateral line placodes in amphibians I. *Development. Zoology (Jena)* 105, 119-146.
- Schlosser, G., 2003. Hypobranchial placodes in *Xenopus laevis* give rise to hypobranchial ganglia, a novel type of cranial ganglia. *Cell Tissue Res* 312, 21-29.

- Schlosser, G., 2005. Evolutionary origins of vertebrate placodes: insights from developmental studies and from comparisons with other deuterostomes. *J Exp Zool B Mol Dev Evol* 304, 347-399.
- Schlosser, G., 2006. Induction and specification of cranial placodes. *Dev Biol* 294, 303-351.
- Schlosser, G., 2010. Making sense of development of vertebrate cranial placodes. *Int Rev Cell Mol Biol* 283, 129-234.
- Schlosser, G., 2014. Early embryonic specification of vertebrate cranial placodes. *Wiley Interdiscip Rev Dev Biol* 3, 349-363.
- Schlosser, G., 2021a. Development of Sensory and Neurosecretory Cell Types. *Vertebrate Cranial Placodes*, vol. 1. CRC Press, Boca Raton.
- Schlosser, G., 2021b. Evolutionary Origin of Sensory and Neurosecretory Cell Types. *Vertebrate Cranial Placodes*, vol. 2. CRC Press, Boca Raton.
- Schlosser, G., Ahrens, K., 2004. Molecular anatomy of placode development in *Xenopus laevis*. *Dev Biol* 271, 439-466.
- Schlosser, G., Awtry, T., Brugmann, S.A., Jensen, E.D., Neilson, K., Ruan, G., Stammler, A., Voelker, D., Yan, B., Zhang, C., Klymkowsky, M.W., Moody, S.A., 2008. *Eya1* and *Six1* promote neurogenesis in the cranial placodes in a *SoxB1*-dependent fashion. *Dev Biol* 320, 199-214.
- Schlosser, G., Northcutt, R.G., 2000. Development of neurogenic placodes in *Xenopus laevis*. *J Comp Neurol* 418, 121-146.
- Schwarting, G.A., Wierman, M.E., Tobet, S.A., 2007. Gonadotropin-releasing hormone neuronal migration. *Semin Reprod Med* 25, 305-312.
- Serres, M.P., Shaughnessy, R., Escot, S., Hammich, H., Cuvelier, F., Salles, A., Rocancourt, M., Verdon, Q., Gaffuri, A.L., Sourigues, Y., Malherbe, G., Velikovskiy, L., Chardon, F., Sassoon, N., Tinevez, J.Y., Callebaut, I., Formstecher, E., Houdusse, A., David, N.B., Pylypenko, O., Echard, A., 2023. MiniBAR/GARRE1 is a dual Rac and Rab effector required for ciliogenesis. *Dev Cell* 58, 2477-2494 e2478.
- Shimozaki, K., 2014. *Sox2* transcription network acts as a molecular switch to regulate properties of neural stem cells. *World J Stem Cells* 6, 485-490.

Shimozaki, K., Zhang, C.L., Suh, H., Denli, A.M., Evans, R.M., Gage, F.H., 2012. SRY-box-containing gene 2 regulation of nuclear receptor tailless (Tlx) transcription in adult neural stem cells. *J Biol Chem* 287, 5969-5978.

Silver, S.J., Davies, E.L., Doyon, L., Rebay, I., 2003. Functional dissection of eyes absent reveals new modes of regulation within the retinal determination gene network. *Mol Cell Biol* 23, 5989-5999.

Simoës-Costa, M., Bronner, M.E., 2015. Establishing neural crest identity: a gene regulatory recipe. *Development* 142, 242-257.

Singh, S., Groves, A.K., 2016. The molecular basis of craniofacial placode development. *Wiley Interdiscip Rev Dev Biol* 5, 363-376.

Sokpor, G., Xie, Y., Rosenbusch, J., Tuoc, T., 2017. Chromatin Remodeling BAF (SWI/SNF) Complexes in Neural Development and Disorders. *Front Mol Neurosci* 10, 243.

Stern, C.D., 2006. Neural induction: 10 years on since the 'default model'. *Curr Opin Cell Biol* 18, 692-697.

Steventon, B., Mayor, R., Streit, A., 2012. Mutual repression between Gbx2 and Otx2 in sensory placodes reveals a general mechanism for ectodermal patterning. *Dev Biol* 367, 55-65.

Streit, A., 2004. Early development of the cranial sensory nervous system: from a common field to individual placodes. *Dev Biol* 276, 1-15.

Streit, A., 2018. Specification of sensory placode progenitors: signals and transcription factor networks. *Int J Dev Biol* 62, 195-205.

Sturm, S., Koch, M., White, F.A., 2000. Cloning and analysis of a murine PIAS family member, PIASgamma, in developing skin and neurons. *J Mol Neurosci* 14, 107-121.

Sun, C., Yu, Z., Wang, Y., Tao, T., 2016. The importin protein karyopherin-beta1 regulates the mice fibroblast-like synoviocytes inflammation via facilitating nucleus transportation of STAT3 transcription factor. *Biochem Biophys Res Commun* 471, 553-559.

Sun, S.K., Dee, C.T., Tripathi, V.B., Rengifo, A., Hirst, C.S., Scotting, P.J., 2007. Epibranchial and otic placodes are induced by a common Fgf signal, but their subsequent development is independent. *Dev Biol* 303, 675-686.

- Sun, Y., Kaneko, S., Li, X.K., Li, X., 2015. The PI3K/Akt signal hyperactivates Eya1 via the SUMOylation pathway. *Oncogene* 34, 2527-2537.
- Surzenko, N., Crowl, T., Bachleda, A., Langer, L., Pevny, L., 2013. SOX2 maintains the quiescent progenitor cell state of postnatal retinal Muller glia. *Development* 140, 1445-1456.
- Suzuki, A., Ueno, N., Hemmati-Brivanlou, A., 1997. *Xenopus* msx1 mediates epidermal induction and neural inhibition by BMP4. *Development* 124, 3037-3044.
- Tadjuidje, E., Hegde, R.S., 2013. The Eyes Absent proteins in development and disease. *Cell Mol Life Sci* 70, 1897-1913.
- Tahk, S., Liu, B., Chernishof, V., Wong, K.A., Wu, H., Shuai, K., 2007. Control of specificity and magnitude of NF-kappa B and STAT1-mediated gene activation through PIASy and PIAS1 cooperation. *Proc Natl Acad Sci U S A* 104, 11643-11648.
- Takanaga, H., Tsuchida-Straeten, N., Nishide, K., Watanabe, A., Aburatani, H., Kondo, T., 2009. Gli2 is a novel regulator of sox2 expression in telencephalic neuroepithelial cells. *Stem Cells* 27, 165-174.
- Talikka, M., Perez, S.E., Zimmerman, K., 2002. Distinct patterns of downstream target activation are specified by the helix-loop-helix domain of proneural basic helix-loop-helix transcription factors. *Dev Biol* 247, 137-148.
- Taranova, O.V., Magness, S.T., Fagan, B.M., Wu, Y., Surzenko, N., Hutton, S.R., Pevny, L.H., 2006. SOX2 is a dose-dependent regulator of retinal neural progenitor competence. *Genes Dev* 20, 1187-1202.
- Tavares, A.L.P., Jourdeuil, K., Neilson, K.M., Majumdar, H.D., Moody, S.A., 2021. Sobp modulates the transcriptional activation of Six1 target genes and is required during craniofacial development. *Development* 148.
- Taylor, K.M., Labonne, C., 2005. SoxE factors function equivalently during neural crest and inner ear development and their activity is regulated by SUMOylation. *Dev Cell* 9, 593-603.
- Tolkunova, E., Malashicheva, A., Parfenov, V.N., Sustmann, C., Grosschedl, R., Tomilin, A., 2007. PIAS proteins as repressors of Oct4 function. *J Mol Biol* 374, 1200-1212.

- Tomioka, M., Nishimoto, M., Miyagi, S., Katayanagi, T., Fukui, N., Niwa, H., Muramatsu, M., Okuda, A., 2002. Identification of Sox-2 regulatory region which is under the control of Oct-3/4-Sox-2 complex. *Nucleic Acids Res* 30, 3202-3213.
- Tootle, T.L., Silver, S.J., Davies, E.L., Newman, V., Latek, R.R., Mills, I.A., Selengut, J.D., Parlikar, B.E., Rebay, I., 2003. The transcription factor Eyes absent is a protein tyrosine phosphatase. *Nature* 426, 299-302.
- Toro, S., Varga, Z.M., 2007. Equivalent progenitor cells in the zebrafish anterior preplacodal field give rise to adenohypophysis, lens, and olfactory placodes. *Semin Cell Dev Biol* 18, 534-542.
- Touhara, K., Vosshall, L.B., 2009. Sensing odorants and pheromones with chemosensory receptors. *Annu Rev Physiol* 71, 307-332.
- Trinkle-Mulcahy, L., Boulon, S., Lam, Y.W., Urcia, R., Boisvert, F.M., Vandermoere, F., Morrice, N.A., Swift, S., Rothbauer, U., Leonhardt, H., Lamond, A., 2008. Identifying specific protein interaction partners using quantitative mass spectrometry and bead proteomes. *J Cell Biol* 183, 223-239.
- Tsuruzoe, S., Ishihara, K., Uchimura, Y., Watanabe, S., Sekita, Y., Aoto, T., Saitoh, H., Yuasa, Y., Niwa, H., Kawasuji, M., Baba, H., Nakao, M., 2006. Inhibition of DNA binding of Sox2 by the SUMO conjugation. *Biochem Biophys Res Commun* 351, 920-926.
- Vierbuchen, T., Ostermeier, A., Pang, Z.P., Kokubu, Y., Sudhof, T.C., Wernig, M., 2010. Direct conversion of fibroblasts to functional neurons by defined factors. *Nature* 463, 1035-1041.
- Wang, L., Baiocchi, R.A., Pal, S., Mosialos, G., Caligiuri, M., Sif, S., 2005. The BRG1- and hBRM-associated factor BAF57 induces apoptosis by stimulating expression of the cylindromatosis tumor suppressor gene. *Mol Cell Biol* 25, 7953-7965.
- Wang, W., Chi, T., Xue, Y., Zhou, S., Kuo, A., Crabtree, G.R., 1998. Architectural DNA binding by a high-mobility-group/kinesin-like subunit in mammalian SWI/SNF-related complexes. *Proc Natl Acad Sci U S A* 95, 492-498.
- Wang, Y., Cortez, D., Yazdi, P., Neff, N., Elledge, S.J., Qin, J., 2000. BASC, a super complex of BRCA1-associated proteins involved in the recognition and repair of aberrant DNA structures. *Genes Dev* 14, 927-939.

- Wattler, F., Wattler, S., Kelly, M., Skinner, H.B., Nehls, M., 1999. Cloning, chromosomal location, and expression analysis of murine Smarce1-related, a new member of the high-mobility 365 group gene family. *Genomics* 60, 172-178.
- Weasner, B., Salzer, C., Kumar, J.P., 2007. Sine oculis, a member of the SIX family of transcription factors, directs eye formation. *Dev Biol* 303, 756-771.
- Wegner, M., 2010. All purpose Sox: The many roles of Sox proteins in gene expression. *Int J Biochem Cell Biol* 42, 381-390.
- Wegner, M., Stolt, C.C., 2005. From stem cells to neurons and glia: a Soxist's view of neural development. *Trends Neurosci* 28, 583-588.
- Wheeler, G.N., Brandli, A.W., 2009. Simple vertebrate models for chemical genetics and drug discovery screens: lessons from zebrafish and *Xenopus*. *Dev Dyn* 238, 1287-1308.
- Whitfield, T.T., 2015. Development of the inner ear. *Curr Opin Genet Dev* 32, 112-118.
- Wong, E.Y., Ahmed, M., Xu, P.X., 2013. EYA1-SIX1 complex in neurosensory cell fate induction in the mammalian inner ear. *Hear Res* 297, 13-19.
- Wood, H.B., Episkopou, V., 1999. Comparative expression of the mouse Sox1, Sox2 and Sox3 genes from pre-gastrulation to early somite stages. *Mech Dev* 86, 197-201.
- Woods, C., Montcouquiol, M., Kelley, M.W., 2004. Math1 regulates development of the sensory epithelium in the mammalian cochlea. *Nat Neurosci* 7, 1310-1318.
- Wray, S., 2010. From nose to brain: development of gonadotrophin-releasing hormone-1 neurones. *J Neuroendocrinol* 22, 743-753.
- Wu, D.K., Kelley, M.W., 2012. Molecular mechanisms of inner ear development. *Cold Spring Harb Perspect Biol* 4, a008409.
- Wu, Y., Guo, Z., Wu, H., Wang, X., Yang, L., Shi, X., Du, J., Tang, B., Li, W., Yang, L., Zhang, Y., 2012. SUMOylation represses Nanog expression via modulating transcription factors Oct4 and Sox2. *PLoS One* 7, e39606.

- Wylie, L.A., Hardwick, L.J., Papkovskaia, T.D., Thiele, C.J., Philpott, A., 2015. Ascl1 phospho-status regulates neuronal differentiation in a *Xenopus* developmental model of neuroblastoma. *Dis Model Mech* 8, 429-441.
- Xu, J., Wong, E.Y., Cheng, C., Li, J., Sharkar, M.T., Xu, C.Y., Chen, B., Sun, J., Jing, D., Xu, P.X., 2014. Eya1 interacts with Six2 and Myc to regulate expansion of the nephron progenitor pool during nephrogenesis. *Dev Cell* 31, 434-447.
- Xu, P.X., 2013. The EYA-SO/SIX complex in development and disease. *Pediatr Nephrol* 28, 843-854.
- Xu, P.X., Adams, J., Peters, H., Brown, M.C., Heaney, S., Maas, R., 1999. Eya1-deficient mice lack ears and kidneys and show abnormal apoptosis of organ primordia. *Nat Genet* 23, 113-117.
- Yamamoto, H., Ihara, M., Matsuura, Y., Kikuchi, A., 2003. Sumoylation is involved in beta-catenin-dependent activation of Tcf-4. *EMBO J* 22, 2047-2059.
- Yamamoto, N., Uchiyama, H., Ohki-Hamazaki, H., Tanaka, H., Ito, H., 1996. Migration of GnRH-immunoreactive neurons from the olfactory placode to the brain: a study using avian embryonic chimeras. *Brain Res Dev Brain Res* 95, 234-244.
- Yi, S.H., Jo, A.Y., Park, C.H., Koh, H.C., Park, R.H., Suh-Kim, H., Shin, I., Lee, Y.S., Kim, J., Lee, S.H., 2008. Mash1 and neurogenin 2 enhance survival and differentiation of neural precursor cells after transplantation to rat brains via distinct modes of action. *Mol Ther* 16, 1873-1882.
- Youn, J.Y., Dunham, W.H., Hong, S.J., Knight, J.D.R., Bashkurov, M., Chen, G.I., Bagci, H., Rathod, B., MacLeod, G., Eng, S.W.M., Angers, S., Morris, Q., Fabian, M., Cote, J.F., Gingras, A.C., 2018. High-Density Proximity Mapping Reveals the Subcellular Organization of mRNA-Associated Granules and Bodies. *Mol Cell* 69, 517-532 e511.
- Yu, Y., Davicioni, E., Triche, T.J., Merlino, G., 2006. The homeoprotein six1 transcriptionally activates multiple protumorigenic genes but requires ezrin to promote metastasis. *Cancer Res* 66, 1982-1989.
- Yu, Y., Khan, J., Khanna, C., Helman, L., Meltzer, P.S., Merlino, G., 2004. Expression profiling identifies the cytoskeletal organizer ezrin and the developmental homeoprotein Six-1 as key metastatic regulators. *Nat Med* 10, 175-181.

- Zhang, F.P., Mikkonen, L., Toppari, J., Palvimo, J.J., Thesleff, I., Janne, O.A., 2008. Sumo-1 function is dispensable in normal mouse development. *Mol Cell Biol* 28, 5381-5390.
- Zhang, L., Yang, N., Huang, J., Buckanovich, R.J., Liang, S., Barchetti, A., Vezzani, C., O'Brien-Jenkins, A., Wang, J., Ward, M.R., Courreges, M.C., Fracchioli, S., Medina, A., Katsaros, D., Weber, B.L., Coukos, G., 2005. Transcriptional coactivator Drosophila eyes absent homologue 2 is up-regulated in epithelial ovarian cancer and promotes tumor growth. *Cancer Res* 65, 925-932.
- Zhang, S., Cui, W., 2014. Sox2, a key factor in the regulation of pluripotency and neural differentiation. *World J Stem Cells* 6, 305-311.
- Zhang, Y., Knosp, B.M., Maconochie, M., Friedman, R.A., Smith, R.J., 2004. A comparative study of Eya1 and Eya4 protein function and its implication in branchio-oto-renal syndrome and DFNA10. *J Assoc Res Otolaryngol* 5, 295-304.
- Zhang, Y., Pak, C., Han, Y., Ahlenius, H., Zhang, Z., Chanda, S., Marro, S., Patzke, C., Acuna, C., Covy, J., Xu, W., Yang, N., Danko, T., Chen, L., Wernig, M., Sudhof, T.C., 2013. Rapid single-step induction of functional neurons from human pluripotent stem cells. *Neuron* 78, 785-798.
- Zheng, J.L., Gao, W.Q., 2000. Overexpression of Math1 induces robust production of extra hair cells in postnatal rat inner ears. *Nat Neurosci* 3, 580-586.
- Zheng, W., Huang, L., Wei, Z.B., Silvius, D., Tang, B., Xu, P.X., 2003. The role of Six1 in mammalian auditory system development. *Development* 130, 3989-4000.
- Zhou, C., Yang, X., Sun, Y., Yu, H., Zhang, Y., Jin, Y., 2016. Comprehensive profiling reveals mechanisms of SOX2-mediated cell fate specification in human ESCs and NPCs. *Cell Res* 26, 171-189.
- Zhu, C.C., Dyer, M.A., Uchikawa, M., Kondoh, H., Lagutin, O.V., Oliver, G., 2002. Six3-mediated auto repression and eye development requires its interaction with members of the Groucho-related family of co-repressors. *Development* 129, 2835-2849.
- Zhu, X., Gleiberman, A.S., Rosenfeld, M.G., 2007. Molecular physiology of pituitary development: signaling and transcriptional networks. *Physiol Rev* 87, 933-963.
- Zou, D., Erickson, C., Kim, E.H., Jin, D., Fritsch, B., Xu, P.X., 2008. Eya1 gene dosage critically affects the development of sensory epithelia in the mammalian inner ear. *Hum Mol Genet* 17, 3340-3356.

Zou, D., Silviu, D., Fritsch, B., Xu, P.X., 2004. Eya1 and Six1 are essential for early steps of sensory neurogenesis in mammalian cranial placodes. *Development* 131, 5561-5572.

Zou, D., Silviu, D., Rodrigo-Blomqvist, S., Enerback, S., Xu, P.X., 2006. Eya1 regulates the growth of otic epithelium and interacts with Pax2 during the development of all sensory areas in the inner ear. *Dev Biol* 298, 430-441.

Zuber, M.E., Gestri, G., Viczian, A.S., Barsacchi, G., Harris, W.A., 2003. Specification of the vertebrate eye by a network of eye field transcription factors. *Development* 130, 5155-5167.

# Appendix A. Solutions

## A.1. General solutions

### **MBS salts, 10x**

51.3 g NaCl

0.75 g KCl

2 g MgSO<sub>4</sub>\*7 H<sub>2</sub>O

23.8 g HEPES

2 g NaHCO<sub>3</sub>

Adjusted pH to 7.6 with NaOH pellets

Adjusted to 1 liter with dH<sub>2</sub>O and autoclaved

### **MBSH, 1x**

100 ml 10x MBS salts

7 ml 0.1 M CaCl<sub>2</sub>

4 ml 5 M NaCl

Adjusted to 1 liter with dH<sub>2</sub>O

### **MBS, 1x**

100 ml 10x MBS salts

7 ml 0.1 M CaCl<sub>2</sub>

Adjusted to 1 liter with dH<sub>2</sub>O

### **Cysteine solution**

4 g Cysteine

Adjusted to 100 ml with dH<sub>2</sub>O

Adjusted pH to 8 with NaOH pellets

**100x Triple antibiotic (3A)**

250 mg gentamycine

4 g penicillin

4 g streptomycin

100 ml dH<sub>2</sub>O

Dispensed into 1 ml aliquots

Stored at -20°C

**A.2. Solutions for X-gal staining and *in situ* hybridization****AP (alkaline phosphatase) buffer**

5 ml 1M Tris (pH 9.5)

2.5 ml 1M MgCl<sub>2</sub>

1 ml 5M NaCl

50 µl Tween-20

Adjusted to 50 ml with dH<sub>2</sub>O

**BCIP, 50 mg/ml** (Merck; cat. no.: 11383221001): store at -20 °C

**Bleaching solution**

8.30 ml dH<sub>2</sub>O

0.5 ml 20x SSC

0.7 ml H<sub>2</sub>O<sub>2</sub> (30%)

0.5 ml formamide

**BBR (Boehringer Blocking Reagent), 10%**

10 g Boehringer Blocking Reagent (Merck; cat. no.: 11096176001)

Adjusted to 100 ml with 1x MAB

Stirred and heated to dissolve

Autoclaved, stored at -20°C in 50 ml aliquots

**DEPC-H<sub>2</sub>O**

Added 1 ml DEPC (Diethylpyrocarbonate) to 1 l dH<sub>2</sub>O

Mixed thoroughly and left to evaporate under fume hood overnight (at least 1 h)

Autoclaved to destroy DEPC, stored at RT

**EDTA, 0.5M**

73.05 g EDTA (Ethylenediaminetetraacetate)

Dissolved in 400 ml dH<sub>2</sub>O, adjusted pH to roughly 8 with NaOH pellets

(will only go into solution at pH>7)

Adjusted to 500 ml with dH<sub>2</sub>O

Added 0.5 ml DEPC

Mixed thoroughly and left to evaporate under fume hood overnight (at least 1 h)

Autoclaved and stored at RT

**EGTA, 0.2M**

7.61 g EGTA

Dissolved in 70 ml dH<sub>2</sub>O, adjusted pH to roughly 8 with NaOH pellets

(will only go into solution at pH>7)

Adjusted to 100 ml with dH<sub>2</sub>O

Added 0.1 ml DEPC

Mixed thoroughly and left to evaporate under fume hood overnight

(at least 1 h)

Autoclaved and stored at RT

**HIGS (heat inactivated goat serum)**

Normal goat serum

Heated for 30 minutes at 60 °C

Stored at 4 °C

**Hybridization buffer**

Prepared in 50 ml falcon tubes

25 ml formamide (Merck; cat. no.: 11814320001)

12.5 ml 20x SSC

50 mg torula yeast RNA (Merck; cat. no.: 10109223001)

5 mg heparin

1ml 50x Denhart's solution (Thermo Fisher; cat. no.: 750018)

50 µl Tween-20

50 mg CHAPS

1 ml 0.5M EDTA

Adjusted to 50 ml with DEPC-H<sub>2</sub>O

Stored at -20°C

**MAB, 10x**

58 g maleic acid

43.8 g NaCl

Dissolved in 400 ml dH<sub>2</sub>O and adjusted pH to 7.5 with NaOH pellets

Adjusted to 500 ml with dH<sub>2</sub>O

Autoclaved and stored at 4°C

**MEMFA**

79 ml DEPC-H<sub>2</sub>O

10 ml 1M MOPS

1 ml 0.2M EGTA

100 µl 1M MgSO<sub>4</sub>

10 ml formaldehyde solution 37% (Merck; cat. no.: 104003)

**MgCl<sub>2</sub>, 1M**

20.33 g MgCl<sub>2</sub>\*6 H<sub>2</sub>O

Adjusted to 100 ml with dH<sub>2</sub>O

Autoclaved and stored at RT

**MgSO<sub>4</sub>, 1M**

12.04 g MgSO<sub>4</sub>

Adjusted to 100 ml with dH<sub>2</sub>O

Added 0.1 ml DEPC

Mixed thoroughly and left to evaporate under fume hood overnight  
(at least 1 h)

Autoclaved and stored at RT

**MOPS, 1M**

104.65g MOPS

10.25 g NaOAc

50 ml 0.5M EDTA

Dissolved in 300 ml dH<sub>2</sub>O, adjusted pH to 7 with NaOH pellets

Adjusted to 500 ml with DEPC-H<sub>2</sub>O

Stored at 4°C

**NaCl, 5M**

146.1 g NaCl

Adjusted to 500 ml with DEPC-H<sub>2</sub>O

Autoclaved and stored at RT

**NBT, 100 mg/ml** (Merck; cat. no.: 11383213001): store at -20 °C

**PB (phosphate buffer), 0.1M**

2.63 g NaH<sub>2</sub>PO<sub>4</sub>\*H<sub>2</sub>O

21.65g Na<sub>2</sub>HPO<sub>4</sub>\*7H<sub>2</sub>O

Dissolved in 800 ml dH<sub>2</sub>O, adjusted pH to 7.4

Adjusted to 1 liter with dH<sub>2</sub>O

Autoclaved and stored at RT

**PBS (phosphate buffered saline), 10x**

80 g NaCl

2 g KCl

14.4 g Na<sub>2</sub>HPO<sub>4</sub> (or 26.4 g Na<sub>2</sub>HPO<sub>4</sub>\*7 H<sub>2</sub>O)

2.4 g KH<sub>2</sub>PO<sub>4</sub>

Dissolved in 800 ml dH<sub>2</sub>O, pH adjusted to 7.4

Adjusted to 1 liter with dH<sub>2</sub>O

Added 1 ml DEPC

Mixed thoroughly and left to evaporate under fume hood overnight  
(at least 1 h)

Autoclaved and stored at RT

**Proteinase K, 25 mg/ml**

25 mg Proteinase K (Merck; cat. no.: 03115836001)

1 ml DEPC-H<sub>2</sub>O

Dispensed into 20 µl aliquots

Stored at -20°C

**RNAse A, 2mg/ml**

25 mg RNAse A (Merck; cat. no.: 10109142001)

12.5 ml dH<sub>2</sub>O

Dispensed into 100 µl aliquots and stored at -20 °C

**RNAse T1 (Merck; cat. no.: R1003)**

Stored at 4°C

**SSC, 20x**

87.65 g NaCl

44.1 g  $C_6H_5Na_3O_7 \cdot 2 H_2O$  (trisodium citrate dihydrate)

Dissolved in 400 ml  $dH_2O$ , adjusted pH to 7

Adjusted to 500 ml with  $dH_2O$

Added 0.5 ml DEPC

Mixed thoroughly and left to evaporate under fume hood overnight

(at least 1 h)

Autoclaved and stored at RT

**TEA, 1M**

66.7 ml 100% TEA (triethanolamine) solution (7.5M)

433.3 ml DEPC- $H_2O$

Stored at 4°C

**Tris pH 9.5, 1M**

60.55 g Tris base

Dissolved in 400 ml  $dH_2O$ , adjusted pH to 9.5

Adjusted to 500 ml with  $dH_2O$

Autoclaved and stored at RT

**X-gal, 50x (50mg/ml)**

0.5 g X-gal

10 ml dimethylformamide

Dispensed into 100  $\mu$ l aliquots

Stored at -20 °C

**X-gal staining solution**

5 ml 0.1M PB  
82.5 mg potassium ferricyanide  
105 mg potassium ferrocyanide  
10  $\mu$ l 1M MgCl<sub>2</sub>  
100  $\mu$ l X-gal 50x

**A.3. Solutions for co-immunoprecipitation****Extraction buffer**

1 ml 0.1M HEPES  
67  $\mu$ l 5M NaCl  
20  $\mu$ l 1M MgCl<sub>2</sub>  
50  $\mu$ l 0.2M EDTA  
100  $\mu$ l 0.1M DTT (not added for extracts prepared for mass spectrometry)  
5  $\mu$ l Tween-20  
Adjusted to 10 ml with dH<sub>2</sub>O  
Added 100  $\mu$ l protease and phosphatase inhibitor cocktail 100x (Thermo Fisher; cat. no.: 78441) just before use

**TBS, 10x**

24 g Tris Base  
88 g NaCl  
Dissolved in 900 ml dH<sub>2</sub>O, adjusted pH to 7.6  
Adjusted to 1 liter with dH<sub>2</sub>O

**Wash buffer**

10 ml 10x TBS  
50 µl Tween-20  
10 ml 5M NaCl  
80 ml dH<sub>2</sub>O

**A.4. Solutions for PAGE and western blotting****Blocking solution**

1x TBST  
3% BSA (bovine serum albumine)

**Borate transfer buffer, 20x**

49.46g boric acid  
14.8 g EDTA  
Dissolved in 1.7 liters dH<sub>2</sub>O, adjusted pH to 8.8 with NaOH pellets  
Adjusted to 2 liters with dH<sub>2</sub>O

**Running buffer**

7.27 g Tris Base  
12.55 g MOPS  
1.2 g SDS  
0.36 g EDTA  
Dissolved and adjusted to 1.2 liters with dH<sub>2</sub>O

**TBS, 10x**

24 g Tris Base  
88 g NaCl  
Dissolved in dH<sub>2</sub>O, adjusted pH to 7.6  
Adjusted to 1 liter with dH<sub>2</sub>O

**TBST, 1x**

1x TBS

0.1% Tween-20

## Appendix B. Primers list and PCR protocol

**Table B.1.** List of PCR primers designed to generate inserts that were subsequently subcloned in pCS2+ or pCDNA-EGFP vectors.

| Generated plasmid               | Primer name           | Sequence (5' to 3')   | Modifications       | Annealing T°    |
|---------------------------------|-----------------------|---|---------------------|-----------------|
| <b>Pias4-C-term-flag/pCS2+</b>  | pias4_F_BH2           | ATGGCGGCGGAGTTAGTG  |                     | 50.2 to 68.2 °C |
|                                 | pias4_R_BH2           | ACAAGCTGATAAGAGGCCTTTC  |                     |                 |
|                                 | Xl_pias4_XhoI_F       | TACTAA <b>CTCGAG</b> ATGGCGGCGGAGTTAGTG   | <b>XhoI</b>         | 50.2 to 64.6 °C |
|                                 | Xl_pias4_XbaI_R       | TACTAC <b>TCTAGA</b> <b>TTACTTATCGTCATCGTCCTTATAGTC</b> ACAAGCTGATAAGAGGCCTTTC                  | <b>XbaI + flag</b>  |                 |
| <b>Garre1-C-term-flag/pCS2+</b> | Xl_kiaa0355_XhoI_F    | TACTAA <b>CTCGAG</b> ATGTATTGCTGTAGTGCTCAGGA  | <b>XhoI</b>         | 50.2 to 64.6 °C |
|                                 | Xl_kiaa0355_XbaI_R    | TACTAC <b>TCTAGA</b> <b>TTACTTATCGTCATCGTCCTTATAGTC</b> GAACTGGTGCAGGTATGAGGGT                  | <b>XbaI + flag</b>  |                 |
| <b>Msh6-C-term-flag/pCS2+</b>   | msh6_F_BH2            | AGTGTGAGGTAGAAGAGTCC  |                     | 50.2 to 68.2 °C |
|                                 | msh6_R_BH2            | CGTGTGTGAGTAAACAAAGC  |                     |                 |
|                                 | Xl_msh6_AsuII_F       | TACTAC <b>TTCGAA</b> CCCGCCATGTCTAAGCAAAA   | <b>AsuII</b>        | 50.2 to 64.6 °C |
|                                 | Xl_msh6_XbaI_R        | TACTAC <b>TCTAGA</b> <b>TTACTTATCGTCATCGTCCTTATAGTC</b> TTGGAGCAACTTCAGCCGCTT                   | <b>XbaI + flag</b>  |                 |
| <b>Sox11-C-term-flag/pCS2+</b>  | Xl_sox11_XhoI_F       | TACTAA <b>CTCGAG</b> ACAGCCATGGTGCAGCGAG  | <b>XhoI</b>         | 50.2 to 64.6 °C |
|                                 | Xl_sox11_XbaI_R       | TACTAC <b>TCTAGA</b> <b>TTACTTATCGTCATCGTCCTTATAGTC</b><br>GTAAGTGAAGACCAAGTCTGAAAA             | <b>XbaI + flag</b>  |                 |
| <b>Zmym3-C-term-flag/pCS2+</b>  | zmym3_F_BH2           | CTTCGTGAAATCTGGTAAGC  |                     | 50.2 to 68.2 °C |
|                                 | zmym3_R_BH2           | TTGTAGAAGCAGTTTAGTGG  |                     |                 |
|                                 | Xl_zmym3_XhoI_F       | TACTAA <b>CTCGAG</b> ATGGAGAGCGAGGAGGGG   | <b>XhoI</b>         | 50.2 to 64.6 °C |
|                                 | Xl_zmym3_XbaI_R       | TACTAC <b>TCTAGA</b> <b>TTACTTATCGTCATCGTCCTTATAGTC</b> GTCTGTGTCCTCCGTGGCAT                    | <b>XbaI + flag</b>  |                 |
| <b>N-term-Strep-Pias4/pCS2+</b> | XhoI_Nstrep_Pias4_F   | TACTAA <b>CTCGAG</b> <b>ATGGCATCATGGTCACATCCACAATTCGAGAAGGGTGCA</b><br>GCGGCGGAGTTAGTGGAGGCGAAG | <b>XhoI + Strep</b> | 64.6 to 71.7 °C |
|                                 | Pias4_Nstrep_XbaI_R   | TACTAC <b>TCTAGA</b> TTAACAAGCTGATAAGAGGCCTTTC  | <b>XbaI</b>         |                 |
| <b>Pias4-C-term-Strep/pCS2+</b> | Xl_pias4_XhoI_F       | TACTAA <b>CTCGAG</b> ATGGCGGCGGAGTTAGTG   | <b>XhoI</b>         | 64.6 to 71.7 °C |
|                                 | Xl_pias4_XbaI_Strep_R | TACTAC <b>TCTAGA</b> <b>TTATTTTCGAACTGCGGGTGGCTCCATCCTCC</b><br>ACAAGCTGATAAGAGGCCTTTC          | <b>XbaI + Strep</b> |                 |
|                                 | Xl_pias4_XhoI_F       | TACTAA <b>CTCGAG</b> ATGGCGGCGGAGTTAGTG   | <b>XhoI</b>         | 68.2 to 71.7 °C |

|                                     |                    |  |                             |                 |
|-------------------------------------|--------------------|--|-----------------------------|-----------------|
| <b>Pias4-C-term-TwinStrep/pcS2+</b> | XbaI-3'TwinStrep_R | TACTAC <b>TCTAGA</b><br>TTACTTCTCGAATTGTGGATGTGACCATGCAGAGCCACCACTACCACCTCCTGAACCGCCAC<br>C TTTTTCGAACTGCGGGTGGCTCCATCCTCC | <b>XbaI +<br/>TwinStrep</b> |                 |
| <b>Pias4-C-term-eGFP/pcDNA3</b>     | pias4_F_ecoRI      | TACTAC <b>GAATTC</b> GGATCTGGTACCATGGCG  | <b>EcoRI</b>                | 58.3 to 71.7 °C |
|                                     | pias4_R_notI       | TACTAC <b>GCGGCCGC</b> GATCCCGATCCCGATCC ACAAGCTGATAAGAGGCCT   | <b>NotI + linker</b>        |                 |
| <b>Smarce1-C-term-eGFP/pcDNA3</b>   | smarce1_F_kpnI     | TACTAC <b>GGTACC</b> ATGTCCAAGCGACCATCG  | <b>KpnI</b>                 | 58.3 to 71.7 °C |
|                                     | smarce1_R_notI     | TACTAC <b>GCGGCCGC</b> GATCCCGATCCCGATCC GTTCTTGATCAGGCTCTTC   | <b>NotI + linker</b>        |                 |
| <b>Sox11-C-term-eGFP/pcDNA3</b>     | sox11_F_kpnI       | TACTAC <b>GGTACC</b> GAGACAGCCATGGTGCAG  | <b>KpnI</b>                 | 58.3 to 71.7 °C |
|                                     | sox11_R_notI       | TACTAC <b>GCGGCCGC</b> GATCCCGATCCCGATCC GTAAGTGAAGACCAAGTCTGAAAA  | <b>NotI + linker</b>        |                 |
| <b>Six1-C-term-eGFP/pcDNA3</b>      | six1_F_kpnI        | TACTAC <b>GGTACC</b> ATGTCTATGCTGCCTCC   | <b>KpnI</b>                 | 58.3 to 71.7 °C |
|                                     | six1_R_notI        | TACTAC <b>GCGGCCGC</b> GATCCCGATCCCGATCC CGATCCCAGATCCACCAG  | <b>NotI + linker</b>        |                 |

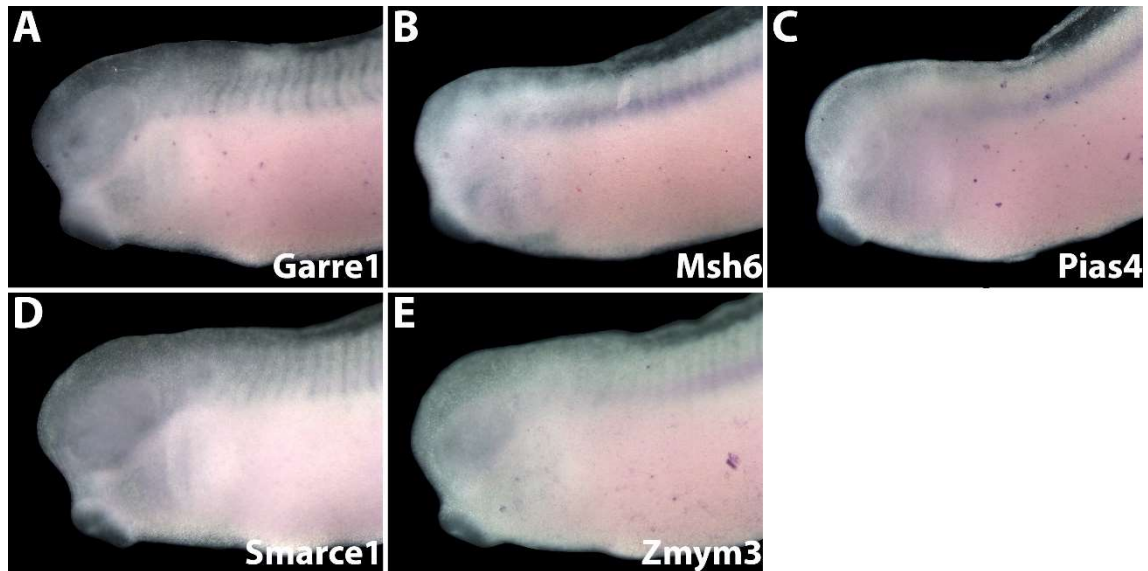
**Table B.2.** PCR reaction mix (20 µl).

|                             |          |
|-----------------------------|----------|
| HF buffer                   | 4 µl     |
| dNTPs 2.5 mM                | 1.6 µl   |
| Primer F 10 µM              | 1 µl     |
| Primer R 10 µM              | 1 µl     |
| Phusion polymerase          | 0.2 µl   |
| Template DNA                | 10 ng    |
| RNAse free H <sub>2</sub> O | to 20 µl |

**Table B.3.** Gradient PCR program.

|                   | <b>Step</b>          | <b>Temp</b> | <b>Time</b>   |
|-------------------|----------------------|-------------|---------------|
|                   | Initial denaturation | 98 °C       | 2'            |
| <b>40 cycles:</b> | Denaturation         | 98 °C       | 10''          |
|                   | Annealing            | (gradient)  | 20''          |
|                   | Elongation           | 72 °C       | (30'' per kb) |
|                   | Final elongation     | 72 °C       | 10'           |
|                   | Store                | 10 °C       |               |

## Appendix C. Sense *in situ* hybridization



**Fig. C.1.** *In situ* hybridization on whole-mount *Xenopus laevis* embryos at stage 27, in lateral views (anterior is to the left), using sense probes for five candidate interaction partners of *eya1*. No staining was present using these probes, except weak, diffuse staining often observed in the pharyngeal pouches (A to E), the optic and otic vesicles (A, D, E) and/or at the level of the notochord (B, C, E).

## Appendix D. MS/MS probable contaminants

**Table D.1.** List of Eya1 candidate protein partners identified by MS/MS, belonging to a class of common contaminants, or individually identified as contaminants in (Gingras et al., 2007) and/or (Trinkle-Mulcahy et al., 2008).

| <b>Protein symbol</b> | <b>Protein name</b>  | <b>Class of contaminants</b>                 |
|-----------------------|--|--|
| <b>Abce1.S</b>        | ATP binding cassette subfamily E member 1  | Eukaryotic translation elongation/initiation |
| <b>Cad.L</b>          | carbamoyl-phosphate synthetase 2, aspartate transcarbamylase, and dihydroorotase | Other  |
| <b>Cand1.S</b>        | cullin-associated and neddylation-dissociated 1                                  | Other  |
| <b>Cltc.L</b>         | clathrin, heavy chain (Hc)   | Other  |
| <b>Copa.L</b>         | COPI coat complex subunit alpha  | Other  |
| <b>Copb1.S</b>        | COPI coat complex subunit beta 1   | Other  |
| <b>Copg1.L</b>        | COPI coat complex subunit gamma 1  | Other  |
| <b>Dync1h1.L</b>      | dynein cytoplasmic 1 heavy chain 1   | Cytoskeletal/structural/motility             |
| <b>Eif2s2.S</b>       | eukaryotic translation initiation factor 2 subunit beta                          | Eukaryotic translation elongation/initiation |
| <b>Eif2s3.L</b>       | eukaryotic translation initiation factor 2 subunit gamma                         | Eukaryotic translation elongation/initiation |
| <b>Eif3a.L</b>        | eukaryotic translation initiation factor 3 subunit A                             | Eukaryotic translation elongation/initiation |
| <b>Eif3a.S</b>        | eukaryotic translation initiation factor 3 subunit A                             | Eukaryotic translation elongation/initiation |
| <b>Eif3b.S</b>        | eukaryotic translation initiation factor 3 subunit B                             | Eukaryotic translation elongation/initiation |
| <b>Eif3c.L</b>        | eukaryotic translation initiation factor 3 subunit C                             | Eukaryotic translation elongation/initiation |
| <b>LOC108706570</b>   | 60S ribosomal protein L9   | Ribosomal                                    |
| <b>Mcm2.S</b>         | minichromosome maintenance complex component 2                                   | Other  |
| <b>Mcm4.L</b>         | minichromosome maintenance complex component 4                                   | Other  |
| <b>Mcm5.L</b>         | minichromosome maintenance complex component 5                                   | Other  |
| <b>Mcm6.2.L</b>       | minichromosome maintenance complex component 6 gene 2                            | Other  |
| <b>Mcm7.L</b>         | minichromosome maintenance complex component 7                                   | Other  |

|                   |                                    |                                  |
|-------------------|------------------------------------|----------------------------------|
| <b>Myh10.S</b>    | myosin, heavy chain 10, non-muscle | Cytoskeletal/structural/motility |
| <b>Myh9.L</b>     | myosin, heavy chain 9, non-muscle  | Cytoskeletal/structural/motility |
| <b>Myh9.S</b>     | myosin, heavy chain 9, non-muscle  | Cytoskeletal/structural/motility |
| <b>Rack1.S</b>    | receptor for activated C kinase 1  | Ribosomal                        |
| <b>Rpl10a.S</b>   | ribosomal protein L10a             | Ribosomal                        |
| <b>Rpl13a.S</b>   | ribosomal protein L13a             | Ribosomal                        |
| <b>Rpl21.L</b>    | ribosomal protein L21              | Ribosomal                        |
| <b>Rpl28.S</b>    | ribosomal protein L28              | Ribosomal                        |
| <b>Rpl38.L</b>    | ribosomal protein L38              | Ribosomal                        |
| <b>Rps10.S</b>    | ribosomal protein S10              | Ribosomal                        |
| <b>Rps5.S</b>     | ribosomal protein S5               | Ribosomal                        |
| <b>Tkt.L</b>      | transketolase                      | Other                            |
| <b>Tuba1c.S</b>   | tubulin alpha 1c                   | Cytoskeletal/structural/motility |
| <b>Tubal3.2.L</b> | tubulin alpha like 3, gene 2       | Cytoskeletal/structural/motility |
| <b>Tubal3.L</b>   | tubulin alpha like 3 gene 1        | Cytoskeletal/structural/motility |
| <b>Tubal3.S</b>   | tubulin alpha like 3 gene 1        | Cytoskeletal/structural/motility |
| <b>Tubb4a.S</b>   | tubulin beta 4A class Iva          | Cytoskeletal/structural/motility |
| <b>Tubb4b.L</b>   | tubulin beta 4B class Ivb          | Cytoskeletal/structural/motility |